EPFL

Thèse n° 8726

The role of immune effectors in controlling *Drosophila*-microbes interactions

Présentée le 28 mai 2021

Faculté des sciences de la vie
Unité du Prof. Lemaitre
Programme doctoral en approches moléculaires du vivant

pour l'obtention du grade de Docteur ès Sciences

par

Alice MARRA

Acceptée sur proposition du jury

Prof. V. Simanis, président du jury
Prof. B. Lemaitre, directeur de thèse
Prof. P. Engel, rapporteur
Prof. F. Leulier, rapporteur
Prof. C. Vorburger, rapporteur

École
polytechnique
fédérale
de Lausanne

2021

Acknowledgments

First of all, I would like to thank Professor Bruno Lemaitre for welcoming me into his laboratory. Thank you Bruno for the confidence, the guidance, and the support you gave me in the years along this path together.

I would like to thank the members of the jury for accepting and evaluating my work and their contribution during the defense of the thesis.

Thanks to all former and present members of the Lemaitre lab. It has been a pleasure collaborate with all of you. The results I got during my work here were also accomplished with your help. A special thanks goes to Florent, a great supervisor and friend. Thank you for always believing in me and for passing to me, with passion and patience, a great wealth of knowledge. I could not have made it without your help. Thank you Samuel, for the dedication you put into your work every day and for being always helpful and willing to discuss with your colleagues, without exception. You have been a precious teacher. Despite the relatively little time we spent together in the lab, thanks to Berra for helping me to grow professionally and emotionally. A big thank you goes to Mark. It has been a real pleasure to collaborate with you over the years. Your help and your positivity were really appreciated! Thanks to Bianca, who was not only a colleague, but also a great friend. Thanks to Hannah for delighting the laboratory with her fantastic sweets and, of course, for the time spent helping me with my work. Thank you Li, for the time spent together in the lab during all these years. I wish you all the best for your new career!

Thanks to Véronique and Mercedes for all their help with the EPFL administration; to Jean Philippe, Fanny and Christophe for keeping the laboratory running smoothly; and to all the people outside of the lab that were also part of this 4-year adventure. A special thanks goes to Fabio with whom I shared joys and sorrows of the PhD experience, and to Radiana. You made Lausanne a homey place to be!

Much gratitude goes to the lifelong friends who have always supported me and with whom I shared a lot. Thank you Serena, Valmira, Anael and Silvia. Thanks for always being there.

Last but not least, I want to thank my mother and father for the love and the support they gave me over the years, and for helping me to make things easier despite the distance.

E Grazie al mio compagno di vita Francesco. Il tuo amore, il tuo coraggio e la tua costanza sono la mia forza. E grazie a Po, il nostro eterno dolce cucciolo.

Abstract

All live beings are in constant interaction with microorganisms that may be beneficial, deleterious or commensal. Insects in particular live in close contact with microorganisms. This is especially true for species, like the fruit fly *Drosophila melanogaster* that feed, lay eggs and develop on or close to decomposing organic matter. In contrast to vertebrates, insects did not evolve an adaptive immune system to combat pathogens selectively. They instead rely on surprisingly efficient innate defense mechanisms for the control and clearance of all microbes without any species-specific targeting. Innate immunity encompasses a wide range of mechanisms that rely on direct pathogen recognition and elimination. In addition, metabolic and behavioral responses also strongly affect the outcome of insect interactions with both pathogenic and non-pathogenic bacteria. Although the *Drosophila* immune system has been extensively described, little is known about the role of immune effectors in tolerating and controlling symbiotic microbes.

For this reason, during my PhD studies, I investigated how *Drosophila melanogaster* immune effectors differentially interact with mutualistic symbionts. First, I investigated the role of some of the host antimicrobials, called antimicrobial peptides and lysozymes, in maintaining the homeostasis of the gut microbiota. I found that both antimicrobial peptides and lysozymes can actively regulate the gut microbiota composition and abundancy, especially during aging.

In a second part of my thesis, I got interested in *Spiroplasma*, a heritable symbiotic bacterium that lives within the fly hemolymph. I characterized the role of the *Drosophila* iron transporter Transferrin 1 (Tsf1) during *Spiroplasma-Drosophila* symbiosis. I first showed that mutant flies for *tsf1* have an impaired *Spiroplasma* load, due to iron relocation from the hemolymph to the fat body, where it becomes inaccessible for *Spiroplasma*. Furthermore, I demonstrated that *Spiroplasma* scavenges host iron only when it is bound to the protein, which points to Tsf1 and iron transport as a control mechanism for hemolymphatic symbionts.

Collectively, my studies contribute to a better understanding of how the innate immune effectors interact with *Drosophila* microbial symbionts to both regulate and maintain stable, long-lasting, interactions.

Keywords: *Drosophila melanogaster*, innate immunity, immune effectors, symbiosis, iron sequestration, gut microbiota, antimicrobial peptides, lysozymes, Transferrin.

Riassunto

Tutti gli esseri viventi sono in costante interazione con microrganismi che possono essere definiti come benefici, deleteri o commensali. Gli insetti in particolare vivono a stretto contatto con microrganismi. Ciò è particolarmente vero per le specie come il moscerino della frutta *Drosophila melanogaster*, che si nutre, depone le uova e si sviluppano sopra o nei pressi della materia organica in decomposizione. A differenza dei vertebrati, gli insetti non hanno sviluppato un sistema immunitario adattativo per combattere selettivamente i patogeni. Si affidano, invece, a meccanismi di difesa innati, sorprendentemente efficienti per il controllo e l'eliminazione di tutti i microbi senza alcun targeting specie-specifico. L'immunità innata comprende un'ampia gamma di meccanismi che si basano sul riconoscimento e sull'eliminazione diretti dei patogeni. Inoltre, anche le risposte metaboliche e comportamentali influenzano fortemente l'esito delle interazioni degli insetti con batteri patogenici e non. Sebbene il sistema immunitario di *Drosophila* sia stato ampiamente descritto, poco si sa sul ruolo degli effettori della risposta immunitaria nel tollerare e controllare i microrganismi simbionti.

Per questo motivo, nella mia tesi di dottorato, ho studiato come gli effettori della risposta immunitaria di *Drosophila melanogaster* interagiscano in modo differenziale con i simbionti mutualistici. In primo luogo, ho studiato il ruolo di alcuni antimicrobici prodotti dall'ospite, chiamati peptidi antimicrobici e lisozimi, nel mantenimento dell'omeostasi del microbiota intestinale. Dai nostri studi è emerso che i peptidi antimicrobici e i lisozimi possono regolare attivamente la composizione e l'abbondanza del microbiota intestinale, specialmente durante il processo di invecchiamento.

In una seconda parte della mia tesi, mi sono interessata a *Spiroplasma*, un batterio simbionte trasmissibile che vive all'interno dell'emolinfa della moscerino e ho caratterizzato il ruolo del ferro trasportatore di *Drosophila* Transferrin 1 (Tsf1) durante la simbiosi *Spiroplasma-Drosophila*. Per prima cosa ho mostrato che i moscerini mutanti per Tsf1 hanno una carica batterica di *Spiroplasma* ridotta a causa del trasferimento del ferro dall'emolinfa all'organo fat-body, dove diventa inaccessibile per *Spiroplasma*. Inoltre, ho dimostrato che *Spiroplasma* acquisice il ferro dell'ospite solo quando esso è legato a Tsf1. Il che indica Tsf1 e il trasporto del ferro come meccanismo di controllo per i simbionti emolinfatici.

Collettivamente, i miei studi contribuiscono a una migliore comprensione di come gli effettori della risposta immunitaria innata interagiscano con i simbionti microbici di *Drosophila* per regolare e mantenere interazioni stabili e durature.

Parole chiave: *Drosophila melanogaster*, immunità innata, effettori della risposta immunitaria, simbiosi, sequestro del ferro, microbiota intestinale, peptidi antimicrobici, lisozimi, Transferrina.

Table of content

Abbreviations

AMPs	Antimicrobial peptides
Boms	Bomanins
DAP	Meso-diaminopimelic acid
Duox	Dual Oxidase
Imd	Immune deficiency pathway
JNK	JUN N-terminal kinase
Lys	Lysozyme
MAMP	Microbe associated molecular pattern
Nox	NADPH oxidase
PGN	Peptidoglycan
PGRP	Peptidoglycan recognition protein
PPO	Prophenoloxidase
PRR	Pattern recognition receptor
ROS	Reactive oxygen species
SR	Scavenger receptor
TEP	Thioster-containing proteins
TLR	Toll-like receptor

Chapter I

Drosophila innate immunity

1. *Drosophila melanogaster* interaction with microbes

Drosophila melanogaster (hereafter *Drosophila*) has been used as a model organism for research for over a century to study genetics. Because of its high level of gene conservation relative to mammals, and because of the ease with which its genome can be manipulated in pursuit of functional genetic studies, *Drosophila* has been widely used as an animal model. It allowed a deeper insight into key biological mechanisms relating to metabolism, development, neurology, diseases and immunity, among others (1–5) **(Figure 1)**.

Drosophila lives and develops on decomposing matter throughout its life cycle. Eggs are laid on rotting fruits, from which larvae hatch and feed on the same substrate. After a few days of feeding, larvae undergo pupation and give rise to mature adults that will keep feeding on decomposing matter, ingesting a complex mix of bacteria and fungi. In the wild, this translates into a high level of exposure to infection by microbes at all life stages (6, 7), including bacteria but also viruses, eukaryotic parasites (nematodes and parasitoid wasps), trypanosomes, microsporidia and fungi (yeasts and filamentous fungi) (8). Each of these categories of pathogens triggers a distinct set of overlapping immune mechanisms.

The continuous feeding of larvae on rotting material and parental feces also allows larvae to acquire mutualistic bacterial species that can colonize their gut, establishing the so-called “gut microbiota” (9).

Symbiosis with gut microbiota is a widespread feature in most eukaryotic taxa. Insects however developed a more intricate interaction with bacteria species living within their host tissues, called endosymbiotic bacteria or endosymbionts. Endosymbionts strongly affect their host physiology, including their metabolic capabilities or their ability to fight against pathogens (2, 10). Unlike the gut microbiota, which is transmitted horizontally, endosymbionts have a vertical transmission that entails some extent of coevolution with their host and a stronger interdependency between the two partners (e.g. most endosymbionts cannot grow outside of their host tissues (11). In *Drosophila*, only two endosymbiotic bacteria have been identified so far: *Wolbachia* and *Spiroplasma* (12). Their peculiar lifestyle and intimacy with their host set them apart from other microbes with regards to their interaction with the host immune system (see below).

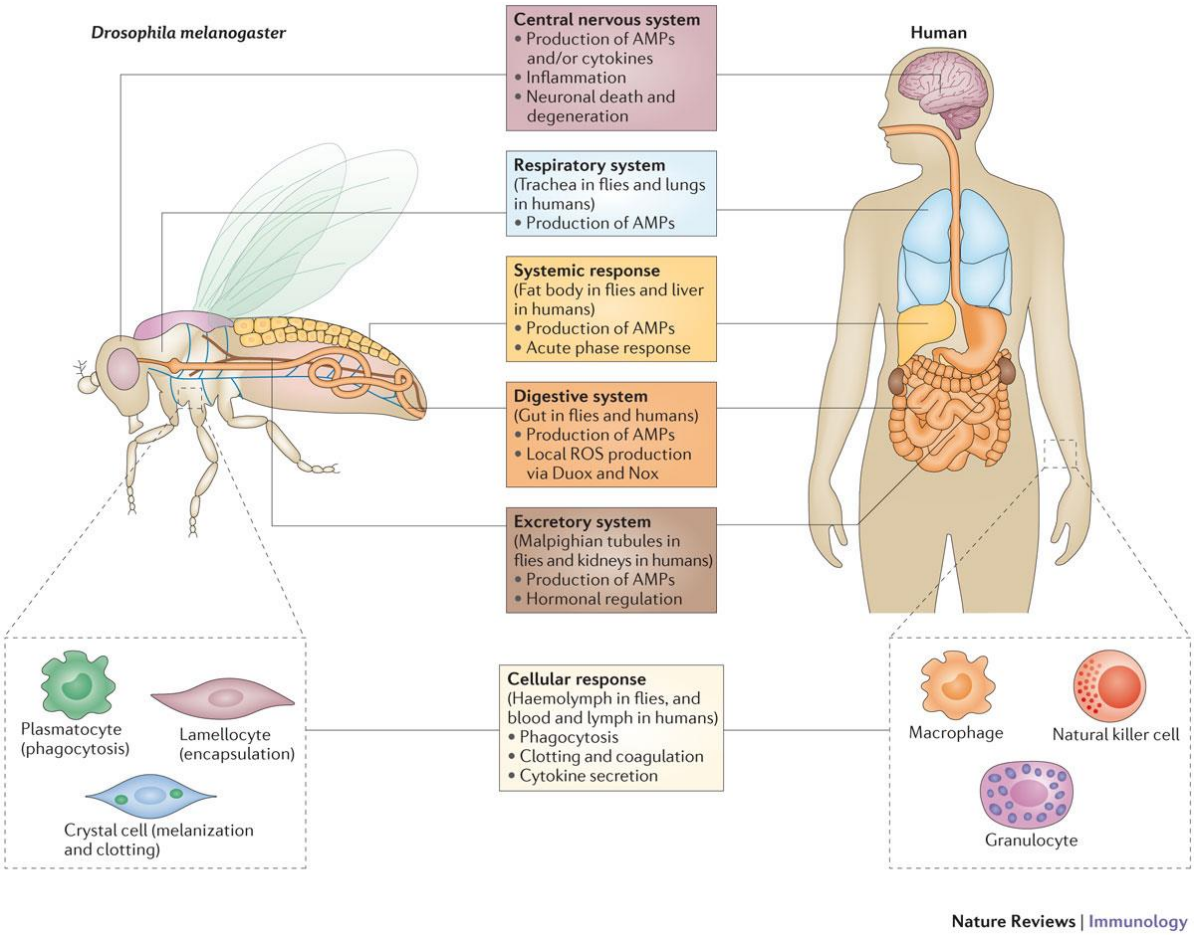

Fig.1 *Drosophila* as a model to study physiology. In spite of its phylogenetic distance, many organs of the fruit fly are analogous in their functions to that of mammals. This analogy is especially important when it comes to their innate immune system. More specifically, the main arms of immune defense are highly conserved (systemic and cellular immune response, see below) and make *Drosophila* a valuable model to study their function (from Buchon *et al*., 2014)

1.1 The *Spiroplasma-Drosophila* interaction

One of the most frequently reported endosymbiont infecting insects, along with *Wolbachia*, is *Spiroplasma spp* (13, 14). *Spiroplasma* are helicoidal bacteria that belong to the Mollicutes class, a group of wall-less bacteria. The genus is very diverse and includes insect, crustacean and plant pathogens, commensal and endosymbiotic species (15). *Spiroplasma poulsonii*, hereafter *Spiroplasma*, can naturally infect *Drosophila melanogaster* in the wild as a facultative, vertically transmitted, endosymbiont (12) **(Figure 2)**. Most strains cause male-killing, a fascinating phenomenon whereby male embryos from *Spiroplasma*-infected mothers die during early embryogenesis (16, 17). Recent studies showed that male-killing involves the

Spiroplasma-encoded toxin Spaid (18), that targets the X-chromosome dosage compensation system in *Drosophila*. Spaid causes the breakage of the male X chromosomes during mitosis (by a yet unknown mechanism) and therefore a massive apoptosis that ends up killing the embryo (18, 19). *Spiroplasma* lives free in flies hemolymph, where it can acquire host metabolites to sustain its growth (20). Being devoid of a cell wall, hence devoid of peptidoglycan and other immunogenic surface motives, *Spiroplasma* is considered as undetectable for the host immune system (21), although some recent studies indicated that the Toll pathway responds mildly to *Spiroplasma* infection (22). *Spiroplasma* infections shorten the fly lifespan, reduces fertility and causes a neurodegenerative phenotype in older flies (21, 23). The cause of this phenotypes it has not fully unraveled yet, although the involvement of cardiolipins or a neurotoxic protein released by *Spiroplasma* have been proposed as putative mechanisms (21, 24).

Although *Spiroplasma* infection appears deleterious for the flies, it can also provide a major benefit, that is protection against fly natural enemies, such as parasitoid wasps and nematodes (25–27). This protection has been linked to the secretion of toxins belonging to the Ribosome-Inactivating Protein (RIP) family by *Spiroplasma*. RIPs accumulate in the hemolymph and target parasitic wasp and nematode ribosomes, hence blocking their protein synthesis and eventually killing them (25, 28). A second hypothesis involves the competition between parasites and *Spiroplasma* for host resources, mainly lipids. *Spiroplasma* thus, would block the parasitoid wasp larva growth by monopolizing these resources (29). This phenotype is a major beneficial effect of *Spiroplasma* infections and studies performed on museum specimens showed that protection against nematodes, most likely drove *Spiroplasma* infection prevalence in fruit flies across North America in only a few decades (30).

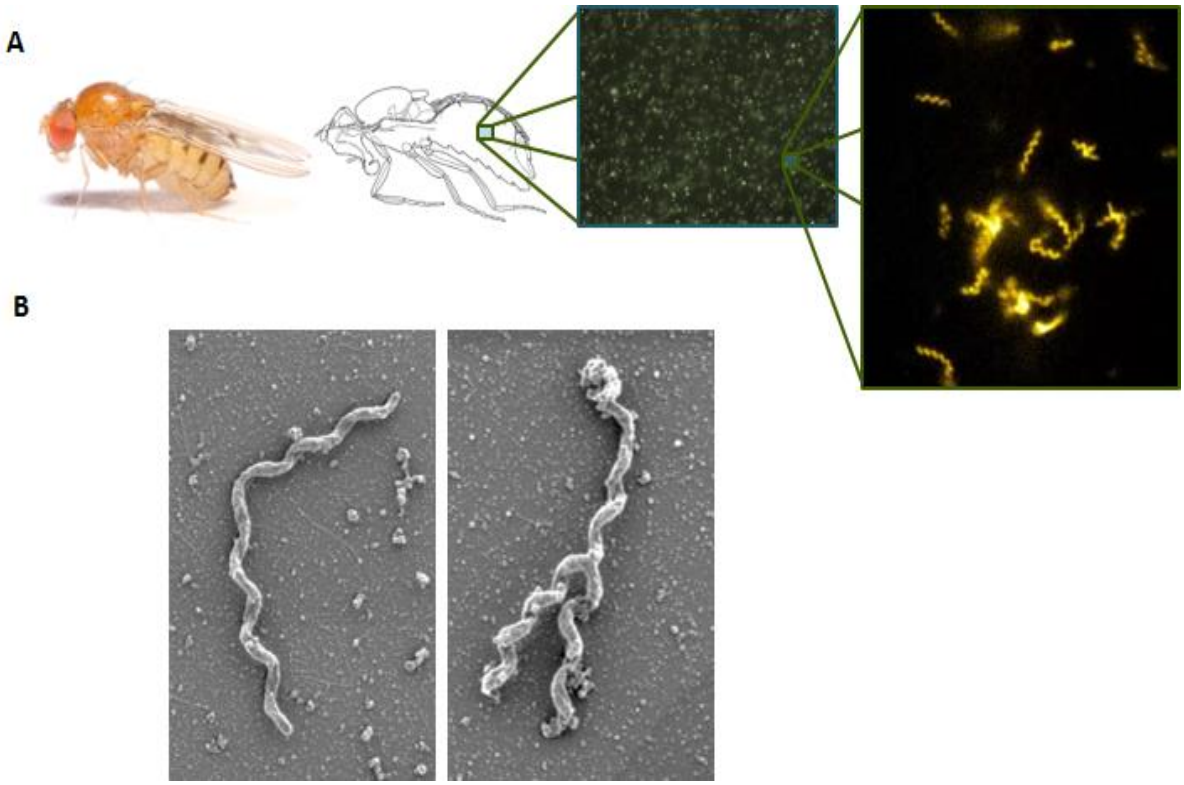

Fig.2 *Spiroplasma poulsonii* : a facultative endosymbiont of *Drosophila melanogaster*. A) *Spiroplasma* lives free in *Drosophila* hemolymph. The green square shows a DNA staining of *Spiroplasma* in a droplet of *Drosophila* hemolymph and the yellow square a higher magnification. Image courtesy of Florent Masson and Alexandre Persat. **B)** Scanning electron microscopy (SEM) of *Spiroplasma* extracted from infected flies. *Spiroplasma* can be found as one elongated body (left) or with a Y-shape upon division by longitudinal scission (right). Modified from Ramond *et al.*, 2016.

2. The defense mechanisms of *Drosophila*

The first defense of *Drosophila* against pathogens is simply to avoid encountering them. These avoidance mechanisms, termed behavioral immunity, have been discovered in several insect species and are suspected to play a major role in reduction of infection at the population level. Insects can, for example, move away from areas containing harmful bacteria or, in some cases, temporarily stop eating until they find a new, non-infectious, diet (31, 32).

However, behavior cannot prevent all encounters. In such cases, the first line of *Drosophila* defense is mechanical and comprises the external cuticle and the gut peritrophic matrix. Both are chitinized structures that prevent the penetration of intruders inside the body cavity. However, if pathogens bypass this first line of defense, flies can mount an immune response built around cellular and humoral mechanisms (7)

The cellular response is mediated by circulating blood cells called hemocytes, which can sense the invaders and participate directly in pathogen clearance in the hemolymph through several mechanisms: phagocytosis, encapsulation, melanization and indirectly the production of clotting factors.

The humoral response on the other hand, relies on the secretion of soluble immune effectors, such as antimicrobial peptides (AMPs). Most of these immune effectors are secreted by the fat body, an organ functionally analogous to the liver of mammals, but some are also produced in other tissues such as microbe-exposed epithelia and hemocytes.

The production of cellular and humoral immune effectors at the whole-organism level is called "systemic" immune response and will be extensively discussed in the next chapters.

3. The systemic antimicrobial response

One of the best-characterized parts of *Drosophila* immunity is the systemic antimicrobial response, which consists mainly of the production of immune effectors by the fat body and hemocytes (33, 34). This response takes place in the body cavity upon the direct entry of the microbes or microbial elicitors through cuticle wounding or by enteric infections if pathogens cross the gut epithelium. Pathogens are recognized by specific receptors called Pattern-Recognition Receptors (PRR), which trigger the selective, pathogen-dependent activation of two NF-kB immune pathways: Toll and Imd. The Toll signaling pathway was initially discovered for its role in the control of dorsoventral patterning in the embryo (35) and it shares some similarities with the mammalian interleukin-1 receptor (IL-1R)/Toll-like receptors

(TLRs)-NF-kB pathways that were discovered thereafter. The Imd pathway is similar to the tumor necrosis factor-receptor (TNF-R) pathway in mammals (36). Activation of the Toll or Imd signaling cascades leads to the transcription of immune genes encoding secreted factors that are subsequently produced and secreted in the hemolymph to fight invaders.

3.1 Microbial recognition

In both vertebrates and arthropods, microbial invasion is sensed by the recognition of specific microbial molecules called Microbe-Associated Molecular Patterns (MAMPs) by dedicated Pattern-Recognition Receptors (PRRs). MAMPs include various molecules such as bacterial lipopolysaccharide (LPS), peptidoglycan (PGN), lipoteichoic acid (LTA) or fungal β-1,3-glucans (37), although *Drosophila* PRRs seem to recognize essentially PGN and β-1,3-glucans (38). Genetic ablation of the genes encoding PRRs significantly impairs the capability of the host to survive microbial infection (38–42). In *Drosophila*, microbial recognition is achieved by PRRs belonging to the family of the Peptidoglycan Recognition Proteins (PGRPs), and the Gram-Negative Binding Proteins (GNBPs) (7, 38). PRR-coding genes are expressed in immune-reactive tissues, including the fat body, hemocytes and the gut. The molecular binding of MAMPs to PRRs is highly specific and allows for preferential activation of the Imd or Toll pathway, the two main immune pathways in *Drosophila*.

The main MAMP determining the preferential activation of the Imd or the Toll pathway is bacterial peptidoglycan (hereafter PGN). PGN is a glucopeptidic polymer found in almost all bacteria. PGN from Gram-negative bacteria differs from most Gram-positive PGN by the presence of meso-diaminopimelic acid (DAP-type) at the third position of the peptide chain instead of an L-Lysine (Lys-type) (43). The recognition of specific forms of PGN explains the ability of *Drosophila* to discriminate between different classes of bacteria, essentially Gram-positive and Gram-negative bacteria.

The most thoroughly characterized PRRs that recognize bacterial PGN belong to the GNBP and PGRP families. PGRPs contain a peptidoglycan-recognition domain that is highly conserved between vertebrates and insects. The *Drosophila* PGRP family comprises 13 genes that are expressed either constitutively or induced upon bacterial infections (38) (see details below).

Some PGRPs have an amidase domain in addition to their peptidoglycan recognition domain. Five amidase-PGRPs (PGRP-LB, -SB1, -SB2, -SC1(a/b), and -SC2) have been identified so far; these amidases remove peptides from the glycan chains and thereby convert PGN into

non-immunogenic fragments (44, 45). PGN degradation by these amidase-PGRPs mitigates the immune response intensity and conserves host resources by anticipating the termination of the immune response (46). Other PRRs, like the Nimrod family, are required for an efficient cellular response in *Drosophila*. They are expressed by the macrophage-like cells called hemocytes, and allow these cells to recognize and properly engulf microbes or to initiate reactions like the melanization process (see details in paragraph 4.2).

3.2 Immune signaling pathways in *Drosophila melanogaster*

3.2.1 The Toll pathway

Elicitation of the Toll pathway upon bacterial infections is mediated by the recognition of Lys-type PGN by PGRP-SA and GNBP1 **(Figure 2)**. Both PGRP-SA and GNBP1 are secreted proteins found in the hemolymph that act upstream of the Toll pathway. Data suggest that GNBP1 and PGRP-SA form a complex in the hemolymph. A proposed function of GNBP1 is to hydrolyze Gram-positive PGN into small fragments optimized for binding to PGRP-SA and stimulating the Toll pathway (40, 47, 48)

The Toll pathway in *Drosophila* is also triggered by fungal structural products, the β-1,3-glucans, which are recognized by GNBP3 (49). This pathway can also be activated by the direct recognition of fungal and bacterial protease activities through a circulating bait protein, Persephone (Psh) (50). Microbial proteases cleave Psh, which leads to its processing by a *Drosophila* Cathepsin (51). The processed Psh then activates the Toll pathway in a similar way to that of the PGRP-SA/GNBP1 and GNBP3 pathways.

The recognition of MAMPs by the Toll pathway receptors leads to the activation of a serine protease cascade in the hemolymph that ends with the cleavage of Spätzle, the Toll receptor ligand **(Figure 2)** (52). The binding of Spätzle to the transmembrane Toll receptor activates an intracellular signaling cascade that leads to the degradation of the inhibitor of κB (IκB) homolog Cactus, which forms a cytoplasmic complex with the two NF-κB-like transcription factors Dif and Dorsal (53, 54). The degradation of Cactus leads to the nuclear translocation of Dorsal and Dif and subsequent induction of genes coding for immune effectors, notably the Bomanins and Drosomycin.

3.2.2 The Imd pathway

Activation of the Imd pathway begins with the recognition of DAP-type PGN by PGRP-LC on the cell membrane triggering the recruitment of the intracellular Imd adaptor, which initiates a complex signaling cascade ending with the activation of the NF-κB-like transcription factor Relish **(Figure 2)** (55). Relish needs to be phosphorylated by the IκB kinase (KKß and IKKγ) and cleaved by the caspase Dredd in order to translocate to the nucleus (53), where it regulates the transcription of many immune genes, notably those coding for the AMPs Diptericin, Cecropin Attacin, Drosocin and Defensin.

The main receptors that activate the Imd pathway are PGRP-LC and PGRP-LE, which sense DAP-type PGN (56–59). PGRP-LC is a transmembrane protein that binds to extracellular PGN (56, 60), while PGRP-LE is located in the cytoplasm and instead detects intracellular pathogens (57, 61), although an extracellular cleaved form has also been identified (58). PGRP-LC and to a lesser extent PGRP-LE regulate the activation of the Imd pathway in the fat body upon systemic infection. PGRP-LE also plays a predominant role in regulating the local immune response in the midgut (62, 63). Another secreted PGRP, PGRP-SD, can promote the activation of the Imd pathway upstream of PGRP-LC by binding to peptidoglycan to promote its relocalisation to PGRP-LC (39).

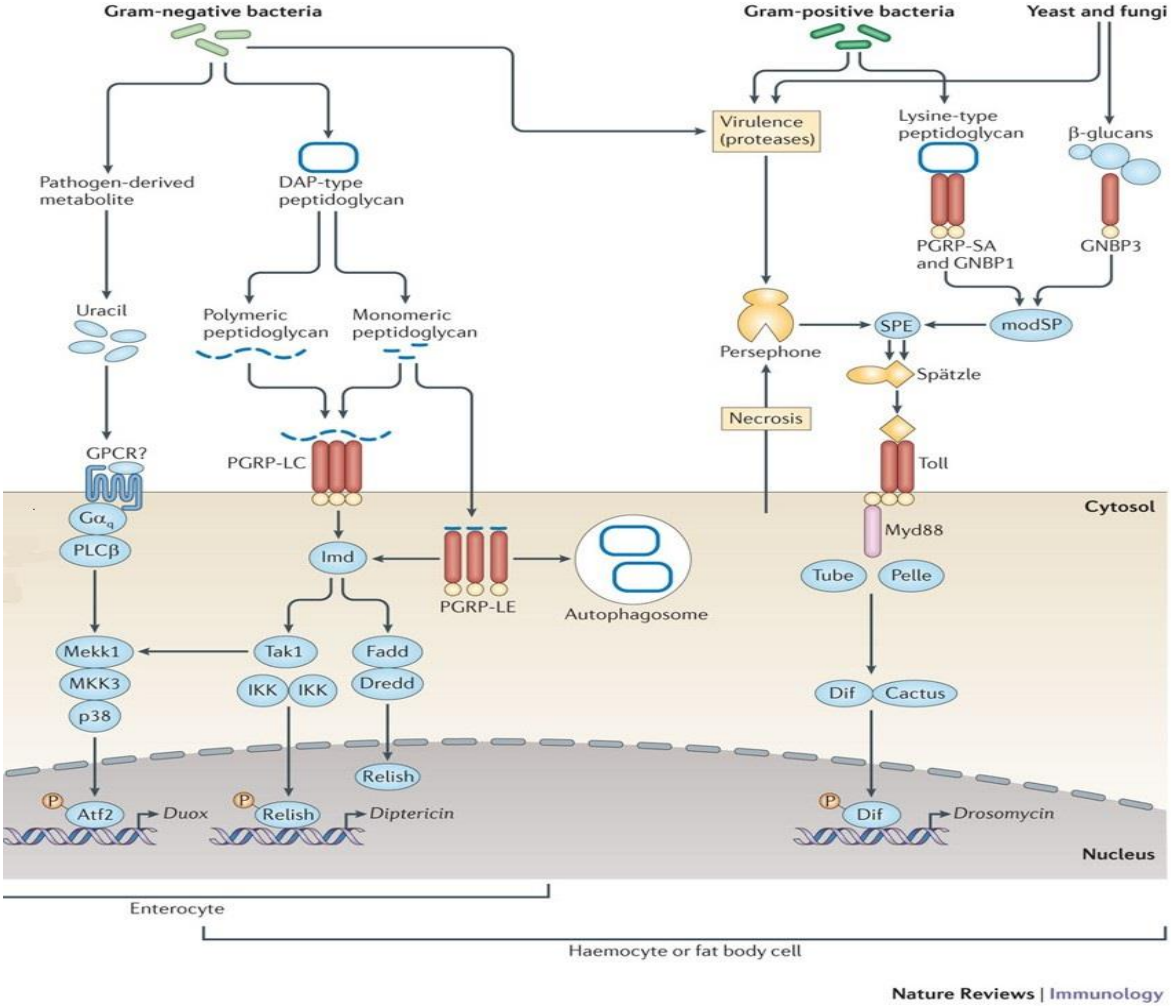

Fig.3 The Toll and Imd pathways. The activation of the Toll and Imd pathways is triggered by the recognition and binding of microbial cell wall components (peptidoglycan) to peptidoglycan recognition proteins (PGRPs). This process activates the transcription and production of antimicrobial peptides that are secreted into the hemolymph and can actively target and kill pathogens. PGRP-LC and PGRP-LE recognize diaminopimelic acid (DAP)-type peptidoglycan from Gram-negative bacteria and certain Gram-positive bacteria, and activate the Imd pathway. PGRP-SA and GNBP1 recognize the lysine-type peptidoglycan of Gram-positive bacteria, and GNBP3 recognizes the β-glucans of yeasts and fungi to activate Toll signalling (From Buchon *et al*., 2014).

3.2.3 Other immune pathways

Two other pathways are involved in the systemic immune response: the JUN N-terminal kinase (JNK) and JAK/STAT pathways. The JNK pathway has been linked to the stress response, wound healing, cell migration, apoptosis, and immune response in both insects and mammals (64–70). It is not activated by microbial products but rather by host factors such as the binding of the TNF-receptor homolog Grindelwald with its ligand Eiger or by Reactive Oxygen Species (ROS). The JNK pathway is also activated down-stream of the Imd pathway at the level of the MAPKKK TAK1 (68, 71, 72). The current model states that Imd signaling bifurcates downstream of TAK1, activating both the JNK kinase Basket and IKK signaling (73). The JNK pathway has been implicated in regulating transcription of AMP coding genes, although its precise role is unclear (73–75).

The JAK/STAT pathway was originally identified through its role in embryonic segmentation in *Drosophila* (76). The four main components of this pathway are the ligands Unpaired (Upd1, Upd2, Upd3), the receptor Domeless (Dome), the Janus kinase JAK (Hopscotch/ Hop), and the transcription factor STAT (STAT92E) (76, 77). Following Upd binding to Dome, the latter dimerizes and activates the JAK kinase. JAK then phosphorylates the cytosolic transcription factor STAT92E to stimulate its nuclear translocation. Once in the nucleus, phospho-STAT92E dimers bind to consensus DNA target sites, where they act as transcriptional activators (77). The JAK-STAT pathway has been shown to regulate genes encoding the complement-like protein Tep2, which is involved in opsonization and phagocytosis (78, 79), and the Turandot stress genes (80). This pathway plays a role in the encapsulation response and hemocyte activation upon immune challenge (81, 82). Moreover, it was demonstrated that mutant flies for the JAK/STAT pathway are more susceptible when infected with *Drosophila* C virus, while they are perfectly resistant to bacterial and fungal infection (83).

4. The humoral immune response

4.1 Humoral immune effectors of the systemic antimicrobial response

The Toll and Imd pathways were initially identified for their role in the regulation of AMP coding genes. After the completion of the *Drosophila* genome, several microarrays have identified many other immune genes that are regulated by these two pathways (84, 85).

De Gregorio *et al*. in 2001, identified about 230 genes upregulated and 170 genes downregulated upon septic injury with a mixture of Gram-positive and Gram-negative bacteria or upon natural infection with the fungus *Beauvaria bassiana* (85). These genes were called *Drosophila* Immune Regulated Genes (DIRGs) and most of them had not previously been associated with the immune response. Some of them can be assigned to specific aspects of the immune response such as signaling, recognition, phagocytosis, coagulation, melanization, ROS detoxification, as well as many small peptides. Furthermore, some DIRGs were induced by infections but their regulation remained unaffected in Toll and Imd double mutants, indicating that other pathways can control the *Drosophila* immune response.

In the next part, I will detail the main types of immune effectors that were identified by these microarrays and discuss their involvement in the immune response.

4.1.1 Antimicrobial peptides

Antimicrobial peptides (AMPs) are small (less than 15 kDa), positively charged, secreted molecules that directly target and kill microbial pathogens (86, 87). The first AMP to be discovered was a Cecropin isolated from the moth *Hyalophora cecropia* (88). Since then, many peptides from various families have been identified in evolutionarily diverse organisms ranging from prokaryotes to multicellular eukaryotes, including invertebrates, vertebrates, and plants (89–91). AMPs mainly act by targeting the negatively charged membranes of microbes (92). Upon encountering microbial cell envelopes, AMPs get embedded in the hydrophobic regions of lipid membranes leading to membrane destabilization and cell death (93). They can be active against Gram-positive and Gram-negative bacteria or fungi (93) **(Figure 3)**. The *Drosophila* genome contains 21 AMP genes that can be grouped into 7 families. Drosocin, Attacins and Diptericins have demonstrated antibacterial activity especially against Gram-negative bacteria (94–97). Drosomycin and Metchnikowin have antifungal properties (98, 99), while Cecropins

and Defensin have both antibacterial (mainly against Gram-positive but also against Gram-negative bacteria) and antifungal activities (100–104) **(Figure 3)**.

Most of the AMP coding genes are inducible and produced by the fat body and, to a lesser extent, by other tissues. They are secreted into the hemolymph during the systemic immune response where they can reach concentrations in the µM range (86). They can also be induced in surface epithelia in a local, tissue-specific immune response. Finally, some of them are produced constitutively in epithelia that are strongly exposed to microbes, like the gut, the trachea or the reproductive tract epithelia (105–108)

If early studies have demonstrated the powerful action of AMPs in killing pathogens *in vitro*, the evidence of their activity *in vivo* came in 2002 when Tzou *et al*., showed that artificially overexpressing single AMP coding genes in flies using the GAL4/UAS system in Imd/Toll double mutants was sufficient to restore the survival of these immune deficient flies when infected with certain pathogens (109).

Other *in vivo* studies on AMP function were, however, based solely on mutants for signaling pathway intermediates, and not directly on AMP mutants because of the inherent difficulty of mutating such small genes. The possibility of creating loss-of-function mutants for single or AMPs groups using the CRISPR/Cas9 technique recently allowed a much more in-depth understanding of their exact contribution to host defense. Hanson *et al*, generated loss-of-function mutants for 10 *Drosophila* AMPs and, through recombinations, produced fly lines lacking groups of AMP coding genes as well as lines lacking all 10 main AMP genes (110). Their study confirmed that AMPs play a major role in the defense against Gram-negative bacteria and to a lesser extent against fungi. Surprisingly however, these flies showed little susceptibility when infected with Gram-positive bacteria. These experiments also indicated specific roles of individual AMPs. For instance, Diptericin plays a major role in the defense against *Providencia rettgeri* infection, while being dispensable to fight against other *Providencia* species. In addition, this paper reveals that combinations of AMPs have a synergistic or additive effect against certain pathogens (110). Besides their role in defense against pathogens, AMPs have been shown to play a role in tumor growth control (111, 112), in neurodegeneration (113, 114) and in aging (86, 115, 116).

4.1.2 The Bomanin family

The Bomanin family (Bom) comprises 12 genes which are transcriptionally regulated by the Toll pathway (117). They were discovered almost 15 years ago (118) as small inducible peptides, but their function as immune effectors has been shown only recently. They share a 16-residue domain and are highly active against fungal species and Gram-positive bacteria (117) **(Figure 3)**.

Clemmons *et al*., 2015, who deleted ten of the twelve Bom-coding genes, gave the first evidence that proved their function during microbial infections *in vivo*. Their results showed that *Boms* deficient flies had an impaired survival upon microbial infection, although their Toll pathway activity was normal. Moreover, they showed that Boms are required for resistance to, rather than tolerance of infection. While Boms contribute to microbial killing in the fly hemolymph, their microbicidal activity *in vitro* has not been fully demonstrated (119).

A.

Dpt

Unknown

Att

Unknown

Dro

Cec

Def

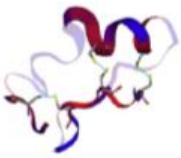

Drs

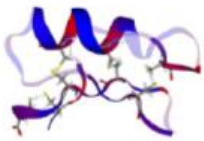

Mtk

Unknown

AMP family	Gene	Location	[in vivo]	Size (AA)	Characteristics	Immune Expression
Diptericin	DptA	2R (55F)	0.5 µM	83	P-rich and G-rich domains, C-terminus amidated, O-glycosylated Thr^{8}, Asp^{52}	Imd
	DptB	2R (55F)		32, 67	Furin cleavage produces two mature peptides: one uncharacterized P-rich peptide and one G-rich with C-terminus presumably amidated	Imd, other
Attacin	AttA	2R (51C)		190	Furin cleavage produces two mature peptides: uncharacterized 9AA short peptide and Attacin G-rich peptide, C-terminus amidated	Imd, Toll, other
	AttB	2R (51C)		190	Furin cleavage produces two mature peptides: uncharacterized 9AA short peptide and Attacin G-rich peptide, C-terminus amidated	Imd, Toll, other
	AttC	2R (50A)		23, 195	Furin cleavage produces two mature peptides: MPAC (P-rich) and Attacin (G-rich) , C-terminus amidated	Imd, other
	AttD	3R (90B)		115	Attacin G-rich domain, lacks a signal peptide	Imd
Drosocin	Dro	2R (51C)	40 µM	19	Furin cleavage, P-rich, O-glycosylated Thr^{11}, and also a 22AA uncharacterized C-terminal peptide	Imd, other
Cecropin	CecA1	3R (99E)	20 µM	39	Alpha-helical, C-terminus amidated	Imd
	CecA2	3R (99E)		39	Alpha-helical, C-terminus amidated	Imd
	CecB	3R (99E)		39	Alpha-helical, C-terminus amidated	Imd
	CecC	3R (99E)		39	Alpha-helical, C-terminus amidated	Imd
	Anp	3R (99E)		34	Alpha-helical	ejaculatory duct (males)
Defensin	Def	2R (46D)	1 µM	40	Furin cleavage produces two peptides: 30AA uncharacterized peptide and Defensin peptide with disulfide bonds mediated by cysteine bridges	Imd
Drosomycin	Drs	3L (63D)	100 µM	44	Disulfide bonds mediated by cysteine bridges	Toll, Imd
	Drs-like1	3L (63D)		44	Disulfide bonds mediated by cysteine bridges	
	Drs-like2	3L (63D)		50	Disulfide bonds mediated by cysteine bridges	JAK-STAT
	Drs-like3	3L (63D)		45	Disulfide bonds mediated by cysteine bridges	JAK-STAT
	Drs-like4	3L (63D)		44	Disulfide bonds mediated by cysteine bridges	
	Drs-like5	3L (63D)		44	Disulfide bonds mediated by cysteine bridges	
	Drs-like6	3L (63D)		46	Disulfide bonds mediated by cysteine bridges	
Metchnikowin	Mtk	2R (52A)	10 µM	26	P-rich	Toll, other
Bomanin *(AMP-like)*	IM1-type (6 genes)	2R (55C)	10-100 µM	16	16-residue Bomanin domain	Toll
	CG5778-type (3 genes)	2R (55C), 3R (94A)		41-97	Bomanin domain with C-terminal tail	Toll
	IM23-type (3 genes)	2R (55C), 3R (94A)		78-134	2 Bomanin domain repeats with intermediate linker	Toll

B.

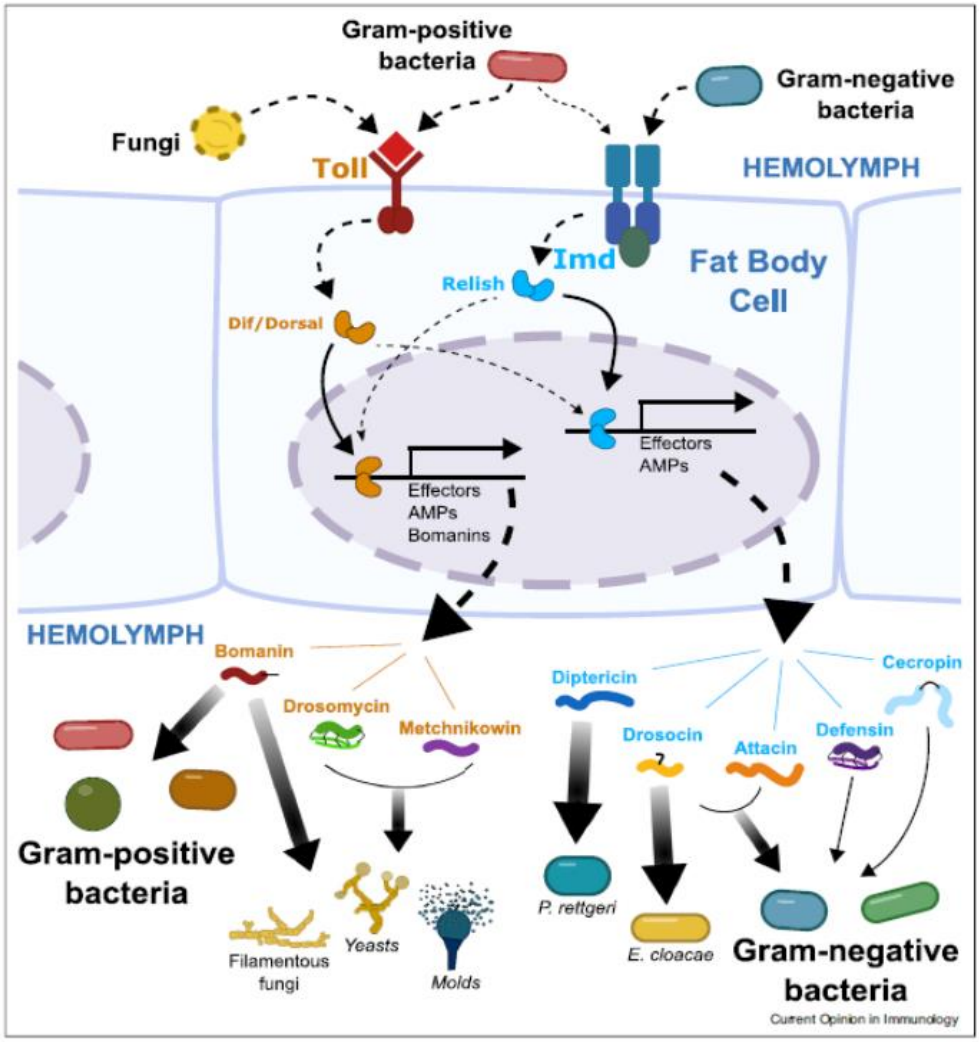

Fig.3 Specificity of *Drosophila* AMPs. **A**) Summary of identified *Drosophila* AMPs and AMP-like peptides (Bomanins). On the left panel, the 3D structure is displayed. The table indicates the chromosomal location, active concentration in the hemolymph upon immune activation, size and gene characteristics of these peptides. **B)** Schematic representation of the systemic antimicrobial response showing the specificity of action of *Drosophila* AMPs. The AMPs and AMP-like peptides are induced upon recognition of specific pathogens. In most cases these effectors show broad-spectrum importance against many pathogens (e.g. Bomanin, the combined action of Drosocin, Attacin and Diptericin). However in some instances, specific AMPs are the primary contributors to a successful defense response (Diptericin against *P. rettgeri*, Drosocin against *E. cloacae*) (Adapted from Hanson *et al*., 2020).

4.1.3 The Turandots family

The Turandots family is a group of eight inducible genes (*tot A, B, C, E, F, M, X* and *Z*) distributed at three different locations in the *Drosophila* genome (80). They code for small

peptides of 11-14 kDa that are produced by the fat body upon infections and are secreted into the hemolymph. All *tot* genes are induced under stresses such as bacterial infections, heat shock, oxidative stress or exposure to UV light, suggesting that all members of this family play a role in *Drosophila* general stress tolerance (80) .

In basal conditions, their expression during development is highly variable. *Tot* genes have slow kinetics of activation compared to that of AMP coding genes. Their expression reaches a peak 16h after infection, while CecropinA and Diptericin A reach their peak after only 3h and 6h respectively, which suggests a role in tolerance or healing after infection rather than a direct antimicrobial effect (80).

The JAK-STAT pathway regulates *totA*, *totM* and *totC* upon septic injury (76, 120). *TotA* activation also requires the Imd pathway and, more precisely, the activation of Relish in the fat body. The induction of *totA* is abolished in stocks carrying Imd pathway mutations (121). However, overexpression of *totA* does not increases resistance to infections compared to wild-type flies.

Recent studies showed that the MAP kinase Mekk1, which is involved in p38 pathway activation and the stress response, is able to upregulate genes that code for small peptides after septic injury, including the Tots. The expression of *totA* and *totM*, which normally are highly induced upon septic injury, was significantly reduced in *Mekk1* mutant flies (120).

Finally, a role of the Tot family during mating has been uncovered. Indeed, mating itself can be source of biological stress such as sexually transmitted infections and injury. Recent studies showed that *Drosophila melanogaster* females induce *totM* and *totC* when they hear the male courtship song (122). These genes are also upregulated in response to the exposure of female reproductive tract to male accessory gland proteins, and TotM provides protection against sexual transmitted infections (123, 124). This latter result is surprising, as Turandots exhibit no antimicrobial activity, so the mechanism of protection remains elusive.

The broad induction of members of the Tot family is compatible with a direct role in the protection against tissue damage. One possibility is that the Tot proteins function as chaperones interacting with denatured proteins in the extracellular environment, preventing their aggregation to facilitate their refolding or recycling. An indirect role for the Tot proteins in the stress response, for instance as signaling molecules, is also possible. Future studies using combined loss-of function mutations may reveal their functions.

4.1.4. Other inducible proteins

Microarray studies revealed the existence of an unexpected number of uncharacterized peptides that do not belong to annotated AMPs, Bomanins or Turandots families, but are strongly induced upon infection (102). The function of these peptides is unknown but some could have antimicrobial activity, or function as opsonins. For instance, two GNBP-like genes, *CG14322* and *CG12780*, are strongly induced upon systemic infection and do not seem to play any regulatory role in Toll and Imd pathway activation (B. Lemaitre, unpublished). These GNBP-like proteins are small secreted proteins containing a glucan-binding site. They are promising antifungal candidates that could act as opsonins favoring fungal detection and subsequent elimination by other immune effectors, or could directly interfere with fungal cell walls.

Secretion of small peptides is just one facet of the systemic antimicrobial response. Microarray analysis has also uncovered many genes encoding large proteins that are likely secreted and induced upon infection. Many of them encode serine proteases and serine protease inhibitors (serpins) that regulate the Toll pathways and melanization (see below). However, proteins involved in iron sequestration (*transferrin*), in ROS detoxification (*catalases*), lipases, carboxypeptidases, opsonins, or proteins that inhibit actin polymerization (*gelsolin*) are also likely to contribute to the immune defense.

4.2 The melanization process

Melanization is a rapid hemolymphatic reaction triggered upon cuticle injury, for example upon penetration of pathogens into the hemolymph when the fly gets pricked. It consists of the *de novo* synthesis and deposition of melanin, which confers a typical black color to the wound site. This reaction plays an essential role in arthropod defense and is involved in encapsulation, wound healing and sequestration of microbes (125). It was also proposed to release toxic intermediates that can kill directly the pathogens, including reactive oxygen species and other metabolic intermediates of the melanin synthesis pathway (126–128). The melanization cascade is triggered by injury or through the recognition of microbial ligands by PRRs, such as PGN and β-(1,3)-glucan (49, 129). Melanization requires the activation of phenoloxidases (PO), enzymes that catalyze the oxidation of mono- and diphenols to orthoquinones, which polymerize nonenzymatically into melanin. Insect POs exist in the hemolymph plasma, in some

specialized hemocytes, and in the cuticle as an inactive pro-phenoloxidase (PPO) form. PPOs are activated by enzymatic cleavage by serine proteases.

Despite extensive genetic studies of the *Drosophila melanogaster* immune response, the melanization reaction remains one of its less well-characterized facets. In the fruit fly, three PPOs have been identified as produced by two types of blood cells: the crystal cells produce PPO1 and PPO2, and the lamellocytes produce PPO3. While PPO3 is always produced in an active form and is likely regulated at the transcriptional level, both PPO1 and PPO2 require proteolytic cleavage to be activated (130). Upon injury, crystal cells rupture and release PPO crystals into the hemolymph, where they are activated by serine proteases. Several studies have analyzed the contribution of melanization to the immune defense, pointing out its importance to resist microbial infection. Mutants carrying either mutations that reduce or abolish PO hemolymphatic activity (131, 132), showed increased susceptibility to large injury (133, 134). Flies lacking activators of PPO like SP7 were highly susceptible to the Gram-negative bacteria *Salmonella typhimurium* and Gram-positive bacteria *Listeria monocytogenes* and *Staphylococcus aureus* (135). In 2019 Duzdic *et al*., used a model of systemic infection with a low dose of *Staphylococcus aureus* to show that the survival of flies upon such challenge relies on the melanization response, but not on Toll signaling or phagocytosis (129).

Studies performed on PPO1 and PPO2 loss-of-function mutants revealed also the importance of PPOs during bacterial infection. Although PPO1,2 double mutants do not show any pigmentation defect, they do not develop any hemolymphatic PO activity upon wounding or following microbial infection, demonstrating that PPO1 and PPO2 are the two main sources of PO activity in the hemolymph of *Drosophila.* Flies lacking these two components are more susceptible to Gram-positive and fungal infections (136).

5. Cellular immune effectors in the systemic response

The humoral response is effectively flanked by the cellular response, where the main actors are specialized circulating cells called hemocytes (137).

Hemocytes are analogous to mammalian white blood cells, which are involved in many different physiological processes during the cellular immune system activation: they participate in the melanization process, in the engulfment and digestion of bacteria, and in encapsulation of large intruders in the hemolymph (138). *Drosophila* relies on three main classes of differentiated hemocytes, each of which has a specific immune function: the plasmatocytes, the crystal cells and the lamellocytes **(Figure 4)**.

The following paragraphs will introduce the main components of the cellular immune branch, giving an overview of the most notable processes in which they are involved.

5.1 The *Drosophila* hemocyte classes

Plasmatocytes represent the 90-95% of the total blood cell population during all developmental stages (139). They share common functional features with mammalian macrophages, being involved in pathogen clearance, engulfment, and removal of dead cells by phagocytosis (138). Moreover, plasmatocytes play a key function during animal development by stimulating the secretion of extracellular matrix (ECM) components (140, 141). The ECM is involved in tissue remodeling, giving plasmatocytes an indirect role in this process (142, 143). Mature larval plasmatocytes also possess antimicrobial activity, producing antimicrobial peptides. They are involved in the first stages of encapsulation by binding to parasitic intruders (144). It has also been proposed that plasmatocytes could clear the hemolymph of intestinal microbiota or pathogens. Indeed, plasmatocyte-deficient flies have more circulating bacteria in the hemolymph and are more susceptible to oral infection with *Serratia marcescens*, a food-borne pathogen known to cross the gut epithelia to infect the hemolymph (145, 146).

The second hemocyte type, called the crystal cells, represents the remaining 5-10% of the blood cell population. Mature crystal cells express PPOs, which are oxidoreductases related to hemocyanins that mediate the melanization process (discussed in the chapter 4.2) (136). These cells are fragile, readily disrupted, and can release their PPO crystals into the hemolymph upon activation. They thus function as storage cells for the large amounts of PPO present in their cytoplasm in crystallized form (147).

Finally, lamellocytes are large flat cells mainly involved in the neutralization and encapsulation of any object too big to be phagocytosed by plasmatocytes. They are rarely present in healthy

larvae and completely absent in embryos and adult flies. Their differentiation from hemocytes can be induced upon stress signals such as tumor growth or parasitization by parasitoid wasps (148).

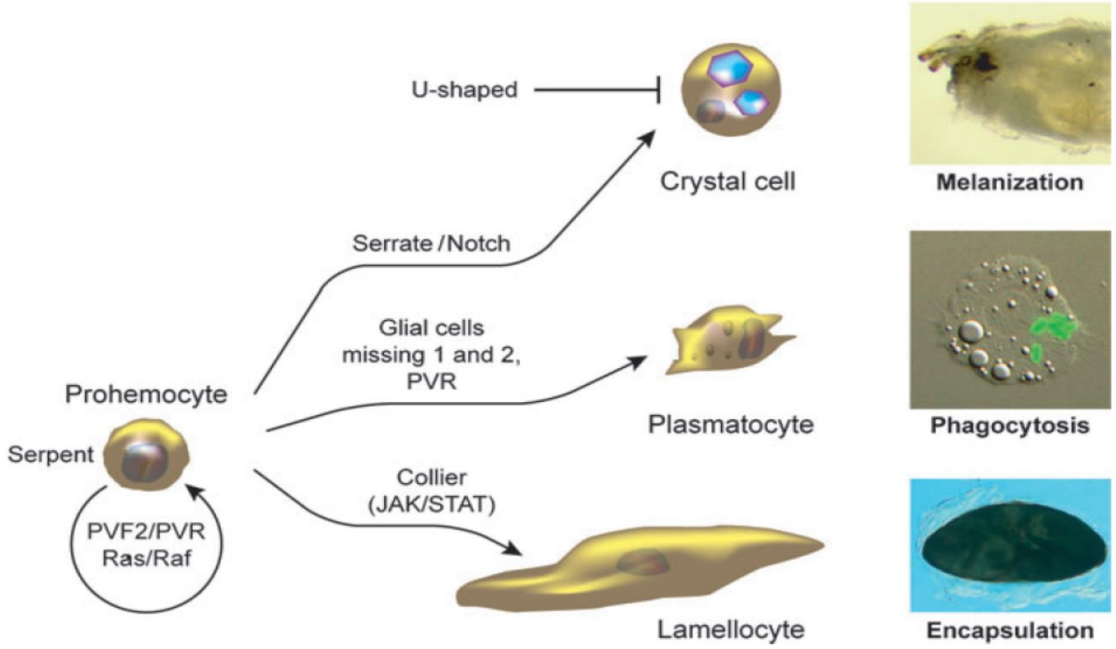

Fig.4 The *Drosophila* hemocytes. *Drosophila* hemocytes originate from multipotent progenitors called prohemocytes, which can differentiate into three mature cell types: plasmatocytes, crystal cells and lamellocytes. Plasmatocytes are phagocytic cells and represent the most abundant hemocyte class at all developmental stages. Lamellocytes are rarely present in healthy larvae and play an essential role in encapsulation of parasitoid wasp eggs. The remaining 5% to 10% of the blood cell population is represented by crystal cells, which are non-phagocytic cells involved in the melanization response and wound healing. Indicated on each arrow are the main pathways and/or factors responsible for hemocyte cell fate determination and proliferation (from Lemaitre and Hoffmann, 2007).

5.1.1 Phagocytosis in *Drosophila*

Phagocytosis is an evolutionary conserved process mediated by phagocytes that consists of the engulfment and subsequent digestion of microorganisms, apoptotic cells and small cell debris. Phagocytosis in *Drosophila* is mainly performed by the plasmatocytes and can be directly initiated via the recognition of MAMPs (for bacteria) or specific membrane phospholipids (for *Drosophila* cells to be cleared) by hemocyte receptors (37, 149). Phagocytosis can also be activated indirectly via opsonins that mark the surface of particles for engulfment so that it can

be detected by phagocytic receptors (78). Upon their recognition, microbes are rapidly internalized. Engulfment relies on a dynamic remodeling of the plasmatocyte plasma membrane, mainly driven by actin cytoskeleton remodeling, resulting in the formation of the so-called phagocytic cup. Actin polymerization pushes the plasmatocyte membrane around the particle, until these protrusions fuse at the leading edges, generating a newly formed phagosome. This initial plasma membrane derived vacuole does not have the ability to digest the internalized material. Instead, newly formed phagosomes undergo a series of subsequent fusion events (called phagosome maturation) with cellular organelles (early endosomes, late endosomes and lysosomes) that promote digestion (138). Rab5 is a key regulator of the initial fusion events. Another GTPase, Rab7, is needed for the late phagosome-lysosome fusion (150–152). Phagosome maturation culminates in the formation of a highly acidic phagolysosome. In its final stages, the phagolysosome acquires important components for particle destruction, such as DNAses and proteases that achieve the complete breakdown of the particle (153).

5.1.1.1 The phagocytic receptors

The phagocytic receptors (scavenger receptors) have a crucial immune role since they mediate the recognition of "non self" particles and therefore their engulfment. Scavenger receptors comprise transmembrane proteins that are expressed by professional phagocytes. One of the first molecules characterized as a hemocyte receptor in *Drosophila* was the class C scavenger receptor (dSR-CI). Early *in vitro* experiments showing that dSR-CI was required for efficient phagocytosis of Gram-negative and Gram-positive bacteria, but not yeast (154, 155). Another important class of scavenger receptor is the B SCr, homologous of the mammalian CD-36, discovered to be important for apoptotic bodies clearance (156).

The exact role of *Drosophila* scavenger receptors is not always well established. For example, the *Drosophila* CD-36 homologue Croquemort was initially shown to be required for recognition and clearance of apoptotic cells (157). However, more recent studies suggest that Croquemort plays a more predominant role in phagosome maturation rather than in particle recognition (158–160).

The Nimrod (Nim) family is a broad family of scavenger receptors that has been recently discovered and characterized. Nimrod receptors contain a sub-type of Epidermal Growth Factor (EGF) repeats, called Nimrod repeats (161). Eater, the most well-characterized Nimrod receptor, is necessary for phagocytosis (162). This receptor is specifically expressed in both larval and adult *Drosophila* plasmatocytes. Several studies using RNAi or an overlapping set of deficiencies removing *eater* have pointed to its crucial role in the phagocytosis of both Gram-

negative and Gram-positive bacteria (162–164), as well as the elimination of bacteria entering the hemolymph by crossing the gut (164). Use of flies carrying a null mutation in *eater* confirmed the importance of Eater in the phagocytosis of Gram-positive, but not Gram-negative bacteria (165). Another well-studied Nimrod receptor is NimC1, a plasmatocyte-specific receptor known to be involved in the phagocytosis of *S. aureus* (166). A *NimC1* null mutant revealed that NimC1 is required for the phagocytosis of latex beads and yeast zymosan particles, but is dispensable for phagocytosis of Gram-negative and Gram-positive bacteria (42). These two examples illustrate how each scavenger receptor has a distinct role in specific microbe recognition and engulfment.

5.1.1.2 Opsonization

Opsonins are molecules that bind to microbes and can promote their engulfment by macrophages. The *Drosophila* genome encodes for 6 thioster-containing proteins (TEPs) which have been proposed to participate in and enhance phagocytosis by the hemocytes (138). Tep genes are specifically expressed in plasmatocytes, in the fat body, and in some barrier epithelia (167). These family members possess a signal peptide which indicate that they are secreted, and three of them (TEP1, TEP2 and TEP4) have been found to be upregulated upon bacterial infection (78). Previous studies in *Drosophila* S2 cells shed light on the function of some Tep members in binding and enhancing phagocytosis of *E. coli* (Tep2), *S. aureus* (Tep3) and *Candida albicans* (Tep6) (168).

Recently, Dostálová *et al* used null mutant flies for four immune-inducible Teps (Tep1, 2, 3 and 4) to show that these proteins act in both the humoral and cellular immune response (79). Indeed, they showed that Teps promote the Toll pathway activation and phagocytosis of Gram-positive bacteria upon infection. Despite these recent results, the specific receptors mediating the uptake of Tep-bound particles remain unknown.

Other potential opsonins comprise secreted members of the Nimrod family and more precisely the Nimrod B subfamily (Nimrod B1-B5). Unlike other Nim family members, which are transmembrane, the NimB proteins are all secreted (166) and NimB1 and NimB2 can bind to bacteria *in vitro* (169). Finally, evidence from the literature points to a potential role of PGRP-SC1A as a secreted opsonin specifically recognizing *S. aureus* bacteria activating the Toll pathway (170).

5.1.2 Other hemocytes immune function

Hemocytes also carry out a variety of functions besides phagocytosis, melanization and opsonin secretion. As an additional *Drosophila* “organ”, they store immune-related molecules that can be released upon infection (144, 171). Plasmatocytes can produce the blood-clotting factor Hemolectin, which is one of the main actors involved in the clotting process. Clotting is a similar mechanism to vertebrate coagulation, which mechanically seals cuticle breaches to avoid a massive loss of hemolymph upon wounding. Clotting therefore belongs to the first line of defense against pathogen invasion and dissemination upon cuticle breaching (172, 173). Septic injury also triggers the expression of antibacterial peptide genes via the Imd pathway in a subset of circulating plasmatocytes (174). Last, hemocytes are believed to play signaling functions between distant immune-responsive tissues. This is illustrated by the release of cytokines such as the JAK-STAT ligand Upd-3 that organize the systemic wound response and stimulate intestinal stem cell proliferation. A recent study suggests that activation of the hemolymph polyols pathway by hemocyte-secreted enzymes relays a danger signal from the gut to the fat body *via* hemocytes (175).

6. The gut as an immune barrier

6.1 The *Drosophila* gut structure

In *Drosophila*, as in other organisms, besides being the site of food digestion and nutrient uptake, the gut acts as one of the first lines of defense against ingested pathogens (176). The gut structure and immune ability make it a hostile environment for microbial proliferation yet it is normally colonized by a transient but well-defined microbiota, showing that immunity is fine-tuned in this organ to discriminate pathogens from beneficial bacteria (177, 178)

The *Drosophila* adult gut structure and physiology is similar to that of vertebrates. It is a tubular and compartmentalized organ with an epithelial monolayer **(Figure 5)**. A semipermeable chitinous membrane called the peritrophic matrix physically separates and protects cells from the lumen, that contains the food and the microbiota, and from bacterial insults (179, 180). Four main cell types compose the epithelium: intestinal stem cells (ISCs), absorptive enterocytes, secretory enteroendocrine cells, and enteroblasts, which are post-mitotic, immature cells that can differentiate as enterocytes (176) **(Figure 5)**. Visceral muscles that pace peristalsis, the processing movement that pushes the food through the gut, surround this epithelium.

The *Drosophila* gut has been extensively studied for its extreme plasticity. It is constantly renewed during the whole fly lifespan and there is a great deal of interest in the steady-state dynamics of its adult progenitor cells, as well as their adaptations to challenges both external (e.g., infection, nutrition) and internal (e.g., aging, reproduction) (176, 181). Intestinal stem cells are key actors of tissue homeostasis. In response to damages, they proliferate in order to maintain the tissue integrity of the organ (176, 182, 183). For example, after ingestion of enteric pathogens, the gut is able to eliminate the damaged or dead cells by shedding cells and shrinking in length. These two mechanisms are considered as part of the immune defense (184, 185). However, this process is reversed within a few hours through ISCs proliferation and differentiation, through which they can replace the lost differentiated cells and restore the tissue structure to ensure resilience after the infection (185).

The gut is composed of three anatomically distinct regions. This regional compartmentalization enables the sequential ingestion of food, digestion and nutrient absorption, and defecation. The anterior part, ectodermally derived, is called the foregut. It produces the peritrophic matrix, is involved in early digestion and microbial control, and is the major site of AMP production. Posterior to the foregut is the midgut, which is endodermally derived. The midgut is commonly regarded as the main digestive/absorptive portion of the gut. The last part is called the hindgut,

again of ectodermal origin, which is responsible for water and ion exchange and defecation (176).

Interestingly, the *Drosophila* immune pathway expression is compartmentalized in the gut as well: the Imd pathway is the main immune pathway in the midgut, while both the Imd and Toll pathways are activated in the foregut and hindgut (186).

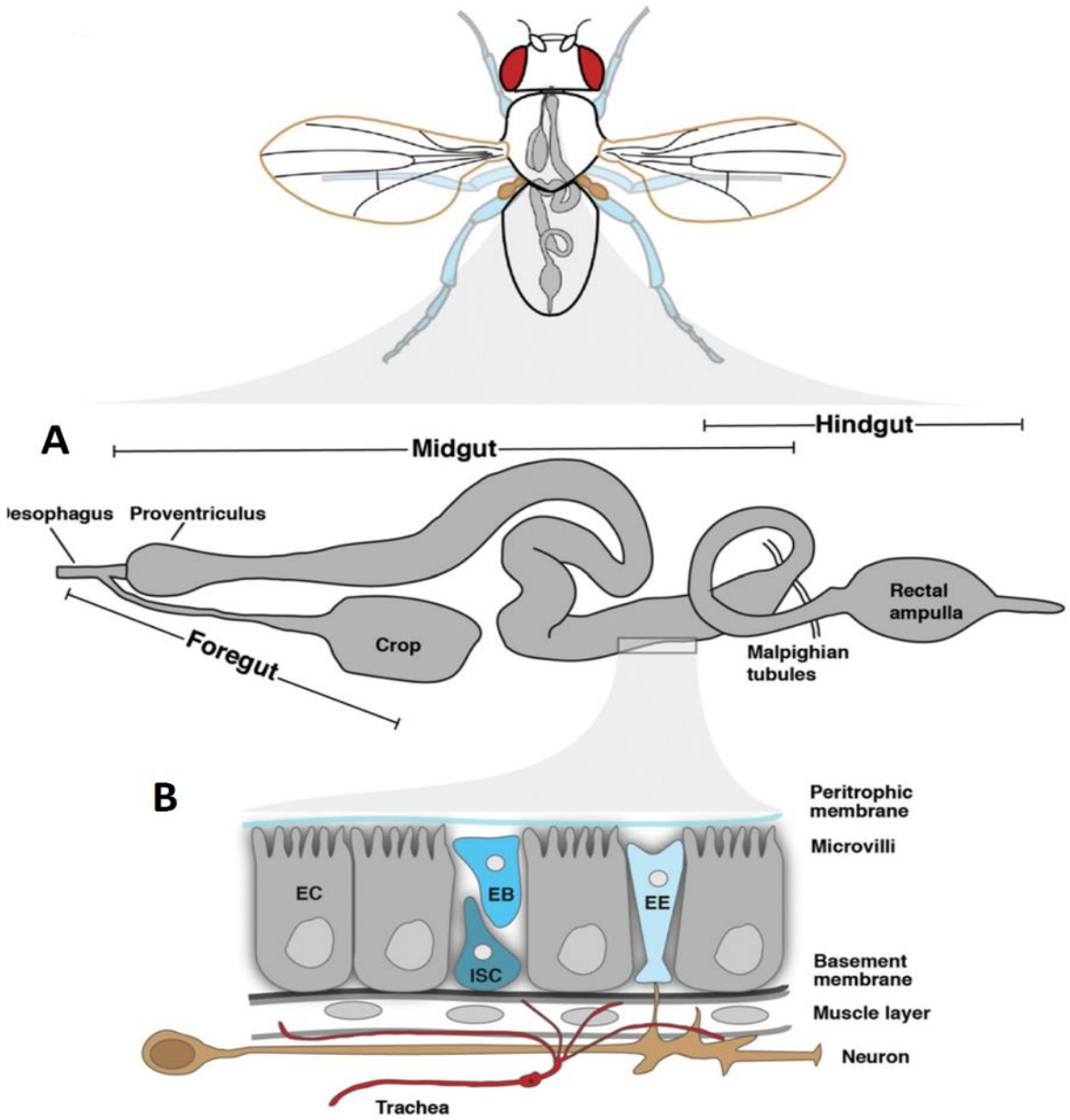

Fig. 5 Schematic illustration of the *Drosophila* digestive tract. **A)** The *Drosophila* digestive tract is composed of three different compartments called respectively the foregut (including the crop, where the food in stored upon ingestion); the midgut, which is the main nutrient absorption domain; the hindgut where the reabsorption of water and minerals takes place. Each portion is further divided in functionally distinct sub-domains. **B)** The midgut epithelium is composed of 4 types of cells: enteroblasts, stem cells, enteroendocrine cells and enterocytes. It is surrounded by a basal membrane and two layers of visceral muscles. The epithelium is protected from direct contact with ingested bacteria by the peritrophic matrix (adapted from Miguel-Aliaga *et al*., 2018)

6.2 The gut immune response

6.2.1 Structural defenses of the gut

The digestive tract is a major route of entry for food-borne pathogens. Some of these microbes produce virulence factors that can disrupt the gut epithelium renewal, leading to systemic infections and to the death of the animal (182, 187). The gut deploys several immune layers to avoid microbial passage into the hemolymph. The first defence is physical: the peritrophic matrix is a chitinous barrier that surrounds the lumen and provides a barrier by preventing the interaction between pathogen and gut cells. It surrounds mainly the midgut, where it is partially permeable and facilitates the absorption of nutrients. The foregut and hindgut are, on the contrary, surrounded by an impermeable cuticle (188). A second poorly defined physical barrier, is provided by a mucus layer, composed of polysaccharides and proteins (mucins), which is located between the peritrophic matrix and the epithelium.

Another important physical factor that allows microbial control in the digestive tract is the presence of an acidic region. This small region is located in the central part of the midgut and contains a specialized cell type, the copper cells, whose membranes are enriched in V-ATPases (189, 190). Secretion of H^+ by copper cells creates a highly acidic zone that kills most bacteria that transit through the gut (190, 191) .

6.2.2 The gut epithelial immunity

6.2.2.1 Secretion of Reactive Oxygen Species

Reactive oxygen species (ROS) are highly reactive oxygen radicals. They are produced by the *Drosophila* gut epithelium in response to bacterial recognition and can contribute to the direct killing of microbes (184, 192, 193) **(Figure 6)**. They also act as second messengers to stimulate the basal epithelium turnover through ISC proliferation (194, 195). The main sources of ROS are Dual Oxidase (Duox) and NADPH oxidase (Nox) (196, 197). Duox generates microbicidal hydrogen peroxide (H_2O_2) and hypochlorous acid (HClO), whereas Nox generates H_2O_2 only. The inhibition of the genes that encode these enzymes leads to an increased susceptibility of *Drosophila* to bacterial oral infection and parasitization (196, 198, 199). Duox is thought to be activated upon the sensing of uracil released by pathogenic bacteria (193, 200, 201), while Nox can be activated by secondary metabolites produced by the resident microbiota, for example lactate released by *Lactobacillus plantarum* (197). However, the production of ROS is a double-

edged sword. High ROS levels due to the over-activation of these enzymes cause damage to the gut epithelium and affects the beneficial microbiota, leading to dysbiosis (195, 202). Dysbiosis induces chronic epithelial stress that stimulates high levels of ISC proliferation, which alters both the differentiation and the renewal of the gut tissue. In physiological conditions, the excess of ROS is detoxified by catalases (196). The mechanism of activation of this anti-oxidative response is currently unknown and does not require either the Toll or the Imd pathways.

6.2.2.2 Secretion of AMPs

AMPs are also produced in the gut against pathogenic bacteria in a regionalized fashion: the Toll pathway is active only in the foregut and hindgut but its immune role in this organ has not been demonstrated yet, whereas the Imd pathway, which is mostly triggered by Gram-negative bacteria, regulates AMPs in the midgut (53). To date, there is no evidence for an AMP-based gut response against Gram-positive bacteria or fungi, although two inducible Drosomycin-like peptides regulated by the JAK-STAT pathway have been identified (203).

The ingestion of Gram-negative bacteria triggers the local immune response by recognition of DAP-type PGN by extracellular PGRP-SD, the transmembrane receptor PGRP-LC, or by the intracellular receptor PGRP-LE in the middle and posterior part of the gut (39, 62, 63). The gut antibacterial response is kept in check by several negative regulators of the Imd pathway **(Figure 6)**. For example, amidase-PGRPs (PGRP-SC1/2, PGRP-LB) hydrolyze PGN to mitigate the activation of the pathway (45, 46, 204, 205). Another negative regulator is the cytoplasmic protein called Poor IMD Response upon Knock-in (Pirk) that interacts with the PGRP-LC cytoplasmic tail and depletes this receptor from the membrane, thus preventing Imd over-activation by the resident microbiota (206–208). Interestingly, the AMPs in the *Drosophila* midgut are also suspected to have different roles beyond traditional immunity. It has been suggested that AMPs produced in the anterior part of the gut could function along with digestive enzymes (many of which are regulated by immune pathways) in the breaking down of microorganisms as they enter the gut for use as food (177).

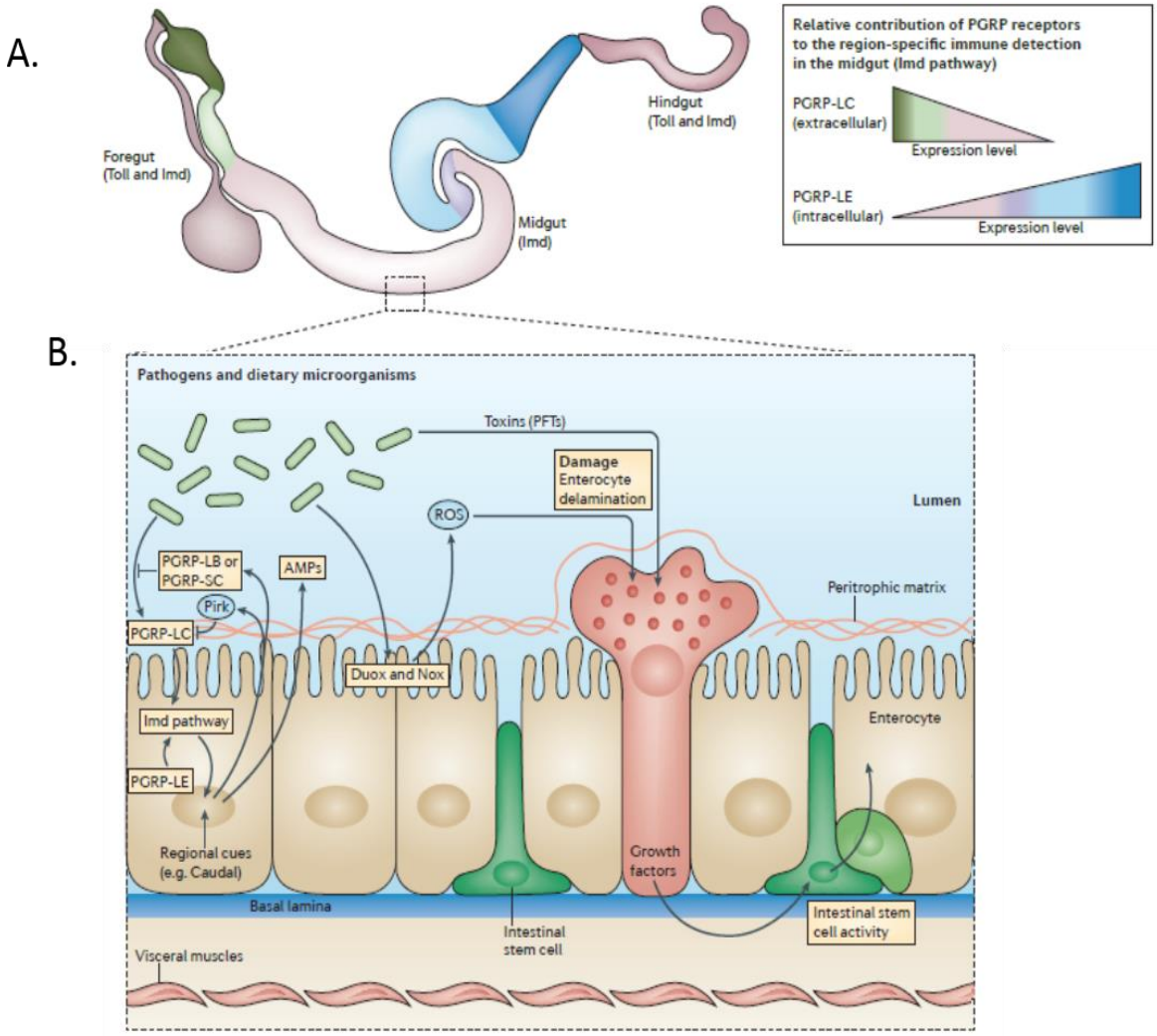

Fig.6 The *Drosophila* intestinal immune response. A) The gut immune response is highly regionalized. The Toll pathway is mainly activated in the foregut and hindgut, while the Imd pathway is mainly induced in the midgut. The bacterial recognition takes place in different gut compartments and relies on PGRPs, like PGRP-LE and PGRP-LC. PGRP-LE is an intracellular receptor and is mainly expressed in the posterior and middle midgut; PGRP-LC on the other hand, is a membrane receptor mainly expressed in the anterior midgut. **B)** Upon bacterial recognition, the gut epithelium expresses several immune effectors in order to efficiently fight the infection. In response to Imd pathway activation, the gut produces antimicrobial peptides (AMPs). It also produces ROS through the activation of Nox and Duox. On the other hand, to prevent the excessive damages that immune system over-activation can cause to the epithelium, the gut expresses negative regulators of the Imd pathway. For example, Poor IMD Response upon Knock-in (Pirk) inhibits Imd, while the amidases PGRP-LB and PGRP-SC can degrade bacterial PGN responsible for PGRP-LC activation (from Buchon *et al*., 2014).

6.3 The *Drosophila* gut microbiota

Drosophila melanogaster carries a simple gut microbiota, which contributes to the regulation of gut morphology, animal growth and nutrition. In the wild, it is composed of up to 30 bacterial species (209), the most commonly found being members of three major families: Lactobacillaceae (e.g. *Lactobacillus*, *Leuconostoc*), Acetobacteraceae (e.g. *Acetobacter*, *Gluconobacter*) and sometimes Enterobacteriaceae (e.g. *Enterococcus*). Yeasts, such as *Hanseniaspora* or *Saccharomyces*, are also frequently found in wild flies. In contrast, when flies are raised in laboratory conditions, the microbiota is highly reduced and comprises mainly the genera *Lactobacillus* (*L. plantarum* and *L. brevis*) and *Acetobacter* (*A. pomorum* and *A. pasteurianus*) (178, 210). Unlike that of mammals, the fly gut microbiota is transient and its maintenance relies on a continuous re-ingestion of bacteria from the food (211). Indeed, when females feed and lay their eggs they also contaminate the food and the chorion of the eggs with their feces. Hence hatching larvae, which feed continuously, ingest the contaminated eggshell and food and get infected by the parental microbiota (178, 211, 212) **(Figure 7)**. The bacterial composition of the microbiota is highly affected by the food on which the flies feed: for instance, a food medium enriched in sucrose should favor the predominance of *Acetobacter* that are efficient at processing it (213). Moreover, the food choice of *Drosophila* is itself affected by the bacterial presence in the food. Larvae and adults are more attracted to food that has been associated with members of the microbiome, like *L. plantarum* or *L. brevis*, most likely through the sensing of molecules released by these bacteria (214).

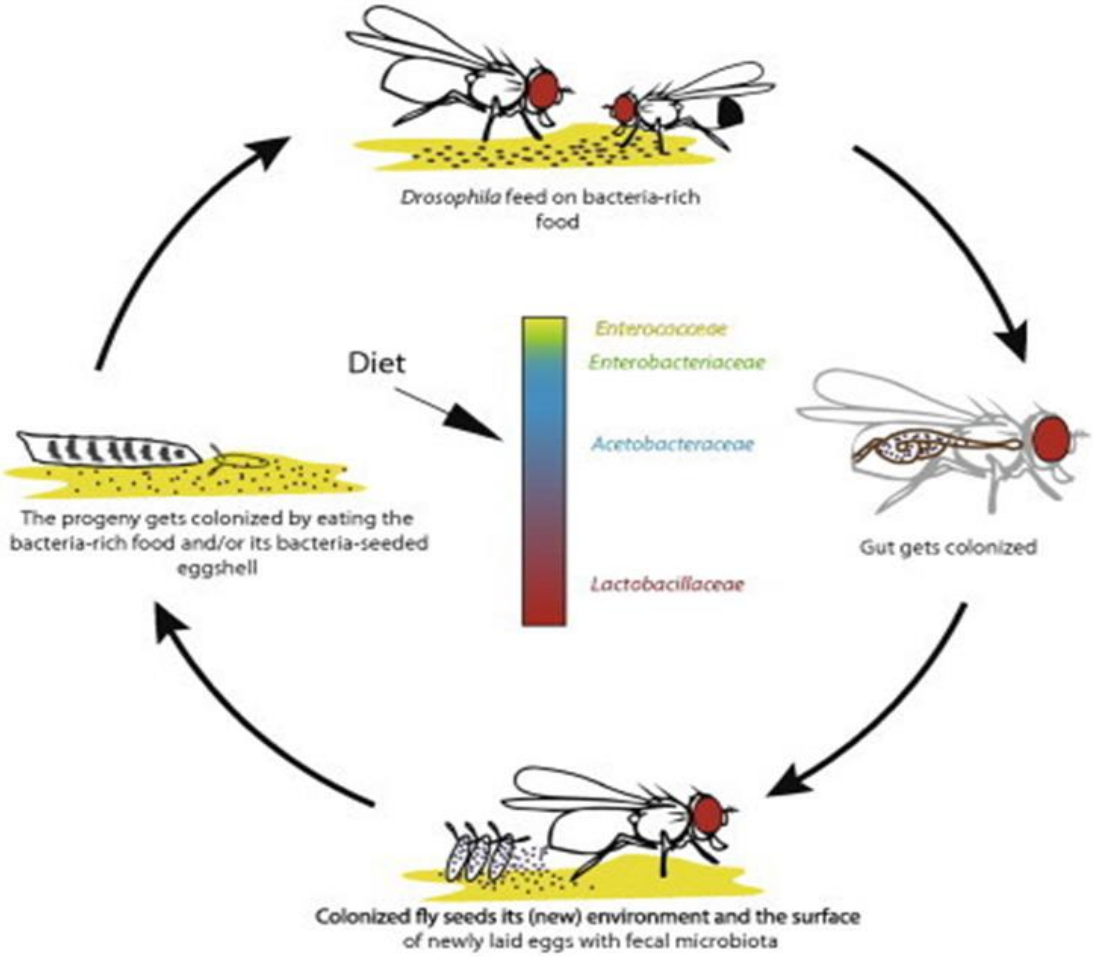

Fig.7 The *Drosophila* gut microbiota establishment. In fruit flies the gut microbiota is maintained by continuous feeding on a diet containing the bacteria. In laboratory conditions, the number of bacterial species is highly reduced and limited to four dominant species (*Enteroccacae, Enterobacteriacae, Acetobacteraceae, Lactobacillacae*), here color-coded according to their relative proportions. *Drosophila's* diet greatly affects this ratio. The gut microbiome inheritance is allowed by the parents fecal deposition on the eggshell of the progeny and in the food where the larvae will feed on. After hatching, larvae eat their contaminated chorion, and hence get contaminated by the parental microbiota (From Erkosar *et al*., 2013).

6.3.1 Role of the gut microbiota in *Drosophila* physiology

In-depth studies on the role of the gut microbiota have been fostered in flies because of the possibility to easily grow flies in axenic (devoid of microbiota) or gnotobiotic (with a controlled microbiota composition) conditions (215). As in vertebrates, the *Drosophila* gut microbiota has a significant impact on the host physiology and functions. It provides a nutritional support to larval growth, stimulates the gut immune system at a basal level, participates in epithelial

morphogenesis, and has systemic impacts on host metabolism and endocrine pathways through the gut–brain axis (216–219). Although axenic flies are viable, they undergo a developmental delay when raised on a poor diet, associated with defects in glucose and lipid storage (217, 220, 221).

The gut microbiota has also a major impact on fly nutrition. It can promote the lifespan of flies raised on a poor diet by complementing the food (217, 221, 222). Bacteria can be used directly as a food source as evidenced by the presence in the gut of lysozymes, digestive enzymes that can digest the bacterial cell wall (213). Moreover, bacterial metabolism increases survival on suboptimal diets, such as high-glucose diets (with low nutritional complexity), by providing the host with supplemental vitamins and essential amino-acids (223).

The gut microbiota can also influence the regulation of host development and growth. It has been shown that bacteria of the *Acetobacter* and *Lactobacillus* genera can improve animal digestion by producing metabolites that stimulate the activation of two important metabolic pathways involved in cellular metabolism: the insulin and TOR pathways (217, 220).

Last, one of the most notable effects of the gut microbiota on the host biology is the basal and continuous stimulation of the ISC proliferation. The presence of indigenous bacteria maintains a basal level of ISC activity by stimulating Nox- and Duox- derived ROS signaling in the gut and activating the JAK/STAT and Epidermal Growth Factor Receptor (EGFR) pathways (184, 197). At the same time, it promotes low-level antibacterial immunity, which, in turn, is thought to regulate microbiota density together with ROS and acidity (186).

6.3.2 The control of *Drosophila* gut microbiota

Contrary to the systemic immune system, which is activated to maintain the complete sterility of the host internal compartment, the epithelial immunity, especially in the gut, must be able to tolerate the presence of commensal bacteria. Adult flies, once they emerge from pupae, have an almost sterile digestive system, which gets colonized by the microbiota after the ingestion of food and feces. The bacterial load in the gut is initially low, but it increases upon fly aging (184, 186, 224). How beneficial microbes are tolerated by the host while their proliferation stays under control, is still an important open question.

The first tolerance mechanism is the compartmentalization of the bacteria in the endoperitrophic space (the lumen space surrounded by the peritrophic matrix), preventing any direct contact between the microbiota and the gut cells and thus diminishing the possibility of triggering strong immune activation (186, 225).

A second strategy to tolerate the microbiota is the compartmentalization of AMP production. Indeed, although the Imd pathway is functional all along the gut, the basal expression of AMP coding genes is mostly restricted to the anterior part of the gut, while their expression is reduced in the posterior side (186). The microbiota reflects the same pattern in terms of localization and proliferation: almost no bacteria have been detected in the anterior part of the gut, while they can colonize the lumen in the posterior part at high density (186). This could be due to the expression of the homeobox gene *caudal* that negatively regulates AMP expression only in the midgut, allowing persistence of the microbiota (226). In *caudal* deficient mutants with high AMP expression in the gut, there is a shift in microbiota composition towards deleterious species (226).

Transcriptome analyses comparing the gut transcriptome of germ-free and conventionally reared flies have shown that the microbiota triggers the expression of several AMP genes in the *Drosophila* gut, notably Attacins AttA and AttD that are mostly regulated by the Imd pathway, and also Drosomycin-like 2 and 3 regulated by JAK-STAT (186). The higher bacterial count in the gut of Imd-deficient flies also supports the notion that intestinal AMPs control the microbiota (186). Interestingly, the major components of the gut microbiota also have a low division rate (210). As bacteria release most of their immunogenic PGN during division, the presence of slow-growing bacteria in the gut ensures a low level of basal immune system elicitation. Negative regulators also reduce immune activity by scavenging peptidoglycan (e.g. the amidases PGRP-LB and PGRP-SC) or disrupting signaling between the PGRP-LC receptor and Imd (e.g. Pirk), as they do during immune defense against pathogens (46, 205, 208). Finally, PGRP-LF, a membrane-bound PGRP, was demonstrated to be a key negative regulator of Imd signaling by sequestering PGN, hence preventing PGRP-LC activation even in the absence of pathogens (227) **(Figure 8)**.

One of the initial, and most rapidly induced, host responses is the production of reactive oxygen and chlorine species (i.e ROS and RCS). While pathogenic bacteria stimulate ROS and RCS production via the dual oxidase system (Duox) (193, 201), the Nox pathway is activated by lactate derived from *Lactobacilli* (197, 198). This dual activation mechanism could be a way to discriminate pathogens from mutualists and to generate a milder ROS response against the microbiota, hence preventing overgrowth without eliminating it (197, 198).

Last, microbiota tolerance is also ensured at the systemic level. PGN release by the microbiota can translocate from the gut to the hemolymph and elicit the Toll pathway systemically. Filtrating cells located under the dorsal cuticle, called nephrocytes, function as PGN scavengers and prevent this chronic Toll activation (228).

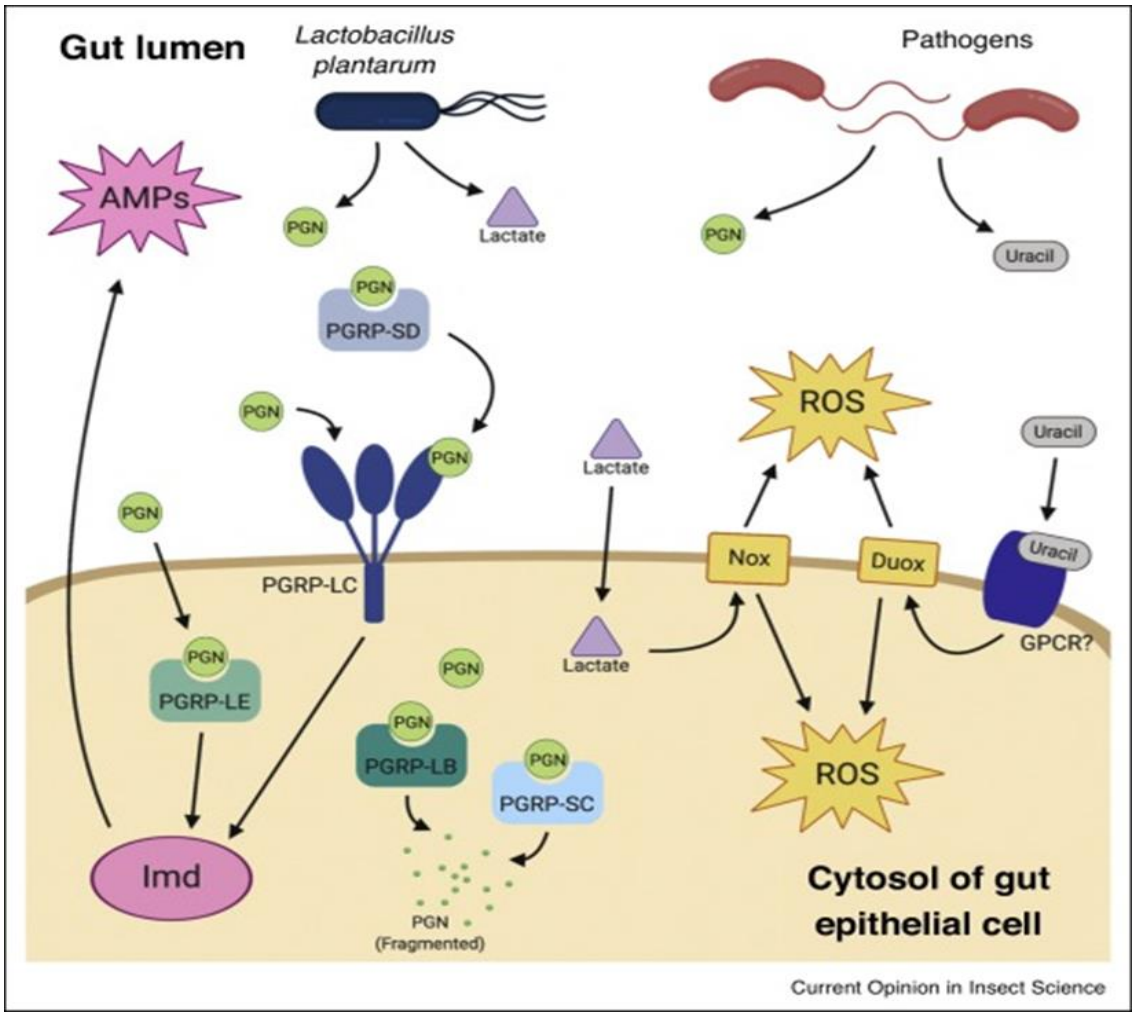

Fig. 8 Gut microbiota control mechanisms. The gut microbiota elicits the activation of the Imd pathway through the release of cell wall components upon division (PGN). These are sensed by the PGRPs and lead to the secretion of AMPs in the gut lumen. PGN activation is shared between mutualistic and pathogenic bacterial species. On the other hand, ROS secretion is differentially controlled: the lactate production by Lactobacillus species leads to the activation of Nox, while Duox is activated by uracil released from pathogens (from Lesperance and Broderick, 2020).

Scope and outline

The study of host-symbiont interactions is a rapidly expanding field as microbes are increasingly considered as major determinants of host physiology, whether they are mutualistic, commensal or pathogenic. Yet, how hosts discriminate between microbes and react adequately to their detection is still a largely unanswered question. This thesis falls within this context and aims to better characterize the mechanisms that allow the host-microbe interaction, in particular the role played by *Drosophila* immune effectors in this context.

The first part of my work **(Chapter II)** focused on the immune mechanisms that keep the gut microbiota under control in homeostatic conditions. The Imd pathway has been identified as the main immune pathway in the gut. However, the fact that it regulates many factors including AMP production, the JNK pathway, digestive enzymes (229) and enterocyte shedding (230) makes it difficult to draw conclusions on the impact of each of its arms in controlling the microbiota and discerning the role of AMPs and lysozymes specifically. To address this point, I have used *AMP* and *lysozymes* null mutant flies and compared their microbiota to that of wild-type flies and of Imd-deficient flies (*relish* null mutants). Using a combination of sequencing analysis and gnotobiotic association experiments, I revealed that both antimicrobial peptides and lysozymes are necessary to maintain the microbiota species balance in the gut, especially during aging.

In the second part of the thesis **(Chapter III)** I worked on non-AMP immune effectors and their function in systemic immunity and symbiosis. I indeed characterized the role of Transferrin 1 (Tsf1), an iron trafficking protein, in the systemic immune defense (See article Iatsenko *et al.* PNAS in the annex of this thesis) and *Drosophila-Spiroplasma poulsonii* interaction. Our studies showed that *tsf1* is an immune inducible gene by both Toll and Imd pathway and that it is necessary to sequester iron from the bacterial usage. Use of a null mutant for *tsf1* reveals that its expression is necessary to fight against certain classes of bacteria and fungi. We demonstrated a mechanism of iron sequestration analogous to that of mammals upon infection, where Tsf1 scavenges iron from the hemolymph and relocates it into the fat body to limit its availability to invading pathogens. In the context of an endosymbiotic relationship, we further demonstrated that *Spiroplasma* growth relies on the host Tsf1 utilization and that the lack of the protein significantly impaired the ability of *Spiroplasma* to colonize the fly.

Finally, I participated in the study of a newly discovered immune effector, called Baramicin, (See article Hanson MA *et al*. submitted in the annex of this thesis). Using *in vivo* and *in vitro* experiments, we showed that these proteins are Toll-regulated and are mainly important to fight against some fungal infections.

Chapter II

Drosophila antimicrobial peptides and lysozymes regulate gut microbiota composition and abundance

A. Marra[1], M.A. Hanson[1], S. Kondo[2], B. Erkosar[1†*], and B. Lemaitre[1†*]

1 Global Health Institute, School of Life Science, École Polytechnique Fédérale de Lausanne (EPFL), Lausanne, Switzerland.

2 Invertebrate Genetics Laboratory, Genetic Strains Research Center, National Institute of Genetics, Mishima, Japan

[†]Joint last authors

*Correspondence: B. Lemaitre (bruno.lemaitre@epfl.ch), B. Erkosar (berra.erkosarcombe@unil.ch)

ORCID IDs:

Hanson: https://orcid.org/0000-0002-6125-3672

Erkosar: https://orcid.org/0000-0003-1152-6772

Lemaitre: https://orcid.org/0000-0001-7970-1667

Author contributions:

AM, BE, BL conceived the study and designed the experiments; AM, BE, MH, collected the data; BE analyzed the data; SK provided critical reagents; AM, BE, MH and BL wrote the manuscript.

Running title: Microbiota and Immune effectors

Keywords: Microbiota, innate immunity, aging, gnotobiotic animals, immune effectors, gut

Abstract

The gut microbiota has a tremendous impact on the physiology and metabolism of animals. Microbiota alteration can lead to diseases such as gut dysplasia, metabolic disorders and neurodegenerative pathologies. Several reports have shown that the immune system plays an important role in shaping both bacterial community composition and abundance in *Drosophila*, and that immune deficit, especially during aging, negatively affects microbiota richness and diversity. However, there has been little study at the effector level to demonstrate how immune pathways regulate the microbiota. A key set of *Drosophila* immune effectors are the antimicrobial peptides (AMPs), which confer defense upon systemic infection. AMPs and lysozymes, a group of digestive enzymes with antimicrobial properties, are expressed in the gut and are good candidates for microbiota regulation. Here, we take advantage of the model organism *Drosophila melanogaster* to investigate the role of AMPs and lysozymes in regulation of gut microbiota structure and diversity.

Using flies lacking AMPs and newly generated lysozyme mutants, we colonized gnotobiotic flies with a defined set of commensal bacteria and analyzed changes in microbiota composition and abundance in vertical transmission and aging contexts through 16S rRNA gene amplicon sequencing. Our study shows that AMPs and, to a lesser extent, lysozymes are necessary to regulate the total and relative abundance of bacteria in the gut microbiota. We also decouple the direct function of AMPs from the IMD signaling pathway that regulates AMPs but also many other processes, more narrowly defining the role of these effectors in the microbial dysbiosis observed in IMD-deficient flies upon aging.

Introduction

The microbiota is the complex array of microbes commonly associated with the digestive tract of animals. This bacterial consortium greatly affects host physiology, for example by promoting immune function or intestinal homeostasis (1–4). Imbalance of the microbiota, called dysbiosis, has been identified as a cause of gut dysplasia and chronic inflammatory diseases, especially during aging (5).

The fruit fly *Drosophila melanogaster* is a powerful model to decipher host-microbe interactions (6–8). Its genetic tractability, the possibility to generate gnotobiotic animals and the simplicity of its natural microbiota have made *Drosophila melanogaster* a convenient model to gain insight into host-microbiota relationships (7, 9, 10). *Drosophila* harbors a simple gut microbiota composed of only a few dominant species, mainly belonging to *Acetobacteraceae* and *Lactobacillaceae*, which influence multiple aspects of fly physiology, such as growth (11, 12), behavior (13), lifespan (14) and infection resistance (15, 16). In turn, the microbiota can be shaped by various host and environmental factors such as food composition, or age of the flies (17–21).

Innate immunity is a key regulator of microbial abundance in *Drosophila* (22–25). Upon acute bacterial infection, *Drosophila* immune responsive tissues (the fat body and hemocytes in systemic infection, and epithelium in local infection) sense microbe-associated molecular patterns (MAMPs) to activate signaling pathways. In *Drosophila*, two immune pathways, the Immune deficiency (IMD) and Toll pathways, regulate the expression of genes encoding immune effectors that fight invading microbes (22, 26, 27). Studies in *Drosophila* have revealed a key role of the IMD pathway in the gut to fight pathogens and keep symbiotic bacteria in check (28–30). It is however unclear how the IMD pathway can effectively combat pathogens but tolerate symbiotic microbiota members in the digestive tract. In fact, the microbiota induces a low level of activation of the IMD pathway (28). Several reports have demonstrated that immune tolerance towards the indigenous microbiota is sustained by several negative feedback loops that prevent hyperactivation of the IMD pathway by peptidoglycan (the bacterial elicitor recognized by IMD pathway) released from commensal bacteria. Enzymatic members of the PGRP family such as PGRP-LB and PGRP-SC1/2 prevent activation of the IMD pathway by actively degrading peptidoglycan (31–33). Other negative regulators such as Pirk, also lower IMD pathway activity upon stimulation. Compartmentalization of the immune response to restricted areas can also favor microbiota growth and control (34, 35). However, IMD pathway

activation is necessary to regulate both microbiota composition and proliferation, and dysregulation of this pathway leads to abnormal bacterial growth and premature death of the host (28, 32, 33, 36). Notably, mutations affecting the IMD transcription factor Relish lead to a higher gut microbiota load and a shifted bacterial composition compared to wild-type flies (28, 37). Moreover, aged *Relish* mutant flies display dysbiosis associated with a loss of gut epithelium integrity and premature death of the animals (21, 38). Collectively, these studies point to an important role of the IMD pathway in control of the microbiota, notably during aging. However, the IMD pathway regulates hundreds of immune effectors, and affects numerous physiological processes such as enterocyte delamination and digestion (39–43). As previous studies have used mutations that suppress the whole pathway (e.g *Relish*), the precise role of individual immune effectors downstream of the IMD pathway in shaping the gut microbial community has remained elusive.

Antimicrobial peptides (AMPs) are small, positively charged molecules that contribute to innate defenses by targeting the negatively charged membranes of microbes (27). These peptides are produced in large quantities by the fat body during systemic infection, but also in local epithelia such as the gut. Seven classic families of inducible AMPs with several isoforms have been identified in *D. melanogaster* (27, 44). Use of CRISPR/CAS9 has recently enabled the generation of individual and combined AMP mutants, allowing direct investigation of their role in host defense (45). Hanson et al. showed that *Drosophila* AMPs are essential for resisting infection by Gram-negative bacteria that trigger the IMD pathway, but appear to be less involved in defense against Gram-positive bacterial infection (45).

Another key group of effector proteins that are potential regulators of Gram-positive bacteria in the gut are the lysozymes (46, 47). Lysozymes specifically cleave peptidoglycan exposed on the cell wall of Gram-positive bacteria (48). The *Drosophila* genome encodes at least 17 putative lysozymes, whose functions have never been formally addressed. Among them, six lysozyme genes (*LysB, D, E, P, S,* and *X*) are clustered in the genome at cytogenetic map position 61F. This group of lysozyme genes, notably *LysB, LysD, LysE,* and *LysP*, is strongly expressed in the digestive tract (46), and may contribute to digestive activities of the gut by degrading peptidoglycan from dietary bacteria. Furthermore, lysozyme genes are expressed in the gut upon microbiota colonization in *Drosophila*, and these proteins have been proposed to modulate immune signaling (28, 31, 49). Lysozymes may contribute to gut immunity either as direct antimicrobials, or by cleaving peptidoglycan and modulating activation of the IMD

pathway (31). As such, AMPs and lysozymes may shape microbiota composition by direct interactions with microbes.

In this study, we decipher the role of two classes of antimicrobial effectors of the *Drosophila* digestive tract, the antimicrobial peptides (AMPs) and the lysozymes, on the gut microbiota. We characterized the microbiota composition in mutant flies lacking either the 14 AMP genes from seven gene families or the four gut-specific lysozyme-encoding genes in a gnotobiotic setup using 16S rRNA gene amplicon sequencing. We also assessed the role of these effectors in controlling the abundance of individual microbiota members by performing mono-association experiments. Finally, we confirmed that certain immune effectors can directly control the proliferation of microbiota members by performing systemic infections. Our findings demonstrate a direct role for both AMPs and lysozymes in controlling both the composition and abundance of the microbiota in *Drosophila melanogaster*.

Results

Impact of AMPs and lysozymes on microbiota composition

To decipher the role of AMPs and lysozymes in the regulation of gut microbiota composition, we performed 16S rRNA gene amplicon sequencing on gnotobiotic flies. DrosDel isogenic flies with the following genotypes were used for all experiments: the wild-type strain w^{1118} (referred to as *w*), a compound mutant strain lacking *Defensin*, *Cecropins (*4 *genes)*, *Drosocin*, *Diptericins* (2 *genes*), *Attacins* (4 *genes*), *Metchnikowin* and *Drosomycin*, referred to as $\Delta AMPs^{14}$ (Carboni et al., in preparation), and a newly-generated lysozyme-deficient mutant (referred to $LysB\text{-}P^{\Delta}$). The $LysB\text{-}P^{\Delta}$ mutation is an 11.5kb deletion, removing *LysC* (a putative pseudogene) and the four lysozyme genes (i.e. *Lys B, LysD, LysE, Lys P*) that are known to be strongly expressed in the digestive tract (46) **(Fig S1)**. As expected, gut extracts from $LysB\text{-}P^{\Delta}$ flies have reduced lysozyme activity *ex vivo* as monitored by their ability to digest peptidoglycan from *E. faecalis* (Fig. S1). We additionally included *Relish* (Rel^{E20}) flies lacking IMD signaling as a comparative control to determine to what extent AMPs contribute to the phenotype of IMD-deficient flies.

To avoid pre-existing microbial community biases in different fly stocks, we performed this analysis in a gnotobiotic system with two different experimental designs. First, we analyzed the microbiota of 12-day old flies with gut bacteria acquired through vertical transmission from gnotobiotic parental flies (i.e. germ-free parents inoculated with a known community upon adult emergence) **(Fig 1A)**. Second, we analyzed aging-dependent changes in the adult microbiota. Here, we inoculated emerging germ-free adults with a known microbiota and analyzed changes in the community structure 10 and 29 days after colonization **(Fig 2A)**. In this way, we uncoupled the effects of juvenile development and metamorphosis from the adult microbiota composition and abundance.

We inoculated the flies with a cocktail of six bacterial isolates that were previously described as common *Drosophila* microbiota members (19), or that were associated with the food that was used in this study (see Methods) (8, 10, 19). These included previously characterized bacterial species as members of the *Drosophila* gut microbiota : *Acetobacter pomorum* (50), *Lactobacillus plantarum* (11), and *Enterococcus faecalis* (51). Our cocktail also included some incompletely characterized bacterial strains: an *Acetobacter sp.* (52), an isolate of *Lactobacillus brevis* and an isolate of *Leuconostoc pseudomesenteroides* (described in Materials and

Methods, Supplementary text 1). *Acetobacter*, a genus of Gram-negative bacteria, and *Lactobacillus plantarum*, a Gram-positive species, both have DAP-type peptidoglycan known to activate the IMD pathway (51, 53–55). In contrast, *Leuconostoc pseudomesenteroides*, *Lactobacillus brevis* (53, 56) and *Enterococcus faecalis* are Gram-positive bacteria with Lysine-type peptidoglycan (57), which typically activates the Toll pathway during systemic infections. Although there is no evidence for a role of the Toll pathway in the midgut (22, 43, 54), Lys-type Gram-positive bacteria can induce a basal immune reaction in the gut through the release of the metabolite uracil, which activates ROS production through the Duox enzyme (58).

16S rRNA gene amplicon sequencing of the six-component cocktail yielded 7 Amplicon Sequence Variants (ASVs (59) are also referred to as zero-noise OTUs (60) or sub-OTUS (61)) across the 72 samples, with a minimum of 42'596 reads per sample after quality and abundance filtering (see methods and Supplementary Table S1 for details). These ASVs mapped to the known species in the inoculum cocktail. Sequencing showed that the *Acetobacter* sp. (52) fraction mapped to two ASVs that were distinguishable by a single nucleotide difference in their 16S amplicon. These ASVs were associated with two closely related species, *A. aceti* and *A. nitrogenifigens* (62, 63), based on their highly similar sequence.

We first focused our analysis on flies with microbiota acquired through vertical transmission from parents raised in a gnotobiotic environment (**Fig 1A**, see Methods). We found that Rel^{E20} and $\Delta AMPs^{14}$ flies harbored communities dominated by *A. nitrogenifigens*, whereas the wild-type strain had a greater prevalence of *La. plantarum* **(Fig 1B)**. In contrast, $LysB\text{-}P^{\Delta}$ flies had highly variable community compositions (see below), suggesting a different mode of action for these genes compared to the AMPs **(Fig 1B)**.

Similarities between bacterial communities were assessed using β-diversity analyses. Dissimilarities between all samples were calculated using Bray-Curtis distances plotted in a multi-dimensional space using Principal Component Analysis (PCoA). This was complemented with an analysis of the dispersal (variability and spread) of the communities, and a permutation based, multivariate analysis of variance was applied to test statistical significance. These analyses showed that community compositions within $LysB\text{-}P^{\Delta}$ and $\Delta AMPs^{14}$ sample groups were more variable than the wild-type (**Fig S2A** , $0.05<p<0.1$), in that . communities of some samples resembled wild-type flies, while others resembled Rel^{E20} flies **(Fig 1C)**. One $LysB\text{-}P^{\Delta}$ sample had a completely different profile to all other samples, with higher abundance of *La. brevis* **(Fig 1B)**. This suggests that the loss of AMPs or lysozymes increases stochasticity in

microbiota composition. Surprisingly however, communities in *Rel*^{E20} mutants were more consistent between replicates, which indicates either that the stochasticity is not due to perturbation of the immune response or that the communities in these mutants stabilize earlier than in other genotypes due to other factors regulated by the IMD pathway.

In terms of community composition, distribution of data in the PCoA shows that *ΔAMPs*^{14} samples mimic *Rel*^{E20} (Pairwise ADONIS: p-adjusted$_{\Delta AMPs\ vs\ Rel}$=0.5), and both differ noticeably from the wild-type, as demonstrated by general colocalization of *ΔAMPs*^{14} and *Rel*^{E20} samples, and separation from the wild-type samples (**Fig 1C**, Pairwise ADONIS: p-adjusted$_{w\ vs\ Rel}$=0.02, p-adjusted$_{w\ vs\ \Delta AMPs}$=0.06). This suggests that loss of AMPs recapitulates the effect of a general loss of the IMD pathway on the microbiota structure. As expected from the variable community composition found in *LysB-P*$^{\Delta}$ mutants **(Fig 1B)**, the PCoA did not reveal a distinct cluster for these samples **(Fig 1C).**

Finally, we measured total bacterial loads in our samples using universal *16S rRNA* gene primers (64) and *Drosophila Actin 5C* primers (52). We did not detect a statistically significant difference in total 16S rRNA gene copy numbers between the different genotypes, indicating that wild-type and mutant flies do not harbor different quantities of microbes in these conditions **(Fig 1D)**.

Overall, our results show that the microbiota composition in *ΔAMPs*^{14} flies is similar to the microbiota of *Rel*^{E20} mutants that completely lack IMD signaling, suggesting that the changes in community composition observed in IMD pathway mutants is at least partly due to the specific loss of AMP production.

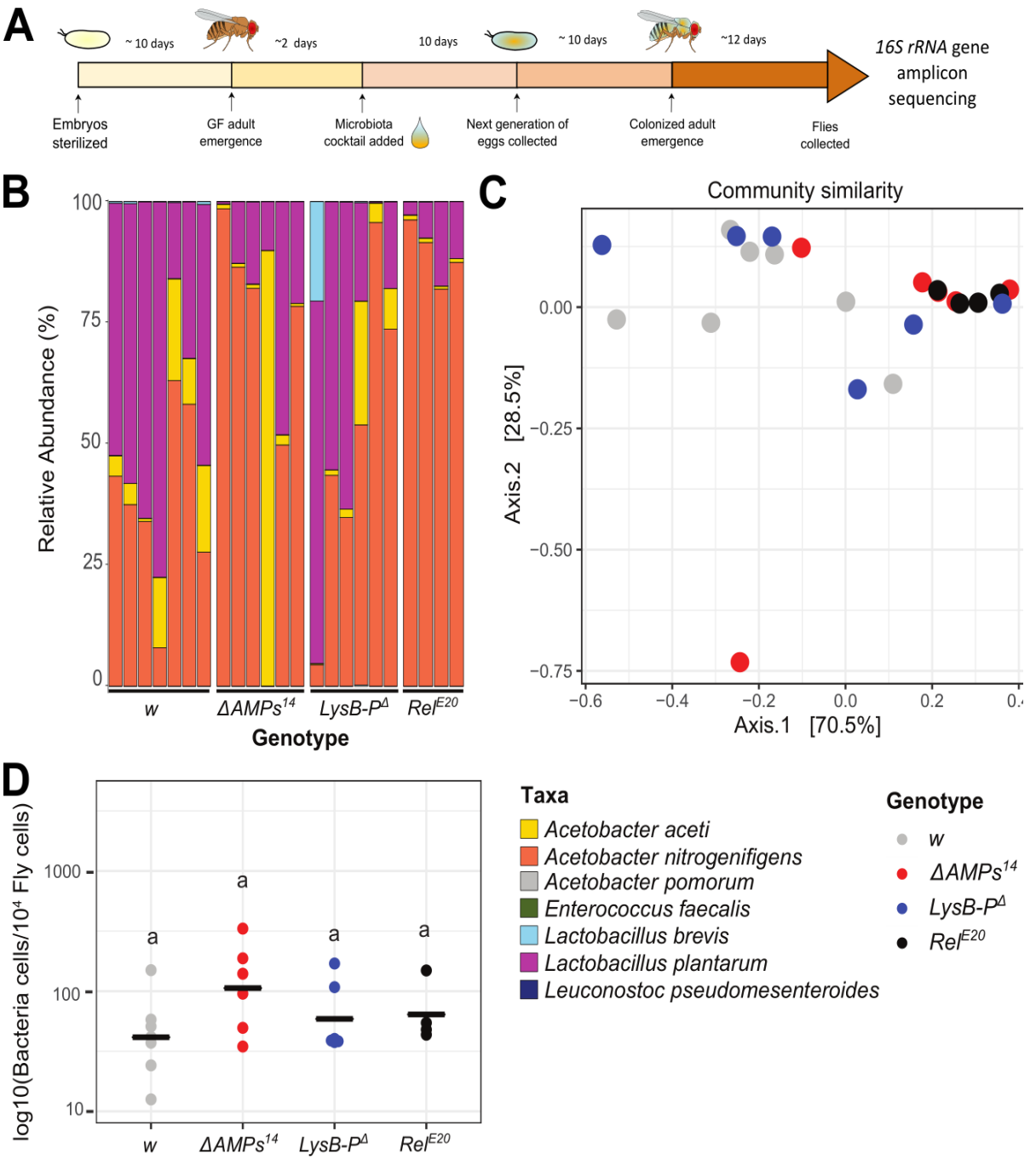

Fig1. The role of AMPs and lysozymes on microbiota composition and abundance in a gnotobiotic vertical transmission setup. A) Scheme of the experimental procedure for fly colonization and collection for 16S rRNA gene amplicon sequencing. Parental embryos were collected, sterilized in 3% bleach and kept on antibiotic food until the adult stage. Emerging germ-free flies were then associated with a bacterial cocktail (microbiota cocktail) containing six representative microbiota members. Their eggs were collected over 3 days, allowed to develop to adulthood, and finally the microbiota of their adult female progeny was analyzed ~12 days after emergence.

Continue in the next page

B) Relative community composition of the gut microbiota in wild-type iso w^{1118} (*w*) wild-type flies, *Relish* (Rel^{E20}), antimicrobial peptide ($\Delta AMPs^{14}$), and gut lysozyme ($LysB\text{-}P^{\Delta}$) mutants as determined by 16S rRNA gene amplicon sequencing. Each bar represents a biological replicate of multiple pooled flies (see **Table S1** numbers of flies included in each sample). C) Principal coordinate analysis (PCoA) of gut communities in *w* wild-type flies, Rel^{E20}, $\Delta AMPs^{14}$ and $LysB\text{-}P^{\Delta}$ as determined by 16S rRNA gene amplicon sequencing. Overall colocalization of $\Delta AMPs^{14}$ (red dots) and Rel^{E20} (black dots) samples and separation of these from wild-type (grey dots) samples shows that $\Delta AMPs^{14}$ and Rel^{E20} samples are similar to each other and differ from wild-type samples. Stochastic distribution of $LysB\text{-}P^{\Delta}$ samples shows high variability in community structures between samples. D) Absolute quantification by qPCR of the total number of bacterial cells normalized to the host gene *Actin5C.* Horizontal black bars show mean values. Details of the statistical outcomes are provided in Supplementary Table S2.

Control of microbiota structure by AMPs and lysozymes during aging

Next, we focused on the microbiota structure of adult flies that were raised in germ-free conditions throughout larval development and colonized only after emergence. We analyzed microbiota of these flies at both 10 and 29 days after colonization **(Fig 2A)**. Here, microbial communities were generally dominated by the two *Acetobacter* variants. 10 days after colonization, *A. aceti* was the most abundant species, whereas by 29 days after colonization, *A. nitrogenifigens* was the dominant species., suggesting distinct competitive ability of the two bacteria tied to the 16S sequence variants detected in our *Acetobacter sp.* isolate.

As Rel^{E20} mutants died earlier than other genotypes during the aging process, only three samples with fewer flies than other genotypes were included for the 29-day time point **(Fig 2B, Table S1)**. Rel^{E20} mutants harbored elevated abundance of *E. faecalis* in 1/3 of the samples, which was not observed in other genotypes. Some samples in this genotype also had higher proportions of *La. plantarum* and *Le. pseudomesenteroides* (in two and three samples respectively) at day 10, a trend that was not observed at day 29 **(Fig 2B)**. However, we cannot conclude whether this change in community structure is real or a consequence of high mortality in this genotype leading to analysis of the survivors only. In contrast to the vertical transmission setup **(Fig S2A)**, Rel^{E20} communities had high dispersal: highest variation was observed at 10 days (Fig S2B), and decreased at 29 days **(Fig S2C)**. This indicates that, at least for this genotype, the microbiota stabilizes over time. This indicates that immunity mutations cause stochasticity in microbiota composition, however the communities are still capable of reaching a stability over a long period of time.

β-diversity and PCoA clearly shows significant (ADONIS p=0.001) separation of the 10-day old and 29-day old flies on the first axis, clearly pointing to aging as the major factor defining the community composition in adults **(Fig 2C)**. Interestingly, in 29-day old flies, *ΔAMPs*^{14} and *Rel*^{E20} were separated from wild-type and *LysB-P*$^{\Delta}$ mutants on the same axis **(Fig 2C)**, indicating that aging and loss of immune effectors act on microbiota composition in similar directions. In 10-day old flies, we did not see similar clustering of samples except for *Rel*^{E20} mutants, which were more widely dispersed on the plot **(Fig 2C)**. This indicates that mutations in IMD pathway act on microbiota composition differently in young versus old flies. A statistically significant Genotype x Age interaction (ADONIS p=0.03) supports this interpretation.

Careful examination of the relative abundance of bacteria in wild-type and mutant flies reveals interesting trends **(Fig 2B)**. We found that wild-type flies maintained *Acetobacter aceti* as the dominant *Acetobacter* ASV even after 29 days, while the proportion of lactobacilli in the community remained small. However, although *Acetobacter aceti* was similarly abundant at 10 days *ΔAMPs*^{14} and *LysB-P*$^{\Delta}$ flies, *Acetobacter nitrogenifigens* became predominant in 29-day samples, and the proportion of lactobacilli in some samples was higher compared to wild-type, particularly in *LysB-P*$^{\Delta}$ flies. This change in relative abundances was even more dramatic in *Rel*^{E20} mutants, which were distinguished by disproportionate loads of *Acetobacter nitrogenifigens* and lactobacilli.

Investigation of each time point separately showed that loss of AMPs (*ΔAMPs*^{14}) did not affect the community composition in 10-day old flies (**Fig 2B**, Pairwise ADONIS, $q_{w\ vs\ \Delta AMPs}$=0.1). However, loss of lysozymes had detectable effects (Pairwise ADONIS, $q_{w\ vs\ Lys}$=0.02) on the abundance of *A. pomorum*, *A. nitrogenifigens*, or *La. brevis* depending on the samples, which further supports the idea of increased stochasticity in *LysB-P*$^{\Delta}$ mutants compared to wild-types. This stochasticity is clearly shown by the community dispersal **(Fig S2B)**.

At 29 days, microbial communities in the wild-type differed from those of *ΔAMPs*^{14}, *LysB-P*$^{\Delta}$ and *Rel*^{E20} genotypes (Pairwise ADONIS p-adjusted$_{w\ vs\ \Delta AMPs}$ =0.04, p-adjusted$_{w\ vs\ Lys}$ =0.04, p-adjusted$_{w\ vs\ Rel}$ =0.04, **Fig 2B**, **2C**). In *ΔAMPs*^{14} the relative abundance of Gram-negative *A. nitrogenifigens* consistently increased, whereas in *LysB-P*$^{\Delta}$ mutants the relative abundance of Gram-positive lactobacilli increased **(Fig 2B)**. This suggests that lysozymes act preferentially on Gram-positive bacteria, and the action of AMPs is limited to *Acetobacteraceae*. As all genotypes contain communities that are similarly variable **(Fig S2C)**, the observed differences

in community composition at day 29 are unlikely to be an artefact of heterogeneity in variance among different groups.

Analysis of the total microbiota abundance showed that bacterial load differed between genotypes mainly in aged flies. At 10 days old, Rel^{E20} flies harbored significantly higher amounts of total bacteria compared to the other genotypes , primarily due to one sample that had a high load typical in 29-day old samples of this genotype **(Fig 2D)**. In 29-day old flies both $\Delta AMPs^{14}$ and particularly Rel^{E20} flies had higher bacterial loads **(Fig 2D)**. These data support the notion that the IMD pathway is crucial in regulating microbiota load as the flies age and that AMPs significantly contribute to this effect of the IMD pathway.

In agreement with previous reports, our data show that microbial community composition shifts and bacterial load increases with age (17, 18, 28), and that this effect is exacerbated by loss of antimicrobials.

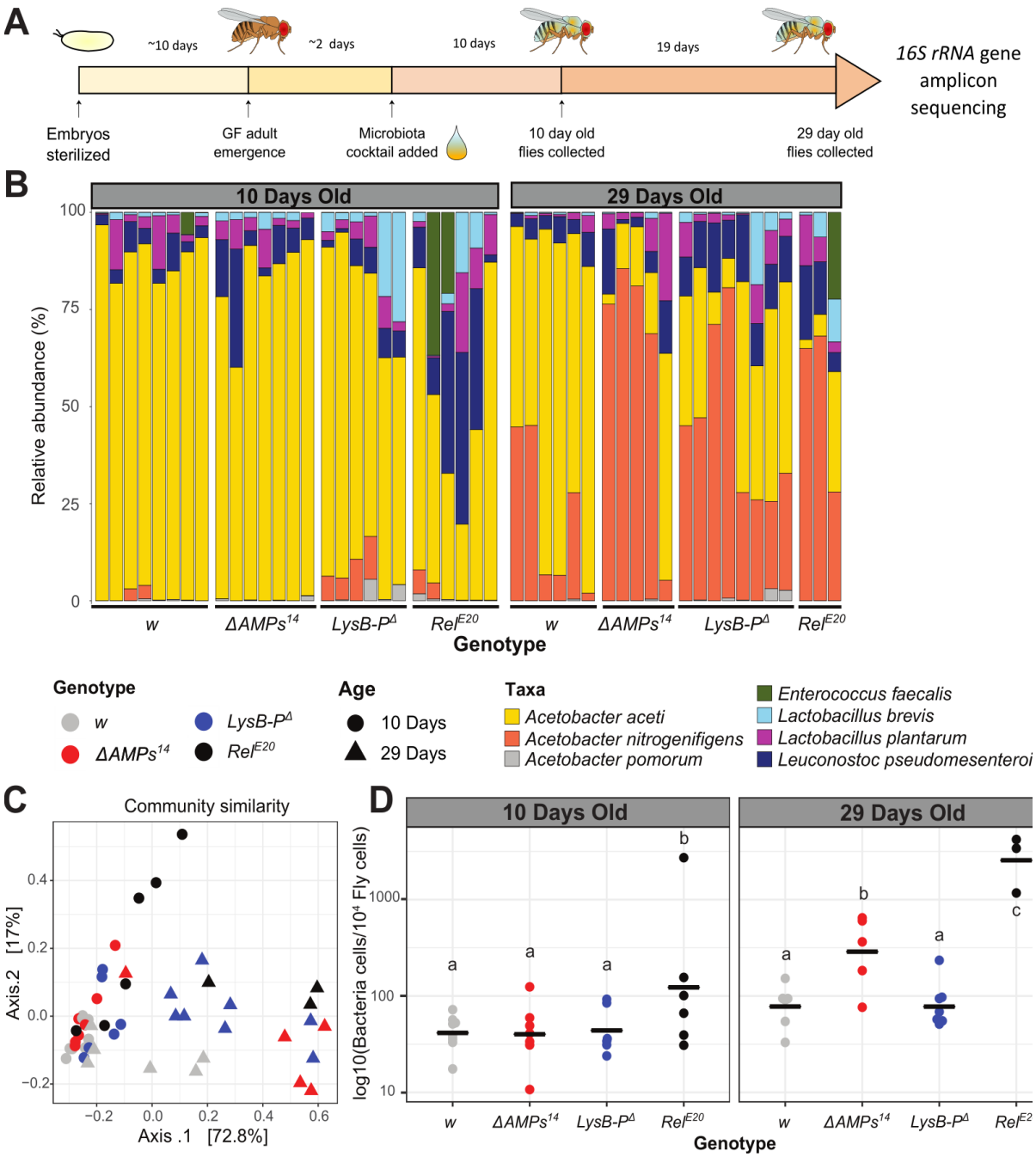

Fig2. The role of AMPs and lysozymes in microbiota composition and abundance on adult microbiota in a gnotobiotic setup. A) Scheme of the experimental procedure for fly colonization and collection for 16S rRNA gene amplicon sequencing. Embryos were collected, sterilized in 3% bleach, and kept on antibiotic food until the adult stage. Emerging germ-free flies were associated with a bacterial cocktail containing six representative microbiota members. Females were collected for DNA extraction and 16S rRNA gene amplicon sequencing 10 and 29 days after colonization. See Table S1 for the number of flies included in each sample. B) Relative community composition of the gut microbiota in iso w^{1118} (*w*) wild-type flies and *Relish* (Rel^{E20}), antimicrobial peptide ($\Delta AMPs^{14}$), and gut lysozyme ($LysB\text{-}P^{\Delta}$) mutants 10 days (left panel) and 29 days (right panel) after colonization. Each bar in the plot represents a biological replicate with a pool of 5 flies each.

Continue in the next page

C) Principal coordinate analysis based on Bray–Curtis dissimilarities on the gut communities of *w* control flies, *Rel*^{E20}, Δ*AMPs*^{14}, and *LysB-P*$^{\Delta}$ mutants 10 and 29 days after colonization based on 16S rRNA gene amplicon sequencing. Separation of the 10-day old (dots) and 29-day old clusters on the first axis, indicates that aging is the major factor defining bacterial community composition in adults. Separation *ΔAMPs*^{14} and *Rel*^{E20} (red and black triangles) from wild-type and *LysB-P*$^{\Delta}$ (grey and blue triangles) on the same axis in 29-day samples indicates that aging and loss of immune effectors act on microbiota composition in similar directions. D) Absolute quantification of the total number of bacterial cells by qPCR, normalized to the host gene *Actin5C.* Horizontal black bars show mean values. Details of the statistical outcomes are provided in Supplementary Table S2.

Effect of AMPs and lysozymes on individual microbiota members

16S rRNA gene amplicon sequencing provided us a first glimpse of how AMPs and gut lysozymes regulate microbiota structure at the community level. To further characterize the effect of these antimicrobials on individual microbiota members, we used a mono-association setup where we colonized flies with each bacterial isolate from the commensal cocktail used in the 16S rRNA gene amplicon sequencing experiment. Germ-free adult females were mono-associated with a single bacterial species and their load was measured 6 days after colonization by qPCR **(Fig 3A)**. We quantified 16S rRNA gene copies using primers that recognize *Acetobacteraceae* (65) and Firmicutes (including *La. plantarum, Le. pseudomesenteroides* and *La. brevis)* and normalized their abundance to host cells using primers for *Actin 5C* (52) **(Fig 3B)**.

As expected, all mono-associated taxa established a higher load in *Rel*^{E20} flies compared to wild-type flies **(Fig 3B)**. Interestingly, abundance of both *Acetobacter sp.* and *A. pomorum* isolates were high in *LysB-P*$^{\Delta}$ but especially in *ΔAMPs*^{14} mutants **(Fig 3B)**, indicating that AMPs most prominently control the proliferation of these Gram-negative microbiota members. Surprisingly, in contrast to shifts towards increased lactobacilli seen in the absence of lysozymes in gnotobiotic experiments **(Fig 1, Fig 2)**, mono-associated *La. plantarum* increased in abundance in the absence of AMPs but not lysozymes **(Fig 3B)**. This was surprising considering that lysozymes are expected to digest Gram-positive bacteria. The differing trends resulting from these approaches may depend on bacterial community dynamics in gnotobiotic experiments, or age-related differences between the experimental setups. Interestingly, *ΔAMPs*^{14} harbored significantly more *E. faecalis* compared to the wild-type *w* (**Fig 3B**, p-adjusted = 0.032), and indeed *ΔAMPs*^{14} had bacterial abundances equivalent or even greater than *Rel*^{E20} flies for all bacterial taxa except *Le. pseudomesenteroides* **(Fig 3B).**

Overall, our data indicate that in the absence of bacterial community dynamics, AMPs and to a lesser extent lysozymes, are major effectors regulating gut microbiota abundance.

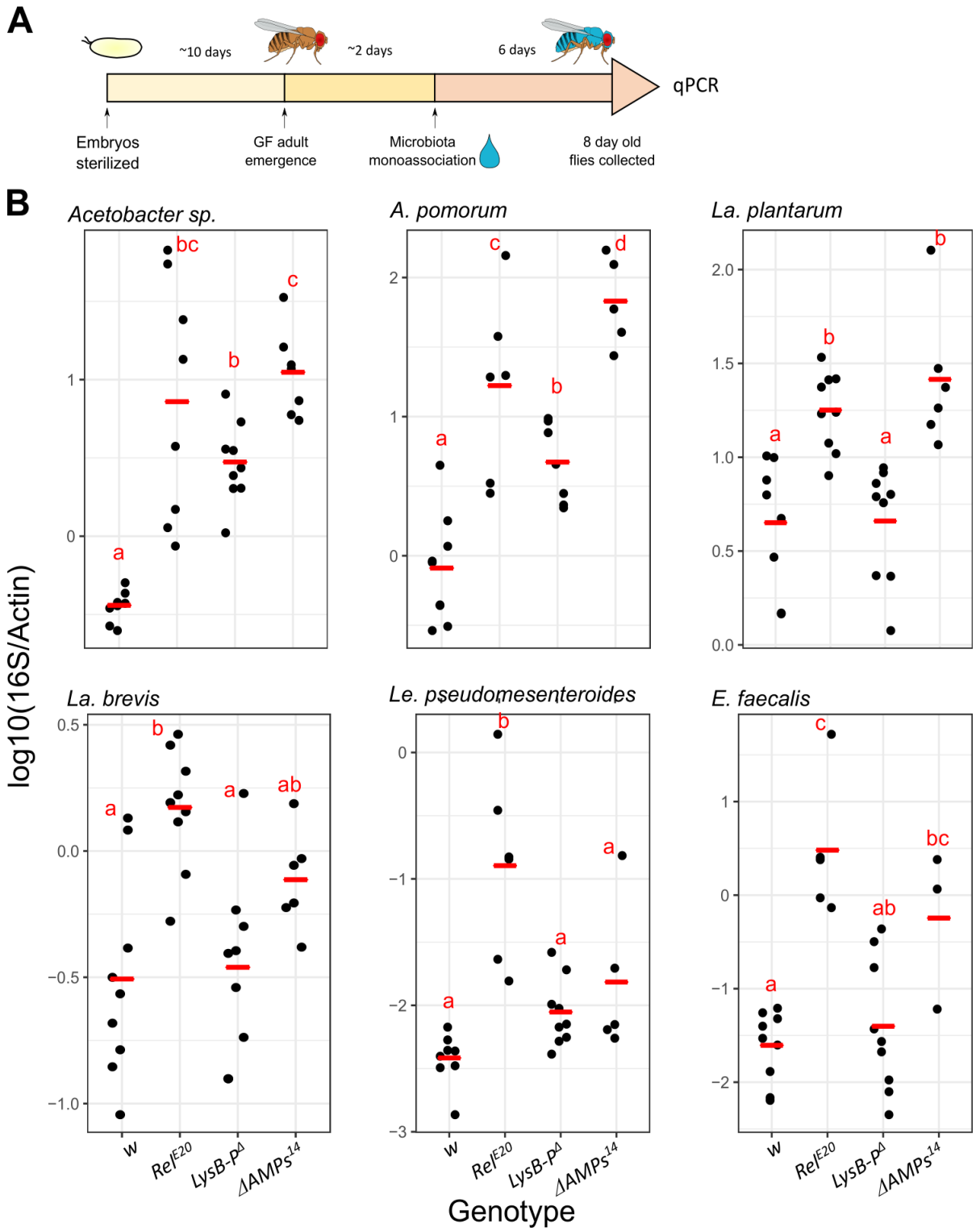

Fig3. Regulation of individual microbiota members in mono-association.

A) Scheme of the experimental procedure of the mono-association experiment. Embryos were collected, sterilized in 3% bleach, and kept on antibiotic food until the adult stage. Newly emerged germ-free flies were then mono-associated with a single bacterial isolate. Six days after colonization, the host and bacterial DNA was extracted and qPCR analysis of the microbial load was performed. B-G) Total microbial load was determined by quantitative PCR (qPCR) in female flies 6 days after mono-association. *iso* w^{1118} (*w*) wild-type flies and *Relish* (Rel^{E20}), antimicrobial peptide ($\Delta AMPs^{14}$), and gut lysozyme ($LysB\text{-}P^{\Delta}$) mutant flies were included. Bacterial loads were assessed by qPCR with family/phylum specific 16S rRNA gene primers and normalized to the host gene *Actin5C*. Red horizontal bars show mean values. Each dot represents a sample containing five individuals. Letters represent statistical significance ($p<0.05$) of adjusted p-values (FDR) from pairwise contrasts obtained from a main general linear mixed model; samples with shared letters are not statistically different from each other.

Systemic infection with microbiota members

In the previous experiments, we showed that a lack of AMPs in the gut significantly affects the microbiota composition and growth. However, it is unclear whether AMPs have preferential antimicrobial activity that selects for core microbiota members, and to date it has not been demonstrated that AMPs directly control members of the microbiota community. Hanson et al. (45) recently showed that *Drosophila* AMPs are primarily active against Gram-negative bacteria, but less so against Gram-positive bacteria. However, this study did not address whether AMPs can control bacterial species commonly found in the gut, with the exception of *E. faecalis* (45).

To address this, we used a systemic infection model to effectively "incubate" gut microbiota members in hemolymph with or without AMPs. Flies that fail to control bacterial proliferation ultimately die (66). We systemically infected flies with three representative bacteria that are normally present in the digestive tract and followed fly survival. We challenged wild-type, $\Delta AMP^{14}s$, Rel^{E20} and spz^{rm7} female flies by clean injury, and with three different bacterial species*: Acetobacter sp.* and *La. plantarum*, which have DAP-type peptidoglycan, and *E. faecalis* which has Lys-type peptidoglycan. Rel^{E20} lack a functional IMD response and are known to be very susceptible to systemic infection by most Gram-negative bacteria and certain classes of Gram-positive bacteria, while *spätzle* (spz^{rm7}) mutants lack Toll immune signaling and are susceptible to Gram-positive bacteria and fungi. We observed that $\Delta AMPs^{14}$ flies were more susceptible to Gram-negative *Acetobacter sp.*, mimicking the susceptibility of *Relish* mutants **(Fig 4)**. As expected, spz^{rm7} flies were highly susceptible to Gram-positive *La. plantarum* and *E. faecalis* infection, dying completely within one week. However, $\Delta AMPs^{14}$

flies did not have increased mortality when infected with these bacterial species. Flies did not die upon clean injury, indicating that the phenotype is specific to bacterial infection and is not due to a technical bias in the experiment **(Fig S3)**.

These systemic infections confirm that AMPs can play a direct role in the control of *Acetobacter sp.*, bacteria typically found in the gut, but have a lesser impact on *La. plantarum* and *E. faecalis* proliferation. This trend is consistent with the results above showing that AMPs most prominently contribute to *Acetobacter* control after gnotobiotic or mono-associative colonization.

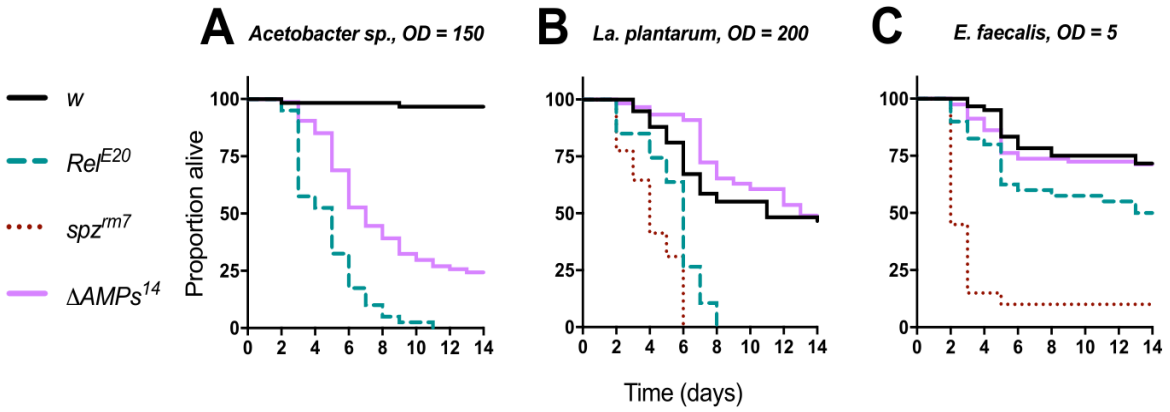

Fig4. Survival upon systemic infection with microbiota bacteria. Female iso w^{1118} wild-type flies (*w*), and *Relish* (Rel^{E20}), antimicrobial peptide ($\Delta AMPs^{14}$) and *spaetzle* (spz^{rm7}) mutants were pricked in the thorax with three common microbiota bacteria: Gram-negative bacterium *Acetobacter sp*. (A) and two Gram-positive bacteria *La. plantarum* (B) and *E. faecalis* (C). $\Delta AMPs^{14}$ mutants were significantly more susceptible than wild-type only to *Acetobacter sp.* infection ($p = .001$), and otherwise resisted infection like wild-type ($p > 0.1$). Pellet densities are reported for all systemic infections as OD600nm.

Discussion

In *Drosophila*, the immune system and particularly the IMD pathway has been robustly demonstrated to be an important regulator of the gut microbiota and intestinal homeostasis (21, 22, 28, 30, 33, 37). Several reports have indicated the importance of the IMD pathway in maintaining balanced microbiota during aging, and mutants for this pathway (e.g *Relish*) have atypical microbiota abundance and composition (28). While it is clear that the IMD pathway is a regulator of the gut microbiota, little is known about the effectors mediating this regulation. In addition to regulating most AMP expression in the gut (21), the IMD pathway regulates other physiological aspects, including expression of digestive enzymes (42), and enterocyte delamination (40, 67, 68). The present work extends these studies by more narrowly defining the role of AMPs and lysozymes by comparing specific loss of these effectors to total loss of IMD signaling.

Our results confirm a prominent role for the IMD pathway in regulating both microbiota load and diversity, especially upon aging (21, 28, 37). The $\Delta AMPs^{14}$ mutant mimics the *Relish* phenotype in many respects, showing that AMPs indeed contribute downstream of IMD to shape the microbiota composition. Our experiments consistently showed an increase in the load of *Acetobacter* species in both Rel^{E20} and $\Delta AMPs^{14}$ flies. The observation that both $\Delta AMPs^{14}$ and Rel^{E20} flies are also susceptible to *Acetobacter* systemic infection, together with previous studies showing that AMPs contribute to survival to Gram-negative bacterial infection (45), provides strong evidence that direct microbicidal activity of AMPs regulates these Gram-negative bacteria. Collectively, this indicates for the first time that the basal level of IMD pathway activity induced by the gut microbiota (28) leads to the production of AMPs that prevent overgrowth of Gram-negative commensals such as *Acetobacter*. Future studies should clarify which AMP(s) among the 14 deleted in the $\Delta AMPs^{14}$ flies regulate *Acetobacter*.

La. plantarum is an important member of *Drosophila* microbiota that is associated to the host both in larval development and adulthood (11, 34, 69). As the DAP-type peptidoglycan found in the cell wall of these bacteria can activate the IMD pathway, we might expect to see an action of AMPs against them. However, previous studies have shown that IMD pathway and AMP mutants are not very susceptible to DAP-type Gram-positive bacteria (70). Moreover, D-Alanylation of *La. Plantarum* lipoteichoic acid has recently been proposed as a mechanism to protect against the action of AMPs and lysozymes (49). Here, we found that the AMPs do play a role in controlling *La. plantarum* abundance in a mono-colonization setup but not when

bacteria are in a community context. This might be due to the dynamics between microbiota members (e.g. competition between different species), or due to differential affinity of AMPs to the peptidoglycan of distinct species. It is possible that the abundance of *La. plantarum* is maintained at a threshold level in the gut and this is naturally achieved in a community through bacterial interactions. However, *La. plantarum* overgrowth can be inhibited by AMPs in a context where it becomes the only dominant member of the community.

The genome of *Drosophila* contains many genes encoding lysozymes, likely as a consequence of living in bacterially enriched habitats (46). Indeed, animals feeding on fermenting medium, such as ruminants or fruit flies, have a much higher number of lysozyme gene copies compared to animals feeding on 'clean food' (71, 72). In many insects, lysozymes are induced upon systemic infection, pointing to a possible role as immune effectors. In contrast, *Drosophila* lysozymes are strongly expressed in the gut, indicating a specific role in the digestive process (46, 47). Of note, one uncharacterized gene annotated as encoding a putative lysozyme (*CG6429*) is strongly induced upon systemic infection, and is partially regulated by the IMD pathway (73).

In this study, we generated a *LysB-P*$^{\Delta}$ mutant deficient for four lysozyme genes strongly expressed in the gut. *LysB-P*$^{\Delta}$ gut extracts have reduced lysozyme activity **(Fig S1)** confirming that these four genes indeed contribute to gut lysozyme activity. As lysozymes are known to digest peptidoglycan and can exhibit bactericidal activity alone or in combination with AMPs (48), we were interested to monitor the impact of lysozymes on the gut microbiota. We expected that loss of lysozymes would have a greater effect on Gram-positive bacteria, as the thin peptidoglycan layer of Gram-negative bacteria is protected by their external LPS membrane. Consistently, 16S rRNA gene amplicon sequencing revealed that *LysB-P*$^{\Delta}$ mutants exhibit increased relative community *Lactobacillus* abundance. However, mono-association experiments revealed a role of lysozymes in suppressing growth of only Gram-negative *Acetobacter* species. This effect was less marked than that of AMP deficient mutants.

An interesting observation of our study is that flies lacking AMPs or lysozymes display greater community stochasticity, similar to the phenotype of *Rel*^{E20} flies. This suggests that multiple factors including AMPs, lysozymes and bacteria-bacteria interactions contribute to stability of the gut microbiota, and that loss of these factors increases stochasticity. It should be noted that our work relies on the use of isogenic fly strains. While the isogenization process homogenizes the genetic background, it also increases the degree of homozygosity along the genome with a possible increase in genetic interactions. Thus, our study on AMPs and lysozymes using the *iso*

Drosdel background should be reinforced by other studies using other backgrounds or alternative approaches.

In *Drosophila*, the induction of antibacterial peptides genes after infection is blocked in IMD pathway mutants, such as *Relish*, resulting in high susceptibility. These flies also cannot control their microbiota load, especially during aging (28). As expected, we found similar gut microbiota structure in *Relish* and *AMP* mutants. Indeed, both genotypes were unable to control the microbiota load and composition, but *Relish* flies had a more severe phenotype, with 16S analysis showing atypical microbial composition at early life stages, and marked inability to control all inoculated bacterial species in mono-association experiments. This is likely due to the multiple roles of the IMD pathway in gut physiology, apoptosis, nutrition and metabolism (40, 74, 75), the loss of which in addition to AMPs may exacerbate gut dysbiosis or hasten the inability of the flies to control microbiota growth. This indicates that although AMPs play an important role in control of microbiota members, they contribute only partially to the dysbiosis of IMD pathway mutant flies.

Collectively, our work is the first to show direct involvement of AMPs and lysozymes in the control of *Drosophila* gut microbiota. Consequences of the loss of these effectors are exacerbated during aging, and their loss contributes to increased microbiota abundance and shifted composition. This work shows that immune effectors typically associated with resistance to pathogenic infections also help shape the beneficial gut community, consistent with the idea that host-symbiont interactions use the same ‘language’ typically associated with pathogenesis (76).

Material and Methods

Bacterial strains and culture conditions

Bacterial strains used in this study and their origins are as follows: *Acetobacter sp*. (52), *Acetobacter pomorum* (50), *Lactobacillus plantarum* (11), *Enterococcus faecalis* (see above) (51). *Lactobacillus brevis* and *Leuconostoc pseudomesenteroides* were isolated from the "Valais" population, collected in the Valais canton of Switzerland in 2007 (77). Briefly, homogenates from 20 flies were spread over MRS-5% Mannitol plates. A single colony was used to prepare liquid cultures (described below) and establish glycerol stocks, as well as for 16S rRNA gene full-length amplification using universal primers. The PCR products were sequenced by Sanger sequencing and assigned to taxa based on a Microbial BLASTn search against the nucleotide database of NCBI (https://blast.ncbi.nlm.nih.gov/Blast.cgi?PAGE_TYPE=BlastSearch&BLAST_SPEC=MicrobialGenomes). See **Supplementary Text 1** for full 16S rRNA gene sequences of these isolates, as well as that of *Acetobacter* sp (52).

A. pomorum and *Acetobacter sp.* were cultivated in Man, Rogosa and Sharpe (MRS)- D-Mannitol 2,5% medium in aerobic conditions at 29°C for at least 18h with agitation. *La. plantarum*, *La. brevis* and *Le. pseudomesenteroides* were cultivated in anaerobic conditions in Man, Rogosa and Sharpe (MRS)- D-Mannitol 2,5% medium at 29°C for at least 18h standing. *E. faecalis* was cultured in Brain Heart Infusion Broth (BHI) medium in aerobic conditions at 37°C for at least 16h with agitation.

Gnotobiotic fly cultivation and media

All experiments were done on flies kept at 25˚C with a 12h dark/light cycle.

Because antibiotic treatments over multiple generations may result in epigenetic effects that may interfere with phenotypes, germ-free flies were freshly generated for each experiment. To do this, embryos were collected from an overnight egg laying on grape juice-agar plates supplemented with yeast. Embryos were washed with tap water, sterilized by soaking in 3% bleach for 3 minutes and were rinsed with autoclaved water 3 times. ~200 eggs were counted on a mesh under a laminar flow hood and were transferred to filter cap falcon tubes (TPP catalogue #87050) containing the autoclaved larval medium (0.79% Agar, 5.2% cornmeal, 11% sucrose, 4% yeast, 1.12% Moldex, and 0.77% propionic acid, where the last two were added

when the medium was <78˚C) supplemented with antibiotics (50µg/µl Ampicilin, 50µg/µl Kanamycin, 10µg/µl Erythromycin, 10µg/µl Tetracyclin).

Upon emergence, 0-2 day old adults were transferred to autoclaved 2% yeast adult medium (all other ingredients were identical to the larval medium) without antibiotics to remain germ-free or to be colonized with commensals. To colonize adults, cultured bacteria were centrifuged at 3000 rpm for 10 minutes and resuspended in sterile PBS to a concentration of ~5 x 10^6 cells per 100µl. To generate the commensal cocktail, 100µl of each bacterial suspension was mixed in 1:1 ratio to maintain the same cell concentration. 50µl of the bacterial suspension was spread over the adult medium using glass beads (3mm diameter) for 10 seconds and the tubes were air dried under the laminar hood for 2 hours. Germ-free adults raised in antibiotic medium were anaesthetized on ice for 10 minutes, and 20-30 adults were transferred to each tube.

To avoid sticky 'biofilm-like' formation on the medium, flies were transferred to fresh medium every 3-4 days. To avoid a decrease in microbial loads, the microbiota of each tube was transferred to the next using glass beads. Briefly, flies were anaesthetized on ice and removed on sterile caps. 10-20 glass beads were transferred to the old tube and shaken for 10 seconds. The beads were then transferred to the new sterile tube and were shaken again for 10 seconds to spread the bacteria around the tubes. Adults were added in the new tubes. Flies were sampled 10 days and 29 days after colonization.

For vertically transmitted microbiota, we let gnotobiotic adults (colonized as described above 3-4 days previously) lay eggs on fresh medium for three days. We let larvae grow in this original medium and began transferring the emerging adults to new tubes 5 days after the first fly emerged. We collected adults 10-15 days after emergence and analyzed their associated bacterial community.

For mono-association experiments, we colonized flies with each isolate that was included in the commensal cocktail. Because during mono-association changes in community structure is not a concern, we maintained the flies in their original tube throughout the experiment. Flies were sampled 6 days after colonization.

DNA extraction and qPCR

DNA extraction was carried out on samples of surface sterilized adults (washed in sterile water and EtOH) using a DNeasy Blood & Tissue Kit (Qiagen). Briefly, flies were homogenized in PBS (at a concentration of 100µl per fly) and 180µl of homogenate was transferred into a new

tube for lysis with 20µl proteinase-K solution and 200µl Buffer ALT. The protocol was finalized using manufacturer's instructions.

The qPCR reactions for absolute quantification were carried out as described in (78) . The universal (78) and *Acetobacter* specific 16S (65), and Actin 5C primers (65) were previously described. Firmicute specific primers (anti-sense primer 5'AGCGTTGTCCGGATTTAT 3', sense primer 5' CATTTCACCGCTACACAT 3') were designed by aligning the 16S rRNA gene sequences of the four Firmicute species that were used in this study. Their specificity (lack of amplification in *Acetobacteraceae*) was determined on plasmid DNA containing specific 16S sequences as well as on DNA extracted from flies mono-associated with microbiota members described in this study.

Standard curves that allowed estimation of the number of bacterial cells per genome equivalent of fly cells were generated from serial dilutions of plasmids containing bacterial 16S sequences and actin sequence. The number of detected 16S rRNA gene copies was corrected by the average number of 16S rRNA operon copies present in the genome of each species. This number was obtained from rrNDB (79).

16S rRNA gene amplicon sequencing and data processing

Amplification of the V4 region of the 16S rRNA gene and library preparation protocol was done as previously described (78) except for the first cycle PCR that was performed with 30 cycles. Libraries were verified by Fragment analyzer, mixed with 10% PhiX library (Illumina #FC-110-3001), and subjected to Illumina MiSeq v3 paired-end sequencing in one lane, with all libraries multiplexed.

Divisive Amplicon Denoising Algorithm 2 (DADA2) pipeline ("dada2" package version 1.14.1 in R) was used to process the sequencing data. All functions were run using the recommended parameters (https://benjjneb.github.io/dada2/tutorial.html) except for "expected errors" during the filtering step which was set to (maxEE=2,5) in "filterAndTrim" function. The RDP database was used for taxonomy assignments. Downstream analyses were performed in R version 3.6.0. Reads belonging to mitochondria, chloroplasts, and eukaryotes were excluded from further analyses ("phyloseq" package version 1.30.0, "subset_taxa" function (80)). Only the variants present in at least 10 samples with a total of 100 reads were retained for downstream analyses ("genefilter" package version 1.68.0, "filterfun_sample" function (81)). To complement the taxonomic classification based on the RDP database, sequence variants were further assigned

to the gut microbiota members based on their alignment to the full 16S rRNA gene sequences obtained by Sanger sequencing of each isolate.

To calculate absolute bacterial abundances, we multiplied the proportions of each taxon by the total 16S rRNA gene copy number present in each sample (as measured by qPCR using the universal 16S primers).

Diversity and statistical analysis

Permutational multivariate analysis of variance (ADONIS, "adonis" function) based on Bray–Curtis distances ("vegdist" function) (82) was used to test the effects of age and genotype on community structure, and "metaMDS" function was used for plotting beta-diversity. For pairwise comparisons of ADONIS, "adonis.pair" function was used from "EcolUtils" package. To test the dispersion of communities we used the function "betadisper" (83, 84) and compared the distances of individual samples to group centroids in multidimensional space using "permutest".

All statistical analyses were performed using R (version 3.6.3). We used general linear mixed models ("lme4" package version 1.1.23) to test for the effects of age, genotype and their interaction (depending on the experimental design) on bacterial loads or dispersion of bacterial communities. Pairwise comparisons were performed using "emmeans" and "pairs" functions ("emmeans" package version 1.5.1). p-values were adjusted using FDR method.

Systemic infection and lifespan assay

Systemic infections were performed by pricking 5-7 day-old conventionally reared adult females in the thorax with a 100-µm-thick insect pin dipped into a concentrated pellet of bacteria. The following bacteria were grown to the respective OD600 concentrations in MRS+Mannitol broth (*Acetobacter sp.,* OD600=150; *La. plantarum,* OD600=200) or BHI (*E.faecalis,* OD600=5); the maximum concentration we could achieve for *Acetobacter sp.* was OD600=150. Infected flies were maintained at 25˚C for experiments. At least three replicate survival experiments were performed for each infection, with 20 flies per vial on standard fly medium without yeast. Survivals were scored daily and flies were flipped to fresh medium every two days.

Survival data were analyzed using the survival package in R 3.6.3 with a Cox proportional hazards model (coxph() function) including experiment as a covariate in the final model when significant.

Acknowledgments

We are grateful to Tadeusz J. Kawecki (University of Lausanne, Switzerland) for providing bacterial isolates; Xiaoxue Li for providing data on *LysB-P*$^{\Delta}$ strain validation; Iatsenko Igor (Max Planck Institute, Germany) for *LysB-P*$^{\Delta}$ strain isogenization; and to Hannah Westlake for critical reading of the manuscript.

Fundings

This work was supported by the Swiss National Science Foundation grant N°310030_185295.

Declaration of interests

The authors declare no competing interests.

Data availability

16S rRNA gene amplicon sequencing data will be submitted to NCBI database upon acceptance.

Supplementary matherials

S1. Lysozyme mutant characterization.

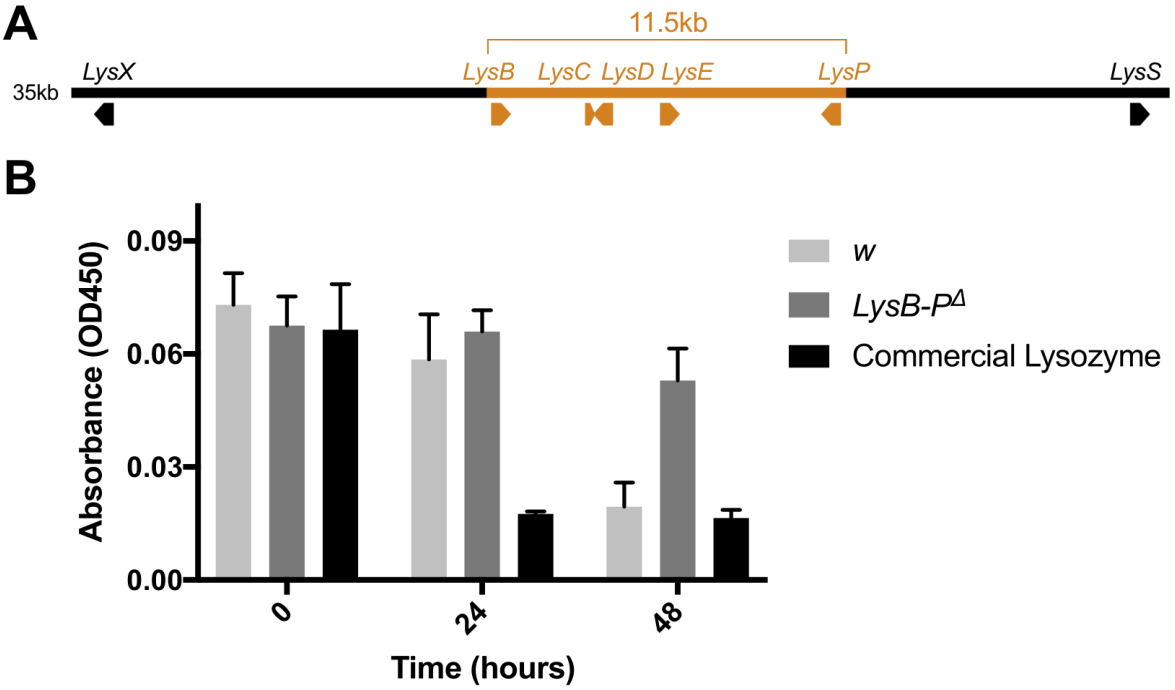

Fig S1. Lysozyme mutant characterization. A) Diagram of the *LysB-P*$^{\Delta}$ mutation, which deletes 11.5kb of nucleotide sequence from the *Drosophila* genome. *LysB-P*$^{\Delta}$ flies lack the four lysozyme genes (*LyB, LysD, LysE, LysP*) that are highly expressed in the gut, and also the *LysC* pseudogene. B) *LysB-P*$^{\Delta}$ mutants have a reduced capacity to degrade peptidoglycan in the gut compared to wild-type flies. Gut extracts from wild-type flies (*w*) and lysozyme mutants (*LysB-P*$^{\Delta}$) were incubated with *E.faecalis* peptidoglycan for 48h. The lysozyme activity was monitored by change in optical density of the peptidoglycan solution. Commercial lysozyme was included as a positive control.

S2. Homogeneity of multivariate dispersals in microbial communities.

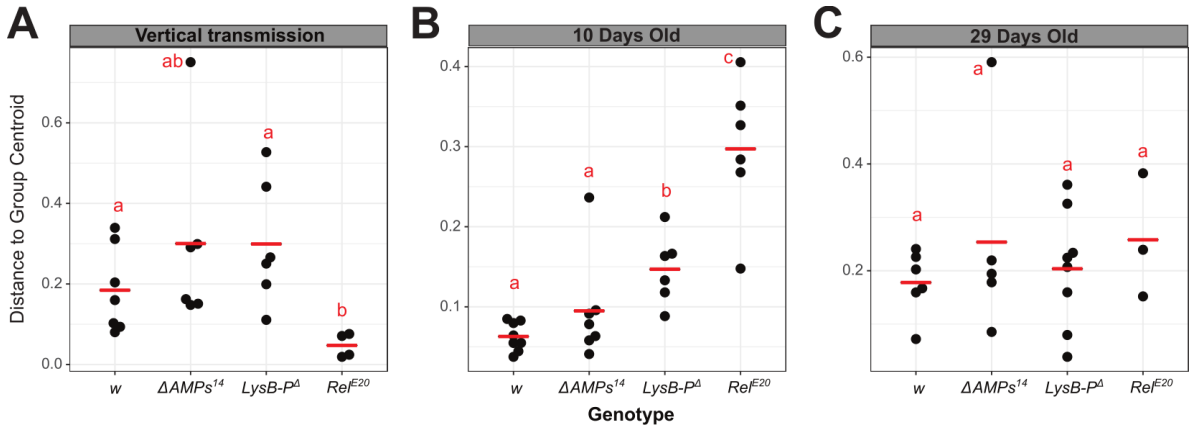

Fig S2. Homogeneity of multivariate dispersals in microbial communities.

Distance to the center of each group (genotype) represents how spread are the communities in the multivariate space (PCoA) in A) a vertical transmission setup, B) 10 days after colonization, and C) 29 days after colonization. Different letters indicate significant differences ($p<0.05$) between p-values upon pairwise comparison, calculated by permutations on multivariate equivalent of variances. A significant difference between groups indicates that samples belonging to one group are more variable in microbiota composition compared to the other group.

S3. Δ*AMPs*^{14} flies survive clean injury.

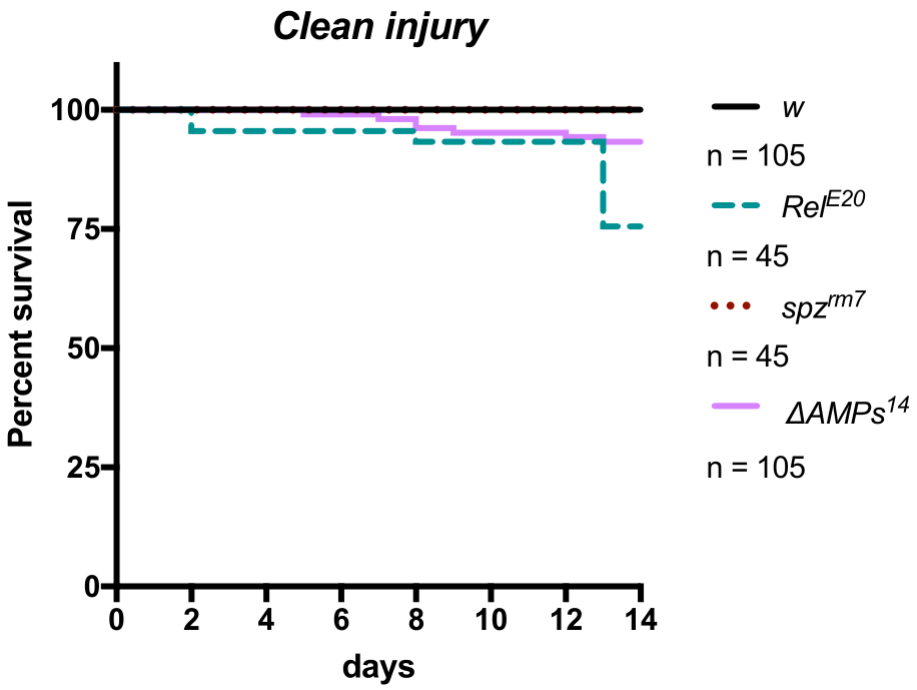

Fig S3. Δ*AMPs*^{14} flies survive clean injury.

Females from indicated genotypes were pricked with a clean 100µm insect pin. No genotype displayed pronounced susceptibility to clean injury.

Sup. Text 1: 16S rRNA gene sequences of La. brevis, *Le. pseudomesenteroides* and *Acetobacter sp*. [REF erkosar 2017] used in this study.

>Lactobacillus_brevis_16S

CCTAATACATGCAAGTCGAACGAGCTTCCGTTGAATGACGTGCTTGCACTGATTT
CAACAATGAAGCGAGTGGCGAACTGGTGAGTAACACGTGGGGAATCTGCCCAGA
AGCAGGGGATAACACTTGGAAACAGGTGCTAATACCGTATAACAACAAAATCCG
CATGGATTTTGTTTGAAAGGTGGCTTCGGCTATCACTTCTGGATGATCCCGCGGCG
TATTAGTTAGTTGGTGAGGTAAAGGCCCACCAAGACGATGATACGTAGCCGACCT
GAGAGGGTAATCGGCCACATTGGGACTGAGACACGGCCCAAACTCCTACGGGAG
GCAGCAGTAGGGAATCTTCCACAATGGACGAAAGTCTGATGGAGCAATGCCGCG
TGAGTGAAGAAGGGTTTCGGCTCGTAAAACTCTGTTGTTAAAGAAGAACACCTTT
GAGAGTAACTGTTCAAGGGTTGACGGTATTTAACCAGAAAGCCACGGCTAACTAC
GTGCCAGCAGCCGCGGTAATACGTAGGTGGCAAGCGTTGTCCGGATTTATTGGGC
GTAAAGCGAGCGCAGGCGGTTTTTTAAGTCTGATGTGAAAGCCTTCGGCTTAACC
GGAGAAGTGCATCGGAAACTGGGAGACTTGAGTGCAGAAGAGGACAGTGGAACT
CCATGTGTAGCGGTGGAATGCGTAGATATATGGAAGAACACCAGTGGCGAAGGC
GGCTGTCTAGTCTGTAACTGACGCTGAGGCTCGAAAGCATGGGTAGCGAACAGG
ATTAGATACCCTGGTAGTCCATGCCGTAAACGATGAGTGCTAAGTGTTGGAGGGT
TTCCGCCCTTCAGTGCTGCAGCTAACGCATTAAGCACTCCGCCTGGGGAGTACGA
CCGCAAGGTTGAAACTCAAAGGAATTGACGGGGGCCCGCACAAGCGGTGGAGCA
TGTGGTTTAATTCGAAGCTACGCGAAGAACCTTACCAGGTCTTGACATCTTCTGCC
AATCTTAGAGATAAGACGTTCCCTTCGGGGACAGAATGACAGGTGGTGCATGGTT
GTCGTCAGCTCGTGTCGTGAGATGTTGGGTTAAGTCCCGCAACGAGCGCAACCCT
TATTATCAGTTGCCAGCATTCAGTTGGGCACTCTGGTGAGACTGCCGGTGACAAA
CCGGAGGAAGGTGGGGATGACGTCAAATCATCATGCCCCTTATGACCTGGGCTAC
ACACGTGCTACAATGGACGGTACAACGAGTTGCGAAGTCGTGAGGCTAAGCTAA
TCTCTTAAAGCCGTTCTCAGTTCGGATTGTAGGCTGCAACTCGCCTACATGAAGTT
GGAATCGCTAGTAATCGCGGATCAGCATGCCGCGGTGAATACGTTCCCGGGCCTT
GTACACACCGCCCGTCACACCATGAGAGTTTGTAACACCCAAAGCCGGTGAGATA
ACCTTCGGGAGTCAGCCGTCTAAGGGACGAT

>Leuconostoc_pseudomesenteroides_16S

GCTAATACATGCAAGTCGAACGCACAGCGAAAGGTGCTTGCACCTTTCAGTGAGT
GGCGAACGGGTGAGTAACACGTGGACAACCTGCCTCAAGGCTGGGGATAACATT
TGGAAACAGATGCTAATACCGAATAAAACTCAGTGTCGCATGACACAAAGTTAA
AAGGCGCTTTGGCGTCACCTAGAGATGGATCCGCGGTGCATTAGTTAGTTGGTGG
GGTAAAGGCCTACCAAGACAATGATGCATAGCCGAGTTGAGAGACTGATCGGCC
ACATTGGGACTGAGACACGGCCCAAACTCCTACGGGAGGCTGCAGTAGGGAATC
TTCCACAATGGGCGAAAGCCTGATGGAGCAACGCCGCGTGTGTGATGAAGGCTTT
CGGGTCGTAAAGCACTGTTGTATGGGAAGAACAGCTAGAATAGGGAATGATTTT
AGTTTGACGGTACCATACCAGAAAGGGACGGCTAAATACGTGCCAGCAGCCGCG
GTAATACGTATGTCCCGAGCGTTATCCGGATTTATTGGGCGTAAAGCGAGCGCAG
ACGGTTGATTAAGTCTGATGTGAAAGCCCGGAGCTCAACTCCGGAATGGCATTGG

AAACTGGTTAACTTGAGTGCAGTAGAGGTAAGTGGAACTCCATGTGTAGCGGTGG
AATGCGTAGATATATGGAAGAACACCAGTGGCGAAGGCGGCTTACTGGACTGTA
ACTGACGTTGAGGCTCGAAAGTGTGGGTAGCAAACAGGATTAGATACCCTGGTA
GTCCACACCGTAAACGATGAACACTAGGTGGTTAGGAGGTTTCCGCCTCTTAGTG
CCGAAGCTAACGCATTAAGTGTTCCGCCTGGGGAGTACGACCGCAAGGTTGAAA
CTCAAAGGAATTGACGGGGACCCGCACAAGCGGTGGAGCATGTGGTTTAATTCG
AAGCAACGCGAAGAACCTTACCAGGTCTTGACATCCTTTGAAGCTTTTAGAGATA
GAAGTGTTCTCTTCGGAGACAAAGTGACAGGTGGTGCATGGTCGTCGTCAGCTCG
TGTCGTGAGATGTTGGGTTAAGTCCCGCAACGAGCGCAACCCTTATTGTTAGTTG
CCAGCATTCAGATGGGCACTCTAGCGAGACTGCCGGTGACAAACCGGAGGAAGG
CGGGGACGACGTCAGATCATCATGCCCCTTATGACCTGGGCTACACACGTGCTAC
AATGGCGTATACAACGAGTTGCCAACCCGCGAGGGTGAGCTAATCTCTTAAAGTA
CGTCTCAGTTCGGATTGTAGTCTGCAACTCGACTACATGAAGTCGGAATCGCTAG
TAATCGCGGATCAGCACGCCGCGGTGAATACGTTCCCGGGTCTTGTACACACCGC
CCGTCACACCATGGGAGTTTGTAATGCCCAAAGCCGGTGGCCTAACCTTTAGGAA
GGAGCCGTCTAAGGCAGACCG

>Acetobacter_sp_16S

atGCaGTcgcanGaaGgCTTCGGCCTTAGTGGCGGacGGGTGAGTAACGCGTAGGAATC
TATCCatGGgtGGGGGATAACTCCGGGAAACTGGAGctAATACCGCATGATACCTGA
GGGTCAAAGGCGCAAGTCGCCTgtGGAGGAGCCTGCGTTTGATTAGCTTGTTGGTG
GGGTAAAGGCCTACCAAGGCGATGATCAATAGCTGGTCTGAGAGGATGATCAGC
CACACTGGGACTGAGACACGGCCCAGACTCCTACGGGAGGCAGCAGTGGGGAAT
ATTGGACAATGGGGGAAACCCTGATCCAGCAATGCCGCGTGTGTGAAGAAGGTT
TTCGGATTGTAAAGCACTTTCGGCGGGGACGATGATGACGGTACCCGCAGAAGA
AGCCCCGGCTAACTTCGTGCCAGCAGCCGCGGTAATACGAAGGGGGCTAGCGTT
GCTCGGAATGACTGGGCGTAAAGGGCGTGTAGGCGGTTTGTACAGTCAGATGTG
AAATCCCCGGGCTTAACCTGGGAGCTGCATTTGATACGTGCAGACTAGAGTATGA
GAGAGGGTTGTGGAATTCTCAGTGTAGAGGTGAAATTCGTAGATATTGGGAAGA
ACACCGGTGGCGAAGGCGGCAACCTGGCTCATTACTGACGCTGAGGCGCGAAAG
CGTGGGGAGCAAACAGGATTAGATACCCTGGTAGTCCACGCTGTAAACGATGTGT
GCTGGATGTTGGGTAACTTAGTTACTCAGTGTCGTAGCTAACGCGATAAGCACAC
CGCCTGGGGAGTACGGCCGCAAGGTTGAACTCAAAGGAATTGACGGGGGCCCGC
ACAAGCGGTGGAGCATGTGGTTTAATTCGAAGCAACGCGCAGAACCTTACCAGG
GCTTGTATGGAGAGGCTGTATTCAGAGATGGATATTTCCCGCAAGGGACCTCTTG
CACAGGTGCTGCATGGCTGTCGTCAGCTCGTGTCGTGAGATGTTGGGTTAAGTCC
CGCAACGAGCGCAACCCTTATCTTTAGTTGCCAGCATGTTTGGGTGGGCACTCTA
AAGAGACTGCCGGTGACAAGCCGGAGGAAGGTGGGGATGACGTCAAGTCCTCAT
GGCCCTTATGTCCTGGGCTACACACGTGCTACAATGGCGGTGAcagTGGGAAGCTA
GATGGTGACATCATGCCGATCTCTAAAAACCGTCTCAGTTCGGATTGCACTCTGC
AACTCGAGTGCATGAAGGTGGAATCGCTAGTAATCGCGGATCAGcatGCCGCGGTG
AATACGTTCCCGGGCCTTGTACAcacCGCCCGTCACaccATGGGAGTTGGnTnaCCTT
AAGCCgGTgaGCGAACCgcaaGAcgcaAGcgGa

Table S1

Sample*	# Flies	initial #reads	Filtered	Denoised F	Denoised R	Merged	Non-chimeras	bacFiltered**
dAMP_1_r1_10d_1	10	198415	119889	119831	119589	117941	117941	117231
dAMP_1_r1_10d_2	10	279472	165273	165226	164800	163304	163304	163040
dAMP_1_r1_29d_1	8	136085	81191	81051	80971	79325	77216	77168
dAMP_1_r1_VerticalTrans_1	5	134880	82475	82440	82332	82003	82003	81882
dAMP_1_r2_10d_1	10	221248	134917	134865	134711	133002	133002	132683
dAMP_1_r2_10d_2	5	285526	174552	174449	174191	171816	170349	167301
dAMP_1_r2_29d_1	6	270998	164534	164494	164341	159733	159502	159425
dAMP_1_r2_29d_2	6	216330	131327	131261	131102	126716	126361	126312
dAMP_1_r2_VerticalTrans_1	7	150429	92007	91961	91771	91457	91266	91232
dAMP_1_r3_VerticalTrans_1	8	123405	74463	74421	74275	73952	73952	73811
dAMP_2_r1_10d_1	10	239915	144406	144346	144124	143049	142999	140812
dAMP_2_r1_10d_2	4	314766	187147	187010	186723	184739	184572	175126
dAMP_2_r1_29d_1	7	344596	206625	205146	206151	197609	191977	191559
dAMP_2_r1_VerticalTrans_1	6	164042	99782	99734	99599	98849	98175	98169
dAMP_2_r2_10d_1	9	140966	85716	85678	85600	84943	84943	84596
dAMP_2_r2_29d_1	10	122801	73717	73636	73468	71662	70645	70578
dAMP_2_r2_VerticalTrans_1	10	170047	99629	99524	99231	97980	96977	96824
dAMP_2_r3_VerticalTrans_1	8	333021	200848	200737	200405	199301	197995	197792
Lys_1_r1_10d_1	10	288237	176047	175950	175743	170804	170376	168492
Lys_1_r1_10d_2	10	288783	176693	176652	176449	171898	171584	170195
Lys_1_r1_29d_1	10	215621	127915	127857	127617	122928	122911	122670
Lys_1_r1_29d_2	8	139254	83476	83390	83228	79880	79875	79591
Lys_1_r1_VerticalTrans_1	8	278798	161179	161141	160870	158477	158274	152621
Lys_1_r2_10d_1	10	213270	129430	129333	129179	125752	125462	124567
Lys_1_r2_10d_2	10	386433	231518	231443	231077	222268	221365	220796
Lys_1_r2_29d_1	10	146137	87704	87647	87447	84829	84408	84183
Lys_1_r2_29d_2	8	200615	121173	121071	120898	117296	117248	116867
Lys_1_r2_VerticalTrans_1	4	283688	168556	168487	167839	165812	165645	165410
Lys_1_r3_VerticalTrans_1	5	334811	196729	196645	196016	193442	193240	192974
Lys_2_r1_10d_1	10	166350	100089	100023	99741	98802	98792	98307
Lys_2_r1_10d_2	10	102189	60615	60566	60449	59555	59555	59344
Lys_2_r1_29d_1	10	221088	134220	134163	133938	130293	130219	130054
Lys_2_r1_29d_2	10	160493	96178	96082	95819	93027	92910	92727
Lys_2_r1_VerticalTrans_1	9	220361	133215	133191	132913	128959	128787	128745

Lys_2_r2_29d_1	8	207383	124019	123937	123695	119557	118835	118659
Lys_2_r2_29d_2	8	124609	75638	75582	75440	72762	72746	72657
Lys_2_r2_VerticalTrans_1	10	231503	140724	140623	140538	137356	137356	136542
Lys_2_r3_VerticalTrans_1	10	237096	142105	142036	141799	138235	138135	137701
Rel_1_r1_10d_1	10	165672	99828	99776	99601	96875	96680	96365
Rel_1_r1_29d_1	5	142222	83914	83858	83656	81733	77845	77832
Rel_1_r2_10d_1	10	177025	105763	105706	105425	103224	103183	103065
Rel_1_r2_10d_2	5	129464	74479	74409	74147	73186	72865	72677
Rel_1_r2_VerticalTrans_1	8	180773	111286	111227	111085	110664	110664	110476
Rel_1_r3_VerticalTrans_1	10	241828	148237	148134	147949	146704	146588	142552
Rel_2_r1_10d_1	9	81990	45776	45756	45581	44972	44972	26135
Rel_2_r1_10d_2	9	186257	108730	108680	108277	107542	107542	105403
Rel_2_r1_29d_1	6	113524	68345	68304	68138	66029	62578	62576
Rel_2_r1_VerticalTrans_1	10	293351	177116	177037	176758	175394	175277	173631
Rel_2_r2_10d_1	10	287915	175016	174980	174737	173714	173670	170228
Rel_2_r2_29d_1	2	92415	54838	54664	54474	51964	45982	42596
Rel_2_r3_VerticalTrans_1	10	200504	120738	120666	120475	119917	119756	119667
w_1_r1_10d_1	10	128717	78558	78511	78429	76910	76910	76720
w_1_r1_10d_2	10	143826	87902	87853	87687	86171	86171	84858
w_1_r1_29d_1	6	207126	125673	125594	125490	121147	121147	120730
w_1_r1_29d_2	6	363182	219169	219066	218786	210104	210021	209582
w_1_r1_VerticalTrans_1	5	266497	156547	156497	155853	153045	152729	148294
w_1_r2_10d_1	9	105442	63734	63650	63589	62063	61933	61359
w_1_r2_10d_2	9	301687	184604	184554	184345	180408	180178	174903
w_1_r2_29d_1	10	120509	72680	72612	72536	70235	70074	69904
w_1_r2_29d_2	10	160109	97560	97493	97357	94195	93970	93833
w_1_r2_VerticalTrans_1	4	206267	120736	120624	120222	118275	118124	117301
w_1_r3_VerticalTrans_1	10	398820	232817	232734	231946	230352	227504	226582
w_2_r1_10d_1	9	192644	115370	115332	115177	114343	114343	113117
w_2_r1_10d_2	9	279236	168568	168517	168218	166890	166869	166488
w_2_r1_29d_1	8	155685	95016	94908	94766	92547	92408	91946
w_2_r1_VerticalTrans_1	10	258499	150454	150375	150009	147933	147770	144601
w_2_r2_10d_1	10	248622	150758	150685	150480	149184	149184	147344
w_2_r2_10d_2	4	378800	228769	228707	228452	226019	226014	224698
w_2_r2_29d_1	10	157947	95484	95413	95275	91478	91478	91234
w_2_r2_VerticalTrans_1	10	142551	86080	86013	85872	83170	83170	81939
w_2_r3_VerticalTrans_1	10	412044	244344	244272	243626	237903	237026	236340
w_2_r4_VerticalTrans_1	10	116841	68387	68299	68072	66661	66645	66111

* Genotype_Colonization Batch_Vial_Age/Life stage_sample replicate

** Reads that were matching tomitochondria, chloroplast or eukaryotes have been removed

Table S2

Fig 1

ADONIS on relative abundances with genotype as a factor, 999 Permutations						
	Df	SumsOfSqs	MeanSqs	F Model	R2	P-value
GENOTYPE	3	0.776	0.2585	2.75	0.303	0.03
RESIDUALS	19	1.784	0.0939		0.697	
Pairwise ADONIS (different model) between genotypes, 1000 permutations						
	F Model	R2	P-value	P-adjusted (FDR)		
dAMP-Lys	0.8553	0.078791	0.491508	0.524476		
dAMP-Rel	0.88605	0.099713	0.524476	0.524476		
dAMP-w	3.7167	0.25255	0.01998	0.05994		
Lys-Rel	3.55123	0.307433	0.085914	0.171828		
Lys-w	3.55123	0.052585	0.497502	0.524476		
Rel-w	17.75694	0.663639	0.003996	0.023976		
Homogeneity of multivariate dispersions with Genotype as a factor, 1000 permutations						
	Df	F Model	P-vALUE			
GENOTYPE	3	2.84				
RESIDUALS	19					
Pairwise comparisions from the same model:						
	Permuted P-value					
dAMP-Lys	0.995					
dAMP-Rel	0.0679					
dAMP-w	0.28					
Lys-Rel	0.015					
Lys-w	0.13					
Rel-w	0.02					

MAIN INTERACTION MODEL						
ADONIS on relative abundances with genotype and age as interacting factors, 999 Permutations						
	Df	SumsOfSqs	MeanSqs	F Model	R2	P-value
GENOTYPE	3	1.0456	0.34855	6.678	0.17489	0.002
AGE	1	2.3922	2.39216	45.835	0.40009	0.001
GENOTYPE X AGE	3	0.4014	0.13379	2.564	0.06713	0.03
RESIDUALS	41	2.1398	0.05219		0.35789	
Pairwise ADONIS (different model) between ages, 1000 permutations						
	SumsOfSqs	MeanSqs	F Model	R2	P-value	
10d - 29d	2.401378	2.401378	31.54751	0.401636	0.000999	
10 DAYS OLD FLIES						
ADONIS on relative abundances with genotype as a factor, 999 Permutations						
	Df	F Model	R2	P-value		
GENOTYPE	3	4.68	0.379	0.001		
RESIDUALS	23		0.621			
Pairwise ADONIS (different model) between genotypes, 1000 permutations						
	F Model	R2	P-value	P-adjusted (FDR)		
dAMP-Lys	2.2833	0.17189	0.090909	0.109091		
dAMP-Rel	4.2014	0.27638	0.042957	0.077922		
dAMP-w	1.8614	0.12525	0.144855	0.144855		
Lys-Rel	3.434	0.25562	0.051948	0.077922		
Lys-w	5.3992	0.31031	0.002997	0.017982		
Rel-w	7.8648	0.39592	0.005994	0.017982		
Homogeneity of multivariate dispersions with Genotype as a factor, 1000 permutations						
	Df	F Model	P-vALUE			
GENOTYPE	3	21.1	0.001			
RESIDUALS	23					
Pairwise comparisions from the same model:						
	Permuted P-value					
dAMP-Lys	0.125					
dAMP-Rel	0.002					
dAMP-w	0.230					
Lys-Rel	0.003					
Lys-w	0.000					
Rel-w	0.000					
29 DAYS OLD FLIES						
ADONIS on relative abundances with genotype as a factor, 999 Permutations						
	Df	F Model	R2	P-value		
GENOTYPE	3	4.26	0.415	0.008		
RESIDUALS	18		0.585			
Pairwise ADONIS (different model) between genotypes, 1000 permutations						
	F Model	R2	P-value	P-adjusted (FDR)		
dAMP-Lys	1.7118	0.134662	0.195804	0.29371		
dAMP-Rel	0.29448	0.046784	0.926074	0.92607		
dAMP-w	8.3592	0.481543	0.01998	0.03996		
Lys-Rel	1.04833	0.104329	0.402597	0.48312		
Lys-w	7.72731	0.391706	0.013986	0.03996		
Rel-w	9.40865	0.573396	0.018981	0.03996		

Bibliography

1. Belkaid Y, Harrison OJ. 2017. Homeostatic Immunity and the Microbiota. Immunity 46:562–576.

2. Kim S, Jazwinski SM. 2018. The Gut Microbiota and Healthy Aging: A Mini-Review. Gerontology 64:513–520.

3. Fung TC, Olson CA, Hsiao EY. 2017. Interactions between the microbiota, immune and nervous systems in health and disease. Nat Neurosci 20:145–155.

4. Boulangé CL, Neves AL, Chilloux J, Nicholson JK, Dumas ME. 2016. Impact of the gut microbiota on inflammation, obesity, and metabolic disease. Genome Med 8:1–12.

5. Zeng MY, Inohara N, Nuñez G. 2017. Mechanisms of inflammation-driven bacterial dysbiosis in the gut. Mucosal Immunol 10:18–26.

6. Douglas AE. 2018. The Drosophila model for microbiome research. Lab Anim (NY) 47:157–164.

7. Ma D, Storelli G, Mitchell M, Leulier F. 2015. Studying host-microbiota mutualism in Drosophila: Harnessing the power of gnotobiotic flies. Biomed J 38:285–293.

8. Broderick NA, Lemaitre B. 2012. Gut-associated microbes of Drosophila melanogaster. Gut Microbes 3:307–321.

9. Ludington WB, Ja WW. 2020. Drosophila as a model for the gut microbiome. PLoS Pathog 16:1–6.

10. Erkosar B, Storelli G, Defaye A, Leulier F. 2013. Host-intestinal microbiota mutualism: “learning on the fly.” Cell Host Microbe 13:8–14.

11. Storelli G, Defaye A, Erkosar B, Hols P, Royet J, Leulier F. 2011. Lactobacillus plantarum promotes drosophila systemic growth by modulating hormonal signals through TOR-dependent nutrient sensing. Cell Metab 14:403–414.

12. Keebaugh ES, Yamada R, Obadia B, Ludington WB, Ja WW. 2018. Microbial Quantity Impacts Drosophila Nutrition, Development, and Lifespan. iScience 4:247–259.

13. Fischer C, Trautman EP, Crawford JM, Stabb E V., Handelsman J, Broderick NA. 2017. Metabolite exchange between microbiome members produces compounds that influence

drosophila behavior. eLife 6:1–25.

14. Lee HY, Lee SH, Lee JH, Lee WJ, Min KJ. 2019. The role of commensal microbes in the lifespan of Drosophila melanogaster. Aging 11:4611–4640.

15. Sansone CL, Cohen J, Yasunaga A, Xu J, Osborn G, Subramanian H, Gold B, Buchon N, Cherry S. 2015. Microbiota-dependent priming of antiviral intestinal immunity in Drosophila. Cell Host Microbe 18:571–581.

16. Fast D, Petkau K, Ferguson M, Shin M, Galenza A, Kostiuk B, Pukatzki S, Foley E. 2020. Vibrio cholerae-Symbiont Interactions Inhibit Intestinal Repair in Drosophila. Cell Rep 30:1088-1100.e5.

17. Clark RI, Salazar A, Yamada R, Fitz-Gibbon S, Morselli M, Alcaraz J, Rana A, Rera M, Pellegrini M, Ja WW, Walker DW. 2015. Distinct Shifts in Microbiota Composition during Drosophila Aging Impair Intestinal Function and Drive Mortality. Cell Rep 12:1656–1667.

18. Li H, Qi Y, Jasper H. 2016. Preventing Age-Related Decline of Gut Compartmentalization Limits Microbiota Dysbiosis and Extends Lifespan. Cell Host Microbe 19:240–253.

19. Pais IS, Valente RS, Sporniak M, Teixeira L. 2018. Drosophila melanogaster establishes a species-specific mutualistic interaction with stable gut-colonizing bacteria. PLoS Biol 16:1–45.

20. Vandehoef C, Molaei M, Karpac J. 2020. Dietary Adaptation of Microbiota in Drosophila Requires NF-κB-Dependent Control of the Translational Regulator 4E-BP. Cell Rep 31:107736.

21. Buchon N, Broderick NA, Chakrabarti S, Lemaitre B. 2009. Invasive and indigenous microbiota impact intestinal stem cell activity through multiple pathways in Drosophila. Genes Dev 23:2333–2344.

22. Buchon N, Silverman N, Cherry S. 2014. Immunity in Drosophila melanogaster-from microbial recognition to whole-organism physiology. Nat Rev Immunol 14:796–810.

23. Lemaitre B, Hoffmann J. 2007. The Host Defense of *Drosophila melanogaster*. Annu Rev Immunol 25:697–743.

24. Royet J, Gupta D, Dziarski R. 2011. Peptidoglycan recognition proteins: Modulators of the microbiome and inflammation. Nat Rev Immunol 11:837–851.

25. Lesperance DNA, Broderick NA. 2020. Gut bacteria mediate nutrient availability in Drosophila diets . Appl Environ Microbiol 87:1–14.

26. Lin SJH, Cohen LB, Wasserman SA. 2020. Effector specificity and function in Drosophila innate immunity: Getting AMPed and dropping Boms. PLoS Pathog 16:1–6.

27. Hanson MA, Cohen LB, Marra A, Iatsenko I, Wasserman SA, Lemaitre B. 2020. The Drosophila Baramicin polypeptide gene protects against fungal infection bioRxiv https://doi.org/10.1101/2020.11.23.394148.

28. Broderick NA, Buchon N, Lemaitre B. 2014. Microbiota-induced changes in Drosophila melanogaster host gene expression and gut morphology. MBio 5:e01117-14.

29. Liehl P, Blight M, Vodovar N, Boccard F, Lemaitre B. 2006. Prevalence of local immune response against oral infection in a Drosophila/Pseudomonas infection model. PLoS Pathog 2:0551–0561.

30. Bosco-Drayon V, Poidevin M, Gomperts Boneca I, Narbonne-Reveau K, Royet J, Charroux B. 2012. Peptidoglycan sensing by the receptor PGRP-LE in the Drosophila gut induces immune responses to infectious bacteria and tolerance to microbiota. Cell Host Microbe 12:153–165.

31. Zaidman-Rémy A, Hervé M, Poidevin M, Pili-Floury S, Kim MS, Blanot D, Oh BH, Ueda R, Mengin-Lecreulx D, Lemaitre B. 2006. The Drosophila Amidase PGRP-LB Modulates the Immune Response to Bacterial Infection. Immunity 24:463–473.

32. Paredes JC, Welchman DP, Poidevin M, Lemaitre B. 2011. Negative regulation by Amidase PGRPs shapes the drosophila antibacterial response and protects the Fly from innocuous infection. Immunity 35:770–779.

33. Charroux B, Capo F, Kurz CL, Peslier S, Chaduli D, Viallat-lieutaud A, Royet J. 2018. Cytosolic and Secreted Peptidoglycan-Degrading Enzymes in Drosophila Respectively Control Local and Systemic Immune Responses to Microbiota. Cell Host Microbe 23:215-228.e4.

34. Ryu J, Kim S, Lee H, Bai JY, Nam Y, Bae J, Lee DG, Shin SC, Ha E, Lee W. 2008. Innate Immune Homeostasis by the Homeobox Gene Caudal and Commensal-Gut

Mutualism in Drosophila. Science (80-) 319:777–782.

35. Neyen C, Runchel C, Schüpfer F, Meier P, Lemaitre B. 2016. The regulatory isoform rPGRP-LC resolves immune activation through ESCRT-mediated receptor clearance. Nat Immunol 17:1150–1158.

36. Zaidman-Rémy A, Poidevin M, Hervé M, Welchman DP, Paredes JC, Fahlander C, Steiner H, Mengin-Lecreulx D, Lemaitre B. 2011. Drosophila immunity: Analysis of PGRP-SB1 expression, enzymatic activity and function. PLoS One 6 (2): e1723.

37. Guo L, Karpac J, Tran SL, Jasper H. 2014. PGRP-SC2 promotes gut immune homeostasis to limit commensal dysbiosis and extend lifespan. Cell 156:109–122.

38. Iatsenko I, Boquete J, Lemaitre B. 2018. Microbiota-Derived Lactate Activates Production of Reactive Oxygen Species by the Intestinal NADPH Oxidase Nox and Shortens Drosophila Lifespan. Immunity 49:929–942.

39. De Gregorio E, Spellman PT, Tzou P, Rubin GM, Lemaitre B. 2002. The Toll and Imd pathways are the major regulators of the immune response in Drosophila 21:2568–2579.

40. Zhai Z, Boquete JP, Lemaitre B. 2018. Cell-Specific Imd-NF-κB Responses Enable Simultaneous Antibacterial Immunity and Intestinal Epithelial Cell Shedding upon Bacterial Infection. Immunity 48:897-910.e7.

41. Myllymäki H, Valanne S, Rämet M. 2014. The Drosophila Imd Signaling Pathway . J Immunol 192:3455–3462.

42. Erkosar B, Defaye A, Bozonnet N, Puthier D, Royet J, Leulier F. 2014. Drosophila microbiota modulates host metabolic gene expression via IMD/NF-κB signaling. PLoS One 9 (4): e94729.

43. Buchon N, Broderick NA, Poidevin M, Pradervand S, Lemaitre B. 2009. Drosophila Intestinal Response to Bacterial Infection: Activation of Host Defense and Stem Cell Proliferation. Cell Host Microbe 5:200–211.

44. Imler J, Bulet P. 2005. Antimicrobial Peptides in Drosophila : Structures , Activities and Gene Regulation. Chem Imunol Allergy 86:1–21.

45. Hanson MA, Dostálová A, Ceroni C, Poidevin M, Kondo S, Lemaître B. 2019. Synergy and remarkable specificity of antimicrobial peptides in vivo using a systematic knockout

approach. eLife 8:e44341.

46. Daffre S, Kylsten P, Samakovlis C, Hultmark D. 1994. The lysozyme locus in Drosophila melanogaster: an expanded gene family adapted for expression in the digestive tract. MGG Mol Gen Genet 242:152–162.

47. Regel R, Matioli SR, Terra WR. 1998. Molecular adaptation of Drosophila melanogaster lysozymes to a digestive function. Insect Biochem Mol Biol 28:309–319.

48. Nash JA, Ballard TNS, Weaver TE, Akinbi HT. 2006. The Peptidoglycan-Degrading Property of Lysozyme Is Not Required for Bactericidal Activity In Vivo. J Immunol 177:519–526.

49. Zaynoun A, Kallassy Awad M, Rejasse A, Courtin P, Gomberts Boneca I, Chapot-Chartier M-P, Sanchis Borja V, El Chamy L. 2019. D-alanylation of Techoic Acids in Bacilli impedes the immune sensing of peptidoglycan in Drosophila. bioRxiv https://doi.org/10.1101/631523.

50. Shin SC, Kim S-H, You H, Kim B, Kim AC, Lee K-A, Yoon J-H, Ryu J-H, Lee W-J. 2011. Drosophila Microbiome Modulates Host Developmental and Metabolic Homeostasis via Insulin Signaling. Science (80-) 334:670–674.

51. Lemaitre B, Reichhart JM, Hoffmann JA. 1997. Drosophila host defense: Differential induction of antimicrobial peptide genes after infection by various classes of microorganisms. Proc Natl Acad Sci U S A 94:14614–14619.

52. Erkosar B, Kolly S, van der Meer JR, Kawecki TJ. 2017. Adaptation to chronic malnutrition leads to reduced dependence on microbiota in Drosophila. MBio 8:e01496.

53. Schleifer KH, Kandler O. 1972. Peptidoglycan types of bacterial cell walls and their taxonomic implications. Bacteriol Rev 36:407–477.

54. Leulier F, Parquet C, Pili-Floury S, Ryu JH, Caroff M, Lee WJ, Mengin-Lecreulx D, Lemaitre B. 2003. The Drosophila immune system detects bacteria through specific peptidoglycan recognition. Nat Immunol 4:478–484.

55. Kaneko T, Goldman WE, Mellroth P, Steiner H, Fukase K, Kusumoto S, Harley W, Fox A, Golenbock D, Silverman N. 2004. Monomeric and polymeric gram-negative peptidoglycan but not purified LPS stimulate the Drosophila IMD pathway. Immunity 20:637–649.

56. Kleerebezem M, Hols P, Bernard E, Rolain T, Zhou M, Siezen RJ, Bron PA. 2010. The extracellular biology of the lactobacilli. FEMS Microbiol Rev 34:199–230.

57. Chang JD, Wallace AG, Foster EE, Kim SJ. 2018. Peptidoglycan Compositional Analysis of Enterococcus faecalis Biofilm by Stable Isotope Labeling by Amino Acids in a Bacterial Culture. Biochemistry 57:1274–1283.

58. Lee KA, Kim SH, Kim EK, Ha EM, You H, Kim B, Kim MJ, Kwon Y, Ryu JH, Lee WJ. 2013. Bacterial-derived uracil as a modulator of mucosal immunity and gut-microbe homeostasis in drosophila. Cell 153:797–811.

59. Callahan BJ, McMurdie PJ, Holmes SP. 2017. Exact sequence variants should replace operational taxonomic units in marker-gene data analysis. ISME J 11:2639–2643.

60. Edgar R. 2016. UNOISE2: improved error-correction for Illumina 16S and ITS amplicon sequencing. bioRxiv https://doi.org/10.1101/081257.

61. Amnon A, Daniel M, Navas-Molina J, Kopylova E, Morton J, Xu ZZ, Eric K, Thompson L, Hyde E, Gonzalez A, Knight R. 2017. Deblur Rapidly Resolves Single-Nucleotide Community Sequence Patterns. Am Soc Microbiol 2:e00191-16.

62. Yamada Y, Yukphan P. 2008. Genera and species in acetic acid bacteria. Int J Food Microbiol 125:15–24.

63. Dutta D, Gachhui R. 2006. Novel nitrogen-fixing Acetobacter nitrogenifigens sp. nov., isolated from Kombucha tea. Int J Syst Evol Microbiol 56:1899–1903.

64. Kešnerová L, Mars RAT, Ellegaard KM, Troilo M, Sauer U, Engel P. 2017. Disentangling metabolic functions of bacteria in the honey bee gut. PLoS Biol 15(12): e2003467.

65. Erkosar B, Yashiro E, Zajitschek F, Friberg U, Maklakov AA, van der Meer JR, Kawecki TJ. 2018. Host diet mediates a negative relationship between abundance and diversity of Drosophila gut microbiota. Ecol Evol 8:9491–9502.

66. Duneau D, Ferdy J-B, Revah J, Kondolf H, Ortiz GA, Lazzaro BP, Buchon N. 2017. Stochastic variation in the initial phase of bacterial infection predicts the probability of survival in D. melanogaster. eLife 6:e28298.

67. Zhai Z, Huang X, Yin Y. 2018. Beyond immunity: The Imd pathway as a coordinator of

host defense, organismal physiology and behavior. Dev Comp Immunol 83:51–59.

68. Petkau K, Ferguson M, Guntermann S, Foley E. 2017. Constitutive Immune Activity Promotes Tumorigenesis in Drosophila Intestinal Progenitor Cells. Cell Rep 20:1784–1793.

69. Cox CR, Gilmore MS. 2007. Native microbial colonization of Drosophila melanogaster and its use as a model of Enterococcus faecalis pathogenesis. Infect Immun 75:1565–1576.

70. Hanson MA, Dostálová A, Ceroni C, Poidevin M, Kondo S, Lemaitre B. 2019. Synergy and remarkable specificity of antimicrobial peptides in vivo using a systematic knockout approach. eLife 8:e44341.

71. Callewaert L, Michiels CW. 2010. Lysozymes in the animal kingdom. J Biosci 35:127–160.

72. Ito Y, Nakamura M, Hotani T, Imoto T. 1995. Insect lysozyme from house fly (Musca domestica) larvae: Possible digestive function based on sequence and enzymatic properties. J Biochem 118:546–551.

73. De Gregorio E, Spellman PT, Tzou P, Rubin GM, Lemaitre B. 2002. The Toll and Imd pathways are the major regulators of the immune response in Drosophila. EMBO J 21:2568–2579.

74. Molaei M, Vandehoef C, Karpac J. 2019. NF-κB Shapes Metabolic Adaptation by Attenuating Foxo-Mediated Lipolysis in Drosophila. Dev Cell 49:802–810.

75. Nandy A, Lin L, Velentzas PD, Wu LP, Baehrecke EH, Silverman N. 2018. The NF-κB Factor Relish Regulates Atg1 Expression and Controls Autophagy. Cell Rep 25:2110-2120.e3.

76. McFall-Ngai M, Heath-Heckman EAC, Gillette AA, Peyer SM, Harvie EA. 2012. The secret languages of coevolved symbioses: Insights from the Euprymna scolopes-Vibrio fischeri symbiosis. Semin Immunol 24:3–8.

77. Joye P, Kawecki TJ. 2019. Sexual selection favours good or bad genes for pathogen resistance depending on males' pathogen exposure. Proc R Soc B Biol Sci 286:20190226.

78. Kešnerová L, Emery O, Troilo M, Liberti J, Erkosar B, Engel P. 2020. Gut microbiota structure differs between honeybees in winter and summer. ISME J 14:801–814.

79. Stoddard SF, Smith BJ, Hein R, Roller BRK, Schmidt TM. 2015. rrnDB: Improved tools for interpreting rRNA gene abundance in bacteria and archaea and a new foundation for future development. Nucleic Acids Res 43:D593–D598.

80. McMurdie PJ, Holmes S. 2013. Phyloseq: An R Package for Reproducible Interactive Analysis and Graphics of Microbiome Census Data. PLoS One 8:e61217–e61217.

81. Gentleman R, Carey V, Huber W, Hahne F. 2018. Genefilter: methods for filtering genes from high-throughput experiments. R package version 1.62. 0. Available here https//bioconductor org/packages/release/bioc/html/genefilter html Accessed June.

82. Bray JR, Curtis JT. 1957. An Ordination of the Upland Forest Communities of Southern Wisconsin. Ecol Monogr 27:325–349.

83. Anderson MJ. 2006. Distance-based tests for homogeneity of multivariate dispersions. Biometrics 62:245–253.

84. Anderson MJ, Ellingsen KE, McArdle BH. 2006. Multivariate dispersion as a measure of beta diversity. Ecol Lett 9:683–693.

Chapter III

The iron transporter Transferrin 1 mediates homeostasis of the endosymbiotic relationship between *Drosophila melanogaster* and *Spiroplasma poulsonii*

Alice Marra, Florent Masson†* and Bruno Lemaitre†*

Global Health Institute, School of Life Sciences, École Polytechnique Fédérale de Lausanne (EPFL), Lausanne, Switzerland

†Joint last authors

* Correspondance: B. Lemaitre (bruno.lemaitre@epfl.ch), F. Masson (florent.masson@epfl.ch)

Running title: Transferrin 1 and *Spiroplasma poulsonii* endosymbiosis

Key words: endosymbiosis, *Spiroplasma*, transferrin, iron sequestration

Abstract

Iron is involved in numerous biological processes in both prokaryotes and eukaryotes and is therefore subject to a tug-of-war between host and microbes upon pathogenic infections. In the fruit fly *Drosophila melanogaster*, the iron transporter Transferrin 1 (Tsf1) mediates iron relocation from the hemolymph to the fat body upon infection as part of the nutritional immune response. The sequestration of iron in the fat body renders it less available for pathogens to proliferate and enhances the host ability to fight the infection. Here we investigate the interaction between host iron homeostasis and the facultative, vertically transmitted, endosymbiont of *Drosophila, Spiroplasma poulsonii*. This low-pathogenicity bacterium is devoid of cell wall and is able to thrive in the host hemolymph without triggering pathogen-responsive canonical immune pathways. However, hemolymph proteomics revealed an enrichment of Tsf1 in infected flies. We find that *S. poulsonii* induces tsf1 expression and triggers an iron sequestration response similarly to pathogenic bacteria. We next demonstrate that free iron cannot be used by *Spiroplasma* while Tsf1-bound iron promotes bacterial growth, underlining the adaptation of *Spiroplasma* to the intra-host lifestyle where iron is mostly protein-bound. Our results show that Tsf1 is used both by the fly to sequester iron and by *Spiroplasma* to forage host iron, making it a central protein in endosymbiotic homeostasis.

Background

The sequestration of trace minerals by a host organism is increasingly recognized as part of a "nutritional" immunity, as it limits microbes' proliferation [1]. Iron in particular is involved in numerous processes in both eukaryotes and prokaryotes, and has been identified as a critical trace metal in determining the outcome of pathogenic infections [2]. Consequently, iron-transporting proteins which are involved in iron sequestration upon infection are under strong selective pressure in the arms race between hosts and pathogens [3].

Similarly to mammals, the fruit fly *Drosophila melanogaster* uses iron sequestration as an immune defense mechanism [4]. *Drosophila* iron transport and storage rely on three Ferritin (Fer) and three transferrin homologues (Tsf1, Tsf2 and Tsf3). Ferritins are involved in iron absorption, transport and storage and are particularly important during embryonic development [5–7]. More recently, Fer1 has also been identified as a potent antioxidant in mitochondria [8]. *Drosophila* Transferrins are considered as transport proteins based on their homology with mammalian Transferrins, although genetics and expression studies have revealed that the three isoforms have distinct and initially unexpected functions. Tsf2 is an integral component of epithelial septate junctions and may have no role in iron transport [9]. Tsf3 is poorly characterized but possibly involved in the circadian rhythm regulation [10]. Tsf1 participates in iron trafficking [11] and is inducible upon infection. Its involvement in nutritional immunity has been experimentally demonstrated: by mediating iron sequestration from the hemolymph to the fat body, it reduces iron availability in the hemolymph and consequently enhances fly resistance to infections by *Pseudomonas aeruginosa* and Mucorales fungi [4].

Iron management is however not central in pathogenic interactions only: a growing number of cooperative iron management strategies is getting described between host and mutualistic microbes [12]. Insects are particularly concerned with associations with endosymbiotic bacteria, i.e. bacteria living within host tissues [13]. Some endosymbionts are intracellular and act as obligate for the host, as they provision nutrients without which the host cannot develop properly [14]. Others are facultative (they do not systematically infect all individuals of their host species) and provide the host with context-dependent ecological advantages, such as a reduction of predation risk [15], feeding specialization [16] or protection against natural enemies [17–21]. Some facultative endosymbionts also evolved the ability to manipulate their host reproduction to enhance their own prevalence in the population [22,23]. As endosymbionts are confined within host tissues, they get supplied with nutrients by carrying on intensive metabolic interactions with their host. These interactions were largely studied for

organic molecules such as amino-acids and vitamins [24], but little is known about the function of trace metals in endosymbiotic homeostasis. Proteomics on a free-living relative of the aphid facultative endosymbiont *Serratia symbiotica* revealed several proteins involved in iron metabolism suspected to participate in host iron acquisition at the nascent stage of symbiosis [25]. The Tsetse fly facultative endosymbiont *Sodalis glossinidius* also expresses genes encoding for iron uptake and transport [26] and a mutant defective for the outer membrane heme transporter HemR has an impaired ability to colonize the host gut, indicating that iron metabolism is important to sustain the tsetse fly symbiotic homeostasis [27]. Iron homeostasis has also been highlighted as a key factor regulating *Wolbachia* interaction with its insect hosts. *Wolbachia* is an extremely widespread endosymbiont that can efficiently manipulate the reproduction of various arthropod hosts by four distinct mechanisms that helped it reach a prevalence of over 80% in some host species [28–30]. It produces Bacterioferritins that scavenge iron to sustain bacterial proliferation and consequently help the host coping with iron overload in the diet [31]. *Wolbachia* infection also confers a fecundity benefit to *Drosophila melanogaster* reared on both low-iron and high-iron diets, indicating a global buffering role of *Wolbachia* for this nutrient [32]. These examples suggest that iron could be an important nutrient in mediating homeostasis in a wider range of insect endosymbioses.

Spiroplasma poulsonii (hereafter *Spiroplasma*) is one of the two heritable endosymbionts that naturally infect *Drosophila* flies, along with *Wolbachia* [33]. *Spiroplasma* belongs to the Mollicutes, a class of bacteria that is devoid of a cell wall. As it does not expose peptidoglycan or other known bacteria-associated molecular patterns on its surface, *Spiroplasma* is not expected to be recognized by the fly immune system, although this assumption is put into question by recent results suggesting a basal stimulation of the Toll pathway [34]. In return, host immunity seems to have no effect on *Spiroplasma* proliferation, suggesting that titer control is rather mediated by metabolic processes [35,36]. *Spiroplasma* lives free in the host hemolymph and gets vertically transmitted by co-opting the yolk uptake machinery of oocytes [37]. Most *Spiroplasma* strains also cause two remarkable phenotypes in *Drosophila*: male killing, whereby infected male offspring is killed during early embryogenesis by the action of a bacterial toxin [38], and protection the host against nematode and parasitoid wasp infections [20,39–41].

The metabolic interactions between *Spiroplasma* and *Drosophila* are still largely elusive, although previous reports showed that the bacterium relies on host circulating diacyglycerides to proliferate [42]. The requirement for other nutrients (amino-acids, vitamins or trace metals for example) has not been explored yet. The genome of *Spiroplasma* encodes for three ferritin-

like genes of which one is induced upon host contact compared to *in vitro* culture, suggesting a role of this in endosymbiosis [43]. This prompted us to investigate the role of iron homeostasis in the *Drosophila-Spiroplasma* symbiosis. We first show that *Drosophila* generates a nutritional immune response against *Spiroplasma* by sequestering iron. Using flies carrying a loss-of-function allele of *tsf1*, we further demonstrate that *Spiroplasma* growth relies on host Tsf1, and that the bacteria uptakes iron when it is Tsf1-complexed and not when it is free. This indicates an evolved ability of *Spiroplasma* to highjack the Tsf1-related iron transport of the host to get access to iron to sustain its own growth.

Results

1. Tsf1 is enriched in *Spiroplasma*-infected flies

A recent proteomics profiling revealed an enrichment of Tsf1 in *Spiroplasma*-infected hemolymph of adult females [34]. Other proteins related to iron transport and storage were identified in the fly hemolymph, notably Fer1HCH and Fer2LCH, but Tsf1 was the only one to be significantly more abundant upon *Spiroplasma* infection (**Fig 1A**). Tsf2 and Tsf3 were not detected in the hemolymph.

We first sought to confirm Tsf1 response to *Spiroplasma* infection by measuring the expression of the *tsf1* gene across fly life stages in infected versus uninfected flies (**Fig 1B**). Both the infection status and the life stage had a significant effect on *tsf1* expression level (p-value Infection = 10^{-4}, p-value LifeStage = 10^{-9}, p-value Interaction = 10^{-4}). Post-hoc testing indicates that *Tsf1* increased expression upon *Spiroplasma* infection was markedly significant only in 2-weeks old adults, but although non significant this tendency was also observed for larval and pupal stages and for 1-week-old adults (**Fig 1B**).

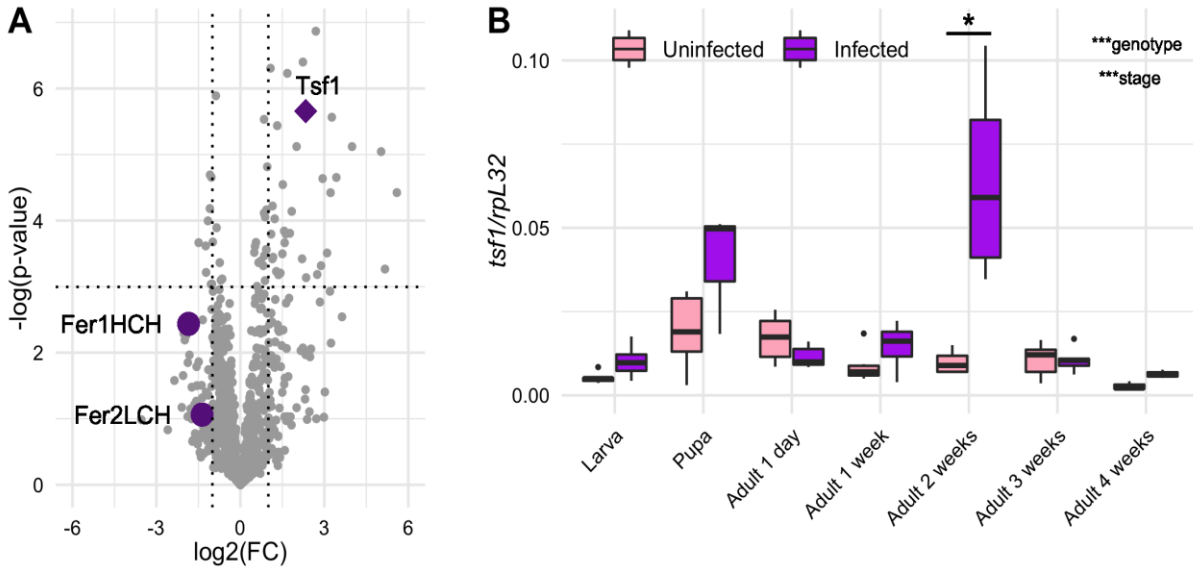

Fig 1 - Tsf1 is enriched in *Spiroplasma* infected flies.

(A) Proteomics profiling of *Spiroplasma*-infected hemolymph from Masson, Rommelaere *et al.* 2021 [34]. FC represents the fold-change between infected and uninfected flies. Dotted lines indicate the significance thresholds (log2(FC) = -1 or 1 for vertical lines, p-value = 0.05 for the horizontal line). Each grey dot represents a protein or a protein group. Purple symbols represent proteins related to iron transport and storage. (B) RT-qPCR quantification of *tsf1* transcript levels in infected versus uninfected flies across life stages. Boxplots indicate the mean and interquartile range. Isolated dots represent outliers. Data was analyzed by two-way ANOVA followed by a Tukey HSD post-hoc testing. Indications in the upper part of the graph display the ANOVA p-values for the factors "*Developmental stage*" (stage) and "genotype". *** = p-value < 0.001 ; ** = p-value < 0.01 ; * = p-value < 0.05.

2. Host Tsf1 is required for *Spiroplasma* growth but not for vertical transmission

The observation that *tsf1* was induced by *Spiroplasma* infection, as well as the Tsf1 enrichment in infected hemolymph, pointed to a possible role of Tsf1 and iron in the regulation of the *Drosophila-Spiroplasma* interaction. To test this we infected a mutant fly line carrying a null *tsf1* allele ($tsf1^{JP94}$, hereafter *tsf1*) [4] and compared the *Spiroplasma* titer to that of the control w^{1118} line over all developmental stages of the fly. Although *tsf1* mutant larvae and early pupae exhibited a normal *Spiroplasma* titer, a marked decreased was observed in late *tsf1* mutant pupae compared to the control (**Fig 2A**). A similar decrease in *Spiroplasma* titer was also observed in 4 weeks old females but not in 1 week old females (**Fig 2B**). In wild-type flies, *Spiroplasma* titer increases over fly development and aging: It dramatically increases at mid-

pupation and then grows exponentially during adulthood [35]. Our results suggest that *tsf1* is required for *Spiroplasma* only at high titer, hence when the most bacteria are competing with the host for iron usage.

Remarkably, the *tsf1* mutant line was unusually difficult to infect by *Spiroplasma* injection and required several attempts before being stably infected. Furthermore, we tried to confirm this phenotype by infecting a stock carrying a chromosomal deficiency containing the *tsf1* gene, and we could not infect this line despite several attempts. This suggests that the lack of *tsf1* makes flies partially refractory to *Spiroplasma* artificial infections. We could however confirm the requirement of *tsf1* for *Spiroplasma* proper growth using RNA interference (RNAi). A RNAi targeting *tsf1* driven by the ubiquitously expressed driver *actin5C-GAL4* led to a normal titer in 1 week old flies and decreased titer in 4 weeks old flies, mimicking the phenotype of the *tsf1* mutant (**Fig 2C**).

Spiroplasma infection severely reduces *Drosophila* lifespan [42]. The *tsf1* mutant line infected with *Spiroplasma* had an increased lifespan compared to infected controls, in accordance with its decreased bacterial titer (**Fig 2D**).

The *tsf1* mutation did not however impair vertical transmission, as evidenced by the stability of the infection over generations and by the titer in embryos that was similar to that from control flies (**Fig 2E**). Male-killing was also unaffected by the *tsf1* mutation as the progeny of the mutant line was 100% female for over two years after the initial infection.

The decreased titer and consequent increased lifespan of the *tsf1* mutant upon *Spiroplasma poulsonii* infection was also observed upon *Spiroplasma citri* acute infection (**Figure S1**). *S. citri* is a closely related species that infects plants and insects with a strict horizontal transmission. It causes lethal infections when injected into the hemolymph of *Drosophila* [35,44]. Similar phenotypes between *S. poulsonii* and *S. citri* indicate *tsf1* requirement is a general requirement of the *Spiroplasma* genus rather than a *S. poulsonii* specificity.

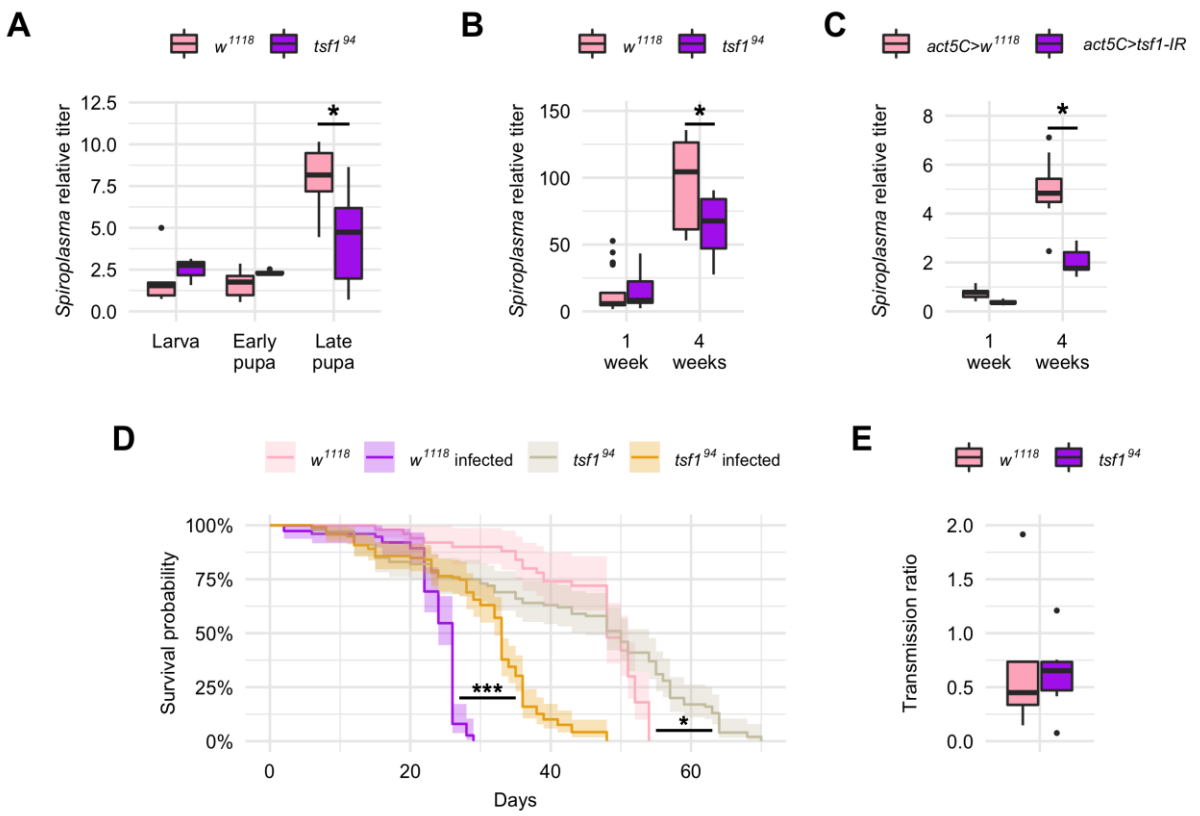

Fig 2 - Tsf1 is required for *Spiroplasma* growth at precise life stages of the host.

Spiroplasma qPCR quantification across developmental stages (A) and in adult females (B) for w^{1118} wild-type flies and *tsf1* mutant flies. (C) *Spiroplasma* qPCR quantification in flies expressing a dsRNA targeting *tsf1* under the control of the ubiquitous *act5C-GAL4* driver. *Spiroplasma* relative titer was calculated as the copy number of the *dnaK* gene normalized by that of the host gene *rps17* following the ΔΔCT method. Boxplots indicate the mean and interquartile range. Isolated dots represent outliers. Data from panels A and B were split for better readability but were analyzed as a whole using a two-way ANOVA followed by Tukey HSD post-hoc testing. * = p-value < 0.05 at the post-hoc testing. (D) Lifespan of infected and uninfected *tsf1* mutant flies compared to their w^{1118} wild-type counterparts (N = 344). Data were analyzed by pairwise Log-Rank test with Benjamini-Hochberg correction for multiple testing. *** = p-value < 0.001; * = p-value < 0.05. (E) Transmission ratio of *tsf1* mutant flies compared to their w^{1118} wild-type counterparts. Transmission was calculated as the *Spiroplasma* relative quantification in embryos normalized by the *Spiroplasma* relative quantification in adult females at the time eggs were laid. Boxplots indicate the mean and interquartile range. Isolated dots represent outliers. Data were analyzed with a Student t-test (not significant).

3. *Spiroplasma* infection triggers iron sequestration in the fat body

Pathogenic infections in *Drosophila* trigger a Tsf1-dependent nutritional immune response whereby iron gets depleted from the hemolymph and sequestrated in the fat body to decrease its availability for invading pathogens [4]. We proceeded with a quantification of total iron in fly tissues to see if a similar defense response was observed upon *Spiroplasma* infection, in wild type and *tsf1* mutant flies (**Fig 3A**). Iron quantification made on whole flies indicated that Tsf1 does not regulate total iron in the fly, and that *Spiroplasma* causes iron depletion in both genotypes (**Fig 3A**). *Spiroplasma*-induced iron depletion was stronger in *tsf1* mutants (-40% in infected flies in average) than in wild type controls (-24% in infected flies in average).

The iron depletion was specific to the hemolymph were *Spiroplasma* reside. The infection caused a significant iron decrease of similar amplitude in both genotypes, although not statistically significant. On the other hand, the iron amount in the fat body was tendentially higher in both genotypes. The trend was statistically significant only in the wild type controls for which iron increase in the fat body reached +59% in average upon infection versus only +29% in average in *tsf1* infected mutants (**Fig 3A**).

To confirm this results, we then monitored iron sequestration in the fat body by an alternative approach. We stained whole flies slices with Perl's Prussian blue, a stain commonly used to detect iron in tissues. The staining revealed iron inclusions in adipocytes from *Spiroplasma*-infected wild-type flies, seen as blue deposits that were undetectable in the fat body of uninfected flies (**Fig 3B**).

Collectively, these results show that *Spiroplasma* induces a nutritional immune response in *Drosophila*. This response translates into iron depletion from the hemolymph and iron sequestration in the fat body. It also indicates that Tsf1 participates in maintaining total iron levels in whole flies and in the iron sequestration in the fat body upon *Spiroplasma* infection, although to a lesser extent compared to the case of an accute infection with pathogenic microbes [4].

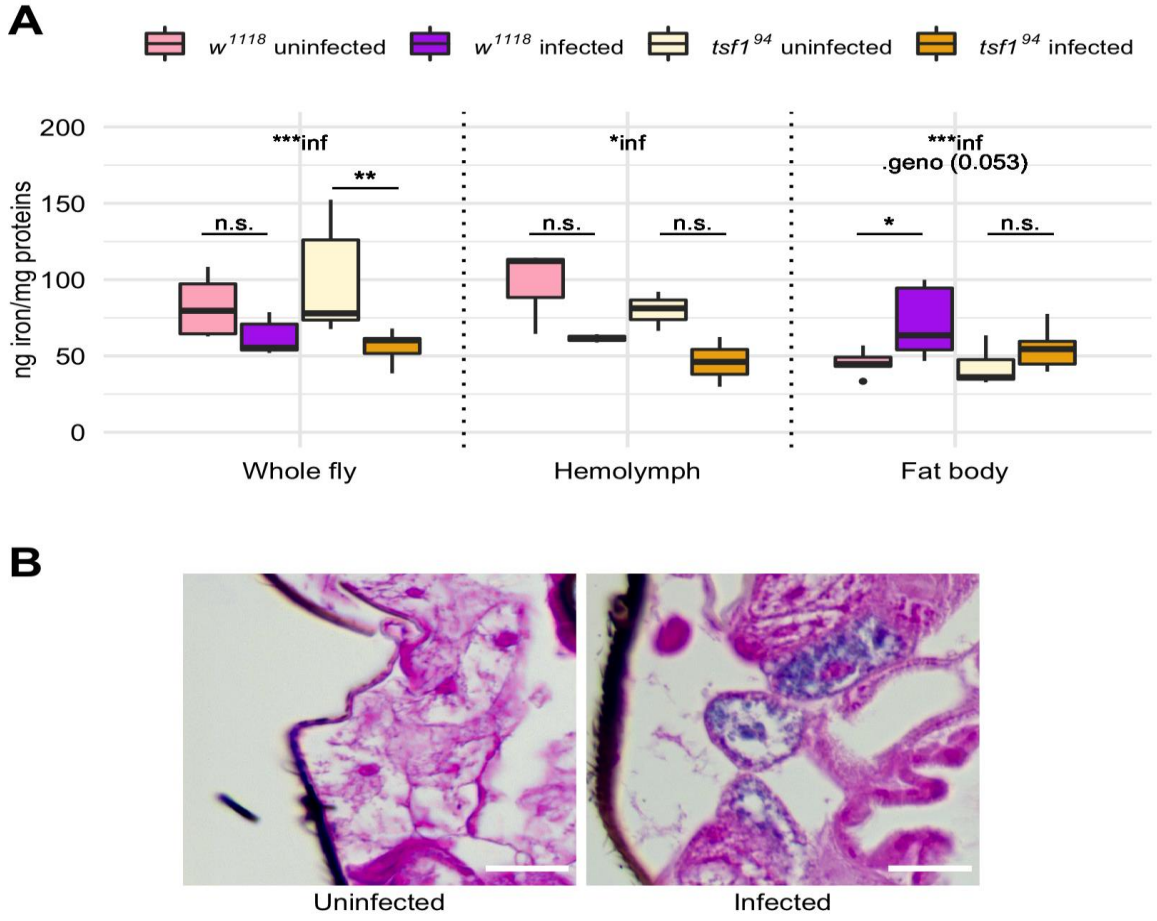

Fig 3 - Iron quantification in fly tissues upon *Spiroplasma* infection.

(A) Iron quantification by ICP-OES in whole flies and in dissected tissues. Iron amount is expressed as ng of iron normalized by mg of proteins in the samples. Boxplots indicate the mean and interquartile range. Isolated dots represent outliers. As samples were independent, data were analyzed by two-way ANOVA per tissue followed by Tukey HSD post-hoc testing. Indications in the upper part of each graph display the ANOVA p-values for the factors "*Spiroplasma* infection" (inf) and "genotype" (geno), when significant. *** = p-value < 0.001 ; ** = p-value < 0.01 ; * = p-value < 0.05. (B) Prussian blue staining on w^{1118} wild-type flies infected or not by *Spiroplasma*. Iron is visible as blue deposits in the cytosol of adipocytes from infected flies only.

4. *Spiroplasma* growth requires Tsf1-complexed iron but not free iron

The negative impact of Tsf1 absence on *Spiroplasma* growth suggests that *Spiroplasma* relies on this protein to get iron. Therefore we investigated whether *Spiroplasma* growth relies on the uptake of free iron or rather on Tsf1-complexed iron. For this, we compared *Spiroplasma* titer in wild type flies raised on a diet either i) enriched in iron through ferric ammonium citrate

(FAC) supplementation, or ii) in which iron was made biologically unavailable by adding the iron chelator bathophenanthrolinedisulfonic acid (BPS). FAC and BPS supplementations were performed on a standard diet (**Fig 4A**) or on an iron-poor diet (**Fig 4B**). We first verified that iron manipulation in the diet had a significant impact on total iron in the flies (**Fig S2**), and then performed *Spiroplasma* titer measurements over three weeks. None of the diet/treatment combination had any significant impact on *Spiroplasma* titer, which indicates that free iron availability is not required for nor detrimental to bacterial growth (**Fig 4A and 4B**).

Upon feeding, iron availability for bacteria living in the hemolymph is however dependent on a series of processes: i) the reduction of free (ferric) iron Fe^{3+} into free (ferrous) iron Fe^{2+} in the gut lumen; ii) Fe^{2+} uptake in the enterocytes through the metal transporter Malvolio; and iii) iron provisioning to the tissues through Fe-S synthesis in the enterocytes, Fe^{3+} complexation with Ferritin or Tsf1, or direct Fe^{3+} export in the hemolymph through multicopper oxidases [6,45,46]. To circumvent all these steps and verify in a more direct fashion the effect of free iron on *Spiroplasma* growth with the least possible bias, we proceeded in injecting FAC or BPS directly in fly thorax and measured *Spiroplasma* titer one week later (**Fig 4C**). Here again we observed no significant effect, although both treatments led to a slightly lower titer (possibly because of the deleterious effects of the compound injection procedure regardless of their iron-related effect, see Discussion section). We also tried to inject bovine hemin, a porphyrin that contains a ferric ion Fe^{3+}. To our surprise, hemin injection caused an upwards trend on *Spiroplasma* titer. The difference was not significant compared to PBS injection, but close to the threshold when compared to other treatments (p-value of the pairwise comparison with FAC injection = 0.041; with BPS injection = 0.059; **Fig 4C**). This could be an indication that iron fosters *Spiroplasma* growth only when complexed to an organic carrier.

We thus wanted to verify if Tsf-complexed iron had a direct positive impact on *Spiroplasma* growth. To this end, we injected commercial mammal Tsf carrying a Fe^{3+} ion (holo-Tsf) or not bound to iron (apo-Tsf) and measured *Spiroplasma* titer after one week (**Fig 4D**). We observed a significant positive effect on *Spiroplasma* growth upon holo-Tsf injection, but not upon apo-Tsf injection. This provides a strong evidence that *Spiroplasma* requires iron complexed to Tsf, and not the Tsf protein itself.

Remarkably, the positive effect of holo-Tsf injection was not observed in *tsf1* mutant flies, pointing that iron-protein complexes have an impact only in presence of the native *Drosophila* Tsf1. Iron binding to Transferrins is a spontaneous, competitive, ionic bounding (illustrated by the ability of other metal ions to replace Fe^{3+} upon competition for the binding site [47,48]), hence ion-exchange from holo- to apo-Tsf are expectable *in vivo*, although this has not been

formally demonstrated due to technical hurdles. An attractive hypothesis to explain *Spiroplasma* titer increase upon holo-Tsf injection could be that iron gets transferred from fully loaded bovine Tsf to partially loaded *Drosophila* Tsf1, where it becomes usable by *Spiroplasma*.

Collectively, these results indicate that *Spiroplasma* is not able to benefit from free iron availability but rather relies on iron complexed with host carrier proteins.

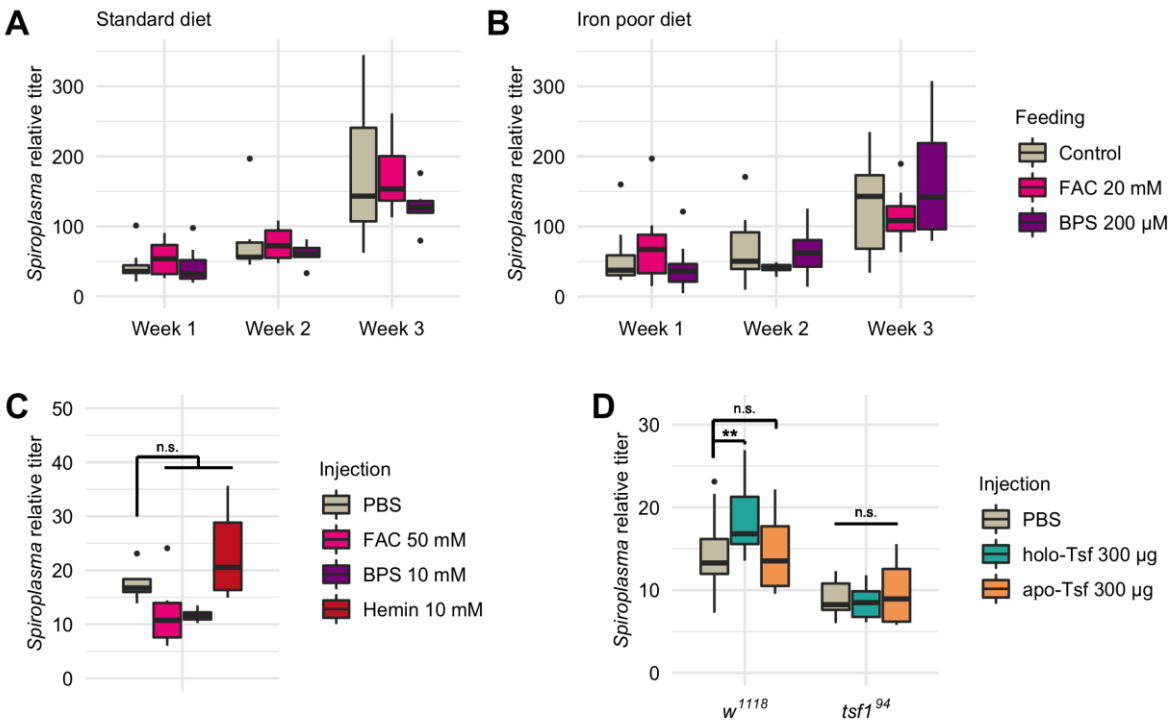

Fig 4 - *Spiroplasma* growth is not affected by free iron but fostered by Tsf-complexed iron.

Spiroplasma quantification in w^{1118} wild-type flies raised on standard (A) or iron poor (B) diet supplemented with FAC or BPS. (C) *Spiroplasma* quantification in w^{1118} flies one week after injection of FAC, BPS or hemin. (D) *Spiroplasma* quantification in w^{1118} wild-type flies or *tsf1* flies one week after injection of holo-Tsf (iron bound) or apo-Tsf (not iron bound). Boxplots indicate the mean and interquartile range. Isolated dots represent outliers. *Spiroplasma* relative titer was calculated as the copy number of the *dnaK* gene normalized by that of the host gene *rps17* following the ΔΔCT method.

Data were analyzed with a two-way ANOVA for panels A and B (no significant effect of the treatment) and C (p-value treatment = 0.099; p-value genotype = 10^{-9}) and with a one-way ANOVA for panel C (p-value treatment = 0.030). TukeyHSD post-hoc testing was performed for pairwise comparisons when the ANOVA p-value was below 0.05. *** = p-value < 0.001 ; ** = p-value < 0.01 ; * = p-value < 0.05.

Discussion

Iron is well established as a disputed nutrient between hosts and microbial pathogens. Its function in insect interactions with their microbial symbionts remains however poorly understood. Here, we demonstrate that iron is also disputed between *Drosophila* and its heritable endosymbiont *Spiroplasma poulsonii*. We show that *Spiroplasma* infection causes an induction of the Tsf1 coding gene in *Drosophila* and a Tsf1 enrichment in the hemolymph of the fly, were *Spiroplasma* resides. By leveraging *Drosophila* genetics, we pinpoint the requirement of *tsf1* gene for a normal *Spiroplasma* growth, especially at the pupal stage and in older flies. We also show that Tsf1 participates in iron sequestration in the fat body upon *Spiroplasma* infection to a lesser extent than upon pathogenic infections, and that *Spiroplasma* requires Tsf-complexed iron to sustain its growth. Collectively, our results pinpoint Tsf1 as a regulator of endosymbiosis stability, as it is central for both the symbiont iron uptake and the host iron transport and sequestration.

The requirement of Tsf1 for *Spiroplasma* growth only at a specific host developmental stage (late pupation) is intriguing. Developmental high-throughput analyses in *Drosophila* revealed a peak of *tsf1* expression at early pupation [49] that translates into steadily increasing protein abundance during the whole pupation process [50]. This suggests an increasing requirement for Tsf1 during host pupation (possibly to sustain the massive tissue remodeling and proliferation), hence a stronger competition with *Spiroplasma* for Tsf1 at this developmental stage specifically. The Tsf1 loss-of-function also had a stronger effect on *Spiroplasma* growth in aging flies, when *Spiroplasma* titer is the highest [35]. Taken together, these results suggest that Tsf1 supply is not limiting bacterial growth when there is a low level of host-symbiont competition for circulating iron. When host demand increases (at pupation) or when symbiont demand increases (along with host aging and titer increase), Tsf1 gets undersupplied and does not cover bacterial needs anymore, which hinders *Spiroplasma* growth.

We show that in the case of the chronic, heritable, infection with *Spiroplasma*, *Drosophila* mounts a nutritional immune response by sequestrating iron. This response resembles that observed in the case of an acute pathogenic infection [4], with the difference that it is only partially mediated by Tsf1. A conceivable explanation would be that Tsf1 could respond steadily to acute stresses, while other proteins, possibly Tsf3, Ferritins or other unsuspected proteins, would mediate long-lasting sequestration.

Our experiments with FAC and BPS injection also proved intriguing as none of the treatment had a positive impact on *Spiroplasma* growth. The BPS experiment indicates that the

bacteria do not directly require free iron. Yet Tsf1 was expected to buffer the FAC supplementation *in vivo*, hence increasing complexed iron availability. An explanation to the lack of positive effect lies in the ability of free iron to produce reactive oxygen species through the Fenton reaction, with deleterious consequences on cells [51,52]. FAC supplementation positive impact could thus be offset by oxidative stress negative impact, resulting in an overall impaired bacterial growth. On the other hand, hemin or holo-Tsf supplementation could provide iron without triggering the Fenton reaction, hence fostering bacterial growth.

Eventually, we show that holo-Tsf extracted from bovine tissues does not improve *Spiroplasma* growth if the native *Drosophila* Tsf1 is absent (in *tsf1* mutant flies). Combined with the inability of *Spiroplasma* to benefit from free iron supplementation, this is an indication that the bacteria evolved an iron uptake mechanism from *Drosophila* Tsf1 that is protein-specific. The genome sequencing of *Spiroplasma poulsonii* revealed evolutionary footprints of its adaptation from a free-living to an intra-host lifestyle. An illustrative example is the pseudogenization of its transporter for trehalose (the main circulating sugar in *Drosophila* hemolymph) that is suspected to prevent bacterial overgrowth, hence assuring the long-term stability of the interaction [53]. We believe the adaptation to Tsf1-complexe iron uptake and not free iron could be another mechanisms coupling *Spiroplasma* growth rate to host metabolism. However, Tsf1 has no known receptor in *Drosophila*, hence the way the protein is internalized by host cells remains elusive, as is the way *Spiroplasma* uptakes iron from it. Further investigation should clarify whether bacterial cells directly internalize the protein, or if iron is scavenged from Tsf1 by means of secreted bacterial proteins.

Material and Methods

Drosophila and *Spiroplasma* stocks

Standard wild type genotype was w^{1118} (Bloomington Stock Center BDSC #3605) for all experiments except proteomics, *tsf1* expression measurements and iron feeding experiments for which Oregon-R (BDSC #5) flies were used. The *tsf1* mutant has been published previously [4] and the UAS-*tsf1*-IR line is publicly available (BDSC #62968). All experiments were carried out with *Spiroplasma poulsonii* strain Uganda-1 (Ug-1) [54] at 25°C.

Diet manipulation

Stocks breeding and experiments were carried out on standard cornmeal medium (35.28 g of cornmeal, 35.28 g of inactivated yeast, 3.72 g of agar, 36 ml of fruits juice, 2.9 ml of propionic acid and 15.9 ml of Moldex for 600 ml of medium) at 25°C. Iron poor diet consisted in 10% yeast, 10% sucrose, and 0.6% agar (w/v) in water [55]. FAC (Sigma F5879) was supplemented in the diet at 20 mM final concentration and BPS (Sigma 146617) at 200 µM final concentration.

Spiroplasma quantification by qPCR

Spiroplasma quantifications were performed as previously described [35] using DnaA109F 5′-TTAAGAGCAGTTTCAAAATCGGG-3′ and DnaA246R 5′-TGAAAAAAACAAACAAATTGTTATTACTTC-3′ [56] to quantify *Spiroplasma dnaA* gene and Dmel.rps17F 5′-CACTCCCAGGTGCGTGGTAT-3′ and Dmel.rps17R 5′-GGAGACGGCCGGGACGTAGT-3′ [57] to quantify *Drosophila rps17* gene. Relative *Spiroplasma* quantification was calculated as the *dnaA* over *rps17* ratio following the ΔΔCT method [58]. Quantifications were made in three biological replicates.

tsf1 expression measurement by RTqPCR

Tsf1 expression was measured by RT-qPCR on pools of 10 individuals at each developmental stage, with three biological replicates, as previously described [4]. Primers used were Tsf1-F 5’-GGATCGCCTGCTGAAGAAGA-3’ and Tsf1-R 5’- CCCGGCAGACCAAAGTACTT-3’ for *tsf1* and rpL32-F 5’-GACGCTTCAAGGGACAGTATCTG-3’ and rpL32-R 5’-

AAACGCGGTTCTGCATGAG-3' for the *Drosophila* housekeeping gene *rpL32* (*rp49*) [59]. Relative quantification of *tsf1* transcript was calculated following the ΔΔCT method [58].

Iron measurement using Inductively Coupled Plasma Optical Emission Spectrometry (ICP-OES)

Flies (N = 10 per sample) were used as a whole or their fat body dissected in phosphate buffer saline (PBS). Hemolymph extraction was performed on large batches of flies by centrifugation on filter cartridges as previously described [4]. Sample preparation and iron quantification was then performed as previously described [4] on a Perkin Elmer Optima 8300 ICP-OES at Laboratoire de Géochimie Environnementale, University of Lausanne, Switzerland. Iron measurements were normalized to the total protein amount in each sample measured using the Pierce™ BCA Protein Assay Kit (Thermofisher).

Prussian blue staining

Prussian blue staining was performed at the Histology Core Facility of EPFL, Lausanne, Switzerland. Briefly, whole flies were fixed in PBS with 4% paraformaldehyde and 0.1 Triton X-100 overnight and embedded in paraffin in a Sakura VIP6. Sections of 5 µM were stained with using a standard Perl's Prussian blue protocol [60] and observed on a Zeiss AxioImager Z1.

***Spiroplasma citri* challenge**

S. citri infections were performed using the GII3 strain kindly provided by Laure Béven from the UMR1332 "Biologie du Fruit et Pathologie," INRAE Bordeaux, France [61,62]. *S. citri* was grown at 32°C in SP4 medium from three days before being injected. 50 µL of culture were centrifuged at 20 000 g for 10 minutes and resuspended in PBS. 9 nL of bacteria suspension or PBS (mock control) were injected in the thorax of young females using a Nanoject II (Drummond) and survival was assessed once a day until all flies died.

Lifespan assessment

Female flies of each genotype/infection status (N = 20 per replicate) were selected within one day after eclosion and kept at 25°C on standard cornmeal medium. Medium was changed and

survival was assessed three times a week until all flies died. At least three replicates were done for each experimental group.

Iron derivative injection

A 18 nL injection of each product (or PBS as mock control) was performed in the thorax of young females using a Nanoject II (Drummond). *Spiroplasma* was quantified by qPCR 7 days after the treatment. FAC (Sigma F5879) was injected at 50 mM, BPS (Sigma 146617) at 10 mM and bovine hemin (Sigma H9039) at 10 mM, bovine holo-Tsf (Sigma T1283) and human apo-Tsf (Sigma T1147) at 300 µg per fly. *Spiroplasma* quantification was performed 7 days after the treatment.

Statistical analyses

Statistical procedures are described in detail in the figure legends along with relevant results. Briefly, RT-qPCR and *Spiroplasma* quantifications were analyzed by ANOVA followed by TukeyHSD multiple comparison post-hoc testing when relevant. Lifespan assays were analyzed by pairwise Log Rang tests with Benjamini-Hochberg correction for multiple testing.

Acknowledgments

We are grateful to Jasquelin Peña and the Laboratoire de Géochimie Environnementale, University of Lausanne, Switzerland for ICP-EOS measurements and the EPFL Histology Core Facility for Prussian Blue staining. We also thank Samuel Rommelaere and Igor Iatsenko for constructive discussions, as well as Fanny Schüpfer for technical help.

Authors' contribution

AM, FM and BL designed the research. AM performed lab work. AM and FM analyzed data. FM wrote the manuscript, which all co-authors revised.

Fundings

This work was supported by the Swiss National Science Foundation grant N°310030_185295.

Competing interests

The authors declare no competing interests.

Supplementary material

S1. *tsf1* mutant phenotype upon *Spiroplasma citri* acute infection.

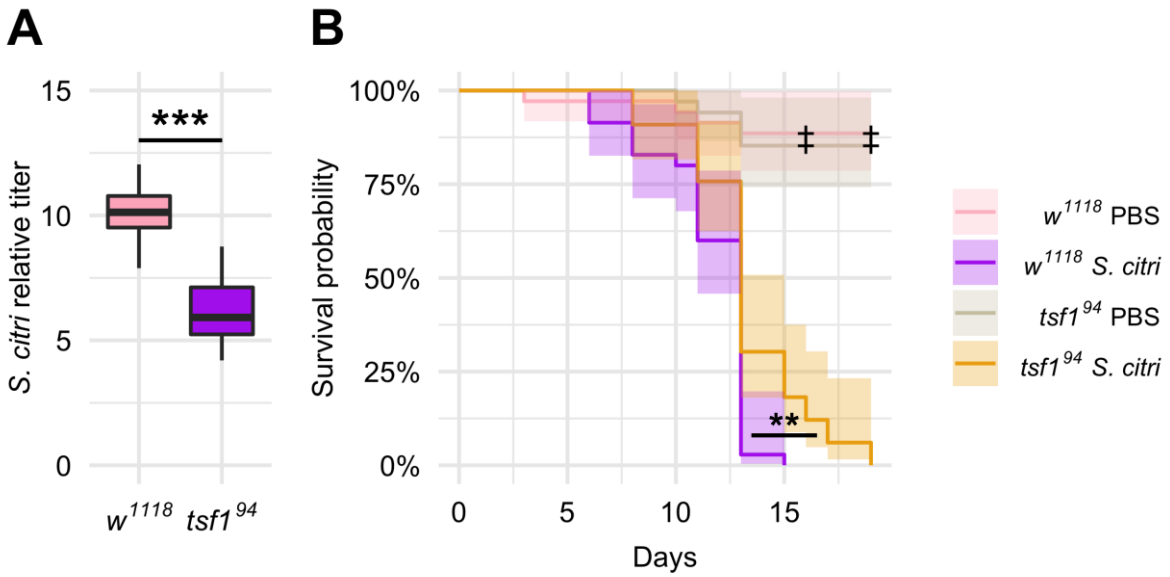

Fig S1. *tsf1* mutant phenotype upon *Spiroplasma citri* acute infection.

(A) *S. citri* quantification in w^{1118} and *tsf1* mutant flies 7 days after injection. Data were analyzed with a Student t-test. *** = p-value < 0.001. (B) Survival of w^{1118} and *tsf1* mutant flies upon PBS buffer or *S. citri* injection (N = 137). Data were analyzed by pairwise Log-Rank test with Benjamini-Hochberg correction for multiple testing. ** = p-value < 0.01. Black crosses on control PBS treatments indicate censored data.

S2. Iron measurement in flies raised on diets with altered iron content.

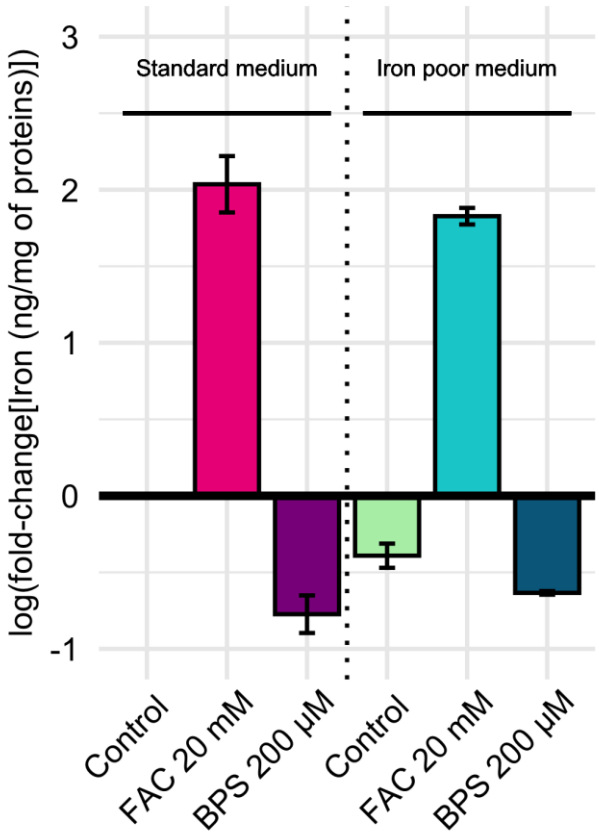

Fig S2. Iron measurement in flies raised on diets with altered iron content. Data is represented as the fold-change in iron content normalized by protein content in flies raised on manipulated diets compared to that of flies raised on control, standard, diet.

References

1. Hennigar SR, McClung JP. 2016 Nutritional Immunity: Starving Pathogens of Trace Minerals. *Am. J. Lifestyle Med.* **10**, 170–173. (doi:10.1177/1559827616629117)

2. Nairz M, Schroll A, Sonnweber T, Weiss G. 2010 The struggle for iron - a metal at the host-pathogen interface. *Cell. Microbiol.* **12**, 1691–1702. (doi:10.1111/j.1462-5822.2010.01529.x)

3. Barber MF, Elde NC. 2014 Escape from bacterial iron piracy through rapid evolution of transferrin. *Science (80-.).* **346**, 1362 LP-1366. (doi:10.1126/science.1259329)

4. Iatsenko I, Marra A, Boquete J-P, Peña J, Lemaitre B. 2020 Iron sequestration by transferrin 1 mediates nutritional immunity in Drosophila melanogaster. *Proc. Natl. Acad. Sci.* **117**, 7317 LP-7325. (doi:10.1073/pnas.1914830117)

5. Missirlis F, Kosmidis S, Brody T, Mavrakis M, Holmberg S, Odenwald WF, Skoulakis EMC, Rouault TA. 2007 Homeostatic Mechanisms for Iron Storage Revealed by Genetic Manipulations and Live Imaging of Drosophila Ferritin. *Genetics* **177**, 89 LP-100. (doi:10.1534/genetics.107.075150)

6. Tang X, Zhou B. 2013 Ferritin is the key to dietary iron absorption and tissue iron detoxification in Drosophila melanogaster. *FASEB J.* **27**, 288–298. (doi:https://doi.org/10.1096/fj.12-213595)

7. González-Morales N, Mendoza-Ortíz MÁ, Blowes LM, Missirlis F, Riesgo-Escovar JR. 2015 Ferritin Is Required in Multiple Tissues during Drosophila melanogaster Development. *PLoS One* **10**, e0133499.

8. Mumbauer S, Pascual J, Kolotuev I, Hamaratoglu F. 2019 Ferritin heavy chain protects the developing wing from reactive oxygen species and ferroptosis. *PLOS Genet.* **15**, e1008396.

9. Tiklová K, Senti K-A, Wang S, Gräslund A, Samakovlis C. 2010 Epithelial septate junction assembly relies on melanotransferrin iron binding and endocytosis in Drosophila. *Nat. Cell Biol.* **12**, 1071–1077. (doi:10.1038/ncb2111)

10. Mandilaras K, Missirlis F. 2012 Genes for iron metabolism influence circadian rhythms in Drosophila melanogaster. *Metallomics* **4**, 928–936. (doi:10.1039/c2mt20065a)

11. Xiao G, Liu Z-H, Zhao M, Wang H-L, Zhou B. 2019 Transferrin 1 Functions in Iron Trafficking and Genetically Interacts with Ferritin in Drosophila melanogaster. *Cell Rep.* **26**, 748–758.e5. (doi:https://doi.org/10.1016/j.celrep.2018.12.053)

12. Chen GY, Ayres JS. 2020 Beyond tug-of-war: Iron metabolism in cooperative host–microbe interactions. *PLOS Pathog.* **16**, e1008698.

13. Masson F, Lemaitre B. 2020 Growing Ungrowable Bacteria: Overview and Perspectives on Insect Symbiont Culturability. *Microbiol. Mol. Biol. Rev.* **84**, e00089-20. (doi:10.1128/MMBR.00089-20)

14. Moran NA, Telang A. 1998 Bacteriocyte-associated symbionts of insects. *Bioscience* **48**, 295–304.

15. Polin S, Le Gallic J-F, Simon J-C, Tsuchida T, Outreman Y. 2015 Conditional Reduction of Predation Risk Associated with a Facultative Symbiont in an Insect. *PLoS One* **10**, e0143728–e0143728. (doi:10.1371/journal.pone.0143728)

16. Tsuchida T, Koga R, Fukatsu T. 2004 Host plant specialization governed by facultative symbiont. *Science (80-.).* **303**, 1989.

17. Teixeira L, Ferreira A, Ashburner M. 2008 The bacterial symbiont Wolbachia induces resistance to RNA viral infections in Drosophila melanogaster. *PLoS Biol* **6**, e2. (doi:08-PLBI-RA-3425 [pii] 10.1371/journal.pbio.1000002)

18. Oliver KM, Russell JA, Moran NA, Hunter MS. 2003 Facultative bacterial symbionts in aphids confer resistance to parasitic wasps. *Proc Natl Acad Sci U S A* **100**, 1803–1807.

19. Scarborough CL, Ferrari J, Godfray HC. 2005 Aphid protected from pathogen by endosymbiont. *Science (80-.).* **310**, 1781. (doi:10.1126/science.1120180)

20. Xie J, Vilchez I, Mateos M. 2010 Spiroplasma Bacteria Enhance Survival of Drosophila hydei Attacked by the Parasitic Wasp Leptopilina heterotoma. *PLoS One* **5**, e12149.

21. Hamilton PT, Perlman SJ. 2013 Host Defense via Symbiosis in Drosophila. *PLoS Pathog.* **9**, e1003808. (doi:10.1371/journal.ppat.1003808)

22. Engelstädter J, Hurst GDD. 2009 The Ecology and Evolution of Microbes that Manipulate Host Reproduction. *Annu. Rev. Ecol. Evol. Syst.* **40**, 127–149. (doi:10.1146/annurev.ecolsys.110308.120206)

23. Hurst GDD, Frost CL. 2015 Reproductive parasitism: maternally inherited symbionts in a biparental world. *Cold Spring Harb. Perspect. Biol.* **7**. (doi:10.1101/cshperspect.a017699)

24. Douglas AE. 2016 How multi-partner endosymbioses function. *Nat. Rev. Microbiol.* **14**, 731–743. (doi:10.1038/nrmicro.2016.151)

25. Renoz F, Champagne A, Degand H, Faber A-M, Morsomme P, Foray V, Hance T. 2017 Toward a better understanding of the mechanisms of symbiosis: a comprehensive proteome map of a nascent insect symbiont. *PeerJ* **5**, e3291–e3291. (doi:10.7717/peerj.3291)

26. Runyen-Janecky LJ, Brown AN, Ott B, Tujuba HG, Rio RVM. 2010 Regulation of high-affinity iron acquisition homologues in the tsetse fly symbiont Sodalis glossinidius. *J. Bacteriol.* **192**, 3780–3787. (doi:10.1128/JB.00161-10)

27. Hrusa G, Farmer W, Weiss BL, Applebaum T, Roma JS, Szeto L, Aksoy S, Runyen-Janecky LJ. 2015 TonB-dependent heme iron acquisition in the tsetse fly symbiont Sodalis glossinidius. *Appl. Environ. Microbiol.* **81**, 2900–2909. (doi:10.1128/AEM.04166-14)

28. Medina P, Russell SL, Corbett-Detig R. 2019 Deep data mining reveals variable abundance and distribution of microbial reproductive manipulators within and among diverse host species. bioRxiv , 679837. (doi:10.1101/679837)

29. Duron O, Bouchon D, Boutin S, Bellamy L, Zhou L, Engelstadter J, Hurst GD. 2008 The diversity of reproductive parasites among arthropods: Wolbachia do not walk alone. *BMC Biol.* **6**, 27. (doi:10.1186/1741-7007-6-27)

30. Werren JH, Baldo L, Clark ME. 2008 Wolbachia: master manipulators of invertebrate biology. *Nat. Rev. Microbiol.* **6**, 741–751. (doi:10.1038/nrmicro1969)

31. Kremer N, Voronin D, Charif D, Mavingui P, Mollereau B, Vavre F. 2009 Wolbachia interferes with ferritin expression and iron metabolism in insects. *PLoS Pathog* **5**, e1000630. (doi:10.1371/journal.ppat.1000630)

32. Brownlie JC, Cass BN, Riegler M, Witsenburg JJ, Iturbe-Ormaetxe I, McGraw EA, O'Neill SL. 2009 Evidence for metabolic provisioning by a common invertebrate endosymbiont, Wolbachia pipientis, during periods of nutritional stress. *PLoS Pathog.*

5, e1000368. (doi:10.1371/journal.ppat.1000368)

33. Mateos M, Castrezana SJ, Nankivell BJ, Estes AM, Markow TA, Moran NA. 2006 Heritable Endosymbionts of Drosophila. *Genetics* **174**, 363–376. (doi:10.1534/genetics.106.058818)

34. Masson F, Rommelaere S, Marra A, Schüpfer F, Lemaitre B. 2021 Dual proteomics of Drosophila melanogaster hemolymph infected with the heritable endosymbiont Spiroplasma poulsonii. *submitted*

35. Herren JK, Lemaitre B. 2011 Spiroplasma and host immunity: Activation of humoral immune responses increases endosymbiont load and susceptibility to certain Gram-negative bacterial pathogens in Drosophila melanogaster. *Cell. Microbiol.* **13**, 1385–1396. (doi:10.1111/j.1462-5822.2011.01627.x)

36. Anbutsu H, Fukatsu T. 2010 Evasion, suppression and tolerance of Drosophila innate immunity by a male-killing Spiroplasma endosymbiont. *Insect Mol. Biol.* **19**, 481–488. (doi:10.1111/j.1365-2583.2010.01008.x)

37. Herren JK, Paredes JC, Schüpfer F, Lemaitre B. 2013 Vertical Transmission of a Drosophila Endosymbiont Via Cooption of the Yolk Transport and Internalization Machinery. *MBio* **4 (2)**, e00532-12. (doi:10.1128/mBio.00532-12)

38. Harumoto T, Lemaitre B. 2018 Male-killing toxin in a bacterial symbiont of Drosophila. *Nature* **557**, 252–255. (doi:10.1038/s41586-018-0086-2)

39. Xie J, Butler S, Sanchez G, Mateos M. 2014 Male killing Spiroplasma protects Drosophila melanogaster against two parasitoid wasps. *Heredity (Edinb).* **112**, 399–408. (doi:10.1038/hdy.2013.118)

40. Ballinger MJ, Perlman SJ. 2017 Generality of toxins in defensive symbiosis: Ribosome-inactivating proteins and defense against parasitic wasps in Drosophila. *PLoS Pathog.* **13**, e1006431. (doi:10.1371/journal.ppat.1006431)

41. Hamilton PT, Peng F, Boulanger MJ, Perlman SJ. 2016 A ribosome-inactivating protein in a Drosophila defensive symbiont. *Proc. Natl. Acad. Sci. U. S. A.* **113**, 350–355. (doi:10.1073/pnas.1518648113)

42. Herren JK, Paredes JC, Schüpfer F, Arafah K, Bulet P, Lemaitre B. 2014 Insect endosymbiont proliferation is limited by lipid availability. eLife **3**, e02964.

(doi:10.7554/eLife.02964)

43. Masson F, Calderon Copete S, Schüpfer F, Garcia-Arraez G, Lemaitre B. 2018 In Vitro Culture of the Insect Endosymbiont Spiroplasma poulsonii Highlights Bacterial Genes Involved in Host-Symbiont Interaction. *MBio* **9(2)**, e00024-18. (doi:10.1128/mBio.00024-18)

44. Regassa LB, Gasparich GE. 2006 Spiroplasmas: evolutionary relationships and biodiversity. *Front. Biosci.* **11**, 2983–3002. (doi:10.2741/2027)

45. Mandilaras K, Pathmanathan T, Missirlis F. 2013 Iron absorption in Drosophila melanogaster. *Nutrients* **5**, 1622–1647. (doi:10.3390/nu5051622)

46. Tang X, Zhou B. 2013 Iron homeostasis in insects: Insights from Drosophila studies. *IUBMB Life* **65**, 863–872. (doi:https://doi.org/10.1002/iub.1211)

47. Ott DB, Hartwig A, Stillman MJ. 2019 Competition between Al(3+) and Fe(3+) binding to human transferrin and toxicological implications: structural investigations using ultra-high resolution ESI MS and CD spectroscopy. *Metallomics* **11**, 968–981. (doi:10.1039/c8mt00308d)

48. Quarles CDJ, Marcus RK, Brumaghim JL. 2011 Competitive binding of Fe3+, Cr3+, and Ni2+ to transferrin. *J. Biol. Inorg. Chem. JBIC a Publ. Soc. Biol. Inorg. Chem.* **16**, 913–921. (doi:10.1007/s00775-011-0792-9)

49. Graveley BR *et al.* 2011 The developmental transcriptome of Drosophila melanogaster. *Nature* **471**, 473–479. (doi:10.1038/nature09715)

50. Casas-Vila N *et al.* 2017 The developmental proteome of Drosophila melanogaster. *Genome Res.* **27**, 1273–1285. (doi:10.1101/gr.213694.116)

51. Li S-W, Liu C-M, Guo J, Marcondes AM, Deeg J, Li X, Guan F. 2016 Iron overload induced by ferric ammonium citrate triggers reactive oxygen species-mediated apoptosis via both extrinsic and intrinsic pathways in human hepatic cells. *Hum. Exp. Toxicol.* **35**, 598–607. (doi:10.1177/0960327115597312)

52. Galaris D, Pantopoulos K. 2008 Oxidative stress and iron homeostasis: mechanistic and health aspects. *Crit. Rev. Clin. Lab. Sci.* **45**, 1–23. (doi:10.1080/10408360701713104)

53. Paredes JC, Herren JK, Schüpfer F, Marin R, Claverol S, Kuo C-H, Lemaitre B, Béven

L. 2015 Genome sequence of the Drosophila melanogaster male-killing Spiroplasma strain MSRO endosymbiont. *MBio* **6(2)**, e02437-14. (doi:10.1128/mBio.02437-14.Editor)

54. Pool JE, Wong a, Aquadro CF. 2006 Finding of male-killing Spiroplasma infecting Drosophila melanogaster in Africa implies transatlantic migration of this endosymbiont. *Heredity (Edinb).* **97**, 27–32. (doi:10.1038/sj.hdy.6800830)

55. Chen K, Ho TS-Y, Lin G, Tan KL, Rasband MN, Bellen HJ. 2016 Loss of Frataxin activates the iron/sphingolipid/PDK1/Mef2 pathway in mammals. *eLife* **5**, e20732. (doi:10.7554/eLife.20732)

56. Anbutsu H, Fukatsu T. 2003 Population dynamics of male-killing and non-male-killing Spiroplasmas in Drosophila melanogaster. *Appl. Environ. Microbiol.* **69**, 1428–1434. (doi:10.1128/AEM.69.3.1428-1434.2003)

57. Osborne SE, Leong YS, O'Neill SL, Johnson KN. 2009 Variation in Antiviral Protection Mediated by Different Wolbachia Strains in Drosophila simulans. *PLOS Pathog.* **5**, e1000656.

58. Pfaffl MW. 2001 A new mathematical model for relative quantification in real-time RT-PCR. *Nucleic Acids Res.* **29**, e45–e45. (doi:10.1093/nar/29.9.e45)

59. Romeo Y, Lemaitre B. 2008 Drosophila immunity: methods for monitoring the activity of Toll and Imd signaling pathways. *Methods Mol. Biol.* **415**, 379–394. (doi:10.1007/978-1-59745-570-1_22)

60. Sheehan DC, Hrapchak BB. 1987 *Theory and practice of histotechnology*. Columbus, Ohio: Battelle Press.

61. Vignault JC, Bové J, Saillard C, Vogel R. 1980 Mise en culture de spiroplasmes à partir de matériel végétal et d'insectes provenant de pays circum-méditerranéens et du Proche-Orient. *C. R. Hebd. Seances Acad. Sci.* **290**, 775–778.

62. Saillard C *et al.* 2008 The abundant extrachromosomal DNA content of the Spiroplasma citri GII3-3X genome. *BMC Genomics* **9**, 195. (doi:10.1186/1471-2164-9-195)

Chapter IV

General discussion and perspectives

The aim of this thesis was to elucidate the molecular mechanisms involved in the control of bacteria-host interactions and, more particularly, the role of immune effectors in symbiotic interactions. To this end, I leveraged the numerous advantages of the genetically tractable model *Drosophila melanogaster* to analyze the impact of immune effectors on the gut microbiota and the endosymbiotic bacterium *Spiroplasma poulsonii.*

The *Drosophila* immune system is composed of several immune modules, some of which share characteristics with the vertebrate innate immune system (53). A hallmark of the *Drosophila* innate immune system is the synthesis of immune effectors and antimicrobials by the fat body and some epithelia (e.g in the trachea and the gut). An extensive array of effectors have been discovered, but their respective contribution to the elimination or control of specific microbes is still elusive. The study of immune effectors is complicated by the fact that the host has multiple strategies to combat microbial infection as such the modes of action of these effectors are diverse. Some effectors directly target pathogens, as exemplified by antimicrobial peptides. In contrast, many immune effectors indirectly contribute to survival by producing toxic molecules (e.g. ROS), by detoxifying microbial toxins, by sequestering metabolites required for microbial growth (e.g. iron sequestration by Transferrin) or by degrading the bacterial cell wall components, making microbes more susceptible to the host weapons (e.g. lysozymes). Many of these immune molecules induced upon infection contribute to a metabolic change that prevents immune and pathogen-induced tissue damage or control bacterial growth, as in the case of microbiota establishment.

It is crucial to consider that host-pathogen and host-symbiont interactions share much of the same ‘language’ of cell and molecular biology, but result in different ‘conversations’, acting to eliminate invaders in the first case, while maintaining beneficial or benign relationships in the second. For example, the detection of MAMPs, which normally triggers immune system activation and pathogen elimination in the host, can be essential for a successful symbiotic establishment (231).

Thus, to fully understand immune effectors in a variety of roles, we must study how they control not only pathogens but also symbionts, and how their function is integrated into host metabolism and physiology.

In the following section, I will discuss the results of the two main projects of this thesis: a clarification of the role of AMP and lysozyme antimicrobials in the establishment and control of gut microbiota homeostasis, and the role of Transferrin 1 in regulation of the *Drosophila* symbiont *Spiroplasma poulsonii*.

Role of immune effectors in the gut homeostasis

As in mammals, the fly gut microbiota contributes to physiological homeostasis (216). However, the establishment of the gut microbiota population comes at a cost for the host. The Imd pathway, which is a main defense against bacterial infection in the gut, has proved to be a key regulator of gut microbiota growth and composition (178, 186, 216). However, the mechanisms allowing the same effectors to establish a protective environment for the microbiota while effectively targeting pathogenic infections are not yet fully established. In this work, we aimed to understand the role of some of these effectors, AMPs and lysozymes, in controlling the microbiota.

We found that AMPs, and to a lesser extent lysozymes, are necessary to regulate the abundance of total gut bacteria and its relative composition, mainly during aging. We found that AMPs are required for homeostatic control of predominantly the Gram-negative bacteria *Acetobacter* during aging, while lysozymes had a minor impact on Gram-positive bacteria. These results are consistent with the idea that the Imd pathway and expression of AMPs are mainly activated upon Gram-negative bacterial infection (232, 233) and that lysozymes are thought to specifically degrade Gram-positive bacterial cell walls but have little or no effect on Gram-negative species (234). However, we did find a minor effect of antimicrobial peptides on some Gram-positive bacterial species, suggesting that they may have a broader impact on microbiota homeostasis. This raises the question of the specificity and mode of action that antimicrobial peptides have against microbiota bacteria. It should be noted that our work relies on the use of isogenic fly strains. While the isogenization process homogenizes the genetic background so that more controlled comparisons are possible, it also increases the degree of homozygosity with possible complex genetic interactions. Thus, our study using the *isogenic Drosdel*

background should be reinforced by other studies in different backgrounds or using other approaches.

Recently, Hanson *et al*. showed that AMPs can selectively target Gram-negative bacteria and to lesser extent fungi, and that they can act in a synergistic or additive modes to kill pathogens upon infection (110). These observations led us to speculate an analogous role for AMPs against the microbiota community. We hypothesize that each antimicrobial peptide expressed in response to the gut microbiota may act differently on the bacterial community, showing synergy or additivity against bacterial species in the gut. By downregulating single or grouped AMPs, further analysis should decipher how AMPs individually or collectively regulate microbiota.

Our work confirmed previous studies showing that gut microbiota composition of adult flies is mainly affected during aging (203). Aging is associated with deterioration of gut compartmentalization, notably the acidic zone (191, 235) that likely leads to bacterial overgrowth, which negatively impacts *Drosophila* gut physiology (197, 202). This increased load of microbiota in the gut with age likely explains the increased expression of AMPs due to chronic activation of the Imd pathway (186). Here we show that specific Imd-related AMPs are required to control gut microbiota composition and abundance, particularly during the aging process. It is paradoxical that microbiota load increases with age despite increased expression of AMPs that control it. This may suggest that most microbiota species can escape the action of AMPs. Alternatively, it cannot be excluded that the increased AMP gene expression does not translate into a higher peptide production. Moreover, studies on germ-free flies suggest that while the microbiota has a positive impact in young flies, the presence of gut bacteria is detrimental upon aging (236). The observation that aging defects are more pronounced in Imd-deficient *Relish* mutants, previously indicated that this pathway plays an important role in gut-microbiota homeostasis (186). Our results extend this by showing that AMPs do contribute to the role of the Imd pathway in the gut during aging, likely by directly limiting microbiota growth.

In *Drosophila*, transmission of the microbiota and colonization of embryo is ensured by the parents, which lay eggs on food contaminated with their feces (178, 211, 212). The newly emerged larvae feed on the contaminated substrate, colonizing the gut. It is also known that the larval and adult microbiota is highly affected by the food content (213, 237). Since some antimicrobial peptides and lysozymes are stable proteins (118), we cannot exclude that some of these effectors produced in the gut lumen may be excreted to the environment in the feces with the microbiota members. An AMP release process in the food may act as an additional early "quality control" step in order to prevent the overgrowth of bacteria deleterious to either the

larvae or adult flies, which re-ingest this microbial community as they feed. Intriguingly, we have observed that certain AMP mutant flies are more difficult to raise due to the growth of sticky bacterial biofilms on the medium (A. Marra, unpublished data). Further analysis will focus on the role of AMPs in shaping the external environment.

The *Drosophila* gut microbiota is typically transient and continuous ingestion is necessary to keep the gut colonized (178). Moreover, laboratory reared flies have an extremely reduced gut community compared to those collected from natural population (209, 237, 238). For example, Pais *et al*, have recently isolated a new bacterial species from the wild which can stably rather than transiently colonize the fly gut, *Acetobacter thailandicus* (209). They showed that this species is beneficial for the host and provides a fitness advantage in wild populations. Finally, functional studies show that bacterial isolates from lab stocks have different properties compared to isolates from wild *Drosophila*. For example, a wild *Lactobacillus plantarum* strain can colonize the gut more efficiently than strains isolated from laboratory flies (239). How host immune effectors can differentially control a stable gut colonizer or a wider natural community throughout animal development is still an open question. This also raises the question of whether antimicrobial peptides can act differently against microbiota from wild and lab populations, and if they can show a high degree of specificity at the species or even strain level.

Signals derived from the gut microbiota are responsible for gut epithelium renewal, which is part of the defense mechanisms against pathogenic insults (184). Altered control of gut microbiota in immune-deficient or aged flies correlates with increased epithelium renewal and dysplasia (184, 197, 240). Moreover, the gut microbiota can confer protection against bacterial and viral infection through mechanisms such as immune priming or niche competition (219, 241). However, the role of immune system activation and immune effectors in these mechanisms is elusive. AMPs and lysozymes are overexpressed in the gut upon bacterial oral infections (177, 235), but their role towards the gut microbiota upon pathogenic infection is unclear. Unpublished data show that after systemic infection with live and heat killed Gram-negative bacteria, AMP mutant flies have an increased bacterial load in the gut compared to the wild-type (M.A. Hanson, personal communication). We also found that germ-free flies lacking AMPs or lysozymes were more susceptible to oral infection with the Gram-negative bacteria *Erwinia carotovora carotovora* and *Pseudomonas entomophila*, compared to conventionally reared flies (A. Marra, unpublished data,). This preliminary evidence suggests an interaction between the gut antimicrobial effectors and the host microbiota in defending against pathogens.

Endosymbiosis and nutritional immunity

Previous studies showed that *Spiroplasma* relies on the host diglycerides for growth (Herren *et al*, 2014). Until recently, circulating lipids availability was the only known limiting factor that can control *Spiroplasma* growth within fly hemolymph. Here, we revealed a significant role of iron complexed to Transferrin 1 in the control of *Spiroplasma* growth. We showed that *tsf1* is upregulated upon *Spiroplasma* infection, and that this upregulation is associated with depletion of iron from the hemolymph, which is relocated to the fat body. This process is reminiscent of the role of Tsf1 in nutritional immunity against pathogenic infections (242). Iatsenko *et al*. showed that *tsf1* transcription is regulated either by the Imd or by the Toll pathway, depending on the microbial elicitors. This suggested that although *Spiroplasma* is devoid of peptidoglycan, it can be detected by at least one of these pathways to trigger *tsf1* upregulation (242). An interesting hypothesis is that secreted proteases from *Spiroplasma* could trigger peptidoglycan-independent activation of the Toll pathway via the circulating protease sensor Perspephone (51). This hypothesis is reinforced by the detection of a low basal activation of the Toll pathway in *Spiroplasma* infected flies (22), although further investigation will be required to validate this. We also show that *Spiroplasma* takes up iron only when it is bound to Tsf1. An alternative hypothesis to explain *tsf1* induction in response to *Spiroplasma* is that iron deprivation is sensed by the flies, prompting upregulation of the iron transporter and iron sequestration in the fat body.

Preliminary data from our lab (F. Masson, personal communication) showed that *Spiroplasma* can adapt to the lack of Tsf1 in *tsf1* mutant flies, and after a small number of generations proliferate in these mutants as efficiently as in wild-type flies. This is likely due to the high rate of mutations of *Spiroplasma poulsonii*, which approaches rates observed in viruses (243). This interesting observation led us to speculate that *tsf1* upregulation and bacterial iron acquisition may be a recent mechanism that *Spiroplasma* has evolved in order to hijack host iron more efficiently, but that other Tsf1-independent mechanisms can take over if Tsf1 is absent.

Overall, this work identifies a new growth-limiting factor involved in *Spiroplasma-Drosophila* symbiosis, and additionally shows that the host nutritional immune-effectors play a role in endosymbiosis maintenance.

Conclusion

The innate immune system is unable to specifically target microbial species, yet our results highlight its incredible ability to respond differentially to the diverse categories of microbes encountered by the fly (pathogenic, mutualistic or endosymbiotic). More importantly, it shows that the effectors used to control symbiotic microbes (AMPs, Tsf1) are the very ones that fight against pathogens upon acute infections. Further research will be needed to better understand how host immunity distinguishes between symbionts and pathogens, beyond effector specificity. Interesting candidates for this distinction are different sensing mechanisms or more likely a fine-tuning of the pathway regulation, the identification of which should be the next significant step in understanding the vast complexity of immune interactions between *Drosophila* and microbes.

Bibliography

1. Mirzoyan Z, Sollazzo M, Allocca M, Valenza AM, Grifoni D, Bellosta P. 2019. Drosophila melanogaster: A model organism to study cancer. Front Genet 10:1–16.

2. Douglas AE. 2018. The Drosophila model for microbiome research. Lab Anim 47:157–164.

3. McGurk L, Berson A, Bonini NM. 2015. Drosophila as an in vivo model for human neurodegenerative disease. Genetics 201:377–402.

4. Musselman LP, Kühnlein RP. 2018. Drosophila as a model to study obesity and metabolic disease. J Exp Biol 121.

5. Capo F, Wilson A, Di Cara F. 2019. The intestine of Drosophila melanogaster: An emerging versatile model system to study intestinal epithelial homeostasis and host-microbial interactions in humans. Microorganisms 7.

6. Panayidou S, Ioannidou E, Apidianakis Y. 2014. Human pathogenic bacteria, fungi, and viruses in *Drosophila*. Virulence 5:253–269.

7. Lemaitre B, Hoffmann J. 2007. The Host Defense of *Drosophila melanogaster*. Annu Rev Immunol 25:697–743.

8. Keebaugh ES, Schlenke TA. 2014. Insights from natural host-parasite interactions: The Drosophila model. Dev Comp Immunol 42:111–123.

9. Erkosar B, Storelli G, Defaye A, Leulier F. 2013. Host-intestinal microbiota mutualism: "learning on the fly." Cell Host Microbe 13:8–14.

10. Keebaugh ES, Yamada R, Obadia B, Ludington WB, Ja WW. 2018. Microbial Quantity Impacts Drosophila Nutrition, Development, and Lifespan. iScience 4:247–259.

11. Masson F, Schüpfer F, Jollivet C, Lemaitre B. 2020. Endosymbiont Spiroplasma poulsonii and Persisting Hurdles. Appl Environ Microbiol 86:e00835-20.

12. Mateos M, Castrezana SJ, Nankivell BJ, Estes AM, Markow TA, Moran NA. 2006. Heritable endosymbionts of Drosophila. Genetics 174:363–376.

13. Medina P, Russell SL, Aswadhati K, Corbett-Detig R. 2019. Deep data mining reveals

variable abundance and distribution of microbial reproductive manipulators within and among diverse host species. bioRxiv https://doi.org/10.1101/679837 .

14. Duron O, Bouchon D, Boutin S, Bellamy L, Zhou L, Engelstädter J, Hurst GD. 2008. The diversity of reproductive parasites among arthropods: Wolbachia do not walk alone. BMC Biol 6:1–12.

15. Regassa LB, Gasparich GE. 2006. Spiroplasmas: evolutionary relationships and biodiversity. Front Biosci 11:2983–3002.

16. Werren JH, Baldo L, Clark ME. 2008. Wolbachia: Master manipulators of invertebrate biology. Nat Rev Microbiol 6:741–751.

17. Montenegro H, Solferini VN, Klaczko LB, Hurst GDD. 2005. Male-killing Spiroplasma naturally infecting Drosophila melanogaster. Insect Mol Biol 14:281–287.

18. Harumoto T, Lemaitre B. 2018. Male-killing toxin in a bacterial symbiont of Drosophila. Nature 557:252–255.

19. Harumoto T, Anbutsu H, Lemaitre B, Fukatsu T. 2016. Male-killing symbiont damages host's dosage-compensated sex chromosome to induce embryonic apoptosis. Nat Commun 7.

20. Herren JK, Paredes JC, Schüpfer F, Arafah K, Bulet P, Lemaitre B. 2014. Insect endosymbiont proliferation is limited by lipid availability. eLife 3:e02964.

21. Herren JK, Lemaitre B. 2011. Spiroplasma and host immunity: Activation of humoral immune responses increases endosymbiont load and susceptibility to certain Gram-negative bacterial pathogens in Drosophila melanogaster. Cell Microbiol 13:1385–1396.

22. Masson F, Rommelaere S, Marra A, Schüpfer F, Lemaitre B. 2021. Dual proteomics of Drosophila melanogaster hemolymph infected with the heritable endosymbiont Spiroplasma poulsonii. bioRxiv https://doi.org/10.1101/2021.02.22.432267.

23. Masson F, Calderon-Copete S, Schüpfer F, Vigneron A, Rommelaere S, Garcia-Arraez MG, Paredes JC, Lemaitre B. 2020. Blind killing of both male and female Drosophila embryos by a natural variant of the endosymbiotic bacterium Spiroplasma poulsonii. Cell Microbiol 22:1–12.

24. Masson F, Copete SC, Schüpfer F, Garcia-Arraez G, Lemaitre B. 2018. In Vitro Culture

of the Insect Endosymbiont Spiroplasma poulsonii Highlights Bacterial Genes Involved in HostSymbiont Interaction 9:1–11.

25. Hamilton PT, Peng F, Boulanger MJ, Perlman SJ. 2016. A ribosome-inactivating protein in a Drosophila defensive symbiont. Proc Natl Acad Sci U S A 113:350–355.

26. Ballinger MJ, Gawryluk RMR, Perlman SJ. 2019. Toxin and genome evolution in a Drosophila defensive symbiosis. Genome Biol Evol 11:253–262.

27. Xie J, Vilchez I, Mateos M. 2010. Spiroplasma bacteria enhance survival of Drosophila hydei attacked by the parasitic wasp Leptopilina heterotoma. PLoS One 5 (8): e12149.

28. Ballinger MJ, Perlman SJ. 2017. Generality of toxins in defensive symbiosis: Ribosome-inactivating proteins and defense against parasitic wasps in Drosophila. PLoS Pathog 13:1–19.

29. Paredes JC, Herren JK, Schüpfer F, Lemaitre B. 2016. The role of lipid competition for endosymbiont-mediated protection against parasitoid wasps in Drosophila. mBio 7:1–8.

30. Jaenike J, Unckless R, Cockburn SN, Boelio LM, Perlman SJ. 2010. Adaptation via symbiosis: Recent spread of a drosophila defensive symbiont. Science (80-) 329:212–215.

31. Keita S, Masuzzo A, Royet J, Kurz CL. 2017. Drosophila larvae food intake cessation following exposure to Erwinia contaminated media requires odor perception, Trpa1 channel and evf virulence factor. J Insect Physiol 99:25–32.

32. Charroux B, Daian F, Royet J. 2020. Drosophila Aversive Behavior toward Erwinia carotovora carotovora Is Mediated by Bitter Neurons and Leukokinin. iScience 23:101152.

33. Lin SJH, Cohen LB, Wasserman SA. 2020. Effector specificity and function in Drosophila innate immunity: Getting AMPed and dropping Boms. PLoS Pathog 16:1–6.

34. Kounatidis I, Ligoxygakis P. 2012. Drosophila as a model system to unravel the layers of innate immunity to infection. Open Biol 2:120075.

35. Anderson K V, Jürgens G, Nüsslein-Volhard C. 1985. Establishment of dorsal-ventral polarity in the Drosophila embryo: Genetic studies on the role of the Toll gene product. Cell 42:779–789.

36. Georgel P, Naitza S, Kappler C, Ferrandon D, Zachary D, Swimmer C, Kopczynski C, Duyk G, Reichhart JM, Hoffmann JA. 2001. Drosophila Immune Deficiency (IMD) Is a Death Domain Protein that Activates Antibacterial Defense and Can Promote Apoptosis. Dev Cell 1:503–514.

37. Akira S, Uematsu S, Takeuchi O. 2006. Pathogen recognition and innate immunity. Cell 124:783–801.

38. Lu Y, Su F, Li Q, Zhang J, Li Y, Tang T, Hu Q. 2020. Pattern recognition receptors in Drosophila immune responses. Dev Comp Immunol 102:103468.

39. Iatsenko I, Kondo S, Mengin-Lecreulx D, Lemaitre B. 2016. PGRP-SD, an Extracellular Pattern-Recognition Receptor, Enhances Peptidoglycan-Mediated Activation of the Drosophila Imd Pathway. Immunity 45:1013–1023.

40. Bischoff V, Vignal C, Boneca IG, Michel T, Hoffmann JA, Royet J. 2004. Function of the drosophila pattern-recognition receptor PGRP-SD in the detection of Gram-positive bacteria. Nat Immunol 5:1175–1180.

41. Costechareyre D, Capo F, Fabre A, Chaduli D, Kellenberger C, Roussel A, Charroux B, Royet J. 2016. Tissue-Specific Regulation of Drosophila NF-κB Pathway Activation by Peptidoglycan Recognition Protein SC. J Innate Immun 8:67–80.

42. Melcarne C, Ramond E, Dudzic J, Bretscher AJ, Kurucz É, Andó I, Lemaitre B. 2019. Two Nimrod receptors, NimC1 and Eater, synergistically contribute to bacterial phagocytosis in Drosophila melanogaster. FEBS J 286:2670–2691.

43. Mengin-Lecreulx D, Lemaitre B. 2005. Structure and metabolism of peptidoglycan and molecular requirements allowing its detection by the Drosophila innate immune system. J Endotoxin Res 11:105–111.

44. Mellroth P, Karlsson J, Steiner H. 2003. A scavenger function for a Drosophila peptidoglycan recognition protein. J Biol Chem 278:7059–7064.

45. Zaidman-Rémy A, Hervé M, Poidevin M, Pili-Floury S, Kim MS, Blanot D, Oh BH, Ueda R, Mengin-Lecreulx D, Lemaitre B. 2006. The Drosophila Amidase PGRP-LB Modulates the Immune Response to Bacterial Infection. Immunity 24:463–473.

46. Charroux B, Capo F, Kurz CL, Peslier S, Chaduli D, Viallat-lieutaud A, Royet J. 2018. Cytosolic and Secreted Peptidoglycan-Degrading Enzymes in Drosophila Respectively

Control Local and Systemic Immune Responses to Microbiota. Cell Host Microbe 23:215-228.e4.

47. Gobert V, Gottar M, Matskevich AA, Rutschmann S, Royet J, Belvin M, Hoffmann JA, Ferrandon D. 2003. Dual Activation of the Drosophila Toll Pathway by Two Pattern Recognition Receptors. Science (80-) 302:2126–2130.

48. Pili-Floury S, Leulier F, Takahashi K, Saigo K, Samain E, Ueda R, Lemaitre B. 2004. In Vivo RNA Interference Analysis Reveals an Unexpected Role for GNBP1 in the Defense against Gram-positive Bacterial Infection in Drosophila Adults. J Biol Chem 279:12848–12853.

49. Ochiai M, Ashida M. 1988. Purification of a beta-1,3-glucan recognition protein in the prophenoloxidase activating system from hemolymph of the silkworm, Bombyx mori. J Biol Chem 263:12056–12062.

50. Gottar M, Gobert V, Matskevich AA, Reichhart J, Wang C, Butt TM, Belvin M, Hoffmann JA. 2006. Dual detection of fungal infection in drosophila through recognition of microbial structures and sensing of virulence factors. Cell 127:1425–1437.

51. Issa N, Guillaumot N, Lauret E, Matt N, Schaeffer-Reiss C, Van Dorsselaer A, Reichhart JM, Veillard F. 2018. The Circulating Protease Persephone Is an Immune Sensor for Microbial Proteolytic Activities Upstream of the Drosophila Toll Pathway. Mol Cell 69:539-550.e6.

52. Arnot CJ, Gay NJ, Gangloff M. 2010. Molecular mechanism that induces activation of Spätzle, the ligand for the Drosophila toll receptor. J Biol Chem 285:19502–19509.

53. Buchon N, Silverman N, Cherry S. 2014. Immunity in Drosophila melanogaster-from microbial recognition to whole-organism physiology. Nat Rev Immunol 14:796–810.

54. Valanne S, Wang J-H, Ramet M. 2011. The Drosophila Toll Signaling Pathway. J Immunol 186:649–656.

55. Myllymäki H, Valanne S, Rämet M. 2014. The Drosophila Imd Signaling Pathway . J Immunol 192:3455–3462.

56. Choe KM, Werner T, Stöven S, Hultmark D, Anderson K V. 2002. Requirement for a peptidoglycan recognition protein (PGRP) in relish activation and antibacterial immune responses in Drosophila. Science (80-) 296:359–362.

57. Takehana A, Katsuyama T, Yano T, Oshima Y, Takada H, Aigaki T, Kurata S. 2002. Overexpression of a pattern-recognition receptor, peptidoglycan-recognition protein-LE, activates imd/relish-mediated antibacterial defense and the prophenoloxidase cascade in Drosophila larvae. Proc Natl Acad Sci U S A 99:13705–13710.

58. Kaneko T, Yano T, Aggarwal K, Lim JH, Ueda K, Oshima Y, Peach C, Erturk-Hasdemir D, Goldman WE, Oh BH, Kurata S, Silverman N. 2006. PGRP-LC and PGRP-LE have essential yet distinct functions in the drosophila immune response to monomeric DAP-type peptidoglycan. Nat Immunol 7:715–723.

59. Leulier F, Parquet C, Pili-Floury S, Ryu JH, Caroff M, Lee WJ, Mengin-Lecreulx D, Lemaitre B. 2003. The Drosophila immune system detects bacteria through specific peptidoglycan recognition. Nat Immunol 4:478–484.

60. Gottar M, Gobert V, Michel T, Belvin M, Duyk G, Hoffmann JA, Ferrandon D, Royet J. 2002. The Drosophila immune response against Gram-negative bacteria is mediated by a peptidoglycan recognition protein. Nature 416:640–644.

61. Yano T, Mita S, Ohmori H, Oshima Y, Fujimoto Y, Ueda R, Takada H, Goldman WE, Fukase K, Silverman N, Yoshimori T, Kurata S. 2008. Autophagic control of listeria through intracellular innate immune recognition in drosophila. Nat Immunol 9:908–916.

62. Bosco-Drayon V, Poidevin M, Gomperts Boneca I, Narbonne-Reveau K, Royet J, Charroux B. 2012. Peptidoglycan sensing by the receptor PGRP-LE in the Drosophila gut induces immune responses to infectious bacteria and tolerance to microbiota. Cell Host Microbe 12:153–165.

63. Neyen C, Poidevin M, Roussel A, Lemaitre B. 2012. Tissue- and Ligand-Specific Sensing of Gram-Negative Infection in Drosophila by PGRP-LC Isoforms and PGRP-LE . J Immunol 189:1886–1897.

64. Biteau B, Karpac J, Hwangbo D, Jasper H. 2011. Regulation of Drosophila lifespan by JNK signaling. Exp Gerontol 46:349–354.

65. Pastor-Pareja JC, Grawe F, Martín-Blanco E, García-Bellido A. 2004. Invasive cell behavior during Drosophila imaginal disc eversion is mediated by the JNK signaling cascade. Dev Cell 7:387–399.

66. Külshammer E, Uhlirova M. 2013. The actin cross-linker filamin/cheerio mediates tumor

malignancy downstream of JNK signaling. J Cell Sci 126:927–938.

67. Willsey HR, Zheng X, Pastor-Pareja J, Willsey AJ, Beachy PA, Xu T. 2016. Localized JNK signaling regulates organ size during development. eLife 5:1–18.

68. Basler K. 2002. Evolution of TNF Signaling Mechanisms: JNK-Dependent Apoptosis Triggered by Eiger, the. Curr Biol 12:1263–1268.

69. Luo X, Puig O, Hyun J, Bohmann D, Jasper H. 2007. Foxo and Fos regulate the decision between cell death and survival in response to UV irradiation. EMBO J 26:380–390.

70. Pinal N, Calleja M, Morata G. 2019. Pro-apoptotic and pro-proliferation functions of the JNK pathway of drosophila: Roles in cell competition, tumorigenesis and regeneration. Open Biol 9(3).

71. Sluss HK, Han Z, Barrett T, Davis RJ, Ip YT. 1996. A JNK signal transduction pathway that mediates morphogenesis and an immune response in Drosophila. Genes Dev 10:2745–2758.

72. Boutros M, Agaisse H, Perrimon N. 2002. Sequential Activation of Signaling Pathways during Innate Immune Responses in Drosophila signaling pathways are activated upon microbial infec-tion. In response to gram-positive and fungal infection, Toll triggers a transcriptional response through the. Dev Cell 3:711–722.

73. Tafesh-Edwards G, Eleftherianos I. 2020. JNK signaling in Drosophila immunity and homeostasis. Immunol Lett 226:7–11.

74. Kallio J, Leinonen A, Ulvila J, Valanne S, Ezekowitz RA, Rämet M. 2005. Functional analysis of immune response genes in Drosophila identifies JNK pathway as a regulator of antimicrobial peptide gene expression in S2 cells 7:811–819.

75. Delaney JR, Stöven S, Uvell H, Anderson K V., Engström Y, Mlodzik M. 2006. Cooperative control of Drosophila immune responses by the JNK and NF-κB signaling pathways. EMBO J 25:3068–3077.

76. Agaisse H, Perrimon N. 2004. The roles of JAK/STAT signaling in Drosophila immune responses. Immunol Rev 198:72–82.

77. Myllymäki H, Rämet M. 2014. JAK/STAT Pathway in Drosophila Immunity. Scand J Immunol 79:377–385.

78. Lagueux M, Perrodou E, Levashina EA, Capovilla M, Hoffmann JA. 2000. Constitutive expression of a complement-like protein in Toll and JAK gain-of-function mutants of Drosophila. Proc Natl Acad Sci U S A 97:11427–11432.

79. Dostálová A, Rommelaere S, Poidevin M, Lemaitre B. 2017. Thioester-containing proteins regulate the Toll pathway and play a role in Drosophila defence against microbial pathogens and parasitoid wasps. BMC Biol 15:1–16.

80. Ekengren S, Hultmark D. 2001. A Family of Turandot -Related Genes in the Humoral Stress Response of Drosophila. Biochem Biophys Res Commun 284:998–1003.

81. Sorrentino RP, Melk JP, Govind S. 2004. Genetic Analysis of Contributions of Dorsal Group and JAK-Stat92E Pathway Genes to Larval Hemocyte Concentration and the Egg Encapsulation Response in Drosophila. Genetics 166:1343–1356.

82. Yang H, Kronhamn J, Ekström J, Korkut GG, Hultmark D. 2015. JAK / STAT signaling in D rosophila muscles controls the cellular immune response against parasitoid infection . EMBO Rep 16:1664–1672.

83. Dostert C, Jouanguy E, Irving P, Troxler L, Galiana-Arnoux D, Hetru C, Hoffmann JA, Imler JL. 2005. The Jak-STAT signaling pathway is required but not sufficient for the antiviral response of drosophila. Nat Immunol 6:946–953.

84. Irving P, Troxler L, Heuer TS, Belvin M, Kopczynski C, Reichhart J, Hoffmann JA, Hetru C. 2001. A genome-wide analysis of immune responses in Drosophila. Pnas 98:15119–15124.

85. De Gregorio E, Spellman PT, Rubin GM, Lemaitre B. 2001. Genome-wide analysis of the Drosophila immune response by using oligonucleotide microarrays. Pnas 98:12590–12595.

86. Hanson MA, Lemaitre B. 2020. New insights on Drosophila antimicrobial peptide function in host defense and beyond. Curr Opin Immunol 62:22–30.

87. Lai Y, Gallo RL. 2009. AMPed up immunity: how antimicrobial peptides have multiple roles in immune defense. Trends Immunol 30:131–141.

88. Steiner H, Hultmark D, Engström Å, Bennich H, Boman HG. 1981. Sequence and specificity of two antibacterial proteins involved in insect immunity. Nature 292:246–248.

89. Tam JP, Wang S, Wong KH, Tan WL. 2015. Antimicrobial peptides from plants. Pharmaceuticals 8:711–757.

90. Tassanakajon A, Somboonwiwat K, Supungul P, Tang S. 2013. Discovery of immune molecules and their crucial functions in shrimp immunity. Fish Shellfish Immunol 34:954–967.

91. Avila EE. 2016. Functions of Antimicrobial Peptides in Vertebrates. Curr Protein Pept Sci 18 (11):1098-1119.

92. Bechinger B, Gorr SU. 2017. Antimicrobial Peptides: Mechanisms of Action and Resistance. J Dent Res 96:254–260.

93. Joo HS, Fu CI, Otto M. 2016. Bacterial strategies of resistance to antimicrobial peptides. Philos Trans R Soc B Biol Sci 371.

94. Imler J, Bulet P. 2005. Antimicrobial Peptides in Drosophila : Structures , Activities and Gene Regulation. Chem Imunol Allergy 86:1–21.

95. Åsling B, Dushay MS, Hultmark D. 1995. Identification of early genes in the Drosophila immune response by PCR-based differential display: the Attacin A gene and the evolution of attacin-like proteins. Insect Biochem Mol Biol 25:511–518.

96. Cudic M, Bulet P, Hoffmann R, Craik DJ, Otvos L. 1999. Chemical synthesis, antibacterial activity and conformation of diptericin, an 82-mer peptide originally isolated from insects. Eur J Biochem 266:549–558.

97. Wicker C, Reichhart JM, Hoffmann D, Hultmark D, Samakovlis C, Hoffmann JA. 1990. Insect immunity. Characterization of a Drosophila cDNA encoding a novel member of the diptericin family of immune peptides. J Biol Chem 265:22493–22498.

98. Fehlbaum P, Bulet P, Michaut L, Lagueux M, Broekaert WF, Hetru C, Hoffmann JA. 1994. Septic injury of drosophila induces the synthesis of a potent antifungal peptide with sequence homology to plant antifungal peptides. J Biol Chem 269:33159–33163.

99. Levashina EA, Ohresser S, Bulet P, Reichhart J -M, Hetru C, Hoffmann JA. 1995. Metchnikowin, a Novel Immune-Inducible Proline-Rich Peptide from Drosophila with Antibacterial and Antifungal Properties. Eur J Biochem 233:694–700.

100. Daffre S, Kylsten P, Samakovlis C, Hultmark D. 1994. The lysozyme locus in Drosophila

melanogaster: an expanded gene family adapted for expression in the digestive tract. MGG Mol Gen Genet 242:152–162.

101. Ekengren S, Hultmark D. 1999. Drosophila cecropin as an antifungal agent. Insect Biochem Mol Biol 29:965–972.

102. De Gregorio E, Spellman PT, Tzou P, Rubin GM, Lemaitre B. 2002. The Toll and Imd pathways are the major regulators of the immune response in Drosophila 21:2568–2579.

103. Cociancich S, Ghazi A, Hetru C, Hoffmann JA, Letellier L. 1993. Insect defensin, an inducible antibacterial peptide, forms voltage-dependent channels in Micrococcus luteus. J Biol Chem 268:19239–19245.

104. Dimarq J -L, Hffman D, Meister M, Bulet P, Lanot R, Reichhart J -M, Hoffmann JA. 1994. Characterization and transcriptional profiles of a Drosophila gene encoding an insect defensin: A study in insect immunity. Eur J Biochem 221:201–209.

105. Akhouayri I, Turc C, Royet J, Charroux B. 2011. Toll-8/tollo negatively regulates antimicrobial response in the drosophila respiratory epithelium. PLoS Pathog 7.

106. Tzou P, Ohresser S, Ferrandon D, Capovilla M, Reichhart JM, Lemaitre B, Hoffmann JA, Imler JL. 2000. Tissue-specific inducible expression of antimicrobial peptide genes in Drosophila surface epithelia. Immunity 13:737–748.

107. Davis MM, Engström Y. 2012. Immune response in the barrier epithelia: Lessons from the fruit fly drosophila melanogaster. J Innate Immun 4:273–283.

108. Tapadia MG, Verma P. 2012. Immune response and anti-microbial peptides expression in malpighian tubules of drosophila melanogaster is under developmental regulation. PLoS One 7 (10): e1002319.

109. Tzou P, Reichhart JM, Lemaitre B. 2002. Constitutive expression of a single antimicrobial peptide can restore wild-type resistance to infection in immunodeficient Drosophila mutants. Proc Natl Acad Sci U S A 99:2152–2157.

110. Hanson MA, Dostálová A, Ceroni C, Poidevin M, Kondo S, Lemaître B. 2019. Synergy and remarkable specificity of antimicrobial peptides in vivo using a systematic knockout approach. eLife 8:e44341.

111. Parvy JP, Yu Y, Dostalova A, Kondo S, Kurjan A, Bulet P, Lemaitre B, Vidal M,

Cordero JB. 2019. The antimicrobial peptide Defensin cooperates with Tumour Necrosis Factor to drive tumour cell death in Drosophila. eLife 8:e45061.

112. Araki M, Kurihara M, Kinoshita S, Awane R, Sato T, Ohkawa Y, Inoue YH. 2019. Anti-tumour effects of antimicrobial peptides, components of the innate immune system, against haematopoietic tumours in Drosophila mxc mutants. Dis Model Mech 12(6).

113. Bozler J, Kacsoh BZ, Chen H, Theurkauf WE, Weng Z, Bosco G. 2017. A systems level approach to temporal expression dynamics in Drosophila reveals clusters of long term memory genes. PLoS Genet 13:e1007054.

114. Azpeleta RB, Wu J, Gill J, Welte R, Seidel C, Si K. 2018. Antimicrobial peptides modulate long-term memory. PLoS Genet 14:e1007440.

115. Seroude L, Brummel T, Kapahi P, Benzer S. 2002. Spatio-temporal analysis of gene expression during aging in Drosophila melanogaster. Aging Cell 1:47–56.

116. Flatt T, Garschall K. 2018. The interplay between immunity and aging in Drosophila. F1000Research 7:1–11.

117. Clemmons AW, Lindsay SA, Wasserman SA. 2015. An Effector Peptide Family Required for Drosophila Toll-Mediated Immunity. PLoS Pathog 11:1–17.

118. Uttenweiler-Joseph S, Moniatte M, Lagueux M, Van Dorsselaer A, Hoffmann JA, Bulet P. 1998. Differential display of peptides induced during the immune response of Drosophila: A matrix-assisted laser desorption ionization time-of-flight mass spectrometry study. Proc Natl Acad Sci U S A 95:11342–11347.

119. Lindsay SA, Lin SJH, Wasserman SA. 2018. Short-Form Bomanins Mediate Humoral Immunity in Drosophila. J Innate Immun 10:306–314.

120. Brun S, Vidal S, Spellman P, Takahashi K, Tricoire H, Lemaitre B. 2006. The MAPKKK Mekk1 regulates the expression of Turandot stress genes in response to septic injury in Drosophila. Genes Cell 11:397–407.

121. Agaisse H, Petersen UM, Boutros M, Mathey-Prevot B, Perrimon N. 2003. Signaling role of hemocytes in Drosophila JAK/STAT-dependent response to septic injury. Dev Cell 5:441–450.

122. Immonen E, Ritchie MG. 2012. The genomic response to courtship song stimulation in

female Drosophila melanogaster. Proc R Soc B Biol Sci 279:1359–1365.

123. McGraw LA, Gibson G, Clark AG, Wolfner MF. 2004. Genes Regulated by Mating, Sperm, or Seminal Proteins in Mated Female Drosophila melanogaster. Curr Biol 14:1509–1514.

124. Zhong W, Mcclure CD, Evans CR, Mlynski DT, Immonen E, Ritchie MG, Priest NK. 2013. Immune anticipation of mating in Drosophila : Turandot M promotes immunity against sexually transmitted fungal infections. Proceeding R Soc B 280 (1773):20132018.

125. Ashida M. 1990. The prophenoloxidase cascade in insect immunity. Res Immunol 141:908–910.

126. Nappi AJ, Vass E. 1993. Melanogenesis and the Generation of Cytotoxic Molecules During Insect Cellular Immune Reactions. Pigment Cell Res 6:117–126.

127. Söderhäll K, Cerenius L. 1998. Role of the prophenoloxidase-activating system in invertebrate immunity. Curr Opin Immunol 10:23–28.

128. Nappi A, Poirié M, Carton YBT-A in P. 2009. The Role of Melanization and Cytotoxic By-Products in the Cellular Immune Responses of Drosophila Against Parasitic Wasps. Adv Parasitol 70:99–121.

129. Dudzic JP, Hanson MA, Iatsenko I, Kondo S, Lemaitre B, Dudzic JP, Hanson MA, Iatsenko I, Kondo S, Lemaitre B. 2019. More Than Black or White : Melanization and Toll Share Regulatory Serine Proteases in Drosophila. Cell Rep 27:1050-1061.e3.

130. Chen Y, Liu F, Yang B, Lu A, Wang S, Wang J, Ling QZ, Li X, Beerntsen BT, Ling E. 2012. Specific amino acids affecting Drosophila melanogaster prophenoloxidase activity in vitro. Dev Comp Immunol 38:88–97.

131. Castillejo-López C, Häcker U. 2005. The serine protease Sp7 is expressed in blood cells and regulates the melanization reaction in Drosophila. Biochem Biophys Res Commun 338:1075–1082.

132. Leclerc V, Pelte N, El Chamy L, Martinelli C, Ligoxygakis P, Hoffmann JA, Reichhart JM. 2006. Prophenoloxidase activation is not required for survival to microbial infections in Drosophila. EMBO Rep 7:231–235.

133. Rämet M, Lanot R, Zachary D, Manfruelli P. 2002. JNK signaling pathway is required for efficient wound healing in Drosophila. Dev Biol 241:145–156.

134. Nam HJ, Jang IH, Asano T, Lee WJ. 2008. Involvement of pro-phenoloxidase 3 in lamellocyte-meidated spontaneous melanization in Drosophila. Mol Cells 26:606–610.

135. Ayres JS, Schneider DS. 2008. A signaling protease required for melanization in Drosophila affects resistance and tolerance of infections. PLoS Biol 6 (12):2764-73.

136. Binggeli O, Neyen C, Poidevin M, Lemaitre B. 2014. Prophenoloxidase Activation Is Required for Survival to Microbial Infections in Drosophila. PLoS Pathog 10 (5):e1004067.

137. Lemaitre B, Hoffmann J. 2007. The Host Defense of Drosophila melanogaster . Annu Rev Immunol 25:697–743.

138. Melcarne C, Lemaitre B, Kurant E. 2019. Phagocytosis in Drosophila: From molecules and cellular machinery to physiology. Insect Biochem Mol Biol 109:1–12.

139. Lanot R, Zachary D, Holder F, Meister M. 2001. Postembryonic hematopoiesis in Drosophila. Dev Biol 230:243–257.

140. Comber JD, Robinson TM, Siciliano NA, Snook AE, Eisenlohr LC. 2011. Functional Macroautophagy Induction by Influenza A Virus without a Contribution to Major Histocompatibility Complex Class II-Restricted Presentation. J Virol 85:6453–6463.

141. Kramerova IA, Kramerov AA, Fessler JH. 2003. Alternative splicing of papilin and the diversity of Drosophila extracellular matrix during embryonic morphogenesis. Dev Dyn 226:634–642.

142. Olofsson B, Page DT. 2005. Condensation of the central nervous system in embryonic Drosophila is inhibited by blocking hemocyte migration or neural activity. Dev Biol 279:233–243.

143. Bunt S, Hooley C, Hu N, Scahill C, Weavers H, Skaer H. 2010. Hemocyte-secreted type IV collagen enhances BMP signaling to guide renal tubule morphogenesis in Drosophila. Dev Cell 19:296–306.

144. Irving P, Ubeda J-M, Doucet D, Troxler L, Lagueux M, Zachary D, Hoffmann JA, Hetru C, Meister M. 2005. New insights into Drosophila larval haemocyte functions through

genome-wide analysis. Cell Microbiol 7:335–350.

145. Braun A, Hoffmann JA, Meister M. 1998. Analysis of the Drosophila host defense in domino mutant larvae, which are devoid of hemocytes. Proc Natl Acad Sci U S A 95:14337–14342.

146. Nehme NT, Liégeois S, Kele B, Giammarinaro P, Pradel E, Hoffmann JA, Ewbank JJ, Ferrandon D. 2007. A model of bacterial intestinal infections in Drosophila melanogaster. PLoS Pathog 3:1694–1709.

147. Rizki TM, Rizki RM, Grell EH. 1980. A Mutant Affecting the Crystal Cells in Drosophila melanogaster. Roux's Arch Dev Biol 99 (2):91-99.

148. Vlisidou I, Wood W. 2015. Drosophila blood cells and their role in immune responses 282:1368–1382.

149. Segawa K, Nagata S. 2015. An Apoptotic "Eat Me" Signal: Phosphatidylserine Exposure. Trends Cell Biol 25:639–650.

150. Kinchen JM, Ravichandran KS. 2010. Identification of two evolutionarily conserved genes regulating processing of engulfed apoptotic cells. Nature 464:778–782.

151. Nieto C, Almendinger J, Gysi S, Gómez-Orte E, Kaech A, Hengartner MO, Schnabel R, Moreno S, Cabello J. 2010. ccz-1 mediates the digestion of apoptotic corpses in C. elegans. J Cell Sci 123:2001–2007.

152. Li W, Zou W, Zhao D, Yan J, Zhu Z, Lu J, Wang X. 2009. C. elegans Rab GTPase activating protein TBC-2 promotes cell corpse degradation by regulating the small GTPase RAB-5. Development 136:2445–2455.

153. Seong CS, Varela-Ramirez A, Aguilera RJ. 2006. DNase II deficiency impairs innate immune function in Drosophila. Cell Immunol 240:5–13.

154. Pearson A, Lux A, Krieger M. 1995. Expression cloning of dSR-CI, a class C macrophage-specific scavenger receptor from Drosophila melanogaster. Proc Natl Acad Sci U S A 92:4056–4060.

155. Rämet M, Pearson A, Manfruelli P, Li X, Koziel H, Göbel V, Chung E, Krieger M, Ezekowitz RAB. 2001. Drosophila scavenger receptor CI is a pattern recognition receptor for bacteria. Immunity 15:1027–1038.

156. Savill J, Hogg N, Ren Y, Haslett C. 1992. Thrombospondin cooperates with CD36 and the vitronectin receptor in macrophage recognition of neutrophils undergoing apoptosis. J Clin Invest 90:1513–1522.

157. Franc NC, Dimarcq JL, Lagueux M, Hoffmann J, Ezekowitz RAB. 1996. Croquemort, a novel drosophila hemocyte/macrophage receptor that recognizes apoptotic cells. Immunity 4:431–443.

158. Guillou A, Troha K, Wang H, Franc NC, Buchon N. 2016. The Drosophila CD36 Homologue croquemort Is Required to Maintain Immune and Gut Homeostasis during Development and Aging. PLoS Pathog 12:1–27.

159. Han C, Song Y, Xiao H, Wang D, Franc NC, Yeh Jan L, Jan YN. 2014. Epidermal Cells Are the Primary Phagocytes in the Fragmentation and Clearance of Degenerating Dendrites in Drosophila. Neuron 81:544–560.

160. Meehan TL, Joudi TF, Timmons AK, Taylor JD, Habib CS, Peterson JS, Emmanuel S, Franc NC, McCall K. 2016. Components of the engulfment machinery have distinct roles in corpse processing. PLoS One 11:1–22.

161. Bork P, Downing AK, Kieffer B, Campbell ID. 1996. Structure and distribution of modules in extracellular proteins. Q Rev Biophys 29:119–167.

162. Kocks C, Cho JH, Nehme N, Ulvila J, Pearson AM, Meister M, Strom C, Conto SL, Hetru C, Stuart LM, Stehle T, Hoffmann JA, Reichhart JM, Ferrandon D, Rämet M, Ezekowitz RAB. 2005. Eater, a transmembrane protein mediating phagocytosis of bacterial pathogens in Drosophila. Cell 123:335–346.

163. Horn L, Leips J, Starz-Gaiano M. 2014. Phagocytic ability declines with age in adult Drosophila hemocytes. Aging Cell 13:719–728.

164. Nehme NT, Quintin J, Cho JH, Lee J, Lafarge MC, Kocks C, Ferrandon D. 2011. Relative roles of the cellular and humoral responses in the Drosophila host defense against three gram-positive bacterial infections. PLoS One 6.

165. Bretscher AJ, Honti V, Binggeli O, Burri O, Poidevin M, Kurucz É, Zsámboki J, Andó I, Lemaitre B. 2015. The Nimrod transmembrane receptor Eater is required for hemocyte attachment to the sessile compartment in Drosophila melanogaster. Biol Open 4:355–363.

166. Kurucz É, Márkus R, Zsámboki J, Folkl-Medzihradszky K, Darula Z, Vilmos P, Udvardy A, Krausz I, Lukacsovich T, Gateff E, Zettervall CJ, Hultmark D, Andó I. 2007. Nimrod, a Putative Phagocytosis Receptor with EGF Repeats in Drosophila Plasmatocytes. Curr Biol 17:649–654.

167. Bou Aoun R, Hetru C, Troxler L, Doucet D, Ferrandon D, Matt N. 2011. Analysis of Thioester-Containing Proteins during the Innate Immune Response of Drosophila melanogaster. J Innate Immun 3:52–64.

168. Stroschein-Stevenson SL, Foley E, O'Farrell PH, Johnson AD. 2006. Identification of Drosophila gene products required for phagocytosis of Candida albicans. PLoS Biol 4:0087–0099.

169. Zsámboki J, Csordás G, Honti V, Pintér L, Bajusz I, Galgóczy L, Andó I, Kurucz É. 2013. Drosophila Nimrod proteins bind bacteria. Cent Eur J Biol 8:633–645.

170. Garver LS, Wu J, Wu LP. 2006. The peptidoglycan recognition protein PGRP-SC1a is essential for Toll signaling and phagocytosis of Staphylococcus aureus in Drosophila. Proc Natl Acad Sci U S A 103:660–665.

171. Kurucz E, Zettervall C, Sinka R, Vilmos P, Pivarcsi A, Ekengren S, Ando I, Hultmark D. 2003. Hemese, a hemocyte-specific transmembrane protein, affects the cellular immune response in Drosophila. Pnas 100:2622–2627.

172. Goto A, Kadowaki T, Kitagawa Y. 2003. Drosophila hemolectin gene is expressed in embryonic and larval hemocytes and its knock down causes bleeding defects. Dev Biol 264:582–591.

173. Lesch C, Goto A, Lindgren M, Bidla G, Dushay MS, Theopold U. 2007. A role for Hemolectin in coagulation and immunity in Drosophila melanogaster. Dev Comp Immunol 31:1255–1263.

174. Reichhart JM, Meister M, Dimarcq JL, Zachary D, Hoffmann D, Ruiz C, Richards G, Hoffmann JA. 1992. Insect immunity: Developmental and inducible activity of the Drosophila diptericin promoter. EMBO J 11:1469–1477.

175. Yang S, Zhao Y, Yu J, Fan Z, Gong S tang, Tang H, Pan L. 2019. Sugar Alcohols of Polyol Pathway Serve as Alarmins to Mediate Local-Systemic Innate Immune Communication in Drosophila. Cell Host Microbe 26:240-251.e8.

176. Miguel-aliaga I, Jasper H, Lemaitre B. 2018. Anatomy and Physiology of the Digestive Tract of Drosophila melanogaster 210:357–396.

177. Broderick NA, Broderick NA. 2016. Friend , foe or food ? Recognition and the role of antimicrobial peptides in gut immunity and Drosophila – microbe interactions. Philos Trans R Soc B Biol Sci 371.

178. Erkosar B, Leulier F. 2014. Transient adult microbiota , gut homeostasis and longevity : Novel insights from the Drosophila model. FEBS Lett 588:4250–4257.

179. Kuraishi T, Binggeli O, Opota O, Buchon N, Lemaitre B. 2011. Genetic evidence for a protective role of the peritrophic matrix against intestinal bacterial infection in Drosophila melanogaster. Proc Natl Acad Sci U S A 108:15966–15971.

180. Shibata T, Maki K, Hadano J, Fujikawa T, Kitazaki K, Koshiba T, Kawabata SI. 2015. Crosslinking of a Peritrophic Matrix Protein Protects Gut Epithelia from Bacterial Exotoxins. PLoS Pathog 11:e1005244.

181. Lemaitre B, Miguel-Aliaga I. 2013. The digestive tract of Drosophila melanogaster. Annu Rev Genet 47:377–404.

182. Bonfini A, Liu X, Buchon N. 2016. From pathogens to microbiota: How Drosophila intestinal stem cells react to gut microbes. Dev Comp Immunol 64:22–38.

183. Jiang H, Tian A, Jiang J. 2016. Intestinal stem cell response to injury: lessons from Drosophila. Cell Mol life Sci 73:3337–3349.

184. Buchon N, Broderick NA, Chakrabarti S, Lemaitre B. 2009. Invasive and indigenous microbiota impact intestinal stem cell activity through multiple pathways in Drosophila. Genes Dev 23:2333–2344.

185. Buchon N, Broderick NA, Kuraishi T, Lemaitre B. 2010. Drosophila EGFR pathway coordinates stem cell proliferation and gut remodeling following infection. BMC Biol 8(185).

186. Broderick NA, Buchon N, Lemaitre B. 2014. Microbiota-induced changes in Drosophila melanogaster host gene expression and gut morphology. mBio 5:e01117-14.

187. Chakrabarti S, Liehl P, Buchon N, Lemaitre B. 2012. Infection-induced host translational blockage inhibits immune responses and epithelial renewal in the Drosophila gut. Cell

Host Microbe 12:60–70.

188. Kenmoku H, Ishikawa H, Ote M, Kuraishi T, Kurata S. 2016. A subset of neurons controls the permeability of the peritrophic matrix and midgut structure in Drosophila adults. J Exp Biol 219:2331–2339.

189. Allan AK, Du J, Davies SA, Dow JAT. 2005. Genome-wide survey of V-ATPase genes in Drosophila reveals a conserved renal phenotype for lethal alleles. Physiol Genomics 22:128–138.

190. Overend G, Luo Y, Henderson L, Douglas AE, Davies SA, Dow JAT. 2016. Molecular mechanism and functional significance of acid generation in the Drosophila midgut. Sci Rep 6:1–11.

191. Li H, Qi Y, Jasper H. 2016. Preventing Age-Related Decline of Gut Compartmentalization Limits Microbiota Dysbiosis and Extends Lifespan. Cell Host Microbe 19:240–253.

192. Kuraishi T, Hori A, Kurata S. 2013. Host-microbe interactions in the gut of Drosophila melanogaster. Front Physiol 4:375.

193. Kim S, Lee W. 2014. Role of DUOX in gut inflammation : lessons from Drosophila model of gut-microbiota interactions. Front Cell Infect Microbiol 3(116).

194. Xu C, Luo J, He L, Montell C, Perrimon N. 2017. Oxidative stress induces stem cell proliferation via TRPA1/RyR-mediated Ca2+signaling in the Drosophila midgut. eLife 6:e22441.

195. Hochmuth CE, Biteau B, Bohmann D, Jasper H. 2011. Redox regulation by keap1 and Nrf2 controls intestinal stem cell proliferation in drosophila. Cell Stem Cell 8:188–199.

196. Ha E-M, Oh C-T, Bae YS, Lee W-J. 2005. A Direct Role for Dual Oxidase in Drosophila Gut Immunity. Science (80-) 310:847–850.

197. Iatsenko I, Boquete J, Lemaitre B. 2018. Microbiota-Derived Lactate Activates Production of Reactive Oxygen Species by the Intestinal NADPH Oxidase Nox and Shortens Drosophila Lifespan. Immunity 49:929–942.

198. Jones RM, Luo L, Ardita CS, Richardson AN, Kwon YM, Mercante JW, Alam A, Gates CL, Wu H, Swanson PA, David Lambeth J, Denning PW, Neish AS. 2013. Symbiotic

lactobacilli stimulate gut epithelial proliferation via Nox-mediated generation of reactive oxygen species. EMBO J 32:3017–3028.

199. Louradour I, Sharma A, Morin-Poulard I, Letourneau M, Vincent A, Crozatier M, Vanzo N. 2017. Reactive oxygen species-dependent Toll/NF-κB activation in the drosophila hematopoietic niche confers resistance to wasp parasitism. eLife 6:e25496.

200. Ha EM, Lee KA, Seo YY, Kim SH, Lim JH, Oh BH, Kim J, Lee WJ. 2009. Coordination of multiple dual oxidase-regulatory pathways in responses to commensal and infectious microbes in drosophila gut. Nat Immunol 10:949–957.

201. Lee KA, Kim SH, Kim EK, Ha EM, You H, Kim B, Kim MJ, Kwon Y, Ryu JH, Lee WJ. 2013. Bacterial-derived uracil as a modulator of mucosal immunity and gut-microbe homeostasis in drosophila. Cell 153:797–811.

202. Guo L, Karpac J, Tran SL, Jasper H. 2014. PGRP-SC2 promotes gut immune homeostasis to limit commensal dysbiosis and extend lifespan. Cell 156:109–122.

203. Buchon N, Broderick NA, Poidevin M, Pradervand S, Lemaitre B. 2009. Drosophila Intestinal Response to Bacterial Infection: Activation of Host Defense and Stem Cell Proliferation. Cell Host Microbe 5:200–211.

204. Bischoff V, Vignal C, Duvic B, Boneca IG, Hoffmann JA, Royet J. 2006. Downregulation of the Drosophila immune response by peptidoglycan- recognition proteins SC1 and SC2. PLoS Pathog 2:0139–0147.

205. Paredes JC, Welchman DP, Poidevin M, Lemaitre B. 2011. Negative regulation by Amidase PGRPs shapes the drosophila antibacterial response and protects the Fly from innocuous infection. Immunity 35:770–779.

206. Lee KZ, Ferrandon D. 2011. Negative regulation of immune responses on the fly. EMBO J 30:988–990.

207. Kleino A, Myllymäki H, Kallio J, Vanha-aho L-M, Oksanen K, Ulvila J, Hultmark D, Valanne S, Rämet M. 2008. Pirk Is a Negative Regulator of the Drosophila Imd Pathway . J Immunol 180:5413–5422.

208. Lhocine N, Ribeiro PS, Buchon N, Wepf A, Wilson R, Tenev T, Lemaitre B, Gstaiger M, Meier P, Leulier F. 2008. PIMS Modulates Immune Tolerance by Negatively Regulating Drosophila Innate Immune Signaling. Cell Host Microbe 4:147–158.

209. Pais IS, Valente RS, Sporniak M, Teixeira L. 2018. Drosophila melanogaster establishes a species-specific mutualistic interaction with stable gut-colonizing bacteria. PLoS Biol 16:1–45.

210. Broderick NA, Lemaitre B. 2012. Gut-associated microbes of Drosophila melanogaster. Gut Microbes 3:307–321.

211. Blum JE, Fischer CN, Miles J, Handelsman J. 2013. Frequent replenishment sustains the beneficial microbiome of Drosophila melanogaster. mBio 4:1–8.

212. Bakula M. 1969. The persistence of a microbial flora during postembryogenesis of Drosophila melanogaster. J Invertebr Pathol 14:365–374.

213. Huang JH, Douglas AE. 2015. Consumption of dietary sugar by gut bacteria determines Drosophila lipid content. Biol Lett 11:12–15.

214. Venu I, Durisko Z, Xu J, Dukas R. 2014. Social attraction mediated by fruit flies' microbiome. J Exp Biol 217:1346–1352.

215. Ma D, Storelli G, Mitchell M, Leulier F. 2015. Studying host-microbiota mutualism in Drosophila: Harnessing the power of gnotobiotic flies. Biomed J 38:285–293.

216. Lesperance DN, Broderick NA. 2020. Microbiomes as modulators of Drosophila melanogaster homeostasis and disease. Curr Opin Insect Sci 39:84–90.

217. Storelli G, Defaye A, Erkosar B, Hols P, Royet J, Leulier F. 2011. Lactobacillus plantarum promotes drosophila systemic growth by modulating hormonal signals through TOR-dependent nutrient sensing. Cell Metab 14:403–414.

218. Fischer C, Trautman EP, Crawford JM, Stabb E V., Handelsman J, Broderick NA. 2017. Metabolite exchange between microbiome members produces compounds that influence drosophila behavior. eLife 6:1–25.

219. Sansone CL, Cohen J, Yasunaga A, Xu J, Osborn G, Subramanian H, Gold B, Buchon N, Cherry S. 2015. Microbiota-dependent priming of antiviral intestinal immunity in Drosophila. Cell Host Microbe 18:571–581.

220. Shin SC, Kim S-H, You H, Kim B, Kim AC, Lee K-A, Yoon J-H, Ryu J-H, Lee W-J. 2011. Drosophila Microbiome Modulates Host Developmental and Metabolic Homeostasis via Insulin Signaling. Science (80-) 334:670–674.

221. Consuegra J, Grenier T, Akherraz H, Rahioui I, Gervais H, da Silva P, Leulier F. 2020. Metabolic Cooperation among Commensal Bacteria Supports Drosophila Juvenile Growth under Nutritional Stress. iScience 23(6).

222. Lee HY, Lee SH, Lee JH, Lee WJ, Min KJ. 2019. The role of commensal microbes in the lifespan of Drosophila melanogaster. Aging (Albany NY) 11:4611–4640.

223. Sannino DR, Dobson AJ, Edwards K, Angert ER, Buchon N. 2018. The Drosophila melanogaster gut microbiota provisions thiamine to its host. mBio 9:1–16.

224. Clark RI, Salazar A, Yamada R, Fitz-Gibbon S, Morselli M, Alcaraz J, Rana A, Rera M, Pellegrini M, Ja WW, Walker DW. 2015. Distinct Shifts in Microbiota Composition during Drosophila Aging Impair Intestinal Function and Drive Mortality. Cell Rep 12:1656–1667.

225. Storelli G, Strigini M, Grenier T, Bozonnet L, Schwarzer M, Daniel C, Matos R, Leulier F. 2018. Drosophila Perpetuates Nutritional Mutualism by Promoting the Fitness of Its Intestinal Symbiont Lactobacillus plantarum. Cell Metab 27:362-377.e8.

226. Ryu J, Kim S, Lee H, Bai JY, Nam Y, Bae J, Lee DG, Shin SC, Ha E, Lee W. 2008. Innate Immune Homeostasis by the Homeobox Gene Caudal and Commensal-Gut Mutualism in Drosophila. Science (80-) 319:777–782.

227. Maillet F, Bischoff V, Vignal C, Hoffmann J, Royet J. 2008. The Drosophila Peptidoglycan Recognition Protein PGRP-LF Blocks PGRP-LC and IMD/JNK Pathway Activation. Cell Host Microbe 3:293–303.

228. Troha K, Nagy P, Pivovar A, Lazzaro BP, Hartley PS, Buchon N. 2019. Nephrocytes Remove Microbiota-Derived Peptidoglycan from Systemic Circulation to Maintain Immune Homeostasis. Immunity 51:625-637.e3.

229. Erkosar B, Defaye A, Bozonnet N, Puthier D, Royet J, Leulier F. 2014. Drosophila microbiota modulates host metabolic gene expression via IMD/NF-κB signaling. PLoS One 9:e94729.

230. Zhai Z, Boquete JP, Lemaitre B. 2018. Cell-Specific Imd-NF-κB Responses Enable Simultaneous Antibacterial Immunity and Intestinal Epithelial Cell Shedding upon Bacterial Infection. Immunity 48:897-910.e7.

231. McFall-Ngai M, Heath-Heckman EAC, Gillette AA, Peyer SM, Harvie EA. 2012. The

secret languages of coevolved symbioses: Insights from the Euprymna scolopes-Vibrio fischeri symbiosis. Semin Immunol 24:3–8.

232. Lemaitre B, Reichhart JM, Hoffmann JA. 1997. Drosophila host defense: Differential induction of antimicrobial peptide genes after infection by various classes of microorganisms. Proc Natl Acad Sci U S A 94:14614–14619.

233. Leulier F, Rodriguez A, Khush RS, Abrams JM, Lemaitre B. 2000. The Drosophila caspase Dredd is required to resist Gram-negative bacterial infection. EMBO Rep 1:353–358.

234. Nash JA, Ballard TNS, Weaver TE, Akinbi HT. 2006. The Peptidoglycan-Degrading Property of Lysozyme Is Not Required for Bactericidal Activity In Vivo. J Immunol 177:519–526.

235. Buchon N, Osman D, David FPA, Yu Fang H, Boquete JP, Deplancke B, Lemaitre B. 2013. Morphological and Molecular Characterization of Adult Midgut Compartmentalization in Drosophila. Cell Rep 3:1725–1738.

236. Brummel T, Ching A, Seroude L, Simon AF, Benzer S. 2004. Drosophila lifespan enhancement by exogenous bacteria. Proc Natl Acad Sci U S A 101:12974–12979.

237. Staubach F, Baines JF, Künzel S, Bik EM, Petrov DA. 2013. Host Species and Environmental Effects on Bacterial Communities Associated with Drosophila in the Laboratory and in the Natural Environment. PLoS One 8 (8):e70749.

238. Chandler JA, Lang J, Bhatnagar S, Eisen JA, Kopp A. 2011. Bacterial communities of diverse Drosophila species: Ecological context of a host-microbe model system. PLoS Genet 7 (9):e1002272.

239. Obadia B, Güvener ZT, Zhang V, Ceja-Navarro JA, Brodie EL, Ja WW, Ludington WB. 2017. Probabilistic Invasion Underlies Natural Gut Microbiome Stability. Curr Biol 27:1999-2006.e8.

240. Fast D, Duggal A, Foley E. 2018. Monoassociation with Lactobacillus plantarum Disrupts Intestinal Homeostatis in Adult Drosophila melanogaster. mBio 9:e011114-18.

241. Davoodi S, Foley E. 2020. Host-Microbe-Pathogen Interactions: A Review of Vibrio cholerae Pathogenesis in Drosophila. Front Immunol 10:1–11.

242. Iatsenko I, Marra A, Boquete JP, Peña J, Lemaitre B. 2020. Iron sequestration by transferrin 1 mediates nutritional immunity in Drosophila melanogaster. Proc Natl Acad Sci U S A 117:7317–7325.

243. Gerth M, Martinez-Montoya H, Ramirez P, Masson F, Griffin JS, Aramayo R, Siozios S, Lemaitre B, Mateos M, Hurst GDD. 2020. Rapid molecular evolution of Spiroplasma symbionts of Drosophila. Mic Gen 7(2).

Curriculum Vitae of Alice Marra

Born in Verbania (IT), 25.09.1990
Avenue de la poste 27, 1020 Renens (CH)
Phone number: +39 3467325386 /+41 787185211
Email: arexis90@gmail.com

Referees:

Bruno Lemaitre, Ecole polytechnique fédérale de Lausanne (EPFL), Lausanne (CH) email : bruno.lemaitre@epfl.ch

Paola Bellosta, Centre for Integrative Biology University of Trento, Trento (IT) email: paola.bellosta@unitn.it

Work experience

- **1.05.2017 – today**: PhD sudent under the supervision of the Professor Bruno Lemaitre at the Ecole polytechnique fédérale de Lausanne (EPFL).

- **01.01.2017-01.01.2017**: post graduate fellowship in Università degli Studi of Milano (IT) under the supervision of the Professor Paola Bellosta.

Education

- From 2014 to 2016: **Master of Biology applied in Biomedical research, University of Milan, department of Biosciences. Average grade:** 110 cum laude

Master thesis*: << Characterization and role of non-muscle myosin II in midgut of the model organism Drosophila melanogaster. >>*

One-year project developed six months in the laboratory of Dr. Paola Bellosta in Università degli
Studi of Milan and six months under the supervision of Dr. Bruno Lemaitre in Global Health Institute in Swiss Federal institute of Technology (EPFL) of Lausanne. The aim of the project was try to analyze the role of motor protein actin associated in *Drosophila* midgut, focusing on stem cells biology.

- From 2010 to 2014: **Bachelor of Science in Biology, University of Milan, department of Biosciences**

Grade: 94/110

Bachelor project: Three months project in human cancer immunology. Investigated the expression profile of specific human melanoma genes and its mechanical ability to invade organs. Research advisor, Prof. Caterina Laporta.

- From 2005 to 2009: **High school diploma focusing on humanities**

Languages

Italian mother tongue , **English** B2 level

Soft Skills

Hard worker, open minded, reliable , proactive, team work and critical mind.

Job related skills

- Protein skills: Western Blot and ELISA
- Molecular biology skills: Plasmid preparation, ligation, transformation, Genomic DNA extraction, total RNA extraction, RT-PCR, PCR, molecular cloning.
- Bacterial strains manipulation and maintenance
- Microscopy skills : immunostaining, confocal microscopy, image analysis
- Maintenance of animals. Deep understanding in *Drosophila* genetic.

Computer skills

Familiar with Windows operating system
Pratical with different softwares:

- GraphPad Prism
- Office
- ImageJ

Teaching experience

- 2017-2020 Practical work and lab assistant in a Biotechnology and Bioengeneer laboratory
- 2020-2021 Teaching assistant in a Physiology and Biochemistry course

Selected List of Attended Congress

- Swiss Drosophila meeting, September 11th-14th 2020, EPFL, Lausanne, Switzerland
- 26th European Drosophila research conference (EDRC), September 5th-8th EPFL, Lausanne, Switzerland
- PhD Summer Course Host-microbe symbioses: from functional to ecological perspectives, Instituto Gulbenkian de Ciência - Fundação Calouste Gulbenkian, July 14th- 26th 2019, Oeiras, Portugal
- 31st French Drosophila meeting October 9th-12th , Belambra Club Les Criques, Hèyres, France

Publications

A. Marra, F. Masson, B. Lemaitre. The iron transporter Transferrin 1 mediates homeostasis of the endosymbiotic relationship between *Drosophila melanogaster* and the bacterium *Spiroplasma poulsonii*. *In prep*.

A. Marra, M.A. Hanson, S. Kondo, B. Erkosar, and B. Lemaitre. *Drosophila* antimicrobials regulate gut microbiota composition and abundance. *In prep*.

I. Iatsenko, **A. Marra**, J.P. Boquete, J. Peña, and B. Lemaitre Iron sequestration by transferrin 1 mediates nutritional immunity in *Drosophila melanogaster.* PNAS 03/2020. https://doi.org/10.1073/pnas.1914830117

M.A. Hanson, L.B. Cohen, **A. Marra**, I. Iatsenko, S.A. Wasserman, B. Lemaitre
The *Drosophila* Baramicin polypeptide gene protects against fungal infection. BioRxv 11/2020. https://doi.org/10.1101/2020.11.23.394148

F. Masson, S. Rommelaere, **A. Marra**, F. Schüpfer, Bruno Lemaitre
Dual proteomics of *Drosophila melanogaster* hemolymph infected with the heritable endosymbiont *Spiroplasma poulsonii*. BioRxv 2/2021 https://doi.org/10.1101/2021.02.22.432267

Annexes

Iron sequestration by transferrin 1 mediates nutritional immunity in *Drosophila melanogaster*

Igor Iatsenko[a,1,2], Alice Marra[a], Jean-Philippe Boquete[a], Jasquelin Peña[b], and Bruno Lemaitre[a,1]

[a]Global Health Institute, School of Life Sciences, École Polytechnique Fédérale de Lausanne, 1015 Lausanne, Switzerland; and [b]Institute of Earth Surface Dynamics, University of Lausanne, 1015 Lausanne, Switzerland

Edited by Alexander S. Raikhel, University of California, Riverside, CA, and approved February 20, 2020 (received for review August 26, 2019)

Iron sequestration is a recognized innate immune mechanism against invading pathogens mediated by iron-binding proteins called transferrins. Despite many studies on antimicrobial activity of transferrins in vitro, their specific in vivo functions are poorly understood. Here we use *Drosophila melanogaster* as an in vivo model to investigate the role of transferrins in host defense. We find that systemic infections with a variety of pathogens trigger a hypoferremic response in flies, namely, iron withdrawal from the hemolymph and accumulation in the fat body. Notably, this hypoferremia to infection requires *Drosophila* nuclear factor κB (NF-κB) immune pathways, Toll and Imd, revealing that these pathways also mediate nutritional immunity in flies. Next, we show that the iron transporter Tsf1 is induced by infections downstream of the Toll and Imd pathways and is necessary for iron relocation from the hemolymph to the fat body. Consistent with elevated iron levels in the hemolymph, *Tsf1* mutants exhibited increased susceptibility to *Pseudomonas* bacteria and Mucorales fungi, which could be rescued by chemical chelation of iron. Furthermore, using siderophore-deficient *Pseudomonas aeruginosa*, we discover that the siderophore pyoverdine is necessary for pathogenesis in wild-type flies, but it becomes dispensable in *Tsf1* mutants due to excessive iron present in the hemolymph of these flies. As such, our study reveals that, similar to mammals, *Drosophila* uses iron limitation as an immune defense mechanism mediated by conserved iron-transporting proteins transferrins. Our in vivo work, together with accumulating in vitro studies, supports the immune role of insect transferrins against infections via an iron withholding strategy.

transferrin | *Drosophila* | nutritional immunity | iron sequestration | innate immunity

Iron plays an indispensable role in numerous physiological processes, such as respiration, the trichloroacetic acid cycle, oxygen transport, gene regulation, and DNA biosynthesis. Owing to its versatile biological utility, iron is an essential element in the biological processes of all living organisms, and is central to metabolic function. As a consequence, iron sequestration by the host is a potent defense against bacterial pathogens, a process termed nutritional immunity (1–7). Early reports dating back to the 1940s documented that intramuscular inoculation of dogs with *Staphylococcus aureus* leads to a precipitous drop in plasma iron levels, which was named hypoferremia of infection (8). This hypoferremic response is an important facet of the innate immune system aimed at limiting iron availability to invading microbes by withholding iron within the cells and tissues. In line with this, individuals who suffer from iron overload due to mutations affecting iron metabolism have an enhanced risk of infection (9). To sequester iron from pathogens, the host relies on a number of iron-binding proteins, among which members of the transferrin family frequently play a prominent role (1, 10). Transferrins are monomeric glycoproteins that are ubiquitous in metazoans. Mammals have four types of transferrin: serum transferrin, lactoferrin, melanotransferrin, and the inhibitor of carbonic anhydrase (11, 12). Among these, serum transferrin and lactoferrin have been implicated in nutritional immunity via iron sequestration from invading pathogens (5, 12). Serum transferrin is abundant in the blood of mammals and primarily functions as an iron transporter by shuttling the iron from the gut to peripheral sites of storage and use (13). Lactoferrin is found on mucosal surfaces, and in biological fluids including milk and saliva, indicating that it is part of the innate immune response; however, there is no functional in vivo data supporting this role (14–16). Due to their high affinity to iron, transferrins have been shown to inhibit the growth of certain microbes (17). While numerous studies reported the potent antimicrobial activity of purified transferrins in vitro, in vivo studies addressing transferrin function are rather limited (10, 15, 18–24). Although hypotransferrinemic (hpx) mice devoid of serum transferrin exist, how they respond to microbial infection has yet to be examined (25). Hence, the in vivo role of transferrins awaits further investigation.

Due to its genetic tractability, *Drosophila melanogaster* has been a model of choice to study innate host defense mechanisms (26). The systemic antimicrobial response is probably the best-characterized immune mechanism in *Drosophila*. It involves the fat body, and, to a lesser extent, hemocytes, producing antimicrobial peptides that are secreted into the hemolymph. This response is regulated at the transcriptional level by two nuclear factor κB (NF-κB) pathways, Toll and Imd, whose inactivation causes a high susceptibility to infection (26–29). However,

Significance

Hosts sequester iron as a strategy to limit pathogen acquisition of this essential nutrient in a process termed nutritional immunity. Due to their in vitro antimicrobial activity, iron-binding proteins transferrins are suspected to play a role in iron sequestration. However, little is known about the in vivo role of transferrins. Here, we found that *Drosophila melanogaster* exhibits infection-induced hypoferremia mediated by Transferrin 1. Due to excessive iron in hemolymph, *Transferrin 1* (*Tsf1*)-deficient flies are hypersusceptible to certain infections. Our study reveals that nutritional immunity is an important, previously unrecognized arm of immune defense in *Drosophila*. Using fly and bacterial genetics, we show that Tsf1 mediates nutritional immunity by sequestering iron from the pathogens in vivo on the whole-organism level.

Author contributions: I.I. and B.L. designed research; I.I., A.M., and J.-P.B. performed research; A.M., J.-P.B., and J.P. contributed new reagents/analytic tools; I.I. analyzed data; and I.I. and B.L. wrote the paper.

The authors declare no competing interest.

This article is a PNAS Direct Submission.

[1]To whom correspondence may be addressed. Email: iatsenko@mpiib-berlin.mpg.de or bruno.lemaitre@epfl.ch.

[2]Present address: Research Group Genetics of Host–Microbe Interactions, Max Planck Institute for Infection Biology, 10117 Berlin, Germany.

This article contains supporting information online at https://www.pnas.org/lookup/suppl/doi:10.1073/pnas.1914830117/-/DCSupplemental.

First published March 18, 2020.

IMMUNOLOGY AND INFLAMMATION

whether nutritional immunity via iron sequestration constitutes a part of the insect defense response has not been studied. There are three transferrin homologs in *Drosophila*: Tsf1, Tsf2, and Tsf3. Tsf2 is a component of epithelial septate junctions (30) and is unlikely to play an antimicrobial role, whereas Tsf3 has not been functionally characterized yet but might play a role in circadian rhythms (31). Tsf1 was recently shown to function as an iron transporter in the hemolymph (the insect blood) similar to mammalian serum transferrin (32). Specifically, fat body-derived Tsf1 is secreted into the hemolymph and transports iron from the gut and hemolymph to the fat body. The *Tsf1* gene is induced upon infections, pointing to its role in host defense (33–35). Proteomic analysis of hemolymph also revealed Tsf1 up-regulation after infection with the fungus *Beauveria bassiana* (36). Transferrin genes have been shown to be up-regulated in response to infection in other insect species, including representatives from Diptera, Coleoptera, Hemiptera, Hymenoptera, and Lepidoptera (21, 22, 37–39). Also, the promoter region of Tsf1 genes from several insects is enriched in putative NF-κB binding sites, supporting the immune role of Tsf1 in these animals (37). Indeed, purified iron-free transferrins from *Sarcophaga bullata, Bombyx mori*, and *Manduca sexta* were shown to have antibacterial activity in vitro, which was dependent on the transferrin's ability to sequester iron (21, 22, 40).

However, the in vivo role of insect transferrins in host defense at the organismal level has never been addressed. In this study, we used *D. melanogaster* as a genetically tractable model to investigate the role of iron and Tsf1 in insect host defense.

Results

***D. melanogaster* Exhibits Infection-Induced Hypoferremia.** Infections in mammals induce a transient depletion of plasma iron (8), motivating us to investigate whether infection-induced hypoferremia also happens in *Drosophila*. To this end, we infected flies by pricking with a range of pathogens, including the Gram-positive bacterium *Micrococcus luteus*, the Gram-negative bacteria *Pectobacterium carotovorum* (*Ecc15*) and *Pseudomonas entomophila*, and the yeast *Candida albicans*. We measured iron content in the extracted hemolymph from unchallenged and infected flies using inductively coupled plasma optical emission spectrometry (ICP-OES). Compared to uninfected flies, there was a significant decrease in hemolymph iron levels in all tested infections (Fig. 1*A*). Importantly, pricking with heat-killed bacteria triggered the same drop in hemolymph iron level as infection with live bacteria (Fig. 1*B*). This suggests that iron withdrawal from hemolymph is a host-mediated process, and does not result from bacterial consumption. To track where hemolymphatic iron might be redistributed to upon infection, we monitored iron levels in other major tissues. The decrease of hemolymph iron after *M. luteus* infection was correlated with a concomitant increase in iron level in the fat body, while other tissues were not affected (Fig. 1*C*). This result suggests that iron was relocated from the hemolymph to the fat body after infection.

Infection-Mediated Hemolymph Iron Depletion Requires the Toll and Imd Pathways. We next explored whether the Toll and Imd immune pathways contribute to the depletion of hemolymphatic iron upon infection. We found that, in contrast to wild-type flies, Toll pathway-deficient mutants, including spz^{rm7}, $GNBP1^{osi}$, $PGRP\text{-}SA^{Seml}$, and $ModSP^{1}$ flies, were unable to remove iron from the hemolymph after *M. luteus* infection, a challenge known to predominantly activate the Toll pathway (27, 33). In fact, iron amount after infection stayed at the same level as in uninfected flies (Fig. 1*D*). Similarly, Imd pathway-deficient mutants $PGRP\text{-}SD^{sk1}$, $PGRP\text{-}LC^{E12}$, and $Relish^{E20}$ were impaired in iron removal from the hemolymph after pricking with *Ecc15* heat-killed bacteria (Fig. 1*E*), which potently activates Imd pathway but does not kill mutant flies (41). Interestingly, in $PGRP\text{-}SD^{sk1}$ mutant, we observed significant decrease in hemolymph iron, but not as strong as in wild-type flies. This result is explained by the fact that $PGRP\text{-}SD^{sk1}$ mutants have only partial reduction in Imd pathway activity, and therefore they have partial hypoferremic response (41, 42). Thus, the Imd and Toll pathways appear to be required for iron withdrawal from hemolymph after infections that activate these pathways.

Transferrin 1 Is Required for Iron Relocation from Hemolymph to Fat Body after Infection. The fact that the Toll and Imd pathways are necessary for iron removal from hemolymph after infection suggests that potential immune effectors downstream of these pathways can transport iron from hemolymph to fat body. A good candidate was the iron transporter transferrin 1 (Tsf1), as transcriptomic studies have shown that this gene is induced upon infection (33, 34). Using RT-qPCR, we showed that this gene is strongly induced by *M. luteus* in a Toll pathway-dependent manner, and by *Ecc15* in an Imd pathway-dependent manner (Fig. 2 *A* and *B*). Importantly, *Tsf1* up-regulation upon infection was tissue-specific and was restricted to the fat body (*SI Appendix*, Fig. S1*A*). Also, *Tsf1* is the only infection-responsive transferrin in *Drosophila*, since none of the other two transferrins was induced by *M. luteus* or *Ecc15* (*SI Appendix*, Fig. S1 *B* and *C*). Using an endogenously GFP-tagged *Tsf1* transgenic line, we additionally confirmed that Tsf1 protein abundance is strongly increased in the hemolymph after both *M. luteus* and *Ecc15* infections (Fig. 2*C*). To further explore the role of Tsf1 in infection-induced iron transport, we generated a *Tsf1* mutant ($Tsf1^{JP94}$) using CRISPR-Cas9. The mutant has two nucleotide substitutions and a single nucleotide deletion, which leads to a frameshift with a premature stop codon at position 19 (Fig. 2*D*). Using qPCR, we showed that there was no *Tsf1* transcript in the $Tsf1^{JP94}$ mutant in contrast to wild-type flies after *M. luteus* infection (*SI Appendix*, Fig. S1*D*). $Tsf1^{JP94}$ mutants were viable and did not show any obvious morphological defects under standard laboratory conditions. Also, both Toll and Imd pathways were induced properly in this mutant, as illustrated by the level of *Drs* and *Dpt* expression after *M. luteus* and *Ecc15* infections, respectively (*SI Appendix*, Fig. S1 *E* and *F*). Next, we compared iron distribution between wild-type and $Tsf1^{JP94}$ mutant tissues after *M. luteus* infection. There was no difference in iron content between uninfected wild-type and $Tsf1^{JP94}$ mutant in the hemolymph and fly tissues. Strikingly, after *M. luteus* infection, $Tsf1^{JP94}$ mutant contained significantly more iron in the hemolymph and significantly less in the fat body compared to wild-type flies (Fig. 2*E*). Overexpression of a wild-type copy of *Tsf1* in the $Tsf1^{JP94}$ mutant background rescued the phenotype (Fig. 2*F*). This result suggests that Tsf1 contributes to the iron relocalization from hemolymph to fat body after infection. To confirm this result and identify the source of Tsf1, we performed tissue-specific RNA interference (RNAi)-mediated *Tsf1* knockdown. Similar to $Tsf1^{JP94}$, flies with ubiquitous *Tsf1* knockdown retain high iron load in the hemolymph after infection (Fig. 2*F*). Fat body-specific, but not gut- or hemocyte-specific, *Tsf1* knockdown recapitulated this phenotype, indicating that the fat body is the major source of Tsf1 (*SI Appendix*, Fig. S1*G*). This result is consistent with a recent study (32) that showed Tsf1 is produced by the fat body and is secreted into the hemolymph (Fig. 2*C*), where it binds to iron and transports it to the fat body. DmTsf1 is homologous to human plasma Transferrin that has been functionally and structurally well characterized. Structure–function analysis has shown that five amino acid residues of hTsf are required for iron binding (11, 12). Sequence homology analysis showed that three out of these five residues are conserved in *Drosophila* Tsf1 (*SI Appendix*, Fig. S2). We substituted these three residues with alanine and generated a fly line that overexpresses this mutated form of *Tsf1* ($UAS\text{-}Tsf1^{Fe\ mut}$) that should

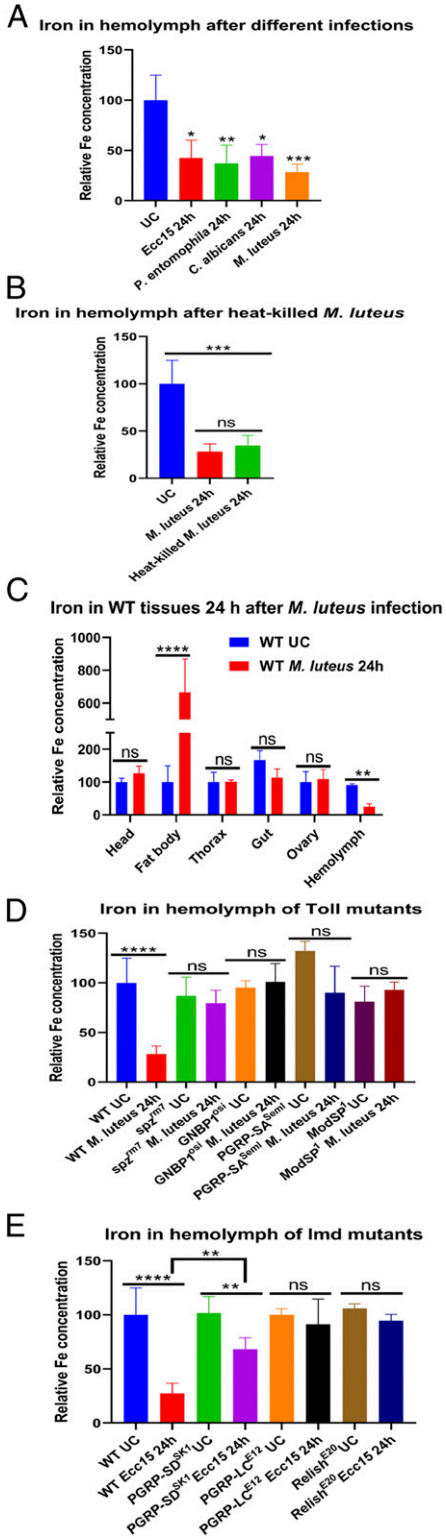

Fig. 1. *D. melanogaster* exhibits infection-induced hypoferremia. (*A* and *B*) Iron content of flies' hemolymph after indicated infections. Asterisks indicate statistical significance relative to unchallenged (UC) (one-way ANOVA) ($n = 50$ flies per treatment). (*C*) Iron content in indicated tissues of wild-type (WT) flies 24 h after *M. luteus* infection compared to uninfected controls ($n = 20$ organs per group, $n = 50$ flies for hemolymph). (*D* and *E*) Hemolymph iron content (*D*) in Toll pathway mutants (*spz*^{rm7}, *GNBP1*^{osi}, *PGRP-SA*^{Seml}, and *ModSP*^{1}) 24 h after *M. luteus* infection and (*E*) in Imd pathway mutants (*PGRP-SD*^{sk1}, *PGRP-LC*^{E12}, and *Relish*^{E20}) 24 h after heat-killed *Ecc15* injection ($n = 50$ flies per group). For all graphs, iron content in uninfected wild-type flies was set to 100, and all other values were expressed as a percentage of this value. The mean and SD of three independent experiments are shown. $^{*}P \leq 0.05$; $^{**}P \leq 0.01$; $^{***}P \leq 0.001$; $^{****}P \leq 0.0001$; ns, nonsignificant, $P > 0.05$.

not bind iron. Overexpression of this mutated version of *Tsf1* did not rescue the *Tsf1*^{JP94} mutant (Fig. 2*F*). This reinforces our conclusion that the ability of Tsf1 to bind iron is necessary to relocate the metal from hemolymph to fat body.

***Transferrin 1* Mutants Are Susceptible to *Pseudomonas* and Mucorales Fungal Infections.** Having shown that Tsf1 mediates the transport of iron upon infection, we investigated the relevance of this immune process in host survival to various pathogens. As shown in *SI Appendix*, Fig. S3, *Tsf1*^{JP94} mutants exhibited wild-type levels of survival after systemic infection with *Ecc15*, *Enterobacter cloacae*, *Listeria monocytogenes*, *Streptococcus pyogenes*, *S. aureus, Enterococcus faecalis*, *C. albicans*, and *B. bassiana* (natural infection). We next explored *Tsf1*^{JP94} mutants' susceptibility to fungi of the order Mucorales and *Pseudomonas* bacteria, the virulence of which is known to be strongly modulated by iron availability (43–45). Interestingly, we observed an increased susceptibility of *Tsf1*^{JP94} mutant and *Tsf1 RNAi* flies to systemic infection with *Cunninghamella bertholletiae*, a representative Mucorales that infects humans (Fig. 3 *A* and *B*). Notably, Toll pathway activation by *C. bertholletiae* was not affected in the *Tsf1*^{JP94} mutant (Fig. 3*C*). Overexpression of wild-type *Tsf1*, but not the iron binding sites mutated form of *Tsf1*, rescued the increased susceptibility of *Tsf1*^{JP94} mutants to this fungus (Fig. 3*D*). We could almost completely rescue the susceptibility of *Tsf1*^{JP94} mutants to *C. bertholletiae* by injection of the iron chelator bathophenanthrolinedisulfonic acid disodium (BPS) (46), suggesting that excessive iron in the hemolymph of *Tsf1*^{JP94} mutants contributes to their increased susceptibility to *C. bertholletiae* (Fig. 3*E*). BPS injection also has a protective effect in wild-type flies, although not as significant as in *Tsf1*^{JP94} mutants. We obtained similar increased sensitivity of *Tsf1*^{JP94} mutants to another Mucorales representative, *Rhizopus oryzae* (Fig. 3*F*), suggesting that transferrins are important for the defense against this group of fungi.

We also observed an increased susceptibility of *Tsf1*^{JP94} and *Tsf1* RNAi flies to systemic infections with two *Pseudomonas* species, *Pseudomonas aeruginosa* (Fig. 4 *A* and *B*) and *P. entomophila* (*SI Appendix*, Fig. S4 *A* and *B*). Consistent with the impaired resistance of *Tsf1*^{JP94} flies, *P. aeruginosa* (Fig. 4*C*) and *P. entomophila* (*SI Appendix*, Fig. S4*C*) reached significantly higher loads in *Tsf1*^{JP94} mutants. As *Tsf1*^{JP94} mutants showed wild-type levels of Imd pathway activation after *P. entomophila* and *P. aeruginosa* infections (*SI Appendix*, Fig. S4*D*), the increased susceptibility of these mutants was not due a general immune deficiency but rather due to their inability to sequester iron away from the hemolymph. Consistent with this, injection of the iron chelator BPS into the hemolymph significantly improves survival of *Tsf1*^{JP94} mutants upon *P. aeruginosa* infection (Fig. 4*D*). Ubiquitous overexpression of wild-type but not the mutated *Tsf1* form was sufficient to rescue the enhanced susceptibility of *Tsf1*^{JP94} mutants to *P. aeruginosa* (Fig. 4*E*) and *P. entomophila* (*SI Appendix*, Fig. S4*E*). Similarly, *P. aeruginosa* elevated load in *Tsf1*^{JP94} mutants was not observed when wild type but not the mutated *Tsf1* form was ubiquitously overexpressed (Fig. 4*F*). Interestingly, overexpression of wild type but not the mutated *Tsf1* form in wild-type background led to a significant reduction in *P. aeruginosa* load (Fig. 4*F*), which correlated with improved survival of the flies (Fig. 4*B*). This protective effect of Tsf1 overexpression is comparable to the effect of BPS injection (Fig. 4*D*), indicating that Tsf1 may function as endogenous iron chelator.

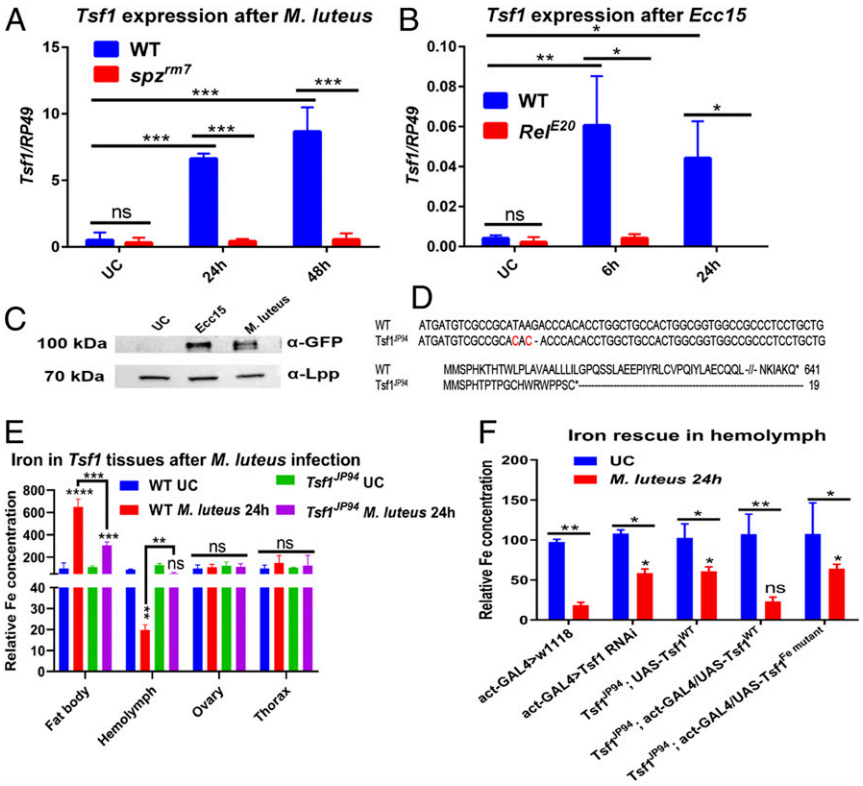

Fig. 2. Contribution of Tsf1 to infection-induced hypoferremia. (*A* and *B*) *Tsf1* expression (*A*) in wild type and *spz*^{rm7} mutants after *M. luteus* infection and (*B*) in wild type and *Rel*^{E20} mutants after *Ecc15* infection, measured by RT-qPCR ($n = 10$ flies per group). (*C*) Western blot of Tsf1-GFP hemolymph extracted 24 h after *M. luteus* or *Ecc15* infection showing Tsf1 induction after these infections. Lipophorin (α-Lpp) was used as a loading control. A representative Western blot out of three independent experiments is shown ($n = 30$ flies per group). (*D*) Nucleotide and amino acid sequence alignment of wild-type and *Tsf1*^{JP94} transferrin. (*E*) Iron content in indicated tissues of wild-type and *Tsf1*^{JP94} flies 24 h after *M. luteus* infection compared to uninfected controls ($n = 20$ organs per group, $n = 50$ flies for hemolymph). Asterisks above the red bars indicate significance relative to wild-type UC. (*F*) Hemolymph iron content of indicated fly genotypes 24 h after *M. luteus* infection compared to uninfected controls ($n = 50$ flies per group). Asterisks above bars indicate significance relative to *act-GAL4 > w1118 M. luteus*-infected. Iron content in uninfected wild-type or *act-GAL4 > w1118* flies was set to 100, and all other values were expressed as a percentage of this value. The mean and SD of three independent experiments are shown unless otherwise stated. $*P \leq 0.05$; $**P \leq 0.01$; $***P \leq 0.001$; $****P \leq 0.0001$; ns, nonsignificant, $P > 0.05$.

Pyoverdine-Mediated Iron Acquisition Is Essential for *P. aeruginosa* Infection in *Drosophila*. Siderophore production by pathogens is a key mechanism for scavenging iron from a variety of host iron sources. Siderophores are small ferric iron chelators capable of binding iron with high affinity, and can therefore effectively outcompete host transferrin (1). *P. aeruginosa* produces large amounts of pyoverdine and pyochelin siderophores that scavenge iron and deliver it to the bacteria (47). We next compared the susceptibility of wild-type and *Tsf1*^{JP94} mutant flies to wild-type *P. aeruginosa* PA14 and to its transposon insertion derivatives *pchE* and *pvdP* that lack the siderophores pyochelin and pyoverdine, respectively (48). As shown in Fig. 5*A*, the *pchE* mutant was as efficient as wild-type *P. aeruginosa* at killing both wild-type and *Tsf1*^{JP94} mutant flies, indicating that pyochelin is not required for *P. aeruginosa* virulence in *Drosophila*. Interestingly, the virulence of *pvdP* mutant was attenuated compared to wild-type *P. aeruginosa* in wild-type flies, indicating that pyoverdine contributes to *Pseudomonas* pathogenicity. In contrast, the pathogenicity of *pvdP* was similar to that of wild-type *P. aeruginosa* when assayed in *Tsf1*^{JP94} mutant background (Fig. 4*B*). In line with this, *pvdP* colony-forming unit (cfus) were the same as for wild-type *P. aeruginosa* in *Tsf1*^{JP94} mutant but were significantly lower in wild-type flies (Fig. 5*C*). To further reinforce the role of pyoverdine, we assessed the survival of flies preinjected prior to infection with flucytosine, a known repressor of pyoverdine (49). We observed that flucytosine was protective in wild-type flies but had no effect in *Tsf1*^{JP94} mutant (Fig. 5*D*), which is similar to what we found with the genetic disruption of pyoverdine (Fig. 5*B*). Using another *P. aeruginosa* strain (PAO1) and its derived pyochelin and pyoverdine mutants (50), we confirmed that pyoverdine is essential for virulence in wild-type flies but not in *Tsf1*^{JP94} mutant (Fig. 5*E*). This result suggests that 1) pyoverdine is necessary for *P. aeruginosa* to acquire iron from wild-type *Drosophila*, and 2) pyoverdine becomes dispensable in *Tsf1*^{JP94} mutant due to excessive iron present in the hemolymph. Additionally, we assessed the virulence of *P. aeruginosa* PAO1 *tonB1* mutants that are defective for siderophore-mediated iron uptake (51). These mutants were severely attenuated in both wild-type and *Tsf1*^{JP94} mutant flies. Nevertheless, they still killed *Tsf1*^{JP94} mutants faster than wild-type flies, likely due to high iron levels in the hemolymph of *Tsf1*^{JP94} mutants (Fig. 5*F*). Thus, using bacterial and fly genetics, we could show that Tsf1 is required for the *Drosophila* defense against certain pathogens, by sequestering iron from hemolymph and limiting pathogen access to this essential element.

Transferrin 1 Plays a Role in Intestinal Immunity. Considering that *Tsf1* is induced by *Ecc15* and *P. entomophila* oral infections in the gut in an Imd pathway-dependent manner (Fig. 6 *A* and *B*) (52), we explored whether this iron transporter is also implicated in intestinal immunity. As shown in Fig. 6*C*, *Tsf1*^{JP94} mutants succumbed faster to *P. entomophila* oral infection compared to wild-type flies. Enterocyte-specific *Tsf1* knockdown by RNAi also resulted in increased sensitivity to *P. entomophila* oral infection (Fig. 6*D*). This increased susceptibility was not due to an impaired Imd pathway activity (*SI Appendix*, Fig. S5*A*) or

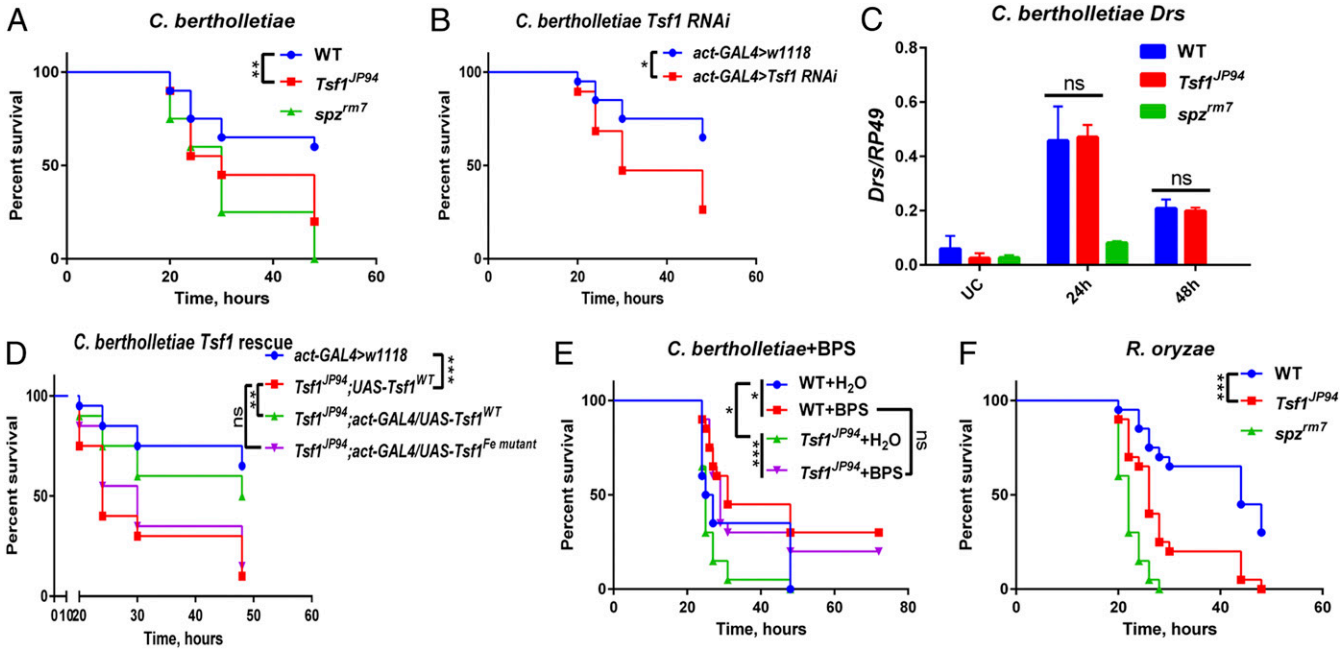

Fig. 3. Tsf1 is required for the defense against Mucorales. (*A*) Survival rates of wild-type, *spz*^{rm7}, *and Tsf1*^{JP94} flies infected with *C. bertholletiae* (10^6 spores per ml). (*B*) Survival rates of flies with ubiquitous knockdown of *Tsf1* is significantly reduced compared to wild-type flies after infection with *C. bertholletiae.* (*C*) *Drs* expression in wild-type, *spz*^{rm7}, *and Tsf1*^{JP94} flies after *C. bertholletiae* infection measured by RT-qPCR (n = 10 flies per group). The mean and SD of three independent experiments are shown. (*D*) Increased susceptibility of *Tsf1*^{JP94} mutant flies to *C. bertholletiae* infection is rescued by the ubiquitous overexpression of the wild-type (*UAS-Tsf1*^{WT}) but not mutated form of *Tsf1* (*UAS-Tsf1*$^{Fe\ mutant}$). (*E*) Survival rates of wild-type and *Tsf1*^{JP94} flies preinjected with 13.4 nL of H_2O (control) or with 13.4 nL of 200 μM iron chelator BPS prior to infection with *C. bertholletiae*. (*F*) Survival rates of wild-type, *spz*^{rm7}, *and Tsf1*^{JP94} flies infected with *R. oryzae* (10^6 spores per mL). Survival graphs show one representative experiment out of three independent experiments with similar results with two or three cohorts of 20 male flies per treatment. *$P \leq 0.05$; **$P \leq 0.01$; ***$P \leq 0.001$; ****$P \leq 0.0001$; ns, nonsignificant, $P > 0.05$.

compromised gut repair, as PH3 staining revealed that *Tsf1*^{JP94} mutants had the same number of proliferating stem cells after *Ecc15* infection as wild-type flies (*SI Appendix*, Fig. S5*B*). In line with this, *upd3*, a ligand of the JAK-STAT pathway playing a crucial role in epithelial renewal (52), was expressed in *Tsf1*^{JP94} mutants at wild-type levels after both *Ecc15* and *P. entomophila* infections (*SI Appendix*, Fig. S5*C*). Importantly, we found that the susceptibility of *Tsf1*^{JP94} mutants to *P. entomophila* oral infection could be rescued by gut-specific overexpression of wild-type but not iron binding-defective *Tsf1* (Fig. 6*E*), indicating that the ability of Tsf1 to bind iron is necessary for defense against *P. entomophila* intestinal infection, similar to its effect in systemic infection. Therefore, Tsf1 plays a similar role in the gut as in the hemolymph. To further reinforce this conclusion, we performed oral infection with *P. aeruginosa* PA14 and observed that *Tsf1*^{JP94} mutants were also more susceptible to this pathogen (Fig. 6*F*). Consistent with systemic infections, pyoverdine-deficient *pvdP* mutant virulence was attenuated in wild-type but not in *Tsf1*^{JP94} mutant flies, while pyochelin-deficient mutant virulence was comparable to wild-type *P. aeruginosa* (Fig. 6*F*). The fact that pyoverdine is unnecessary for virulence in *Tsf1*^{JP94} mutant suggests that there is enough available iron in the guts of these flies. Indeed, we could detect significantly more iron in *Tsf1*^{JP94} mutant guts compared to wild-type unchallenged guts (*SI Appendix*, Fig. S5*D*). We conclude that iron sequestration by transferrin is also a potent mechanism contributing to intestinal immunity.

Discussion

Despite the well-established role of iron and iron-binding proteins in mammalian immunity, their role in insect immunity remains understudied. Using *D. melanogaster* as a model, we found that 1) flies trigger a hypoferremic response after infection to limit iron availability to invading microbes, and 2) the iron transporter Tsf1 mediates nutritional immunity by sequestering iron from invading pathogens (see model in *SI Appendix*, Fig. S6).

In mammals, hypoferremia of infection has been known since the 1940s and is characterized by iron withdrawal from the serum and accumulation in storage organs, like the liver (8). Consistent with mammalian studies, we discovered that flies trigger a hypoferremic response upon challenge with a variety of pathogens. During this response, iron was relocated from the hemolymph to the fat body, which is the equivalent of mammalian liver. Given that the same response was also triggered by heat-killed bacteria, depleting hemolymph iron appears to be a host-mediated process. Notably, this mechanism requires the *Drosophila* Toll and Imd pathways, since mutants for these pathways were not able to induce a hypoferremic response to infection. Thus, beyond regulating antimicrobial effector-mediated immunity, the Toll and Imd pathways also mediate nutritional immunity in flies.

We hypothesized that Tsf1 might play a major role in *Drosophila* nutritional immunity downstream of Toll and Imd pathways. Out of the three *Drosophila* transferrins, Tsf1 is consistently induced by a variety of immune challenges (33, 34, 36). Using a *Transferrin* null mutant, we indeed found that Tsf1 is required for iron trafficking from the hemolymph to the fat body after infection. Therefore, our study agrees with a recently published work that Tsf1 is indeed an iron transporter (32). However, in contrast to Xiao et al. (32), who used a *Tsf1 RNAi*, we did not observe any lethality or developmental defects in *Tsf1*^{JP94} mutants and *Tsf1 RNAi*. This discrepancy could be due to the fact that we used different RNAi lines targeting different parts of the transcript or because, in contrast to Xiao et al., we used conditional knockdown specifically during adult stage.

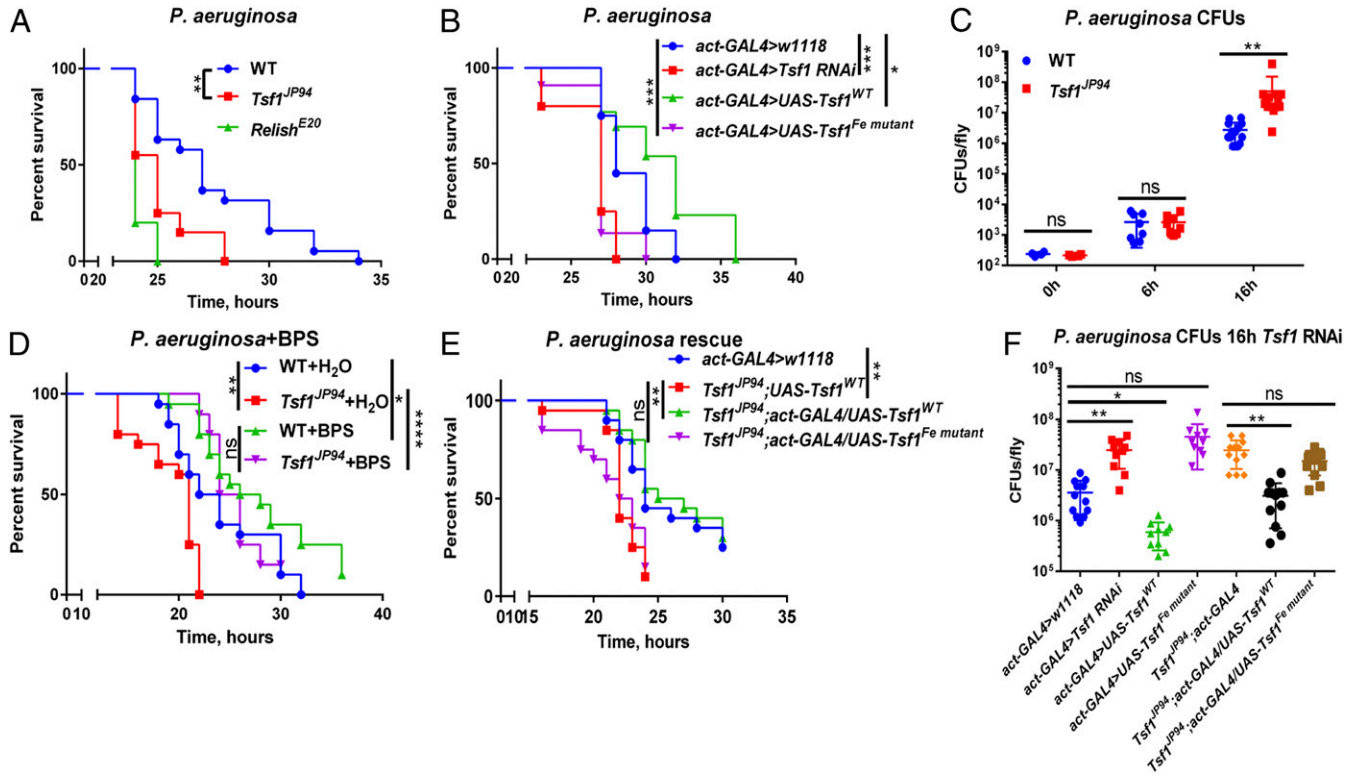

Fig. 4. Tsf1-mediated iron sequestration protects against *P. aeruginosa* infection. (*A*) Survival rates of wild-type, *Rel*^{E20}, and *Tsf1*^{JP94} flies infected with *P. aeruginosa*. (*B*) Survival rates of flies with ubiquitous knockdown of *Tsf1*, and overexpression of either wild-type (*UAS-Tsf1*^{WT}) or mutated *Tsf1* after *P. aeruginosa* infection. (*C*) Measurement of *P. aeruginosa* burden at different time points after infection of wild type and *Tsf1*^{JP94} mutant. (*D*) Survival rates of wild-type and *Tsf1*^{JP94} flies preinjected with 13.4 nL of H_2O (control) or with 13.4 nL of 200 μM iron chelator BPS prior to infection with *P. aeruginosa*. (*E*) Increased susceptibility of *Tsf1*^{JP94} mutant flies to *P. aeruginosa* infection is rescued upon ubiquitous overexpression of wild-type (*UAS-Tsf1*^{WT}) but not mutated form of *Tsf1* (*UAS-Tsf1*$^{Fe\ mutant}$). (*F*) *Pseudomonas aeruginosa* load 16 h after infection of flies with indicated genotypes. For cfu counts, each dot represents cfus from a pool of five animals, calculated per fly. The mean and SD are shown. Survival graphs show one representative experiment out of three independent experiments with similar results with two or three cohorts of 20 male flies per treatment. $^*P \leq 0.05$; $^{**}P \leq 0.01$; $^{***}P \leq 0.001$; $^{****}P \leq 0.0001$; ns, nonsignificant, $P > 0.05$.

Our study raises an intriguing question regarding how Tsf1 relocates iron specifically to the fat body and not to other tissues. One possibility could be that fat body expresses transferrin receptor that directs iron transport by Tsf1. To date, no transferrin receptor homolog has been identified in *Drosophila* (and other insects). Finding this receptor and mechanism of iron uptake by the fat body during infection would be an interesting future research avenue.

Despite the elevated level of iron in the hemolymph, *Tsf1*^{JP94} mutants did not show any increased susceptibility to the majority of pathogens that we tested, including several Gram-positive and Gram-negative bacteria, fungi, and yeast. However, we observed increased susceptibility of *Tsf1*^{JP94} mutants to Mucorales fungi and to *Pseudomonas* bacteria. This increased susceptibility was linked to the ability of Tsf1 to bind iron, as we could not rescue *Tsf1*^{JP94} mutants' susceptibility with a form of *Tsf1* mutated in iron binding sites. Given that Mucorales virulence is known to be enhanced by increased iron supply (43), it is reasonable to assume that *Tsf1*^{JP94} flies are more susceptible to these infections because of elevated hemolymph iron levels. *P. aeruginosa* virulence is also known to be strongly regulated by iron. The importance of iron to *P. aeruginosa* is exemplified by the fact that 6% of its transcribed genes are iron responsive (44, 45). Not surprisingly, these bacteria evolved a diversity of mechanisms to scavenge iron from a variety of host iron sources. Siderophore production is one such mechanism. Pyoverdine and pyochelin are two major siderophores produced by *P. aeruginosa* (47), and pyoverdine is essential for *P. aeruginosa* pathogenesis in various mammalian and invertebrate host models (48, 53–55). A recent study showed that *P. aeruginosa* mutants for the algR regulator are deficient for pyoverdine production, and virulence is attenuated in the algR mutant in a *Drosophila* oral infection model (56). In line with this, we showed that the *P. aeruginosa* pyoverdine mutant is less pathogenic compared to its wild-type counterpart during both systemic and oral infections. Importantly, *Tsf1*^{JP94} mutant flies were killed by the *P. aeruginosa* pyoverdine mutant as efficiently as by wild-type bacteria. This suggests that 1) pyoverdine is necessary for iron acquisition by *P. aeruginosa* during *Drosophila* infection and, 2) in the absence of transferrin, pyoverdine becomes unessential, as there is an excess of free iron. The extreme dependence of *P. aeruginosa* on iron makes these bacteria vulnerable to iron chelation therapy by transferrin, which has been proposed as a novel antimicrobial therapy (24). Efficacy of such therapy is also supported by our results showing that Tsf1 overexpression is sufficient to increase the survival of flies to *Pseudomonas* infections.

Why Tsf1 flies are not sensitive to the majority of pathogens is an intriguing question that our work raises. A likely explanation for this result is that, beyond iron sequestration, the host relies on other arms of defense, like phagocytosis or production of antimicrobial peptides, to combat pathogens. Those additional arms of defense might be sufficient to eliminate most pathogens at the infectious doses we used, even if iron sequestration is impaired. There is accumulating evidence that some elements of the immune system are specifically required against certain pathogens. For instance, from *Drosophila* studies, it is known that melanization is important to survive *S. aureus* infection (57),

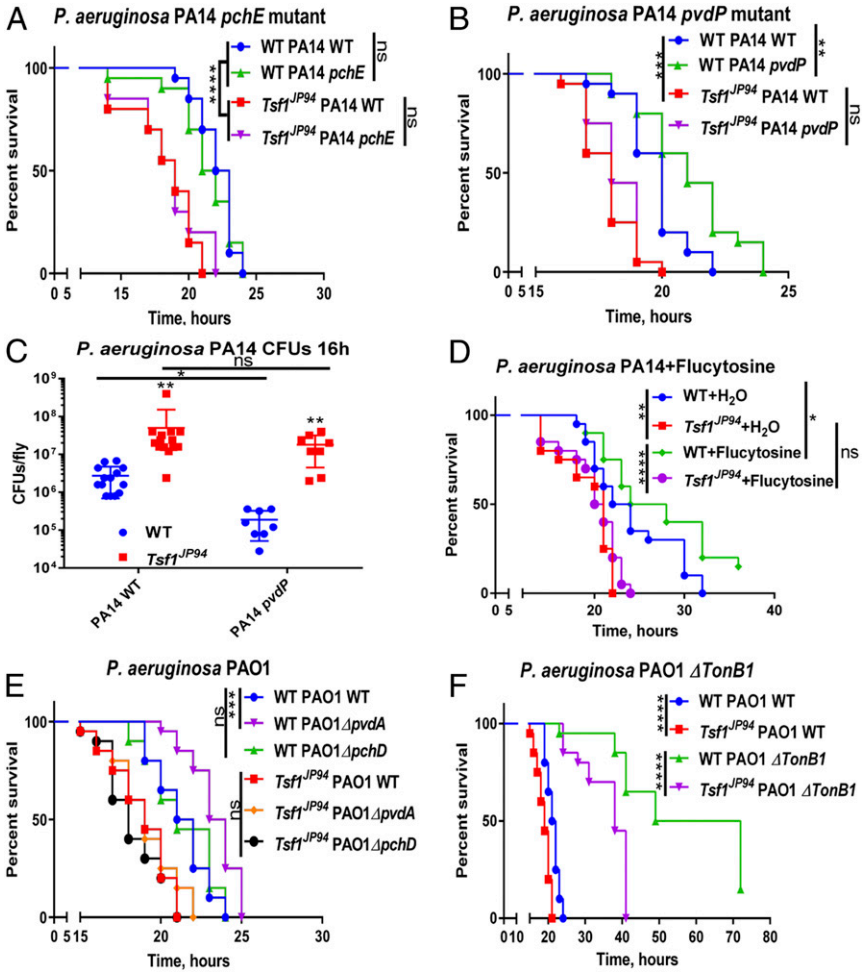

Fig. 5. Pyoverdine is required for *P. aeruginosa* virulence against wild-type but not *Tsf1*^{JP94} flies. (*A* and *B*) Survival rates of wild-type and *Tsf1*^{JP94} mutant flies infected with (*A*) wild-type, pyochelin-deficient *pchE* or (*B*) pyoverdine-deficient *pvdP P. aeruginosa* PA14. (*C*) Measurement of wild-type and *pvdP PA14* load 16 h after infection of wild-type and *Tsf1*^{JP94} flies. Each dot represents cfus from a pool of five animals, calculated per fly. The mean and SD are shown. (*D*) Survival rates of wild-type and *Tsf1*^{JP94} flies preinjected with 13.4 nL of H_2O (control) or with 13.4 nL of 100 μM repressor of pyoverdine flucytosine prior to infection with *P. aeruginosa*. (*E* and *F*) Survival rates of wild-type and *Tsf1*^{JP94} flies infected with wild-type, (*E*) *ΔpchD*, *ΔpvdA*, and (*F*) *ΔTonB1 P. aeruginosa* PAO1. Survival graphs show one representative experiment out of three independent experiments with similar results with two or three cohorts of 20 male flies per treatment. $^*P \leq 0.05$; $^{**}P \leq 0.01$; $^{***}P \leq 0.001$; $^{****}P \leq 0.0001$; ns, nonsignificant, $P > 0.05$.

phagocytosis [*S. aureus* and *Salmonella typhimurium* (58, 59)], the antimicrobial peptide Diptericin [*Providencia rettgeri* (60, 61)], and Drosocin [*E. cloacae* (61)]. Our study suggests that iron sequestration is an important defense mechanism against Mucorales and *Pseudomonas*, while, in the case of other pathogens, other arms of defense might play a more prominent role. It will be an interesting avenue for future research to explore functional redundancy between different arms of the host defense against specific pathogens.

Taken together, our results reveal that nutritional immunity is an important arm of innate immune defense in *Drosophila*. Using fly and bacterial genetics, we showed that the iron transporter Tsf1 mediates nutritional immunity by sequestering iron from the pathogens in vivo on the whole-organism level. So far, two studies have identified immune-related phenotypes resulting from RNAi-mediated knockdown of transferrin: increased prevalence of trypanosome infections in *Glossina morsitans*, and increased mortality of *Bacillus thuringiensis*-infected *Plutella xylostella* (62, 63). Those in vivo and accumulating in vitro studies support the immune role of insect transferrins against infections via an iron withholding strategy. Considering the multifactorial function of iron beyond immunity, our work opens avenues for future research addressing the role of transferrins in the host physiology.

Materials and Methods

Pathogen Strains and Survival Experiments. The bacterial strains used and their respective optical densities (OD) at 600 nm were, unless otherwise stated, the Gram-negative bacteria *P. carotovorum* (*Ecc15*, OD 200), *E. cloacae β12* (OD 200), *P. entomophila* (OD 1), *P. aeruginosa* PA14 (OD 1), *P. aeruginosa* PA14 *pvdP* (OD 1), *P. aeruginosa* PA14 *pchE* (OD 1), *P. aeruginosa* PAO1 (OD 1), *P. aeruginosa* PAO1 *ΔpvdA* (OD 1), *P. aeruginosa* PAO1 *ΔpchD* (OD 1), and *P. aeruginosa* PAO1 *ΔtonB1* (OD 1); the DAP-type peptidoglycan-containing Gram-positive bacteria *L. monocytogenes BUG2377* (, OD 40); the Lys-type peptidoglycan containing Gram-positive bacteria *M. luteus* (OD 200), *S. aureus* (OD 0.5), *S. pyogenes* ATCC19615 (OD 200), and *E. faecalis* OG1RF (OD 15); and the yeast *C. albicans* (OD 200). Microbes were cultured in Brain-Heart Infusion Broth (*L. monocytogenes* and *E. faecalis*), Yeast extract-Peptone-Glucose Broth (*C. albicans*), or Luria Broth (all others) at 29 °C (*E. carotovora*, *M. luteus*, *C. albicans*, and *P. entomophila*) or 37 °C (all others). To compare the virulence of *P. aeruginosa* wild type and siderophore mutants, bacteria were grown in M9 minimal media at 37 °C to stimulate siderophore production. *P. aeruginosa* PAO1 *ΔtonB1* mutant was grown in media supplemented with 100 μM $FeSO_4$. The *pvdP* and *pchE P. aeruginosa* PA14 mutants were grown in the presence of 15 μg/mL gentamicin. Spores of the entomopathogenic fungus *B. bassiana 802* and

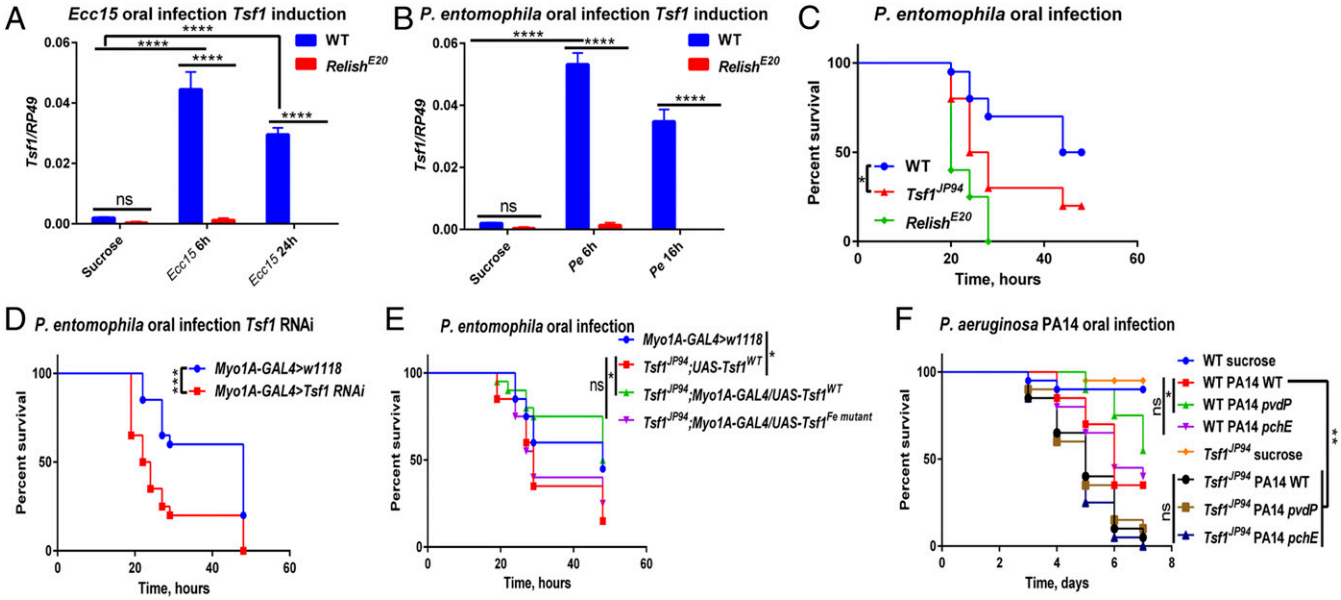

Fig. 6. Tsf1 contributes to intestinal immunity. (*A* and *B*) *Tsf1* expression in wild-type and *Rel*^{E20} guts after (*A*) *Ecc15* and (*B*) *Pe* infection, measured by RT-qPCR ($n = 20$ guts per group). The mean and SD of three independent experiments are shown. (*C*) Survival rates of wild-type, *Rel*^{E20}, *and Tsf1*^{JP94} flies orally infected with *P. entomophila*. (*D*) Survival rates of flies with gut-specific (*Myo1A*) knockdown of *Tsf1* are significantly reduced compared to wild-type flies after *Pe* oral infection. (*E*) Increased susceptibility of *Tsf1*^{JP94} mutant flies to *Pe* oral infection is rescued by gut-specific overexpression of the wild-type (*UAS-Tsf1*^{WT}) but not mutated form of *Tsf1* (*UAS-Tsf1*$^{Fe\ mutant}$). (*F*) Survival rates of wild-type and *Tsf1*^{JP94} flies orally infected with wild-type, *pchE*, and *pvdP P. aeruginosa* PA14. Survival graphs show one representative experiment out of three independent experiments with similar results with two to three cohorts of 20 flies per treatment. $^*P \leq 0.05$; $^{**}P \leq 0.01$; $^{***}P \leq 0.001$; $^{****}P \leq 0.0001$; ns, nonsignificant, $P > 0.05$.

Mucorales *C. bertholletiae* 506313 and *R. oryzae* 557969 were grown on malt agar plates at 29 °C for ∼3 wk until sporulation. Natural infections were performed by shaking anesthetized flies in a Petri dish containing a sporulating culture of *B. bassiana*. Systemic infections (septic injury) were performed by pricking adult flies (2 d to 5 d old) in the thorax with a thin needle previously dipped into a concentrated pellet of a bacterial culture or in a suspension of *fungal* (*C. bertholletiae* and *R. oryzae*) spores. Infected flies were subsequently maintained at 29 °C (most of the infections) or at 25 °C (*E. faecalis*, *S. aureus*, *S. pyogenes*, and *P. aeruginosa*). In some experiments, flies were injected prior to infection with 13.4 nL of 200 μM BPS (iron chelator) or with 13.4 nL of 100 μM Flucytosine using a Nanoject apparatus (Drummond). Oral infections were performed as described previously (42, 52, 64). At least two vials of 20 flies were used for survival experiments, and survivals were repeated at least three times.

Iron Measurement Using ICP-OES. Flies were infected with different pathogens as described above. Right before hemolymph collection, 50 flies were pricked in the thorax to breach the cuticle and increase hemolymph yield. These flies were placed on a 10-μm filter of an empty mobicol spin column (MoBiTec), covered with glass beads, and centrifuged for 5 min at 4 °C, 5,000 rpm. Then 5 μL of hemolymph per each sample were digested with 0.5 mL of 32% ultrapure hydrochloric acid (VWR Chemicals) under heating conditions (60 °C) for 2 h; 9.5 mL of nitric acid was added to each sample, and the total iron concentration was measured using ICP-OES (Perkin-Elmer Optima 8300 ICP-OES). To measure iron content of tissues, tissues of interest were dissected in phosphate-buffered saline and digested in 0.5 mL of 32% ultrapure hydrochloric acid at 60 °C for 2 h. The samples were filtered to remove impurities and any undigested material. Protein concentration in digested samples was determined using the Pierce BCA protein assay kit. Iron concentration in each sample was normalized to the total protein amount to standardize sample size differences.

RT-qPCR. For quantification of messenger RNA, whole flies ($n = 10$) or dissected tissues ($n = 20$) were collected at indicated time points. Total RNA was isolated using TRIzol reagent and dissolved in RNase-free water. Five hundred nanograms of total RNA was then reverse-transcribed in 10-μL reactions using PrimeScript RT (Takara) and random hexamer primers. The qPCR was performed on a LightCycler 480 (Roche) in 96-well plates using the LightCycler 480 *SYBR Green* I Master Mix. RP49 was used as a housekeeping gene for normalization.

All data are available in the manuscript and *SI Appendix*.

ACKNOWLEDGMENTS. We appreciate the gifts of *P. aeruginosa* PA14 pyoverdine mutants from Natalia Kirienko (Rice University) and Mucorales isolates from Dimitrios P. Kontoyiannis (University of Texas MD Anderson Cancer Center). We are extremely grateful to Prof. Paolo Visca and Daniela Visaggio for kindly and timely providing *P. aeruginosa* PAO1 mutant strains. We thank the Bloomington Stock Centre and the Vienna Drosophila Resource Center for fly stocks. We are grateful to Laetitia Monbaron (University of Lausanne) for the ICP-OES analysis of the samples, and to Mark Hanson for critical reading of the manuscript. This work was partially funded by Swiss National Science Foundation Sinergia Grant CRS II5_186397.

1. J. E. Cassat, E. P. Skaar, Iron in infection and immunity. *Cell Host Microbe* **13**, 509–519 (2013).
2. M. I. Hood, E. P. Skaar, Nutritional immunity: Transition metals at the pathogen-host interface. *Nat. Rev. Microbiol.* **10**, 525–537 (2012).
3. E. E. Johnson, M. Wessling-Resnick, Iron metabolism and the innate immune response to infection. *Microbes Infect.* **14**, 207–216 (2012).
4. C. A. Lopez, E. P. Skaar, The impact of dietary transition metals on host-bacterial interactions. *Cell Host Microbe* **23**, 737–748 (2018).
5. S. T. Ong, J. Z. Ho, B. Ho, J. L. Ding, Iron-withholding strategy in innate immunity. *Immunobiology* **211**, 295–314 (2006).
6. U. E. Schaible, S. H. E. Kaufmann, Iron and microbial infection. *Nat. Rev. Microbiol.* **2**, 946–953 (2004).
7. M. P. Soares, G. Weiss, The iron age of host-microbe interactions. *EMBO Rep.* **16**, 1482–1500 (2015).
8. G. E. Cartwright *et al.*, The anemia associated with chronic infection. *Science* **103**, 72 (1946).
9. F. A. Khan, M. A. Fisher, R. A. Khakoo, Association of hemochromatosis with infectious diseases: Expanding spectrum. *Int. J. Infect. Dis.* **11**, 482–487 (2007).
10. A. Bezkorovainy, "Antimicrobial properties of iron-binding proteins" in *Diet and Resistance to Disease*, M. Phillips, A. Baetz, Eds. (Springer, 1981), pp. 139–154.
11. L. A. Lambert, H. Perri, P. J. Halbrooks, A. B. Mason, Evolution of the transferrin family: Conservation of residues associated with iron and anion binding. *Comp. Biochem. Physiol. B Biochem. Mol. Biol.* **142**, 129–141 (2005).
12. L. A. Lambert, Molecular evolution of the transferrin family and associated receptors. *Biochim. Biophys. Acta* **1820**, 244–255 (2012).
13. K. Gkouvatsos, G. Papanikolaou, K. Pantopoulos, Regulation of iron transport and the role of transferrin. *Biochim. Biophys. Acta* **1820**, 188–202 (2012).
14. S. Farnaud, R. W. Evans, Lactoferrin—A multifunctional protein with antimicrobial properties. *Mol. Immunol.* **40**, 395–405 (2003).

15. H. Jenssen, R. E. W. Hancock, Antimicrobial properties of lactoferrin. *Biochimie* **91**, 19–29 (2009).
16. P. P. Ward, M. Mendoza-Meneses, P. W. Park, O. M. Conneely, Stimulus-dependent impairment of the neutrophil oxidative burst response in lactoferrin-deficient mice. *Am. J. Pathol.* **172**, 1019–1029 (2008).
17. A. L. Schade, L. Caroline, An iron-binding component in human blood plasma. *Science* **104**, 340–341 (1946).
18. R. R. Arnold, M. Brewer, J. J. Gauthier, Bactericidal activity of human lactoferrin: Sensitivity of a variety of microorganisms. *Infect. Immun.* **28**, 893–898 (1980).
19. S. H. M. Rooijakkers *et al*., Human transferrin confers serum resistance against *Bacillus anthracis*. *J. Biol. Chem.* **285**, 27609–27613 (2010).
20. P. P. Ward, O. M. Conneely, Lactoferrin: Role in iron homeostasis and host defense against microbial infection. *Biometals* **17**, 203–208 (2004).
21. E.-Y. Yun *et al*., *Bombyx mori* transferrin: Genomic structure, expression and antimicrobial activity of recombinant protein. *Dev. Comp. Immunol.* **33**, 1064–1069 (2009).
22. L. M. Brummett, M. R. Kanost, M. J. Gorman, The immune properties of *Manduca sexta* transferrin. *Insect Biochem. Mol. Biol.* **81**, 1–9 (2017).
23. K. W. Bruhn, B. Spellberg, Transferrin-mediated iron sequestration as a novel therapy for bacterial and fungal infections. *Curr. Opin. Microbiol.* **27**, 57–61 (2015).
24. L. Lin *et al*., Transferrin iron starvation therapy for lethal bacterial and fungal infections. *J. Infect. Dis.* **210**, 254–264 (2014).
25. J. T. Bu, T. B. Bartnikas, The use of hypotransferrinemic mice in studies of iron biology. *Biometals* **28**, 473–480 (2015).
26. B. Lemaitre, J. Hoffmann, The host defense of *Drosophila melanogaster*. *Annu. Rev. Immunol.* **25**, 697–743 (2007).
27. N. Buchon, N. Silverman, S. Cherry, Immunity in *Drosophila melanogaster*—From microbial recognition to whole-organism physiology. *Nat. Rev. Immunol.* **14**, 796–810 (2014).
28. D. Ferrandon, J.-L. Imler, C. Hetru, J. A. Hoffmann, The *Drosophila* systemic immune response: Sensing and signalling during bacterial and fungal infections. *Nat. Rev. Immunol.* **7**, 862–874 (2007).
29. T. Tanji, Y. T. Ip, Regulators of the toll and Imd pathways in the *Drosophila* innate immune response. *Trends Immunol.* **26**, 193–198 (2005).
30. K. Tiklová, K.-A. Senti, S. Wang, A. Gräslund, C. Samakovlis, Epithelial septate junction assembly relies on melanotransferrin iron binding and endocytosis in *Drosophila*. *Nat. Cell Biol.* **12**, 1071–1077 (2010).
31. K. Mandilaras, F. Missirlis, Genes for iron metabolism influence circadian rhythms in *Drosophila melanogaster*. *Metallomics* **4**, 928–936 (2012).
32. G. Xiao, Z.-H. Liu, M. Zhao, H.-L. Wang, B. Zhou, Transferrin 1 functions in iron trafficking and genetically interacts with ferritin in *Drosophila melanogaster*. *Cell Rep.* **26**, 748–758.e5 (2019).
33. E. De Gregorio, P. T. Spellman, G. M. Rubin, B. Lemaitre, Genome-wide analysis of the *Drosophila* immune response by using oligonucleotide microarrays. *Proc. Natl. Acad. Sci. U.S.A.* **98**, 12590–12595 (2001).
34. K. Troha, J. H. Im, J. Revah, B. P. Lazzaro, N. Buchon, Comparative transcriptomics reveals CrebA as a novel regulator of infection tolerance in *D. melanogaster*. *PLoS Pathog.* **14**, e1006847 (2018).
35. T. Yoshiga *et al*., *Drosophila melanogaster* transferrin. Cloning, deduced protein sequence, expression during the life cycle, gene localization and up-regulation on bacterial infection. *Eur. J. Biochem.* **260**, 414–420 (1999).
36. F. Levy, P. Bulet, L. Ehret-Sabatier, Proteomic analysis of the systemic immune response of *Drosophila*. *Mol. Cell. Proteomics* **3**, 156–166 (2004).
37. D. L. Geiser, J. J. Winzerling, Insect transferrins: Multifunctional proteins. *Biochim. Biophys. Acta* **1820**, 437–451 (2012).
38. T. Yoshiga, V. P. Hernandez, A. M. Fallon, J. H. Law, Mosquito transferrin, an acute-phase protein that is up-regulated upon infection. *Proc. Natl. Acad. Sci. U.S.A.* **94**, 12337–12342 (1997).
39. K. Mandilaras, T. Pathmanathan, F. Missirlis, Iron absorption in *Drosophila melanogaster*. *Nutrients* **5**, 1622–1647 (2013).
40. A. Ciencialová *et al*., Mapping the peptide and protein immune response in the larvae of the fleshfly *Sarcophaga bullata*. *J. Pept. Sci.* **14**, 670–682 (2008).
41. I. Iatsenko, S. Kondo, D. Mengin-Lecreulx, B. Lemaitre, PGRP-SD, an extracellular pattern-recognition receptor, enhances peptidoglycan-mediated activation of the Drosophila Imd pathway. *Immunity* **45**, 1013–1023 (2016).
42. I. Iatsenko, J.-P. Boquete, B. Lemaitre, Microbiota-derived lactate activates production of reactive oxygen species by the intestinal NADPH oxidase nox and shortens Drosophila lifespan. *Immunity* **49**, 929–942.e5 (2018).
43. G. Chamilos *et al*., *Drosophila melanogaster* as a model host to dissect the immunopathogenesis of zygomycosis. *Proc. Natl. Acad. Sci. U.S.A.* **105**, 9367–9372 (2008).
44. A. A. Reinhart, A. G. Oglesby-Sherrouse, Regulation of *Pseudomonas aeruginosa* virulence by distinct iron sources. *Genes (Basel)* **7**, E126 (2016).
45. M. L. Vasil, U. A. Ochsner, The response of *Pseudomonas aeruginosa* to iron: Genetics, biochemistry and virulence. *Mol. Microbiol.* **34**, 399–413 (1999).
46. R. E. Cowart, F. L. Singleton, J. S. Hind, A comparison of bathophenanthrolinedisulfonic acid and ferrozine as chelators of iron(II) in reduction reactions. *Anal. Biochem.* **211**, 151–155 (1993).
47. P. Visca, F. Imperi, I. L. Lamont, Pyoverdine siderophores: From biogenesis to biosignificance. *Trends Microbiol.* **15**, 22–30 (2007).
48. N. V. Kirienko *et al*., *Pseudomonas aeruginosa* disrupts *Caenorhabditis elegans* iron homeostasis, causing a hypoxic response and death. *Cell Host Microbe* **13**, 406–416 (2013).
49. F. Imperi *et al*., Repurposing the antimycotic drug flucytosine for suppression of *Pseudomonas aeruginosa* pathogenicity. *Proc. Natl. Acad. Sci. U.S.A.* **110**, 7458–7463 (2013).
50. F. Minandri *et al*., Role of iron uptake systems in *Pseudomonas aeruginosa* virulence and airway infection. *Infect. Immun.* **84**, 2324–2335 (2016).
51. H. Takase, H. Nitanai, K. Hoshino, T. Otani, Requirement of the *Pseudomonas aeruginosa tonB* gene for high-affinity iron acquisition and infection. *Infect. Immun.* **68**, 4498–4504 (2000).
52. N. Buchon, N. A. Broderick, M. Poidevin, S. Pradervand, B. Lemaitre, *Drosophila* intestinal response to bacterial infection: Activation of host defense and stem cell proliferation. *Cell Host Microbe* **5**, 200–211 (2009).
53. J. M. Meyer, A. Neely, A. Stintzi, C. Georges, I. A. Holder, Pyoverdin is essential for virulence of *Pseudomonas aeruginosa*. *Infect. Immun.* **64**, 518–523 (1996).
54. N. V. Kirienko, F. M. Ausubel, G. Ruvkun, Mitophagy confers resistance to siderophore-mediated killing by *Pseudomonas aeruginosa*. *Proc. Natl. Acad. Sci. U.S.A.* **112**, 1821–1826 (2015).
55. A. Zaborin *et al*., Red death in *Caenorhabditis elegans* caused by *Pseudomonas aeruginosa* PAO1. *Proc. Natl. Acad. Sci. U.S.A.* **106**, 6327–6332 (2009).
56. A. S. Little *et al*., *Pseudomonas aeruginosa* AlgR phosphorylation status differentially regulates pyocyanin and pyoverdine production. *MBio* **9**, e02318-17 (2018).
57. J. P. Dudzic, M. A. Hanson, I. Iatsenko, S. Kondo, B. Lemaitre, More than black or white: Melanization and toll share regulatory serine proteases in *Drosophila*. *Cell Rep.* **27**, 1050–1061.e3 (2019).
58. A. Defaye *et al*., Genetic ablation of *Drosophila* phagocytes reveals their contribution to both development and resistance to bacterial infection. *J. Innate Immun.* **1**, 322–334 (2009).
59. B. Charroux, J. Royet, Elimination of plasmatocytes by targeted apoptosis reveals their role in multiple aspects of the *Drosophila* immune response. *Proc. Natl. Acad. Sci. U.S.A.* **106**, 9797–9802 (2009).
60. R. L. Unckless, S. M. Rottschaefer, B. P. Lazzaro, The complex contributions of genetics and nutrition to immunity in *Drosophila melanogaster*. *PLoS Genet.* **11**, e1005030 (2015).
61. M. A. Hanson *et al*., Synergy and remarkable specificity of antimicrobial peptides in vivo using a systematic knockout approach. *eLife* **8**, e44341 (2019).
62. J. Kim, Y. Kim, A viral histone H4 suppresses expression of a transferrin that plays a role in the immune response of the diamondback moth, *Plutella xylostella*. *Insect Mol. Biol.* **19**, 567–574 (2010).
63. M. J. Lehane, W. Gibson, S. M. Lehane, Differential expression of fat body genes in *Glossina morsitans morsitans* following infection with *Trypanosoma brucei brucei*. *Int. J. Parasitol.* **38**, 93–101 (2008).
64. N. Vodovar *et al*., *Drosophila* host defense after oral infection by an entomopathogenic *Pseudomonas* species. *Proc. Natl. Acad. Sci. U.S.A.* **102**, 11414–11419 (2005).

The Drosophila Baramicin polypeptide gene protects against fungal infection

M.A. Hanson[1*], L.B. Cohen[2], A. Marra[1], I. Iatsenko[1,3], S.A. Wasserman[2], and B. Lemaitre[1]

1 Global Health Institute, School of Life Science, École Polytechnique Fédérale de Lausanne (EPFL), Lausanne, Switzerland.
2 Division of Biological Sciences, University of California San Diego (UCSD), La Jolla, California, United States of America.
3 Max Planck Institute for Infection Biology, 10117, Berlin, Germany.
* Corresponding author: M.A. Hanson (mark.hanson@epfl.ch), B. Lemaitre (bruno.lemaitre@epfl.ch)

ORCID IDs:
Hanson: https://orcid.org/0000-0002-6125-3672
Cohen: https://orcid.org/0000-0002-6366-570X
Iatsenko: https://orcid.org/0000-0002-9249-8998
Wasserman: https://orcid.org/0000-0003-1680-3011
Lemaitre: https://orcid.org/0000-0001-7970-1667

Abstract

The fruit fly *Drososphila melanogaster* combats microbial infection by producing a battery of effector peptides that are secreted into the haemolymph. Technical difficulties prevented the investigation of these short effector genes until the recent advent of the CRISPR/CAS era. As a consequence, many putative immune effectors remain to be characterized and exactly how each of these effectors contributes to survival is not well characterized. Here we describe a novel *Drosophila* antifungal peptide gene that we name *Baramicin A*. We show that *BaraA* encodes a precursor protein cleaved into multiple peptides via furin cleavage sites. *BaraA* is strongly immune-induced in the fat body downstream of the Toll pathway, but also exhibits expression in the nervous system. Importantly, we show that flies lacking *BaraA* are viable but susceptible to the enomopathogenic fungus *Beauveria bassiana*. Consistent with *BaraA* being directly antimicrobial, overexpression of *BaraA* promotes resistance to fungi and the IM10-like peptides produced by *BaraA*

synergistically inhibit growth of fungi in vitro when combined with a membrane-disrupting antifungal. Surprisingly, *BaraA* males but not females display an erect wing phenotype upon infection. Collectively, we identify a new antifungal immune effector downstream of Toll signalling, improving our knowledge of the *Drosophila* antimicrobial response.

Introduction

The innate immune response provides the first line of defence against pathogenic infection. This reaction is usually divided into three stages: i) the recognition of pathogens through dedicated pattern recognition receptors, ii) the activation of conserved immune signalling pathways and iii) the production of immune effectors that target invading pathogens [1,2]. The study of invertebrate immune systems has led to key observations of broad relevance, such as the discovery of phagocytosis [3], antimicrobial peptides (AMPs) [4], and the implication of Toll receptors in metazoan immunity [5]. Elucidating immune mechanisms, genes, and signalling pathways has greatly benefited from investigations in the fruit fly *Drosophila melanogaster*, which boasts a large suite of molecular and genetic tools for manipulating the system. One of the best-characterized immune reactions of *Drosophila* is the systemic immune response. This reaction involves the fat body (an analog of the mammalian liver) producing immune effectors that are secreted into the haemolymph. In *Drosophila*, two NF-κB signalling pathways, the Toll and Imd pathways, regulate most inducible immune effectors: the Toll pathway is predominantly activated in response to infection by Gram-positive bacteria and fungi [5,6], while the immune-deficiency pathway (Imd) responds to the DAP-type peptidoglycan most commonly found in Gram-negative bacteria and a subset of Gram-positive bacteria [7]. These two signalling pathways regulate a transcriptional program that results in the massive synthesis and secretion of humoral effector peptides [6,8]. Accordingly, mutations affecting the Toll and Imd pathways cause extreme susceptibilities to systemic infection that reflect the important contribution of these pathways to host defence. The best-

characterized immune effectors downstream of these pathways are antimicrobial peptides (AMPs). AMPS are small and often cationic peptides that disrupt the membranes of microbes, although some have more specific mechanisms [9]. Multiple AMP genes belonging to seven well-characterized families are induced upon systemic infection [10]. However transcriptomic analyses have revealed that the systemic immune response encompasses far more than just the canonical AMPs. Many uncharacterized genes encoding small secreted peptides are induced to high levels downstream of the Toll and Imd pathways, pointing to the role for these peptides as immune effectors [11]. In parallel, MALDI-TOF analyses of the haemolymph of infected flies revealed the induction of 24 peaks - mostly corresponding to uncharacterized peptides - that were named "IMs" for Immune-induced Molecules (IM1-IM24) [8]. Many of the genes that encode these components of the immune peptidic secretome have remained largely unexplored. This is mainly due to the fact that these IMs belong to large gene families of small genes that were until recently difficult to disrupt by mutagenesis.

The CRISPR/Cas9 gene editing approach now allows the necessary precision to delete small genes, singly or in groups, providing the opportunity to dissect effector peptide functions. In 2015 a family of 12 related IM-encoding genes, unified under the name *Bomanins*, were shown to function downstream of Toll. Importantly, a deletion removing 10 out of the 12 Bomanins revealed their potent contribution to defence against both Gram-positive bacteria and fungi [12]. While Bomanins contribute significantly to Toll-mediated defence, their molecular functions are still unknown and it is unclear if they are directly antimicrobial [13]. Two other IMs encoding IM4 and IM14 (renamed *Daisho1* and *Daisho2*, respectively) were shown to contribute downstream of Toll to resistance against specific fungi. Interestingly, Daisho peptides bind to fungal hyphae, suggesting direct antifungal activity [14]. Finally a systematic knock-out analysis of *Drosophila* AMPs revealed that they play an important role in defence against Gram-negative bacteria and some fungi, but surprisingly little against Gram-positive bacteria [15]. An unforeseen finding from these recent studies is the high degree of AMP-pathogen specificity: this is perhaps

best illustrated by the specific requirement for *Diptericin*, but not other AMPs, in defence against *Providencia rettgeri* [15,16]. Collectively, these studies in *Drosophila* reveal that immune effectors can be broad or specific in mediating host-pathogen interactions. Understanding the logic of the *Drosophila* effector response will thus require a careful dissection of the remaining uncharacterized immune induced peptides.

Previous studies identified an uncharacterized Toll-regulated gene called *IMPPP/CG33470*, which we rename "*BaraA*" (see below), that encodes several IMs, indicating a role in the humoral response. Here, we have improved the annotation of IMs produced by *BaraA* to include: IM10, IM12 (and its sub-peptide IM6), IM13 (and its sub-peptides IM5 and IM8), IM22, and IM24. Using a *BaraA* reporter, we show that *BaraA* is not only immune-induced in the fat body, but also expressed in the head, and nervous system tissue including the eyes, and ocelli. Importantly, we show that flies lacking *BaraA* are viable but susceptible to specific infections, notably by the entomopathogenic fungus *Beauveria bassiana*. Consistent with this, the IM10-like peptides produced by *BaraA* inhibit fungal growth in vitro when combined with the antifungal Pimaricin. Surprisingly, *BaraA* deficient males also display a striking erect wing behaviour upon infection. Collectively, we identify a new antifungal immune effector downstream of Toll signalling, improving our knowledge of the *Drosophila* antimicrobial response.

Results:

BaraA is regulated by the Toll pathway

Previous microarray studies from De Gregorio et al. [11] suggest that *BaraA* is primarily regulated by the Toll pathway, with a minor input from the Imd pathway (**Fig.** 1A). Consistent with this, we found several putative NF-κB binding sites upstream of the *BaraA* gene (guided by previous reports [17–19]). Notably there are

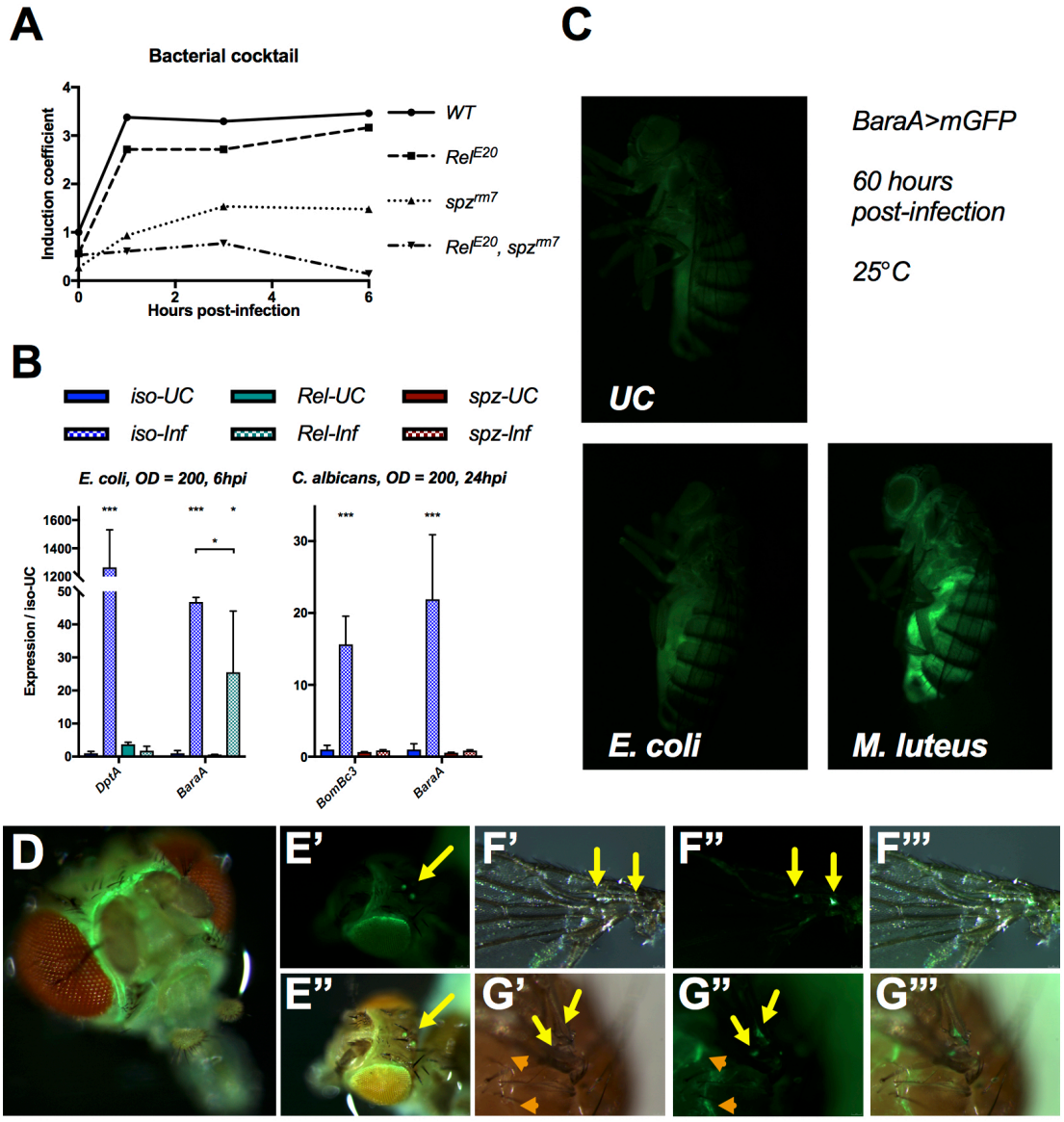

Figure 1: *BaraA* is an immune-induced gene regulated by the Toll pathway. A) Expression profile of *BaraA* upon bacterial challenge by a mixture of *E. coli* and *M. luteus* (from De Gregorio et al. [11]). Induction coefficient is a complex calculation of log-fold change reported in De Gregorio et al. [11], and values are given relative to wild type unchallenged expression levels. B) *BaraA* expression profiles in wild-type, spz^{rm7} and Rel^{E20} flies upon septic injury with the Gram-negative bacterium *E. coli* and the yeast *C. albicans*. *DptA* and *BomBc3* were used as inducible control genes for the Imd and Toll pathways respectively. Floating asterisks indicate significance relative to *iso-UC* where: * = $p < .05$ and, *** = $p < .001$. C) Use of a *BaraA* reporter reveals that *BaraA* induction upon infection is primarily driven by the fat body in adults, and results in a much stronger GFP signal upon pricking with *M. luteus* (which stimulates the Toll pathway) compared to *E. coli* (which stimulates the Imd pathway). Representative images taken 60h (adults) after handling alone (UC) or infection with *E. coli* or *M. luteus* (OD=200). D-G) *BaraA>mGFP* is highly expressed in the head (D), at the border of the eyes and in the ocelli (E), in the wing veins (F-G yellow arrows), and beneath the cuticle in the thorax (H, orange arrows).

two putative binding sites for Relish, the transcription factor of the Imd pathway and three putative binding sites for the Dif/Dorsal transcription factors acting downstream of Toll (**Fig.** S1A). We challenged wild type flies and Imd or Toll pathway mutants (*Rel*^{E20} and *spz*^{rm7} respectively) with the Gram-negative bacterium *Escherichia coli*, the yeast *Candida albicans*, or the Gram-positive bacterium *Micrococcus luteus*. RT-qPCR analysis confirms that *BaraA* is induced by infection with *E. coli*, *C. albicans*, or *M. luteus (***Fig.** 1B and **Fig.** S1B). *BaraA* remains highly inducible in a *Relish* mutant background, albeit at slightly reduced level compared to the wild type. However *BaraA* expression is abolished in *spz*^{rm7} flies. Collectively, the expression pattern of *BaraA* is reminiscent of the antifungal peptide gene *Drosomycin* with a primary input by the Toll pathway and a minor input from the Imd pathway [10,20].

To further characterize the expression of *BaraA*, we generated a *BaraA-Gal4* transgene in which 1675bp of the *BaraA* promoter sequence is fused to the yeast transcription factor Gal4. Use of *BaraA-Gal4>UAS-mCD8-GFP* (referred to as *BaraA>mGFP*) reveals that *BaraA* is strongly induced in the fat body 60h post infection by *M. luteus*, but less so by *E. coli* pricking (**Fig.** 1C); dissections confirmed this GFP signal is produced by the fat body. Larvae pricked with *M. luteus* also show a robust GFP signal primarily stemming from the fat body when examined 2hpi (**Fig.** S1C). We also observed a strong constitutive GFP signal in the headcase of adults (**Fig.** 1D), including the border of the eyes and the ocelli (**Fig.** 1E). Dissection confirmed that the *BaraA* reporter is expressed in brain tissue, notably in the central ventral brain furrow. Other consistent signals include GFP in the wing veins and subcutaneously along borders of thoracic pleura in adults (**Fig.** 1F-G), and in spermatheca of females (**Fig.** S1D). There was also sporadic GFP signal in other tissues that included the larval hindgut, the dorsal abdomen of developing pupae, and the seminal vesicle of males. These expression patterns largely agree with data reported in FlyAtlas1 [21].

Baramicin A encodes a precursor protein cleaved into multiple peptides

Previous studies using bioinformatics and proteomics have suggested that four highly immune-induced peptides (IM10, IM12, IM13, and IM24) are encoded in tandem as a single polypeptide precursor by *IMPPP/BaraA* [8,22]. Some less-abundant sub-peptides (IM5, IM6, and IM8) are also produced by additional cleavage of IM12 and IM13 [22]. Using a newly generated null mutant ("*ΔBaraA,*" described below), we analyzed haemolymph samples of wild type and *ΔBara* flies infected with a bacterial mixture of *E. coli* and *M. luteus* by MALDI-TOF analysis. We confirmed the loss of the seven immune-induced peaks corresponding to IMs 5, 6, 8, 10, 12, 13, and 24 in *ΔBaraA* flies (**Fig.** 2A). We also noticed that an additional immune-induced peak at ~5975 Da was absent in our *BaraA* mutants. Upon re-visiting the original studies that annotated the *Drosophila* IMs, we realized this peak corresponded to IM22, whose sequence was never determined [8,22] (see supplementary information for details). We subjected haemolymph from infected flies to LC-MS proteomic analysis following trypsin digestion and found that in addition to the known IMs of *BaraA* (IMs 5, 6, 8, 10, 12, 13, and 24), trypsin-digested fragments of the *BaraA* C-terminus peptide were also detectable in the haemolymph (**Fig.** S2). The range of detected fragments did not match the full length of the C-terminus exactly, as the first four residues were absent in our LC-MS data (a truncation not predicted to arise via trypsin cleavage). The *BaraA* C-terminus lacking these four residues has a calculated mass of 5974.5 Da, exactly matching the observed mass of the IM22 peak absent in *BaraA* mutant flies. Furthermore in other *Drosophila* species these four residues of the *BaraA* C-terminus are instead an RXRR furin cleavage motif (**Fig.** S3A). Therefore IM22 cleavage in other species, even by an alternate cleavage process, should result in the same maturated IM22 domain as found in *D. melanogaster*. Taken together, we conclude that IM22 is the mature form of the BaraA protein C-terminus.

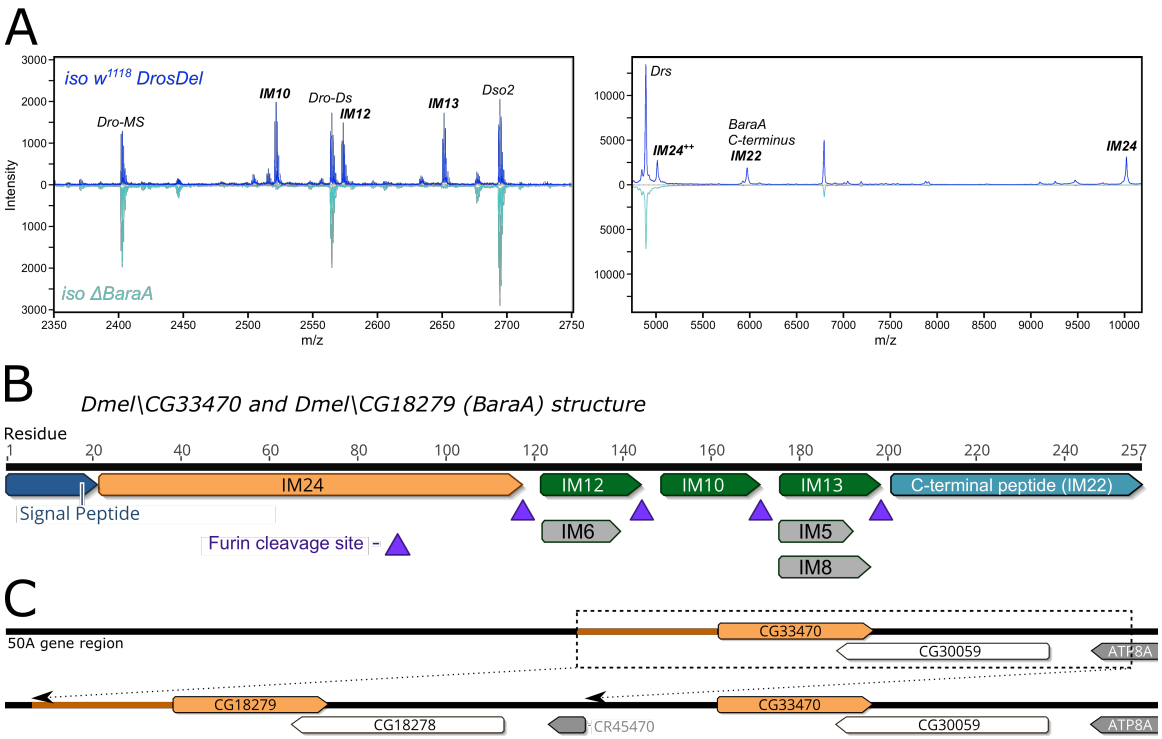

Figure 2: The *BaraA* gene structure. A) MALDI-TOF analysis of haemolymph from *iso w*^{1118} wild-type and *iso ΔBaraA* flies 24 hours post-infection (hpi) confirms that *BaraA* mutants fail to produce the IM10-like and IM24 peptides. *iso ΔBaraA* flies also fail to produce an immune-induced peak at ~5794 Da corresponding to IM22 (the C-terminal peptide of BaraA, see supplementary information). B) The *BaraA* gene encodes a precursor protein that is cleaved into multiple mature peptides at RXRR furin cleavage sites. The sub-peptides IMs 5, 6, and 8 are additional minor cleavage products of IM12 and IM13. IM22 is additionally cleaved following its GIND motif (Fig. S2 and S3A). C) There is a *BaraA* locus duplication event present in the Dmel_R6 reference genome. This duplication is not fixed in laboratory stocks and wild-type flies (Hanson and Lemaitre, 2020; in prep.).

Thus, a single gene, *BaraA*, contributes to one third of the originally described *Drosophila* IMs. These peptides are encoded as a polypeptide precursor interspersed by furin cleavage sites (e.g. RXRR) (**Fig.** 2B). We note that the IM10, IM12 and IM13 peptides are tandem repeats of related peptides, which we collectively refer to as "IM10-like" peptides (**Fig.** S3B). The IM22 peptide also contains a similar motif as the IM10-like peptides (**Fig.** S3A-B), suggesting a related biological activity. We name this gene "*Baramicin A*" (symbol: *BaraA*) for the Japanese idiom Bara Bara (バラバラ), meaning "to break apart;" a reference to the fragmenting structure of the *Baramicin* precursor protein and its many peptidic products.

A BaraA duplication is present in some laboratory stocks

Over the course of our investigation, we realized that *IMPPP (CG18279)* was identical to its neighbour gene *CG33470* owing to a duplication event of the *BaraA* locus present in the *D. melanogaster* reference genome. The exact nature of this duplication is discussed in a separate article (Hanson and Lemaitre; in prep). In brief, the duplication involves the entire *BaraA* gene including over 1kbp of 100% identical promoter sequence, and also the neighbouring sulfatase gene CG30059 and the 3' terminus of the *ATP8A* gene region (**Fig.** 2C). We distinguish the two daughter genes as *BaraA1 (CG33470)* and *BaraA2 (CG18279).* Available sequence data suggests the *BaraA1* and *BaraA2* transcripts are 100% identical. We analyzed the presence of the *BaraA* duplication using a PCR assay spanning the junction of the duplicated region (supplementary data file 1). Interestingly, *BaraA* copy number is variable in common lab strains and wild flies, indicating this duplication event is not fixed in *D. melanogaster* (Hanson and Lemaitre; in prep).

Over-expression of BaraA improves the resistance of immune deficient flies

Imd, Toll deficient flies are extremely susceptible to microbial infection as they fail to induce hundreds of immune genes, including antimicrobial peptides [11]. It has been shown that over-expression of even a single AMP can improve the resistance of *Imd, Toll* deficient flies [23]. As such, immune gene over-expression in *Imd, Toll* immune-compromised flies provides a direct assay to test the ability of a gene to contribute to defence independent of other immune effectors. We applied this strategy to *Baramicin A* by generating flies that constitutively express *BaraA* using the ubiquitous *Actin5C-Gal4* driver *(Act-Gal4)* in an immune-deficient Rel^{E20}, spz^{rm7} double mutant background (**Fig.** S4A). In these experiments, we pooled results from both males and females due to the very low availability of homozygous *Rel, spz* adults, particularly when combined with *Act-Gal4*. Overall, similar trends were seen in both sexes, and separate male and female survival curves are shown in **Fig.** S4.

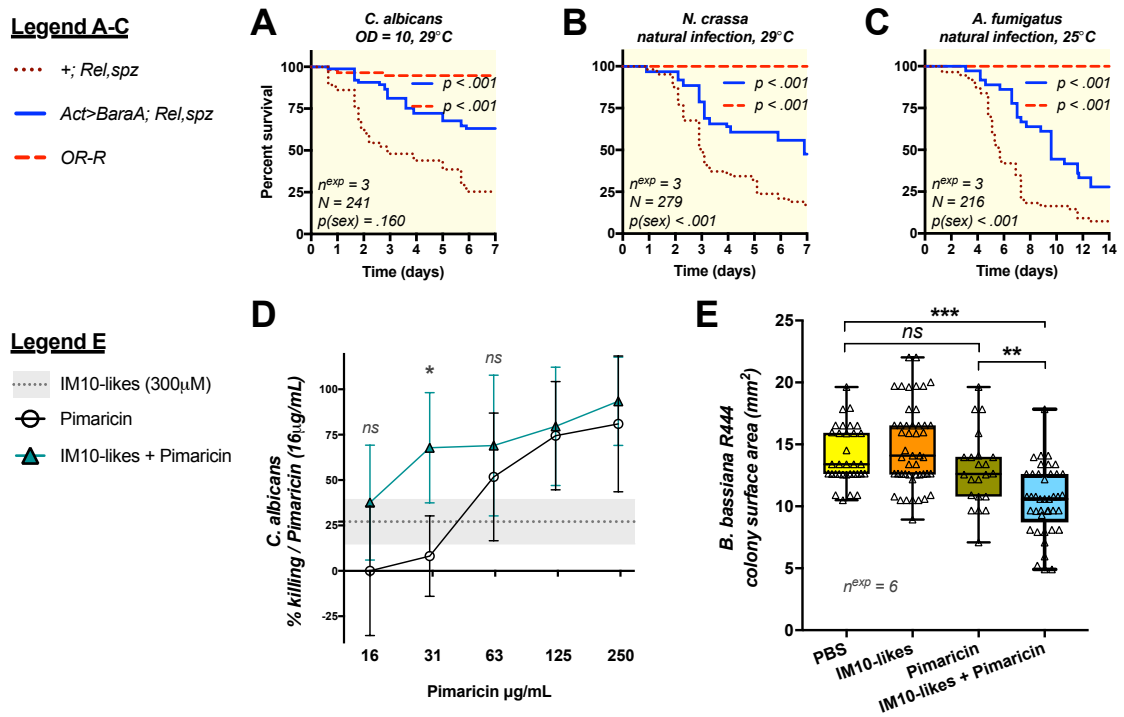

Figure 3: Overexpression of *BaraA* partially rescues the susceptibility of *Rel, spz* flies against fungi and BaraA IM10-like peptides inhibit fungal growth in vitro. A-C) Overexpression of *BaraA* (*Act>BaraA)* rescues the susceptibility of *Rel, spz* flies upon systemic infection with *C. albicans* (A), or natural infection with either *N. crassa* or *A. fumigatus* (B-C). Survivals represent pooled results from males and females (see Fig. S4 for sex-specific survival curves). D) A 300µM cocktail of the three IM10-like peptides improves the killing activity of the antifungal Pimaricin against *C. albicans* yeast. Error bars and the shaded area (IM10-likes alone) represent ±1 standard deviation from the mean. Killing activity (%) was compared against no-peptide controls, then normalized to the activity of Pimaricin alone. E) The IM10-like peptide cocktail also synergizes with Pimaricin to inhibit mycelial growth of *B. bassiana strain R444*. The diameters of individual colonies of *B. bassiana* were assessed after four days of growth at 25°C after peptide treatment, and surface area calculated as πr^2.

Ubiquitous *BaraA* expression marginally improved the survival of *Rel, spz* flies upon infection with *M luteus* bacteria, however there was no effect upon infection with *E. coli* (**Fig. S4B-C**). On the other hand, ubiquitous expression of *BaraA* provided a more pronounced protective effect against infection by a variety of fungal pathogens. This was true upon pricking with *C. albicans* (**Fig.** 3A), or upon natural infections using *Aspergillus fumigatus* or *Neurospora crassa* filamentous fungi (**Fig.** 3B-C). This over-expression study reveals that *BaraA* alone can partially rescue the susceptibility of *Imd, Toll* deficient flies to infection, and points to a more prominent role for *BaraA* in antifungal defence.

IM10-like peptides display antifungal activity in vitro

The Baramicin A gene encodes a polypeptide precursor that ultimately produces multiple mature peptides. However the most prominent *BaraA* products are the 23-residue IM10, 12, and 13 peptides (collectively the "IM10-like" peptides); indeed three IM10-like peptides are produced for every one IM24 peptide (**Fig.** 2B), and IM22 also bears an IM10-like motif (**Fig.** S3). This prompted us to explore the in vitro activity of the BaraA IM10-like peptides as potential AMPs.

We synthesized IM10, IM12, and IM13 and performed in vitro antimicrobial assays with these three IM10-like peptides using a 1:1:1 cocktail with a final concentration of 300μM (100 μM each of IM10, IM12, and IM13). Using a protocol adapted from Wiegand et al. [24], we monitored the microbicidal activity of this peptide cocktail either alone, or in combination with membrane-disrupting antibiotics that facilitate peptide entry into the cell. We based this approach on previous studies that showed that the microbicidal activities of Abaecin-like peptides, which target the bacterial DNA chaperone *DnaK,* increase exponentially in combination with a membrane disrupting agent [25–27]. We did not detect any killing activity of our IM10-like peptide cocktail alone against *Pectobacterium carotovora Ecc15* (hereafter *"Ecc15"*), *Enterococcus faecalis,* or *C. albicans*. We also found no activity of IM10-like peptides against *Ecc15 or E. faecalis* when co-incubated with a sub-lethal dose of Cecropin or Ampicillin respectively. However, we observed a synergistic interaction between IM10-like peptides and the antifungal Pimaricin against *C. albicans* (**Fig.** 3D). Co-incubation of the IM10-like cocktail with Pimaricin significantly improved the killing activity of Pimaricin at 32μg/mL relative to either treatment alone. While not statistically significant, the combination of IM10-like cocktail and Pimaricin also outperformed either the IM10-like cocktail alone or Pimaricin alone across the entire range of Pimaricin concentrations tested.

We next co-incubated dilute preparations of *B. bassiana* strain R444 spores under the same conditions as used previously with *C. albicans*, plated 2μL droplets, and assessed the diameters and corresponding surface area of colonies derived from individual spores after 4 days of growth at 25°C to assess growth rate. We found that neither the IM10-like cocktail nor Pimaricin alone affected surface area relative to PBS buffer control alone (Tukey's HSD: $p = 0.656$ and 0.466 respectively). However in combination, the IM10-like cocktail plus Pimaricin led to significantly reduced colony size compared to either treatment alone, corresponding to a 19-29% reduction in surface area relative to controls (**Fig.** 3E, Tukey's HSD: $p < .01$ in all cases). This indicates that incubation with IM10-like peptides and Pimaricin synergistically inhibits *B. bassiana* mycelial growth, revealing an otherwise cryptic antifungal effect of the BaraA IM10-like peptides.

Overall, we found that IM10-like peptides alone do not kill *C. albicans* yeast or impair *B. bassiana* mycelial growth in vitro. However, IM10-like peptides seem to synergize with the antifungal Pimaricin to inhibit growth of both of these fungi.

BaraA deficient flies broadly resist like wild type upon bacterial infection

To further characterize *BaraA* function, we generated a null mutation of *BaraA* by replacing the 'entire' *BaraA* locus with a dsRed cassette using CRISPR mediated homology-directed repair with fly stocks that contain only one *BaraA* gene copy (BL2057 and BL51323). After isolation, this mutation ($BaraA^{SW1}$) was then backcrossed once to a lab strain of w^{1118} (used in [12–14]) to remove a second site mutation (see materials and methods). The resulting w^{1118}; $BaraA^{SW1}$ flies are hereon referred to as *"w; ΔBaraA*." Finally, the $BaraA^{SW1}$ mutation was isogenized by seven rounds of backcrossing into the w^{1118} *DrosDel* isogenic genetic background (*iso* w^{1118}) [28] as described in Ferreira et al and are hereon referred to as "*iso ΔBaraA*" [29]. Relevant to this study, both our *OR-R* and *DrosDel iso* w^{1118} wild type lines contain the duplication and thus have both *BaraA1 and A2* genes, while *w; ΔBaraA*

and *iso ΔBaraA* flies lack *BaraA* entirely. In the following experiments, we compare the immune response of both *w; ΔBaraA* and *iso ΔBaraA* and focused only on phenotypes that were consistent in both genetic backgrounds.

We validated these mutant lines by PCR, qPCR and MALDI-TOF peptidomics (**Fig.** 2A, supplementary data file 1). *BaraA*-deficient flies were viable with no morphological defect. Furthermore, *ΔBaraA* flies have wild type Toll and Imd signalling responses following infection, indicating that *BaraA* is not required for the activation of these signaling cascades (**Fig.** S5A-C). Moreover, *BaraA* mutant flies survive clean injury like wild type (**Fig.** S5D), and have comparable lifespan to wild type flies (**Fig.** S5E). We next challenged *BaraA* mutant flies using our two genetic backgrounds with a variety of pathogens. We included susceptible Imd deficient Rel^{E20} flies, Toll deficient spz^{rm7} flies and *Bomanin* deficient $Bom^{\Delta 55C}$ flies as comparative controls. We observed that *BaraA* null flies have comparable resistance as wild type to infection with the Gram-negative bacterium *Ecc15* (**Fig.** S6A), or with the Gram-positive bacterium *B. subtilis* (**Fig.** S6B). In contrast, we saw a mild increase in the susceptibility of *w; ΔBaraA* flies to infection by the Gram-positive bacterium *E. faecalis* (HR = +0.73, $p = .014$). We also saw an early mortality phenotype in *iso ΔBaraA* flies (at 3.5 days, $p < .001$), although this was not ultimately statistically significant (**Fig.** 4A; $p = .173$). This mild susceptibility was also observed using flies carrying the *BaraA* mutation over a deficiency (*ΔBaraA/Df(BaraA))*, as well as in flies ubiquitously expressing *BaraA* RNAi (**Fig.** S7); however none of these sets of survival experiments individually reached statistical significance. Overall, the susceptibility of *BaraA* mutants to *E. faecalis* is mild, but consistent using a variety of genetic approaches.

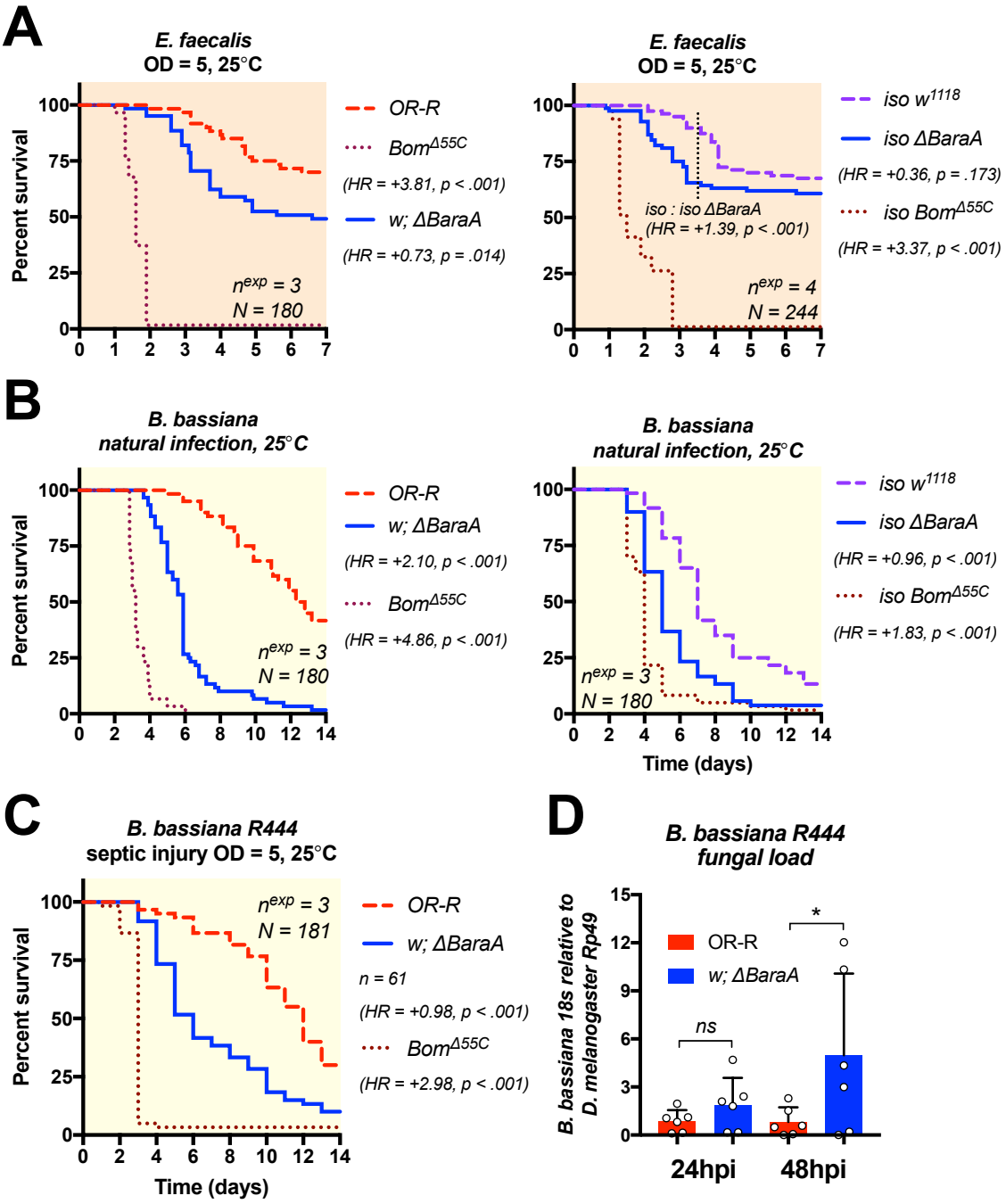

Figure 4: *ΔBaraA* flies are most susceptible to fungal infection. A) *BaraA* mutants with two different genetic backgrounds (here called *w* or *iso*) display a mild susceptibility to systemic infection with *E. faecalis*. This presents as an earlier mortality in the *iso* background (dotted line, p < .001). However, survival in *iso ΔBaraA* flies was not significantly different from wild type at seven days post-infection (p = .173). B) *BaraA* mutants in both backgrounds are susceptible to natural infection with the entomopathogenic fungus *B. bassiana*. C-D) Increased susceptibility (C) and fungal load (D) of *ΔBaraA* flies upon systemic infection by *B. bassiana strain R444*.

BaraA mutant flies are highly susceptible to Beauveria fungal infection

Entomopathogenic fungi such as *B. bassiana* represent an important class of insect pathogens [6]. They have the ability to directly invade the body cavity by digesting and crossing through the insect cuticle. The Toll pathway is critical to survive fungal pathogens as it is directly responsible for the expression of *Bomanin*, *Daisho*, *Drosomycin* and *Metchnikowin* antifungal effectors [12,14,15,30,31]. The fact that i) *BaraA* is Toll-regulated, ii) BaraA IM10-like peptides display antifungal activity in vitro, and iii) *BaraA* overexpression improves the resistance of *Imd, Toll* deficient flies against fungi all point to a role for *BaraA* against fungal pathogens.

We infected *BaraA* mutants and wild type flies by rolling flies in sporulating *B. bassiana* petri dishes. Strikingly, both *w; ΔBaraA* and *iso ΔBaraA* flies displayed a pronounced susceptibility to natural infection with *B. bassiana* (HR = +2.10 or +0.96 respectively, $p < .001$ for both) (**Fig.** 4B). An increased susceptibility to fungi was also observed using flies carrying the *BaraA* mutation over a deficiency (**Fig.** S8A) or that ubiquitously express *BaraA* RNAi (**Fig.** S8B). Moreover, constitutive *BaraA* expression (*Act-Gal4>UAS-BaraA)* in an otherwise wild type background improves survival to *B. bassiana* relative to *Act-Gal4>OR-R* controls (HR = -0.52, $p = .010$) (**Fig.** S8C). Finally, we used a preparation of commercial *B. bassiana R444* spores (BB-PROTEC, Andermatt Biocontrol) to perform controlled systemic infections by pricking flies with a needle dipped in spore solution. In these experiments we monitored both survival and fungal load using qPCR primers specific to the *B. bassiana* 18S rRNA gene [32]. As seen with natural infection, *BaraA* mutants were highly susceptible to *Beauveria* systemic infection (**Fig.** 4C). Moreover, *BaraA* mutants suffered increased fungal load by 48 hours after infection (**Fig.** 4D).

Collectively, our survival analyses point to an important role for *BaraA* in defence against the entomopathogenic fungus *B. bassiana*. Consistent with a direct effect of *BaraA* on fungi, we observe a susceptibility of *BaraA* mutants to infection that is correlated with increased proliferation of *B. bassiana*.

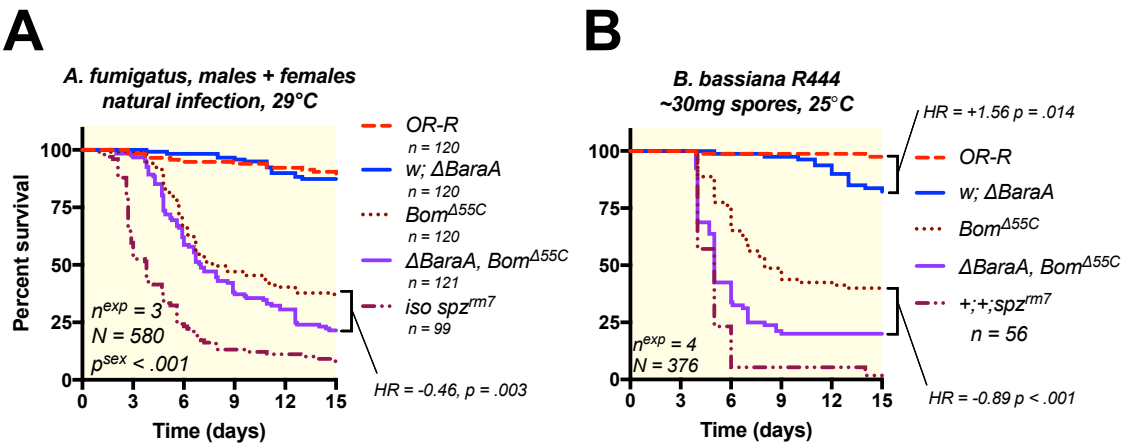

Figure 5: *BaraA* contributes to antifungal defence independent of *Bomanins*. A) *ΔBaraA* , *Bom*$^{\Delta 55C}$ double mutant flies were more susceptible than either mutation alone to natural infection with *A. fumigatus* (see Fig. S6C-D for sex-specific survival curves). B) *ΔBaraA* , *Bom*$^{\Delta 55C}$ double mutant flies were similarly more susceptible than individual mutants when given a mild (30mg of spores) *Beauveria* natural infection by *B. bassiana R444*.

BaraA contributes to antifungal defence independent of Bomanins

Use of compound mutants carrying multiple mutations in effector genes has shown that some of them additively contribute to host resistance to infection [15]. Compound deletions of immune genes can also reveal contributions of immune effectors that are not detectable via single mutant analysis [15,33,34]. Recent studies have indicated that *Bomanins* play a major role in defence against fungi [12,13], though their mechanism of action is unknown. It is possible that *Bomanin* activity relies on the presence of *BaraA*, or vice versa. This prompted us to investigate the interaction of *Bomanins* and *BaraA* in defence against fungi. To do this, we recombined the *Bom*$^{\Delta 55C}$ mutation (that removes a cluster of 10 *Bomanin* genes) with *ΔBaraA.* While natural infection with *Aspergillus fumigatus* did not induce significant mortality in *BaraA* single mutants (**Fig.** S6C-D), we observed that combining *ΔBaraA* and *Bom*$^{\Delta 55C}$ mutations increases fly susceptibility to this pathogen relative to *Bom*$^{\Delta 55C}$ alone (HR = -0.46, p = .003; **Fig.** 5A). We next exposed these *ΔBaraA*, *Bom*$^{\Delta 55C}$, double mutant flies to natural infection with 30mg of commercial spores of *B. bassiana R444*, which we found to be a less virulent *Beauveria* infection model. This is equivalent to approximately 60 million spores,

much of which are removed afterwards upon fly grooming. When using this infection method, we found that *BaraA* mutation markedly increases the susceptibility of $Bom^{\Delta 55C}$ mutant flies (HR = -0.89, $p < .001$), approaching spz^{rm7} susceptibility (**Fig.** 5B).

We conclude that the contribution of *BaraA* to defence does not rely on the presence of *Bomanins*, and vice versa. This finding is consistent with the ability of constitutively expressed *BaraA* to improve survival outcome even in *Imd, Toll* deficient flies. Taken together, these results suggest *BaraA* improves survival against fungi independent of other effectors of the systemic immune response, consistent with a direct effect on invading fungi.

ΔBaraA males display an erect wing phenotype upon infection

While performing infections with *A. fumigatus*, we observed a high prevalence of *BaraA* mutant flies with upright wings (**Fig.** 6A-B), a phenotype similar to the effect of disrupting the gene encoding the "*erect wing"* (*ewg*) transcription factor [35]. Curiously, this erect wing phenotype was most specifically observed in males. Upon further observation, erect wing was observed not only upon *A. fumigatus* infection, but also upon infections with all Gram-positive bacteria and fungi tested (**Table** S1). Increased prevalence of erect wing flies was observed upon infection with both live (**Fig.** 6C) and heat-killed *E. faecalis* (**Fig.** 6D), but less so upon clean injury or via infection with the Gram-negative bacteria *Ecc15* (**Fig.** S9A-B). Thus, the erect wing phenotype appears to be observed in *BaraA* mutants in response to stimuli known to activate the Toll pathway, but does not require a live infection.

Such a phenotype in infected males has never been reported, but is reminiscent of the wing extension behaviour of flies infected by the brain-controlling "zombie" fungus *Enthomopthera muscae* [36]. Intrigued by this phenotype, we further explored its prevalence in other genetic backgrounds. We

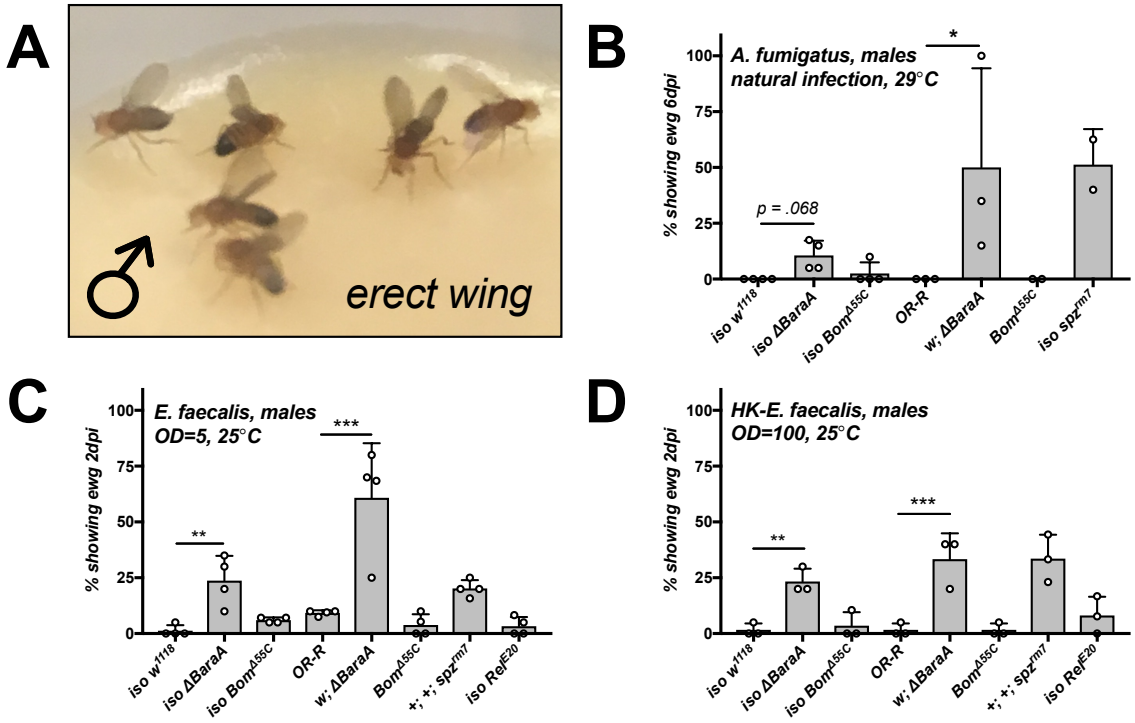

Figure 6: *ΔBaraA* males display an erect wing phenotype upon infection. A) *ΔBaraA* males displaying erect wing six days after *A. fumigatus* natural infection. B-D) *spz*^{rm7} and *ΔBaraA* males, but not *Bom*$^{\Delta 55C}$ or *Rel*^{E20} flies display the erect wing phenotype upon natural infection with *A. fumigatus* (B), or septic injury with live (C) or heat-killed *E. faecalis* (D). Barplots show the percentage of flies displaying erect wing following treatment, with individual data points reflecting replicate experiments. Additional challenges are shown in Table S1.

next confirmed that this phenotype was also observed in other *BaraA*-deficient backgrounds such as *Df(BaraA)/ΔBara*; however the penetrance was variable from one background to another. Erect wing was also observed in *ΔBaraA*/+ heterozygous flies (*Df(BaraA)/+* or *ΔBaraA*/+), indicating that the lack of *BaraA* on one chromosome was sufficient to cause the phenotype (**Fig.** S9C and **Table** S1). Moreover, *spz*^{rm7} flies that lack functional Toll signalling phenocopy *ΔBaraA* flies and display erect wing, but other immune-deficient genotypes such as mutants for the Toll-regulated *Bomanin* effectors (*Bom*$^{\Delta 55C}$), or *Rel*^{E20} mutants that lack Imd signalling, did not readily display erect wing (**Fig.** 6C-D, **Table** S1). Thus the erect wing phenotype is not linked to susceptibility to infection, but rather to loss of *BaraA* upon stimuli triggering the Toll immune pathway. This phenotype suggests

an additional effect of *BaraA* on tissues related to the wing muscle or in the nervous system.

Discussion:

Seven *Drosophila* AMP families were identified in the 1980s-1990s either by homology with AMPs characterized in other insects or owing to their abundant production and microbicidal activities in vitro [37]. In the 2000s, genome annotations revealed the existence of many additional paralogous genes from the seven well-defined families of AMPs [38,39]. At that time, microarray and MALDI-TOF analyses also revealed the existence of many more small immune-induced peptides, which may function as AMPs [8,22]. Genetic analyses using loss of function mutations have recently shown that some of these peptides do play an important role in host defence, however key points surrounding their direct microbicidal activities remain unclear. In 2015, *Bomanins* were shown to be critical to host defence using genetic approaches, but to date no activity in vitro has been found [12,13]. Two candidate AMPs, Listericin [40] and GNBP-like3 [41], were shown to inhibit microbial growth upon heterologous expression using S2 cell lines or bacteria respectively. Most recently, Daisho peptides were shown to bind to fungal hyphae ex vivo, and are required for resisting fungal infection in vivo [14]. However the mechanism and direct microbicidal activity of these various peptides at physiological concentrations was not assessed.

In this study, we provide evidence from four separate experimental approaches that support adding *BaraA* to the list of bona-fide antifungal peptides. First, the *BaraA* gene is strongly induced in the fat body upon infection resulting in abundant peptide production. *BaraA* is also tightly regulated by the Toll pathway, which orchestrates the antifungal response. Second, loss of function study shows that *BaraA* contributes to resistance against fungi. *BaraA* mutation increases susceptibility to *B. bassiana*, and this is coupled with increased *B. bassiana*

proliferation. Third, the antifungal activity of *BaraA* is independent of other key effectors. Over-expression of *BaraA* in the absence of other inducible peptides increased resistance of *Imd, Toll* deficient flies to various fungi including *C. albicans*, *A. fumigatus*, and *N. crassa*. Moreover *BaraA, Bomanin* double mutants suffered greater susceptibility than *Bomanin* mutants alone upon natural infection, even with a relatively avirulent fungal pathogen (*A. fumigatus*). Fourth, and lastly, a cocktail of the *BaraA* IM10-like peptides possesses antifungal activity against *C. albicans* and *B. bassiana* in vitro when co-incubated with the membrane disrupting antifungal Pimaricin.

While it is difficult to estimate the concentration of BaraA peptides in the haemolymph of infected flies, it is expected based on MALDI-TOF peak intensities that the IM10-like peptides should reach concentrations similar to other AMPs (up to 100μM) [10,20]; our in vitro assays used a peptide cocktail at the upper limit of this range. AMPs are often - but not exclusively – positively charged. This positive charge is thought to recruit these molecules to negatively charged membranes of microbes [10]. However the net charges at pH=7 of the IM10-like peptides are: IM10 +1.1, IM12 +0.1, and IM13 -0.9. Given this range of net charge, IM10-like peptides are not overtly cationic. However some AMPs are antimicrobial without being positively charged, exemplified by human Dermicidin [42] and anionic peptides of Lepidoptera that also synergize with membrane-disrupting agents [43]. More extensive in vitro experiments with additional fungi should confirm the range of BaraA peptide activities, and assay the potential activities of IM22 and IM24, which were not included in this study.

Our study also reveals that the *Baramicin A* gene alone produces at least 1/3 of the initially reported IMs. In addition to the IM10-like peptides and IM24 that were previously assigned to *BaraA* [22], we show IM22 is encoded by the C terminus of *BaraA*, and is conserved in other *Drosophila* species. The production of multiple IMs encoded as tandem repeats between furin cleavage sites is built-in to the BaraA protein design akin to a "protein operon." Such tandem repeat organization is rare,

but not totally unique among AMPs. This structure was first described in the bumblebee AMP Apidaecin [44], and has since also been found in Drosocin of *Drosophila neotestacea* [45]. In *D. melanogaster*, several AMPs are furin-processed including Attacin C and its pro-peptide MPAC, wherein both parts synergize in killing bacteria [25]. Therefore, furin cleavage in Attacin C enables the precise co-expression of distinct peptides with synergistic activity. It is interesting to note that IM10-like peptides did not show antifungal activity in the absence of membrane disruption by Pimaricin. An attractive hypothesis is that longer peptides encoded by BaraA such as IM22 and IM24 could contribute to the antifungal activity of *BaraA* by membrane permeabilization, allowing the internalization of IM10-like peptides. Indeed, the BaraA IM24 peptide is a short Glycine-rich peptide (96 AA) that is positively-charged (charge +2.4 at pH=7). These traits are shared by amphipathic membrane-disrupting AMPs such as Attacins [10], however the precise role for the Baramicin IM24 domain remains to be determined.

An unexpected observation of our study is the display of an erect wing phenotype by *BaraA* deficient males upon infection. Our study suggests that this is not a consequence of the genetic background, but rather relies on the activation of the Toll pathway in the absence of *BaraA*. Erect wing is also induced by heat-killed bacteria, and is not observed in *Bomanin* or *Relish* mutants, indicating that the erect wing phenotype is not a generic consequence of susceptibility to infection. The *erect wing* gene, whose inactivation causes a similar phenotype, is a transcription factor that regulates synaptic growth in developing neuromuscular junctions [35]. This raises the intriguing hypothesis that immune processes downstream of the Toll ligand Spaetzle somehow affect wing neuromuscular junctions, and that *BaraA* modulates this activity. Another puzzling observation is the sexual dimorphism exhibited for this response. Male courtship and aggression displays involve similar wing extension behaviours. Koganezawa et al. [46] showed that males deficient for *Gustatory receptor 32a (Gr32a)* failed to unilaterally extend wings during courtship display. *Gr32a*-expressing cells extend into the subesophageal ganglion where they contact mAL, a male-specific set of interneurons involved in unilateral wing display

[46]. One possible explanation for the male specific effects of BaraA could be that *BaraA* mediates this effect through interactions with such male-specific neurons. *BaraA* is highly produced in the fat body upon infection but also expressed in the nervous system (**Fig.** 1D-E and FlyAtlas1 [21]). Further studies should decipher whether the preventative effect of *BaraA* on the erect wing phenotype is cell autonomous or linked to BaraA peptides secreted into the haemolymph. Recent studies have highlighted how NF-κB signalling in the brain is activated by bacterial peptidoglycan [47], and that immune effectors expressed either by fat body surrounding the brain or from within brain tissue itself affect memory formation [41]. Moreover, an AMP of nematodes regulates aging-dependent neurodegeneration through binding to its G-protein coupled receptor, and this pathway is sufficient to trigger neurodegeneration following infection [48]. Thus immune-inducible AMPs can have striking interactions with neurological processes. As such, future studies characterizing the role of *BaraA* in the erect wing phenotype should provide insight on interactions between systemic immunity and host physiology more generally.

Here we describe a complex immune effector gene that produces multiple peptide products. *BaraA* encodes many of the most abundant immune effectors induced downstream of the Toll signalling pathway, and indeed *BaraA* promotes survival upon fungal infection. How each peptide contributes to the immune response and/or erect wing behaviour will be informative in understanding the range of effects immune effectors can have on host physiology. This work and others also clarifies how the cocktail of immune effectors produced upon infection acts specifically during innate host defence reactions.

Materials and methods:

Fly genetics and sequence comparisons

Sequence files were collected from FlyBase [49] and recently-generated sequence data [45,50] and comparisons were made using Geneious R10. Putative NF-κB binding sites were annotated using the Relish motif "GGRDNNHHBS" described in Copley et al. [18] and a manually curated amalgam motif of "GGGHHNNDVH" derived from common Dif binding sites described previously [17,19]. Gene expression analyses were performed using primers described in supplementary data file 1, and further microarray validation for *BaraA* expression comes from De Gregorio et al. [11].

The *UAS-BaraA* and *BaraA-Gal4* constructs were generated using the TOPO pENTR entry vector and cloned into the pTW or pBPGUw Gateway™ vector systems respectively. The *BaraA-Gal4* promoter contains 1675bp upstream of *BaraA1* (but also *BaraA2,* sequence in supplementary information). The *BaraA-Gal4* construct was inserted into the VK33 attP docking site (BDSC line #24871). The $BaraA^{SW1}$ (*ΔBaraA)* mutant was generated using CRISPR with two gRNAs and an HDR vector by cloning 5' and 3' region-homologous arms into the pHD-dsRed vector, and consequently *ΔBaraA* flies express dsRed in their eyes, ocelli, and abdomen. *ΔBaraA* was generated using the Bloomington stocks BL2057 and BL51323 as these backgrounds contain only one copy of the *BaraA* locus. The induction of the immune response in these flies was validated by qPCR and MALDI-TOF proteomics, wherein we discovered an aberrant *Dso2* locus in these preliminary $BaraA^{SW1}$ flies. We thus backcrossed the $BaraA^{SW1}$ mutation once with a standard w^{1118} background (used in [12–14]) and screened for wild type *Dso2* before use in any survival experiments. Additionally, *ΔBaraA* was isogenized into the *DrosDel* w^{1118} isogenic background for seven generations before use in isogenic fly experiments as described in Ferreira et al. [29].

A full description of fly stocks used for crosses and in experiments is provided in supplementary data file 1.

Microbe culturing conditions

Bacteria and *C. albicans* yeast were grown to mid-log phase shaking at 200rpm in their respective growth media (Luria Bertani, Brain Heart Infusion, or Yeast extract-Peptone-Glycerol) and temperature conditions, and then pelleted by centrifugation to concentrate microbes. Resulting cultures were diluted to the desired optical density at 600nm (OD) for survival experiments, which is indicated in each figure. The following microbes were grown at 37°C: *Escherichia coli strain 1106* (LB), *Enterococcus faecalis* (BHI), and *Candida albicans* (YPG). The following microbes were grown at 29°C: *Erwinia carotovora carotovora (Ecc15)* (LB) and *Micrococcus luteus* (LB). For filamentous fungi and molds, *Aspergillus fumigatus* was grown at 37°C, and *Neurospora crassa* and *Beauveria bassiana* were grown at room temperature on Malt Agar in the dark until sporulation. *Beauveria bassiana strain R444* commercial spores were produced by Andermatt Biocontrol, product: BB-PROTEC.

Survival experiments

Survival experiments were performed as previously described [15], with 20 flies per vial with 2-3 replicate experiments. 3-5 day old males were used in experiments unless otherwise specified. As *Rel, spz* double mutant flies and largely wild type backgrounds differ drastically in their immune competence, we selected pathogens, infection routes, and temperatures to provide infection models that could best reveal phenotypes in these disparate genetic backgrounds. For fungi natural infections, flies were flipped at the end of the first day to remove excess fungal spores from the vials. Otherwise, flies were flipped thrice weekly. Statistical

analyses were performed using a Cox proportional hazards (CoxPH) model in R 3.6.3. We report the hazard ratio (HR) alongside p-values as a proxy for effect size in survival experiments. Throughout our analyses, we required $p < .05$ as evidence to report an effect as significant, but note interactions with |HR| near or above 0.5 as potentially important provided p-value approached .05, and tamp down importance of interactions that were significant, but have relatively minor effect size (|HR| less than 0.5) in our discussion of the data.

Erect wing scoring

The erect wing phenotype was scored as the number of flies with splayed wings throughout a distinct majority of the period of observation (30s); if unclear, the vial was monitored an additional 30s. Here we define splayed wings as wings not at rest over the back, but did not require wings to be fully upright; on occasion wings were held splayed outward at ~45° relative to the dorsal view, and often slightly elevated relative to the resting state akin to male aggressive displays. Sometimes only one wing was extended, which occurred in both thoracic pricking and fungi natural infections; these flies were counted as having erect wing. In natural infections, the typical course of erect wing display developed in two fashions at early time points, either: i) flies beginning with wings slightly splayed but not fully upright, or ii) flies constantly flitting their wings outward and returning them to rest briefly, only to flit them outward again for extended periods of time. Shortly after infection, some flies were also observed wandering around with wings beating at a furious pace, which was not counted as erect wing. However at later time points erect wing flies settled more permanently on upright splayed wings. Erect wing measurements were taken daily following infection, and erect wing flies over total flies was converted to a percent. Data points in **Fig.** 6B-D represent % with erect wing in individual replicate experiments with ~20 flies per vial. Flies stuck in the vial, or where the wings had become sticky or mangled were not included in totals. **Table** S1 reports mean percentages across replicate experiments for all pathogens

and genotypes where erect wing was monitored. Days post-infection reported in **Table** S1 were selected as the final day prior to major incidents of mortality. For *E. faecalis* live infections, *Bom*$^{\Delta 55C}$ and *spz*^{rm7} erect wing was taken at 1dpi due to major mortality events by 2dpi specifically in these lines.

Erect wing measurements were performed in parallel with survival experiments, which often introduced injury to the thorax below the wing possibly damaging flight muscle. It is unlikely that muscle damage explains differences in erect wing display. First: we noticed erect wing initially during natural infections with *A. fumigatus*, and observed erect wing upon *B. bassiana R444* and *Metarhizium rileyi PHP1705* natural infections (**Table** S1; *M. rileyi* = NOMU-PROTEC, Andermatt Biocontrol). Second: only 1 of 75 total *iso w*^{1118} males displayed erect wing across 4 systemic infection experiments with *E. faecalis*. For comparison: 19 of 80 total *iso ΔBaraA* and 48 of 80 *w; ΔBaraA* flies displayed erect wing (**Table** S1). Future studies might be better served using an abdominal infection mode, which can have different infection dynamics [51]. However we find erect wing display to be robust upon either septic injury or natural infection modes.

IM10-like peptide in vitro activity

The 23-residue Baramicin peptides were synthesized by GenicBio to a purity of >95%, verified by HPLC. An N-terminal pyroglutamate modification was included based on previous peptidomic descriptions of Baramicins IM10, IM12, and IM13 [52], which we also detected in our LC-MS data (**Fig.** S2). Peptides were dissolved in DMSO and diluted to a working stock of 1200μM in 0.6% DMSO; the final concentration for incubations was 300μM in 0.15% DMSO. For microbe-killing assays, microbes were allowed to grow to log-growth phase, at which point they were diluted to ~50cells/μL. Two μL of culture (~100 cells), and 1μL water or antibiotic was mixed with 1μL of a 1:1:1 cocktail of IM10, IM12, and IM13 peptides to a final concentration of 300μM total peptides; 1μL of water + DMSO (final concentration = 0.15% DMSO) was used as a negative control. Four μL microbe-

peptide solutions were incubated for 24h at 4°C. Microbe-peptide cultures were then diluted to a final volume of 100μL and the entire solution was plated on LB agar or BiGGY agar plates. Colonies were counted manually. For combinatorial assays with bacteria, *C. albicans* yeast, and *B. bassiana R444* spores, peptide cocktails were combined with membrane disrupting antimicrobials effective against relevant pathogens beginning at: 10 μM Cecropin A (Sigma), 500μg/mL ampicillin, or 250μg/mL Pimaricin (commercially available as "Fungin," InVivogen), serially diluted through to 0.1 μM, 0.5μg/mL, and 4μg/mL respectively.

Beauveria bassiana R444 spores were prepared by dissolving ~30mg of spores in 10mL PBS, and then 4μL microbe-peptide solutions were prepared as described for *C. albicans* followed by incubation for 24h at 4°C; this spore density was optimal in our hands to produce distinct individual colonies. Then, 4μL PBS was added to each solution and 2μL droplets were plated on malt agar at 25°C. Colony diameters were measured 4 days after plating by manually analyzing colony diameters in InkScape v0.92. Experimental batches were included as co-variates in one-way ANOVA analysis. The initial dataset approached violating Shapiro-Wilk assumptions of normality ($p = 0.061$) implemented in R 3.6.3. We subsequently removed four colonies from the analysis, as these outliers were over two standard deviations lower than their respective mean (removed colonies: PBS 0.15cm, PBS 0.25cm, IM10-like+Pimaricin 0.21cm, and a second IM10-like+Pimaricin colony of 0.21cm); the resulting Shapiro-Wilk p-value = 0.294, and both QQ and residual plots suggested a normal distribution. Final killing activities and colony surface areas were compared by One-way ANOVA with Holm-Sidak multiple test correction (*C. albicans*) and Tukey's honest significant difference multiple test correction (*B. bassiana R444*).

Gene expression analyses

RNA was extracted using TRIzol according to manufacturer's protocol. cDNA was reverse transcribed using Takara Reverse Transcriptase. qPCR was performed using PowerUP mastermix from Applied Biosystems at 60°C using primers listed in supplementary data file 1. Gene expression was quantified using the PFAFFL method [53] with *Rp49* as the reference gene. Statistical analysis was performed by one-way ANOVA with Holm-Sidak's multiple test correction or student's t-test. Error bars represent one standard deviation from the mean.

Proteomic analyses

Raw haemolymph samples were collected from immune-challenged flies for MALDI-TOF proteomic analysis as described in [14,15]. MALDI-TOF proteomic signals were confirmed independently at facilities in both San Diego, USA and Lausanne, CH. In brief, haemolymph was collected by capillary and transferred to 0.1% TFA before addition to acetonitrile universal matrix. Representative spectra are shown. Peaks were identified via corresponding m/z values from previous studies [8,22]. Spectra were visualized using mMass, and figures were additionally prepared using Inkscape v0.92.

Author contributions:

MAH planned experiments, performed bioinformatic analyses, infection experiments, and in vitro assays. BL supervised the project and MAH and BL wrote the manuscript. LC planned and generated the *BaraA* deletion and performed key descriptive experiments and observations. AM assisted with infection and in vitro assays. MH, II, and SAW generated and supplied critical fly stock reagents and provided constructive commentary.

Acknowledgements:

This research was supported by Sinergia grant CRSII5_186397 and Novartis Foundation 532114 awarded to Bruno Lemaitre, and by National Institute of Health (NIH) grant R01 GM050545 to Steven Wasserman. We thank Jean-Philippe Boquete for assistance with the generation of Gal4 and UAS constructs. We would also like to acknowledge the technical expertise provided by the proteomics and mass spectrometry facilities in both UCSD and EPFL, and specifically Adrien Schmid. The name "*Baramicin*" was partly inspired by Eichero Oda's character "Buggy," a Bara-Bara superhuman. Finally, we further thank Huang et al. (*in preparation*) for their cooperation in publishing initial descriptions of the *BaraA* gene, and for stimulating discussion.

References:

1. Lemaitre B, Hoffmann J. The Host Defense of Drosophila Melanogaster. Annual Review of Immunology. 2007;25: 697–743. doi:10.1146/annurev.immunol.25.022106.141615

2. Kurz CL, Ewbank JJ. Caenorhabditis elegans: An emerging genetic model for the study of innate immunity. Nature Reviews Genetics. 2003;4: 380–390. doi:10.1038/nrg1067

3. Kaufmann SHE. Immunology's foundation: the 100-year anniversary of the Nobel Prize to Paul Ehrlich and Elie Metchnikoff. Nat Immunol. 2008;9: 705–712. doi:10.1038/ni0708-705

4. Steiner H, Hultmark D, Engström \AA, Bennich H, Boman HG. Sequence and specificity of two antibacterial proteins involved in insect immunity. Nature. 1981;292: 246–248. doi:10.1038/292246a0

5. Lemaitre B, Nicolas E, Michaut L, Reichhart JM, Hoffmann JA. The dorsoventral regulatory gene cassette spatzle/Toll/Cactus controls the potent antifungal response in Drosophila adults. Cell. 1996;86: 973–983. doi:10.1016/S0092-8674(00)80172-5

6. Lemaitre B, Reichhart JM, Hoffmann JA. Drosophila host defense: differential induction of antimicrobial peptide genes after infection by various classes of microorganisms. Proceedings of the National Academy of Sciences of the United States of America. 1997;94: 14614–9. doi:10.1073/pnas.94.26.14614

7. Lemaitre B, Kromer-Metzger E, Michaut L, Nicolas E, Meister M, Georgel P, et al. A recessive mutation, immune deficiency (imd), defines two distinct control pathways in the Drosophila host defense. Proc Natl Acad Sci U S A. 1995;92: 9465–9469. doi:10.1073/pnas.92.21.9465

8. Uttenweiler-Joseph S, Moniatte M, Lagueux M, Van Dorsselaer a, Hoffmann J a, Bulet P. Differential display of peptides induced during the immune response of Drosophila: a matrix-assisted laser desorption ionization time-of-flight mass spectrometry study. Proceedings of the National Academy of Sciences of the United States of America. 1998;95: 11342–11347. doi:10.1073/pnas.95.19.11342

9. Lazzaro BP, Zasloff M, Rolff J. Antimicrobial peptides: Application informed by evolution. Science. 2020;368. doi:10.1126/science.aau5480

10. Hanson MA, Lemaitre B. New insights on Drosophila antimicrobial peptide function in host defense and beyond. Curr Opin Immunol. 2020;62: 22–30. doi:10.1016/j.coi.2019.11.008

11. De Gregorio E, Spellman PT, Tzou P, Rubin GM, Lemaitre B. The Toll and Imd pathways are the major regulators of the immune response in Drosophila. EMBO Journal. 2002;21: 2568–2579. doi:10.1093/emboj/21.11.2568

12. Clemmons AW, Lindsay SA, Wasserman SA. An Effector Peptide Family Required for Drosophila Toll-Mediated Immunity. PLoS Pathogens. 2015;11. doi:10.1371/journal.ppat.1004876

13. Lindsay SA, Lin SJH, Wasserman SA. Short-Form Bomanins Mediate Humoral Immunity in Drosophila. J Innate Immun. 2018;10: 306–314. doi:10.1159/000489831

14. Cohen LB, Lindsay SA, Xu Y, Lin SJH, Wasserman SA. The Daisho Peptides Mediate Drosophila Defense Against a Subset of Filamentous Fungi. Front Immunol. 2020;11: 9. doi:10.3389/fimmu.2020.00009

15. Hanson MA, Dostálová A, Ceroni C, Poidevin M, Kondo S, Lemaitre B. Synergy and remarkable specificity of antimicrobial peptides in vivo using a systematic knockout approach. eLife. 2019;8. doi:10.7554/elife.44341

16. Unckless RL, Howick VM, Lazzaro BP. Convergent Balancing Selection on an Antimicrobial Peptide in Drosophila. Current Biology. 2016;26: 257–262. doi:10.1016/j.cub.2015.11.063

17. Busse MS, Arnold CP, Towb P, Katrivesis J, Wasserman SA. A κB sequence code for pathway-specific innate immune responses. EMBO Journal. 2007;26: 3826–3835. doi:10.1038/sj.emboj.7601798

18. Copley RR, Totrov M, Linnell J, Field S, Ragoussis J, Udalova IA. Functional conservation of Rel binding sites in drosophilid genomes. Genome Research. 2007;17: 1327–1335. doi:10.1101/gr.6490707

19. Tanji T, Yun E-Y, Ip YT. Heterodimers of NF-κB transcription factors DIF and Relish regulate antimicrobial peptide genes in Drosophila. Proceedings of the National Academy of Sciences. 2010;107: 14715–14720. doi:10.1073/pnas.1009473107

20. Ferrandon D, Jung AC, Criqui MC, Lemaitre B, Uttenweiler-Joseph S, Michaut L, et al. A drosomycin-GFP reporter transgene reveals a local immune response in Drosophila that is not dependent on the Toll pathway. EMBO Journal. 1998;17: 1217–1227. doi:10.1093/emboj/17.5.1217

21. Robinson SW, Herzyk P, Dow JAT, Leader DP. FlyAtlas: database of gene expression in the tissues of Drosophila melanogaster. Nucleic Acids Research. 2013;41: D744–D750. doi:10.1093/nar/gks1141

22. Levy F, Rabel D, Charlet M, Bulet P, Hoffmann JA, Ehret-Sabatier L. Peptidomic and proteomic analyses of the systemic immune response of Drosophila. Biochimie. 2004;86: 607–616. doi:10.1016/j.biochi.2004.07.007

23. Tzou P, Reichhart J-M, Lemaitre B. Constitutive expression of a single antimicrobial peptide can restore wild-type resistance to infection in immunodeficient Drosophila mutants. Proceedings of the National Academy of Sciences of the United States of America. 2002;99: 2152–2157. doi:10.1073/pnas.042411999

24. Wiegand I, Hilpert K, Hancock REW. Agar and broth dilution methods to determine the minimal inhibitory concentration (MIC) of antimicrobial substances. Nature Protocols. 2008. doi:10.1038/nprot.2007.521

25. Rabel D, Charlet M, Ehret-Sabatier L, Cavicchioli L, Cudic M, Otvos L, et al. Primary Structure and in Vitro Antibacterial Properties of the Drosophila melanogaster Attacin C Pro-domain. Journal of Biological Chemistry. 2004;279: 14853–14859. doi:10.1074/jbc.M313608200

26. Rahnamaeian M, Cytry ska M, Zdybicka-Barabas A, Dobslaff K, Wiesner J, Twyman RM, et al. Insect antimicrobial peptides show potentiating functional interactions against Gram-negative bacteria. Proceedings of the Royal Society B: Biological Sciences. 2015;282: 20150293–20150293. doi:10.1098/rspb.2015.0293

27. Kragol G, Lovas S, Varadi G, Condie BA, Hoffmann R, Otvos L. The antibacterial peptide pyrrhocoricin inhibits the ATPase actions of DnaK and prevents chaperone-assisted protein folding. Biochemistry. 2001;40: 3016–3026. doi:10.1021/bi002656a

28. Ryder E, Blows F, Ashburner M, Bautista-Llacer R, Coulson D, Drummond J, et al. The DrosDel collection: A set of P-element insertions for generating custom chromosomal aberrations in Drosophila melanogaster. Genetics. 2004;167: 797–813. doi:10.1534/genetics.104.026658

29. Ferreira ÁG, Naylor H, Esteves SS, Pais IS, Martins NE, Teixeira L. The Toll-dorsal pathway is required for resistance to viral oral infection in Drosophila. PLoS Pathog. 2014;10: e1004507. doi:10.1371/journal.ppat.1004507

30. Levashina EA, Ohresser S, Bulet P, Reichhart J -M, Hetru C, Hoffmann JA. Metchnikowin, a Novel Immune-Inducible Proline-Rich Peptide from Drosophila with Antibacterial and Antifungal Properties. European Journal of Biochemistry. 1995;233: 694–700. doi:10.1111/j.1432-1033.1995.694_2.x

31. Fehlbaum P, Bulet P, Michaut L, Lagueux M, Broekaert WF, Hetru C, et al. Insect immunity: Septic injury of drosophila induces the synthesis of a potent antifungal peptide with sequence homology to plant antifungal peptides. Journal of Biological Chemistry. 1994;269: 33159–33163.

32. Zhang Y, Zhao J, Fang W, Zhang J, Luo Z, Zhang M, et al. Mitogen-Activated Protein Kinase hog1 in the Entomopathogenic Fungus Beauveria bassiana Regulates Environmental Stress Responses and Virulence to Insects. AEM. 2009;75: 3787–3795. doi:10.1128/AEM.01913-08

33. Dudzic JP, Hanson MA, Iatsenko I, Kondo S, Lemaitre B. More Than Black or White: Melanization and Toll Share Regulatory Serine Proteases in Drosophila. Cell Reports. 2019;27: 1050-1061.e3. doi:10.1016/j.celrep.2019.03.101

34. Binggeli O, Neyen C, Poidevin M, Lemaitre B. Prophenoloxidase Activation Is Required for Survival to Microbial Infections in Drosophila. PLoS Pathogens. 2014;10. doi:10.1371/journal.ppat.1004067

35. DeSimone SM, White K. The Drosophila erect wing gene, which is important for both neuronal and muscle development, encodes a protein which is similar to the sea urchin P3A2 DNA binding protein. Mol Cell Biol. 1993;13: 3641–3649. doi:10.1128/MCB.13.6.3641

36. Elya C, Lok TC, Spencer QE, McCausland H, Martinez CC, Eisen M. Robust manipulation of the behavior of Drosophila melanogaster by a fungal pathogen in the laboratory. eLife. 2018;7: e34414. doi:10.7554/eLife.34414

37. Imler J-L, Bulet P. Antimicrobial peptides in Drosophila: structures, activities and gene regulation. Chemical immunology and allergy. 2005;86: 1–21. doi:10.1159/000086648

38. Hedengren M, Borge K, Hultmark D. Expression and evolution of the Drosophila attacin/diptericin gene family. Biochemical and biophysical research communications. 2000;279: 574–81. doi:10.1006/bbrc.2000.3988

39. Khush RS, Lemaitre B. Genes that fight infection: what the Drosophila genome says about animal immunity. Trends Genet. 2000;16: 442–449. doi:10.1016/s0168-9525(00)02095-3

40. Goto A, Yano T, Terashima J, Iwashita S, Oshima Y, Kurata S. Cooperative regulation of the induction of the novel antibacterial Listericin by peptidoglycan recognition protein LE and the JAK-STAT pathway. J Biol Chem. 2010;285: 15731–15738. doi:10.1074/jbc.M109.082115

41. Barajas-azpeleta R, Wu J, Gill J, Welte R. Antimicrobial peptides modulate long-term memory. PLoS Genetics. 2018; 1–26. doi:10.1371/journal.pgen.1007440

42. Steffen H, Rieg S, Wiedemann I, Kalbacher H, Deeg M, Sahl H-G, et al. Naturally processed dermicidin-derived peptides do not permeabilize bacterial membranes and kill microorganisms irrespective of their charge. Antimicrob Agents Chemother. 2006;50: 2608–2620. doi:10.1128/AAC.00181-06

43. Zdybicka-Barabas A, Mak P, Klys A, Skrzypiec K, Mendyk E, Fiołka MJ, et al. Synergistic action of Galleria mellonella anionic peptide 2 and lysozyme against Gram-negative bacteria. Biochim Biophys Acta. 2012;1818: 2623–2635. doi:10.1016/j.bbamem.2012.06.008

44. Casteels-Josson K, Capaci T, Casteels P, Tempst P. Apidaecin multipeptide precursor structure: a putative mechanism for amplification of the insect antibacterial response. The EMBO journal. 1993;12: 1569–78. doi:10.1002/j.1460-2075.1993.tb05801.x

45. Hanson MA, Hamilton PT, Perlman SJ. Immune genes and divergent antimicrobial peptides in flies of the subgenus Drosophila. BMC evolutionary biology. 2016;16: 228. doi:10.1186/s12862-016-0805-y

46. Koganezawa M, Haba D, Matsuo T, Yamamoto D. The Shaping of Male Courtship Posture by Lateralized Gustatory Inputs to Male-Specific Interneurons. Current Biology. 2010;20: 1–8. doi:10.1016/j.cub.2009.11.038

47. Kurz CL, Charroux B, Chaduli D, Viallat-Lieutaud A, Royet J. Peptidoglycan sensing by octopaminergic neurons modulates Drosophila oviposition. Elife. 2017;6. doi:10.7554/eLife.21937

48. Lezi E, Zhou T, Koh S, Chuang M, Sharma R, Pujol N, et al. An Antimicrobial Peptide and Its Neuronal Receptor Regulate Dendrite Degeneration in Aging and Infection. Neuron. 2018;97: 125-138.e5. doi:10.1016/j.neuron.2017.12.001

49. Gramates LS, Marygold SJ, Dos Santos G, Urbano JM, Antonazzo G, Matthews BB, et al. FlyBase at 25: Looking to the future. Nucleic Acids Research. 2017;45: D663–D671. doi:10.1093/nar/gkw1016

50. Hill T, Koseva BS, Unckless RL. The genome of Drosophila innubila reveals lineage-specific patterns of selection in immune genes. Molecular Biology and Evolution. 2019. doi:10.1093/molbev/msz059

51. Chambers MC, Jacobson E, Khalil S, Lazzaro BP. Thorax injury lowers resistance to infection in Drosophila melanogaster. Infect Immun. 2014;82: 4380–4389. doi:10.1128/IAI.02415-14

52. Verleyen P, Baggerman G, D'Hertog W, Vierstraete E, Husson SJ, Schoofs L. Identification of new immune induced molecules in the haemolymph of Drosophila melanogaster by 2D-nanoLC MS/MS. Journal of Insect Physiology. 2006;52: 379–388. doi:10.1016/j.jinsphys.2005.12.007

53. Pfaffl MW. A new mathematical model for relative quantification in real-time RT-PCR. Nucleic Acids Res. 2001;29: e45. doi:10.1093/nar/29.9.e45

54. Tyler-Cross R, Schirch V. Effects of amino acid sequence, buffers, and ionic strength on the rate and mechanism of deamidation of asparagine residues in small peptides. J Biol Chem. 1991;266: 22549–22556.

Supplemental figure and table captions:

Figure S1: Supplemental *BaraA* expression patterns. A) 400bp of upstream sequence from *BaraA* annotated with putative *Rel* or *Dif/dl* binding sites (included in supplemental data file 1). **B)** Expression of *BaraA in wild-type* and *spz^{rm7} flies* following injury with the Gram-positive bacteria *M. luteus* . **C)** The *BaraA>mGFP* reporter line shows a robust induction of GFP 2hpi upon pricking with *M. luteus* in larvae. **D)** Expression of *BaraA>mGFP* in the spermatheca of females (yellow arrow). Representative images shown.

Figure S2: LCMS coverage of trypsin-digested and detected BaraA peptides aligned to the protein coding sequence. Peptide fragments cover the whole precursor protein barring furin site-associated motifs. Additionally, two peptide fragments are absent: i) the first 4 residues of the C-terminus ("GIND," not predicted *a priori*), and ii) the C-terminus peptide's "RPDGR" motif, which is predicted as a degradation product of Trypsin cleavage and whose size is beyond the minimum range of detection. Without the GIND motif, the mass of the contiguous C-terminus is 5974.5 Da, matching the mass observed by MALDI-TOF for IM22 (**Fig.** 2A). The N-terminal Q residues of IM10, IM12, IM13, and IM24 are pyroglutamate-modified, as described previously [22]. The asparagine residues of IM10-like peptides are sometimes deamidated, likely as a consequence of our 0.1% TFA sample collection method as "NG" motifs are deamidated in acidic conditions [54].

Figure S3: Alignments of BaraA peptide motifs. A) Aligned IM22 peptides of *Drosophila Baramicin A-like* genes, with the IM10-like 'VWKRPDGRTV' motif noted. The GIND residues at the N-terminus are cleaved off in *Dmel\BaraA* by an unknown process, and this site is similarly cleaved at RXRR furin cleavage site in subgenus Drosophila flies. As a consequence, the mature IM22 peptide is predicted to be the same across species even when different cleavage mechanisms are utilized. **B)** Alignment of the three IM10-like peptides of *D. melanogaster BaraA* with the "VXRPXRTV" motif noted.

Figure S4: *Over-expression of BaraA partially* rescues *Rel, spz* double mutant susceptibility to infection in both males and females. A) validation of the *UAS-BaraA* construct in the *Rel, spz* background. **B)** Overexpressing *BaraA* did not improve the survival of *Rel, spz* flies upon *E. coli* infection. **C)** Overexpressing *BaraA* only marginally improves survival of *Rel, spz* females, but not males, upon *M. luteus* infections. Infections using a higher dose tended to kill 100% of *Rel, spz* flies regardless of sex or expression of *BaraA*, suggesting that if *BaraA* overexpression does affect susceptibility to *M. luteus*, this effect is possible within only a narrow window of *M. luteus* concentration. **D-F)** Overexpressing *BaraA* improves survival of *Rel, spz* male and female flies upon injury with *C. albicans* **(D)** or natural infection with *A. fumigatus* **(E)** and *N. crassa* **(F).** P-values are shown for each biological sex in an independent CoxPH model not including the other sex relative to *Rel, spz* as a reference.

Figure S5: RT-qPCR shows that the expression of *BomBc3* **(A)** *Drs* **(B)** and *DptA* **(C)** is wild-type 18hpi in *iso ΔBaraA* flies. **D)** *BaraA* mutants survive clean injury like wild-type flies. **E)** *iso ΔBaraA* flies have similar lifespan compared with the *iso* w^{1118} wild-type (males + females, *iso vs. iso ΔBaraA*: HR = 0.26, p = .118).

Figure S6: Additional survivals using *ΔBaraA* flies in two distinct genetic backgrounds upon infection by a diversity of microbes. A) No significant susceptibility of *ΔBaraA* flies to *Ecc15* infection. **B)** *w; ΔBaraA but not iso ΔBaraA* flies exhibit a marginal susceptibility to *B. subtilis* (HR > 0.5, p = .099). **C-D)** *w; ΔBaraA* males were slightly susceptible to *A. fumigatus* natural infection (HR > 0.5, p = .078), but not females, nor isogenic flies. Additional infections using *ΔBaraA,* $Bom^{\Delta 55C}$ double mutant flies reveal that *BaraA* mutation increases the susceptibility of $Bom^{\Delta 55C}$ flies in both males and females (cumulative curves shown in **Fig.** 5A). Blue backgrounds = Gram-negative bacteria, orange backgrounds = Gram-positive bacteria, yellow backgrounds = fungi.

Figure S7: Additional survival analyses reveal only a minor contribution of *BaraA* to defence against infection by *E. faecalis*. A) Crosses with a genomic deficiency (*Df(BaraA)*) leads to increased susceptibility in both the *w* background and isogenic DrosDel background, with *Df(BaraA)/ΔBaraA* flies suffering the greatest mortality in either crossing scheme. Both deficiency crosses yielded an earlier susceptibility in *BaraA*-deficient flies (shown with dotted black lines), however neither experiment ultimately reached statistical significance. **B)** *BaraA* RNAi flies (*Act>BaraA-IR*) suffered greater mortality than *Act>OR-R* or *OR-R/BaraA-IR* controls, but this was not statistically significant at α = .05; p-values reported are comparisons to *Act>BaraA-IR* flies.

Figure S8: Additional survival analyses reveal a consistent contribution of *BaraA* to defence against natural infection with *B. bassiana*. A) Crossing with a genomic deficiency (*Df(BaraA)*) leads to increased susceptibility of *Df(BaraA)/ΔBaraA* flies for both the *w* background and isogenic DrosDel background relative to wild-type controls (p < .05). **B)** *Act>BaraA-IR* flies were more susceptible than the *OR-R* wild-type (p = .008) and *OR>BaraA-IR* (p = .004), although not significantly different from our *Act>OR-R* control (p = .266). **C)** Overexpressing *BaraA* (*Act>UAS-BaraA*) improved survival against *B. bassiana* relative to *Act>OR-R* controls (HR = -0.52, p = 0.010).

Figure S9: Frequency of erect wing display following additional challenges. A-B) Erect wing frequencies 2dpi after clean injury **(A)**, or *Ecc15* septic injury **(B)**. The erect wing frequencies of flies pricked by HK-*E. faecalis* (**Fig.** 6D) are included in brown in **A** and **B** to facilitate direct comparison with the frequency observed upon Toll pathway activation. **C)** The frequency of erect wing display is increased following *E. faecalis* septic injury in *ΔBaraA/+* or *Df(BaraA)/+* flies. Data points are pooled from *w; ΔBaraA* and *iso ΔBaraA* crosses after *E. faecalis* infections shown in **Fig.** S7A and data in **Table** S1.

Table S1: Erect wing frequencies from various infection experiments.
Following initial erect wing observations upon *A. fumigatus* natural infection, we scored erect wing frequency in all subsequent survival experiments. Data represent the mean % of males displaying erect wing ± one standard deviation. n exp = number of replicate experiments performed, and dpi ewg taken = days post-infection where erect wing data were recorded. We additionally performed natural infections with *Metarhizium rileyi* that generally did not cause significant mortality even in *ΔBaraA, Bom*$^{\Delta 55C}$ double mutant males, but nevertheless induced erect wing specifically in *ΔBaraA* males and *spz*^{rm7} controls. Bacterial infections were performed by septic injury, while fungal challenges were natural infections performed by rolling flies in spores.

Supplementary information:

Identification of the BaraA C-terminus as IM22 from Uttenweiler-Joseph et al.

In 1998, Uttenweiler-Joseph et al. [8] described 24 immune-induced molecules by MALDI-TOF and informed predictions suggested that *BaraA* could encodes several of them [22]. We generated a knock out mutant for the *BaraA* gene (*BaraA*^{SW1}), which we validated by MALDI-TOF peptidomic analysis. Strikingly, we noticed an immune-induced peak at ~5981 Da in Linear mode collections that is absent in *ΔBaraA* flies (**Fig.** 2A); this mass closely resembled the 5984 Da estimated mass of IM22 from Uttenweiler-Joseph et al. [8], for which sequence was never determined. We took the Linear masses reported for then-unknown IMs from Uttenweiler-Joseph et al. [8] and post-hoc generated a standard curve with now-confirmed mass values from Levy et al. [22]. Our post-hoc standard curve corrects the mass of IM22 as found in Uttenweiler-Joseph et al. [8] to be 5973.5 Da. Using the same approach with our own linear data we find a mass of 5975.1 Da for our 5981 Da peak (supplementary data file 1). With LCMS proteomics, we confirmed that the *BaraA* C-terminus is cleaved to remove 4 N-terminal residues, which should produce a putative 5974.5 Da peptide (**Fig** S2). Together these observations indicate the *BaraA* C-terminus encodes the following 53-residue mature peptide, matching the estimated mass of IM22: ARVQGENFVA RDDQAGIWDN NVSVWKRPDG RTVTIDRNGH TIVSGRGRPA QHY.

The *BaraA* gene is therefore involved in the production of over one third of the classical *Drosophila* IMs from Uttenweiler-Joseph et al. [8], including: IM5, 6, 8, 10, 12, 13, 20 (doubly-charged IM24 [22]), 22, and 24.

Sequence of the BaraA-Gal4 promoter construct

The following 1675bp sequence was cloned from the DrosDel isogenic background into the pBPGUw vector to drive a downstream Gal4 gene, and inserted into the VK33 attP docking site using BDSC line #24871:

Dif/dorsal binding site **(bold)***:* **GGGHHNNDVH**

Rel binding site (underline): GGRDNNHHBS

>iso_DrosDel_BaraA_promoter-Gal4

CTGCTACTCCTCTACACATTCGACTCCTTCGCCTTGCTGGCTGGGAAAAAATTTTGCATA
ATTTATGTGGGTGCCGCGCACACGGAGGTCCCGACGGATTCGAAGTATCCGAAGGATTCG
AAAGGAAAACAACGCACGAGCACCACGGCCAACTGATTTAAATGCAATTGCACTGAAGT
ATTTTGTTTGGCGAACGAAGCTGGATGAAATAGGGGGGTGTGGGGTTTTCTATTGAGAC
ATCTGCACGTGCAACCGGAAACATCCGAAGAGAACAGCACAGGCCGGGCTACGCCGGGCA
ATTTCTTTTCATTTGCCAAGGTGTTGAGTTGCACCAACATTCGACATCGACGTGGCCAGA
AGCCAACAAAAGCCAAGAGCCAAACCCCTTTTTGTGGTCACAAGTGTCGTCTATTTGTCG
TGGGCATCTTGGGCACCTTGGGCATCCTCGACATCCTTGCCATTTTGGTCTGGCCAAGAC
AAACAACCAGCAAATTTAGTGTATTTTGTGCATTTTTAAAATTGTCCAAATTTATGTGA
CACGCTGCGCCAATTGATCAGATTAAATAAACATGAGGCCAAGCGAATCGAATTTGGCTT
CACCAAGAAGACAATGCAGTCTGTATTCAAATGGGTGGGCGCATCCACCAAGCGGTGAAT
ACAGTGACCGCTCGCTATAATGGACGGTCAGGTGTTACTTTAACTTAAAAAAATATGTA
ACAAATCTTATCAAGTTTGAAATAGATTGAAATAGATTTGGTTATTGCATTCGAAAGAT
ATATATTAAATTCGAATATTCCAAGAAATTTCATGAGAATGTCACTTATGTCATGAGAT
TATATTAACGTACGAATAAACAATGTATTTTCCAAAATTAAAAATAAAATTTAATTTAA
TTACGCAGTACCTTTACACTATCAGTCGGAGGTAATAACTCATATAATTAGATTAGCATT
AGATTTTAAAGCGAAAAACACTTAAAAGCTGAAATTATTAGACAACACTCTTAAATTAG
TCGAGCTGATATATAGCCTCAAGTTTTGCTTAAATCCAAAGATAAAGGAATGCCTTCAA
AAATATATTTTGTTTTATACCAAGTGACAGCAGAGAATGGGGTTGCAATATCTTAAAAG
AGTTTCACTTAGCCAATATTTACTGCCATTGTTGGCCACCAAATAGTAGCAACCAGAGAC
TTCCAGGAATATATTCTCGTGTCAAATGCAATCCACTTTAAATGCAACTATCTGGCGGCT
AAGAAAACCCGACAGTTTGATTCAAGTCGACGAAACAATATAAGCACGTGCTAAATAAA
GAGACCTATGCAGTTAATACTCTTGTCATATTATAATATAATTTAGTGACATAAGTTGC
ATGGTATACGAGTACTGAACAAGTTATGGCAGCTTTTCCAAATAAGCGATCACATATTCC
GCGGGATGATGGGTGGATTTCTAGCATATGTGGATGCTTAATGGCTTATTGC**GGGTCAG**
GGCGGCGCAATCTGTTC**AGAAATTCCC**GAACGCACACCCATTTCAGATCAGATTGTGAC
GTTTT**GGGAAATTCT**TGACGATCGGTGTAAACAAGCTCAGCAACCAGATTCGATGGCTA
TTTGCCGGCTATAAATACTAGAAACCATTCGATTGCACTCAGTTGAAGCTGGGCTCTGGA
ACAGATCACA